Redesign of bridges Twentekanaal in UHPC

MSc Thesis

7 March 2021

Company	Witteveen+Bos
MSc thesis project	Redesign of bridges Twentekanaal in Ultra-High Performance Concrete
Document	MSc Thesis
Status	Final version
Version	D1.0
Date	7 March 2021

Author	ing. M. Dorland
Student id	4719980
Degree programme	MSc Civil Engineering
Track	Structural Engineering – Concrete Structures

Company Supervisors	ing. T. Petersen RC ir. A. ten Voorde
Supervisors TU Delft	Dr. ir. Y. Yang Dr. ir. M.A.N. Hendriks Dr. ir. S. Grünewald

PREFACE

This report comprises my MSc thesis, which focusses on the redesign of existing bridges across the Twentekanaal in Ultra-High Performance Concrete. By finalizing this project, I am concluding my master studies at TU Delft, that were preceded by my bachelor studies in Arnhem. During my studies I have discovered my interest in structural design, concrete structures and, especially, existing structures. It is because of this reason that I decided to search for a graduation topic within this field.

Existing structures provide both opportunities and challenges to engineers and society. The importance of reliable infrastructure for society is evident, and structures such as bridges and viaducts are essential links in the network. The 'vervangingsopgave' as faced by the Dutch infrastructural sector is therefore not only a purely technical challenge, but it is of relevance to society as a whole. The development of new concepts that provide durable and sustainable solutions in dealing with existing structures may therefore be very promising and beneficial. The potential of one of such concepts will be demonstrated in this report. It involves the application of UHPC to redesign existing concrete structures by applying new UHPC decks in combination with the reuse of existing foundations.

Writing a thesis is an uphill process. Moreover, the strange times we are in has added another dimension to this challenge. Thus, it becomes even more important to thank those who played a role in this endeavour. First of all, I would like to mention and thank Yuguang Yang, Max Hendriks and Steffen Grünewald from TU Delft, for their interest in the topic and their constructive feedback. I am also grateful to my colleagues from Witteveen+Bos. I would especially like to thank Tom Petersen, who has guided me through the process of shaping and managing the project, and Arjan ten Voorde, who shared his knowledge on structural design and has helped me finding my way through the process of bridge design. Finally, I would like to thank my parents, for their support during my seven and a half year of study, and my girlfriend, who has been so understanding and patient.

I hope that this project may yield a small contribution to finding solutions to deal with the 'vervangingsopgave', and that it will spark the curiosity and enthusiasm of others to explore innovative solutions within the field of existing structures.

Wishing you a pleasant reading,

Maarten Dorland
Delft, 7 March 2021

SUMMARY

Within the Dutch infrastructure there is the challenge of having to replace or strengthen a large number of existing structures within the upcoming years. This challenge also provides the opportunity to develop new concepts, the promising concept described in this report involves the application of UHPC to redesign the decks of existing concrete bridges in combination with the reuse of existing foundations. It is expected that by applying UHPC a higher slenderness and lower self-weight can be achieved compared to the existing structures, which compensates for the increased variable loads. This would increase the reusability of existing foundations, resulting in saving time and material and in reducing hindrance and environmental impact.

The Twentekanaal comprises many bridges of which various have similar characteristics and were built in the same period. This canal was therefore selected as the topic of this project. The main question of the project is what the redesign of the existing bridges across the Twentekanaal in UHPC should be like in order to obtain a design which complies to the current standards and enables the reuse of the existing foundation of the bridges without having to modify them due to the increase of vertical variable loads. To limit the scope of the project, the new deck should be constructed using prefabricated beams.

Not all bridges could be considered in-depth simultaneously. Therefore, one representative bridge was selected after which the results for this bridge would be generalised onto all other relevant bridges across the canal. The Eefdesebrug was selected for this task. This concrete tied arch bridge across the canal near Zutphen was selected for its span, which is 68 m, and its year of construction, which was 1955. To determine the full potential of the project, it was investigated up to what extent the results for the Eefdesebrug could be projected onto other bridges across the canal. An inventory was set up containing all bridges, in total 37 bridges or bridges part of larger engineering structures were identified, characterised and compared based on bridge category, year of construction and dimensions. This resulted in a total of twelve bridges with similar characteristics, to which the results of the redesign of the Eefdesebrug could potentially be generalised to.

After the potential of the project had been determined, the focus was placed on the redesign of the Eefdesebrug, which was carried out following a stepwise approach. The design stage was decomposed into four phases: the preliminary design, detailed design, optimization and final design. After each phase, the global goal of the project was reflected by means of a weight comparison with the existing bridge. The design would be based on the Eurocode, supplemented by the AFGC-SETRA 2013 guideline, because the Eurocode is not applicable to UHPC.

The first design phase, the preliminary design, focussed on establishing the first dimensions of the deck and determining the feasibility of the project goal based on the self-weight of the new design. The preliminary design resulted in a 26% increase of the self-weight of the structure compared to the existing bridge. However, given the conservative approach, the large number of possible improvements and the potential to optimisation, the project goal was deemed to be feasible. During the detailed design phase, a more complete and accurate analysis was performed to obtain better insight into the structural behaviour of the bridge, and to identify the best options for optimization. The various improvements and refinements incorporated in the design and design approach resulted in a 33% reduction of self-weight compared to the preliminary design and a 16% reduction compared to the existing structure.

The goal of the optimization phase was to achieve a further reduction of the self-weight, by means of varying the dimensions as obtained during the previous phase. New dimensions were established based on capacity, concrete cover, spacing between pretensioned strands and overall stability of the beam, using the results of the detailed design as the starting point. The optimizations resulted in an additional 18% decrease of the self-weight compared to the detailed design. It was concluded that with the given type of cross section and the chosen approach, only limited room remained for further weight reduction. The design stage was therefore concluded. This final design comprises pretensioned box beams with a slenderness of 36, resulting in a 32% reduction of self-weight compared to the existing bridge.

In addition to the design verifications, executional aspects were also considered in the design. The two most stringent criteria were the maximum number of pretensioned prestressing strands and the transportation and placement of the beams. By means of a reference project the transportation and placement of the beams was proven to be feasible. In the final design the number of strands was brought back below the maximum number of strands that can be applied in practice.

With the design stage concluded, the global assessment of the existing foundation was carried out. A criterion for reuse of the existing foundation was formulated: the summation of vertical forces due to the permanent actions and variable actions in the new situation should be smaller than or at most equal to the summation of those forces in the existing situation. The permanent loads of the existing structure were determined based on design drawings. To determine the variable loads, the GBV 1950 and VOSB 1938 were consulted; these former codes were most likely used for the design of the existing bridge. Because of differences in safety philosophies between these former codes and the Eurocode and uncertainty in the safety margin used in the original design of the existing foundation, the comparison was carried out without the use of partial load factors.

The results of the comparison indicated a 32% decrease of the self-weight between the final design and the existing structure, while the variable loads increased with 31% between the VOSB 1938 and the Eurocode. In total the vertical forces on the foundation decreased with 21%. As typical for concrete bridges of larger spans, the self-weight of the existing Eefdesebrug was the largest contributor to the vertical loads. The criterion for reuse of the existing foundation was therefore satisfied and the possibility of reuse of the foundation of the Eefdesebrug without modifications for increased vertical variable loads had therewith been demonstrated.

It was subsequently investigated what may be expected if the solution for the Eefdesebrug would be applied onto the group of twelve aforementioned bridges. Using the results for the Eefdesebrug it was possible to estimate the dimensions for the other bridges and to consider the vertical forces acting upon the foundations. The remark was made that for bridges with smaller spans additional unfavourable effects may occur in the results that are not covered by projecting the results for the Eefdesebrug directly onto these bridges. Under the assumption that the criterion for reuse as formulated for the Eefdesebrug also holds for the other bridges and that additional unfavourable effects in the results for bridges with smaller spans remain within the 21% margin found for the Eefdesebrug, it is expected that the solution for the Eefdesebrug can be applied to all twelve bridges.

The results of the project demonstrate the potential of the concept of designing slender UHPC decks in combination with the reuse of existing foundations as one of the possible solution strategies in dealing with the replacement task. The application of such concepts results in saving time and material, and thus in reducing hindrance and environmental impact. This makes the given solution strategy into an interesting direction for further research and developments in the field of UHPC and its applications in the infrastructure. In time this may result into a new construction method that can compete with more conventional approaches.

SAMENVATTING

De Nederlandse infrastructuur staat voor de uitdaging om de komende jaren een groot aantal bestaande constructies te moeten vervangen of versterken. Deze uitdaging biedt ook de kans nieuwe concepten te ontwikkelen. Het veelbelovende concept dat in dit rapport wordt uitgewerkt omvat het herontwerp van dekken van bestaande betonnen bruggen in UHSB in combinatie met het hergebruik van bestaande funderingen. Verwacht wordt dat de toepassing van UHSB zal resulteren in een hogere slankheid en een lager eigen gewicht vergeleken met de bestaande constructies. Dit compenseert de toegenomen variabele belastingen, resulteert in een toename van de herbruikbaarheid van de bestaande funderingen, een besparing van tijd en materiaal en een reductie van hinder en impact op milieu.

Het Twentekanaal omvat een groot aantal bruggen met vergelijkbare karakteristieken die gebouwd zijn in dezelfde periode en is daarom uitgekozen als het onderwerp van het project. De hoofdvraag is wat het herontwerp van de bestaande bruggen over het Twentekanaal in UHSB moet zijn om een ontwerp te verkrijgen dat voldoet aan de vigerende normen, en dat hergebruik van de bestaande fundering mogelijk maakt zonder dat er versterkingen nodig zijn ten gevolge van toegenomen verticale variabele belastingen. De oplossingsrichting is beperkt tot geprefabriceerde liggers.

Niet alle bruggen konden tegelijk uitgebreid worden beschouwd. Daarom werd er één representatief object gekozen voor het herontwerp, waarna de resultaten werden gegeneraliseerd naar de andere relevante bruggen over het kanaal. De Eefdesebrug bij Zutphen werd hiervoor uitgekozen. Deze betonnen boogbrug met trekband werd geselecteerd vanwege de overspanning (deze bedraagt 68 m) en het bouwjaar (1955). Om de potentie van het project te bepalen werd onderzocht tot op welke hoogte de resultaten van de Eefdesebrug konden worden geprojecteerd op de andere bruggen. Er werd een inventarisatie uitgevoerd waarbij een totaal van 37 bruggen is gevonden, beschreven en vergeleken op basis van categorie, bouwjaar en afmetingen. In totaal bleken er twaalf gelijkende bruggen te zijn waarnaar de resultaten van het herontwerp van de Eefdesebrug mogelijk konden worden gegeneraliseerd.

Vervolgens werd gefocust op de Eefdesebrug. Het ontwerpstadium van het project werd stapsgewijs uitgewerkt en werd daartoe opgedeeld in vier fasen: het voorontwerp, gedetailleerde ontwerp, optimalisatiefase en het uiteindelijke ontwerp. Na elke fase werd gereflecteerd op het hoofddoel van het project aan de hand van een vergelijking van het eigen gewicht met dat van de bestaande brug. Het ontwerp werd gebaseerd op bepalingen uit de Eurocode, aangevuld met bepalingen uit de AFGC-SETRA 2013 omdat de Eurocode niet van toepassing is voor UHSB.

Tijdens de eerste ontwerpfase, het voorontwerp, werd een eerste inschatting gemaakt van de afmetingen van het dek en werd op basis van het eigen gewicht van het resultaat bepaald of het projectdoel haalbaar zou zijn. Het eigen gewicht nam met 26% toe ten opzichte van dat van de bestaande brug. Maar gezien de conservatieve aanpak, het grote aantal mogelijke verfijningen en de potentie tot optimalisatie werd het projectdoel haalbaar geacht. Voor het gedetailleerde ontwerp werd een meer complete en nauwkeurige analyse uitgevoerd om het gedrag van de constructie beter te begrijpen en om de meest kansrijke mogelijkheden voor de optimalisatie te vinden. De diverse verbeteringen en verfijningen die werden verwerkt in het ontwerp en de ontwerpaanpak resulteerden in een reductie van het eigen gewicht van 33% ten opzichte van het voorontwerp en 16% ten opzichte van de bestaande brug.

Het doel van de optimalisatiefase was een verdere reductie van het eigen gewicht te realiseren door middel van het variëren van de afmetingen zoals verkregen uit het gedetailleerde ontwerp. Nieuwe afmetingen werden vastgesteld aan de hand van capaciteit, betondekking, afstand tussen de voorspanstrengen en de stabiliteit van de ligger, waarbij de afmetingen die volgden uit het gedetailleerde ontwerp werden gebruikt als uitgangspunt. De optimalisatie resulteerde in een reductie van het eigen gewicht van 18% ten opzichte van het gedetailleerde ontwerp. Er werd geconcludeerd dat met de gekozen doorsnede en aanpak verdere optimalisatie slechts zeer beperkt mogelijk zou zijn, de ontwerpfase werd daarmee dan ook afgerond. Het uiteindelijke ontwerp bestaat uit kokerliggers voorgespannen met voorgerekt staal en met een slankheid van 36. Het ontwerp resulteerde in een reductie van het eigen gewicht van 32% ten opzichte van de bestaande brug.

Naast de ontwerpberekeningen zijn ook uitvoeringsaspecten beschouwd. De twee meest beperkende criteria waren het maximumaantal voorspanstrengen en het transporteren en plaatsen van de liggers. Middels een referentieproject werd aangetoond dat het transporteren en plaatsen van de liggers mogelijk is. In het uiteindelijke ontwerp was het aantal voorspanstrengen teruggebracht tot onder het maximumaantal dat in de praktijk kan worden toegepast.

Na het afronden van het ontwerp werd de globale beschouwing van de fundering uitgevoerd. Er werd een criterium voor hergebruik van de bestaande fundering geformuleerd: de sommatie van de verticale krachten door permanente- en veranderlijke belastingen in de nieuwe situatie dienen kleiner of ten hoogste gelijk te zijn aan de sommatie van deze krachten in de bestaande situatie. De permanente belastingen van de bestaande brug werden vastgesteld aan de hand van tekeningen. Om de variabele belastingen te bepalen zijn de GBV 1950 en de VOSB 1938 geraadpleegd, deze normen zijn waarschijnlijk toegepast bij het ontwerpen van de bestaande brug. Vanwege verschillen in de veiligheidsfilosofie tussen deze oude normen en de Eurocode en onzekerheid in de veiligheidsmarge die is toegepast in het originele ontwerp van de fundering werd de vergelijking uitgevoerd zonder het toepassen partiële belastingfactoren.

De vergelijking leverde een afname van het eigen gewicht op van 32% tussen het uiteindelijke ontwerp en de bestaande brug, terwijl de variabele belastingen met 31% zijn toegenomen tussen de VOSB 1938 en de Eurocode. In totaal namen de verticale krachten met 21% af tussen beide situaties. Zoals te verwachten voor betonnen bruggen met grotere overspanningen leverde het eigen gewicht van de Eefdesebrug de grootste bijdrage aan de totale verticale belastingen. Er was daarmee voldaan aan het criterium voor hergebruik van de bestaande fundering en daarmee was de mogelijkheid tot hergebruik van de fundering van de Eefdesebrug zonder versterking voor toegenomen verticale belastingen aangetoond.

Vervolgens werd onderzocht wat kan worden verwacht als deze oplossing van de Eefdesebrug wordt toegepast op de voornoemde groep van twaalf bruggen. Aan de hand van het herontwerp van de Eefdesebrug was het mogelijk de afmetingen van de andere bruggen te schatten en kon worden gekeken naar de verticale belastingen op de funderingen. Er werd opgemerkt dat bij kleinere overspanningen ongunstige effecten kunnen optreden, die niet verrekend worden als de resultaten voor de Eefdesebrug direct op deze bruggen wordt toegepast. Onder de aanname dat het criterium voor het hergebruik van de fundering, zoals geformuleerd voor de Eefdesebrug, ook geldt voor de andere bruggen en dat de ongunstige effecten voor bruggen met kleinere overspanningen binnen de 21%-marge blijven zoals gevonden voor de totale verticale krachten bij de Eefdesebrug, wordt verwacht dat de oplossing voor de Eefdesebrug kan worden toegepast op de groep van twaalf gelijkende bruggen over het kanaal.

De resultaten van het project geven de potentie aan van een concept waarbij het ontwerp van slanke UHSB dekken wordt gecombineerd met het hergebruik van bestaande funderingen als één van de mogelijke oplossingsrichtingen voor de vervangingsopgave. De toepassing van een dergelijk concept resulteert in een besparing van tijd en materiaal en een afname van hinder en negatieve effecten op het milieu. De gepresenteerde oplossing levert een interessante richting op voor verder onderzoek en ontwikkeling op het gebied van UHSB en de toepassingen ervan in de infrastructuur. Dit zou op termijn kunnen resulteren in een nieuwe bouwmethode die concurrerend is met meer conventionele methodes.

TABLE OF CONTENT

SYMBOLS

General symbols

Symbol	Definition
E_d	Design value of effect of actions
R_d	Design value of the resistance
C_d	Limiting design value of the relevant serviceability criterion
G_k	Characteristic value of a permanent action
P	Relevant representative value of a prestressing action
Q_k	Characteristic value of a single variable action
γ_G	Partial factor for permanent actions
γ_P	Partial factor for prestressing actions
γ_Q	Partial factor for variable actions
ξ	Reduction factor for unfavourable permanent actions G
ψ_0	Factor for combination value of a variable action
ψ_1	Factor for frequent value of a variable action
ψ_2	Factor for quasi-permanent value of a variable action

Concrete

Symbol	Definition	Unit
ρ	Density	[kg/m^3]
l_f	Fibre length	[mm]
f_{ck}	Characteristic value cylinder compressive strength	[N/mm^2]
$f_{ck,cube}$	Characteristic value cube compressive strength	[N/mm^2]
f_{cm}	Mean value cylinder compressive strength	[N/mm^2]
ε_{c3}	Strain at reaching concrete compressive strength	[‰]
ε_{cu3}	Maximum compressive strain at ULS	[‰]
f_{ctm}	Mean value axial tensile strength	[N/mm^2]
$f_{ctk,el}$	Characteristic elastic (5% fractile value) tensile strength	[N/mm^2]
f_{ctfk}	Characteristic maximal post-cracking stress (stress at $w = 0{,}30$)	[N/mm^2]
K_{global}	Global fibre orientation factor	[-]
K_{local}	Local fibre orientation factor	[-]
E_{cm}	Modulus of elasticity	[N/mm^2]
G	Shear modulus	[N/mm^2]
v	Poisson ratio	[-]
α	Coefficient of thermal expansion	[K^{-1}]
φ	Creep factor	[-]
α	Factor for shape of concrete compressive zone	[-]
β	Factor position centre of gravity concrete compressive zone	[-]
α_{cc}	Factor for long term effects and unfavourable loading (compression)	[-]
α_{ct}	Factor for long term effects and unfavourable loading (tension)	[-]

Prestressing steel

Symbol	Definition	Unit
f_{pk}	Characteristic value tensile strength	[N/mm^2]
$f_{p0,1k}$	Characteristic 0,1% proof-stress of prestressing steel	[N/mm^2]
f_{pd}	Design value steel stress	[N/mm^2]
σ_{pm0}	Maximum allowed stress directly after tensioning	[N/mm^2]
$\sigma_{p,max}$	Maximum prestressing stress during tensioning	[N/mm^2]
E_p	Modulus of elasticity	[N/mm^2]
ε_{uk}	Characteristic value strain at failure	[‰]
η	Bond factor	[-]
η_1	Factor accounting for bond conditions	[-]
κ	Factor for bond strength improvement due to the presence of fibres	[-]
α_1	Factor depending on method of releasing the strands	[-]

α_2	Factor depending on the type of tendon	[-]
μ	Friction coefficient	[-]
k	Unintentional angular rotation due to the Wobble-effect	[rad]
w_{set}	Estimated wedge set	[mm]

Fatigue

Symbol	Definition	Unit
$\Delta\sigma_{Rsk}$	Stress range at N* cycles	[N/mm^2]
N^*	Number of cycles with single stress range	[-]
k_1	Stress exponent first branch of S-N curve	[-]
k_2	Stress exponent second branch of S-N curve	[-]
m	Number of intervals with constant amplitude	[-]
n_1	Actual number of cycles with constant amplitude in interval 'i'	[-]
N_i	Number of cycles with constant amplitude in interval 'i' until failure	[-]
R_i	Stress ratio	[-]
D_{Ed}	Fatigue damage factor	[-]
$E_{cd,min,i}$	Minimum compressive stress level in interval 'i'	[-]
$E_{cd,max,i}$	Maximum compressive stress level in interval 'i'	[-]
$\sigma_{cd,max,i}$	Highest compressive stress in a cycle in interval 'i'	[N/mm^2]
$\sigma_{cd,min,i}$	Lowest compressive stress in a cycle in interval 'i'	[N/mm^2]

Partial material factors

Symbol	Definition	Unit
γ_C	Partial factor for concrete	[-]
$\gamma_{C,fat}$	Partial factor for fatigue of concrete	[-]
γ_{cf}	Partial factor for fibre-reinforced concrete under tension	[-]
γ_S	Partial factor for reinforcing or prestressing steel	[-]
$\gamma_{S,fat}$	Partial factor for reinforcing or prestressing steel under fatigue loading	[-]

Abbreviations

AFGC	Association Française de Génie Civil
EC	Eurocode
GBV	Gewapend Beton Voorschriften
NEN	Nederlandse Norm
RBK	Richtlijnen Beoordeling Kunstwerken
ROK	Richtlijnen Ontwerp Kunstwerken
RWS	Rijkswaterstaat
SETRA	Service d'études sur les transports, les routes et leurs aménagements
SIA	Societé suisse des ingénieurs
TGB	Technische Grondslagen voor Bouwvoorschriften
VOSB	Voorschriften voor het Ontwerpen van Stalen Bruggen

1

INTRODUCTION TO THE PROJECT

1.1 Project background

Within the Dutch infrastructure there is the challenge of having to replace or strengthen a large number of existing structures within the upcoming years, the 'replacement task', or 'vervangingsopgave'. Many existing bridges and viaducts within the main infrastructure network were built in the 60's and 70's for a service life often lower than the 100 years that are more or less standard in the nowadays practice of bridge design. Moreover, due to an increase in traffic loads and the increase of the number of vehicles, the service life of these structures is in practice even shorter than the service life these structures were designed for.

Although it may be a challenge for the infrastructure, it is also an opportunity to develop new concepts. In (Reitsema, Lukovic, & Hordijk, 2016) it is illustrated that the application of innovative materials and methods could prove to be helpful in finding solutions to this challenge:

- Advanced Cementitious Materials (ACM's) such as ultra-high performance concrete allow for the design of, for example, more slender and lighter concrete decks;

- Accelerated Bridge Construction (ABC) is a concept that comprises methods to reduce the on-site time required for the construction or replacement of bridges. This contributes to, for example, the minimization of impact on traffic (hindrance).

However, an important remark is made: the application of advanced cementitious materials is still limited in practice, which hinders innovation. This raises the question how these concepts can be applied in practice. Therefore, there is an interest to analyse existing bridges following the described line of reasoning, by designing a new UHPC deck, an example of an advanced cementitious material, for an existing bridge while investigating the possibility of reusing the existing foundation, an example of accelerated bridge construction. This might prove to be a promising concept for existing bridges that have to be replaced. The hypothesis is as follows:

''If one redesigns the bridge deck of an existing bridge using UHPC, then a higher slenderness and lower dead-weight can be achieved compared to the original situation, which compensates for the increased traffic loads and therefore increases the reusability of the existing foundation.''

An important factor in formulating this hypothesis is the relationship between the properties of UHPC and the importance of achieving a higher slenderness of the structure under consideration. A higher slenderness implies lower dead weight, which might compensate for the traffic loads that have increased since the existing structure was built. This might eventually result in the possibility of reusing the foundation of an existing bridge without having to increase its vertical load capacity.

The replacement task does not limit itself to a single structure though. Therefore, the Twentekanaal has been selected as the topic of the project. This canal comprises a large number of bridges, among which are several structures that were built in roughly the same period and that have similar characteristics. The period in which these bridges were constructed contributes to the relevance of the project.

Because not all bridges can be considered in-depth simultaneously, a representative bridge has been selected as a testcase for the redesign: the Eefdesebrug, see Figure 1. This bridge, which has been chosen because of its span and year of construction, is located near Zutphen and was originally constructed in 1932 as

one of a series of bridges crossing the canal. After the first bridge was destroyed in the second world war, the current bridge was built in 1955.

Figure 1 Side view of the Eefdesebrug

The value of the concept of designing slender structures using UHPC in combination with reuse of the existing foundation lies in the fact that by reuse of the existing foundation time and material can be saved, which means that hindrance for traffic and the surrounding area, as well as environmental impact, are reduced. The results of this project might provide useful insights into the potential of this concept, thus contributing to finding new and promising solutions to deal with the replacement task.

1.2 Reading guide

The outline of this report is as follows:

Chapter 2: In the second chapter the problem analysis is elaborated based on the introduction and hypothesis as given in this chapter. In addition, the approach to the project is discussed;

Chapter 3: In the third chapter the background knowledge required for successful elaboration of the project is discussed. This chapter comprises information regarding the Twentekanaal and Eefdesebrug, UHPC and prefab bridges;

Chapter 4: In the fourth chapter the potential to generalise the results of the redesign of the Eefdesebrug is explored by identifying bridges crossing the Twentekanaal with similar characteristics;

Chapter 5: The fifth chapter covers different aspects of the design calculations and verifications that will be performed in elaborating the redesign, such as available codes and guidelines, selecting a specific guideline on UHPC, constitutive laws and various UHPC verifications;

Chapter 6: In the sixth chapter the main outline of the design stage is discussed, as well as the four design phases it comprises. The framework of the design stage is also defined by formulating assumptions, boundary conditions and requirements that hold for all design phases;

Chapter 7: In the seventh chapter the preliminary design, which involves the first actual design calculations, is discussed. Specific attention is dedicated to the main design considerations and to the verification of the feasibility of the project by performing a weight calculation;

Chapter 8: In the eighth chapter the detailed design is discussed which involves a more comprehensive set of calculations and verifications as well as refinements compared to the preliminary design, with the goal to gain more understanding of the behaviour of the structure and to identify options for optimization;

Chapter 9: The ninth chapter covers the optimization of the design resulting into a final design, with which the design stage is concluded. The optimization is carried out in a stepwise manner: after the approach is chosen, new dimensions are established and the verifications are carried out;

Chapter 10: The tenth chapter covers the global assessment of the foundation of the Eefdesebrug by comparing the vertical forces acting upon the foundation in the new situation, the aforementioned final design, and the existing situation;

Chapter 11: In the eleventh chapter the solution for the Eefdesebrug is projected onto the group of bridges with similar characteristics that was identified in the fourth chapter. In addition, attention is paid to the actual application of the solution;

Chapter 12: In the eleventh chapter the project is reflected upon, limitations to the results are listed, the conclusion is formulated and recommendation for further research are given.

2

PROBLEM ANALYSIS

2.1 Project goal

The goal of the project is defined as follows:

"To design an ultra-high performance concrete bridge deck for the existing bridges across the Twentekanaal, in such a way that the existing foundations can be reused with only limited modifications."

2.2 Representative structure and project scope

To narrow down the problem, the scope of the project has been defined as follows:

- **Structure under consideration**: The structure under consideration for the redesign in this project is the Eefdesebrug. Further elaborations solely refer to the redesign of this structure unless specifically stated otherwise.

- **Substructure and superstructure**: The focus of the design work is the superstructure (i.e. the deck and arch of the current bridge). Therefore, from now on the term 'redesign' refers to the redesign of the superstructure unless specifically stated otherwise.

- **Analysis of the foundation**: The focus of the design is on the superstructure. The analysis of the foundation is limited to a comparison of the vertical load on the foundation in both the new and old situation, the horizontal loads are not taken into consideration.

- **Bridge type**: To keep the focus on the redesign instead of studying different variants for the bridge type, restrictions are made to the allowed bridge types. The goal is to design a prefabricated beam deck, other structural types are not considered.

- **Codes & guidelines**: The starting point with respect to codes and standards is that the redesign has to comply with the Eurocode including the Dutch national annex. Additional codes and guidelines may be used if and only if the Eurocode and Dutch national annex lack certain information required for the elaboration of the project (e.g. no information particularly about UHPC) or if the Eurocode and Dutch national annex refer to these particular documents.

- **Comparison of materials and structural types**: The focus of the project is on the reusability of existing foundations in combination with redesign using UHPC. Therefore, all other aspects such as comparisons with other materials or structural types will not be included in the project. The use of other materials is only allowed if this is required for the successful application of UHPC. Possible examples of this are prestressing steel or reinforcing steel.

2.3 Main research question

The main research question of the project is defined as follows:

"What should the redesign of the existing bridges across the Twentekanaal in UHPC be like in order to obtain a design which complies to the current standards and enables the reuse of the existing foundation of the bridges without having to modify them due to the increase of vertical variable loads?"

2.4 Project activities and approach

The total project can be decomposed into multiple project phases or activities. Figure 2 gives an overview of the different project activities as well as the relationships between the different activities.

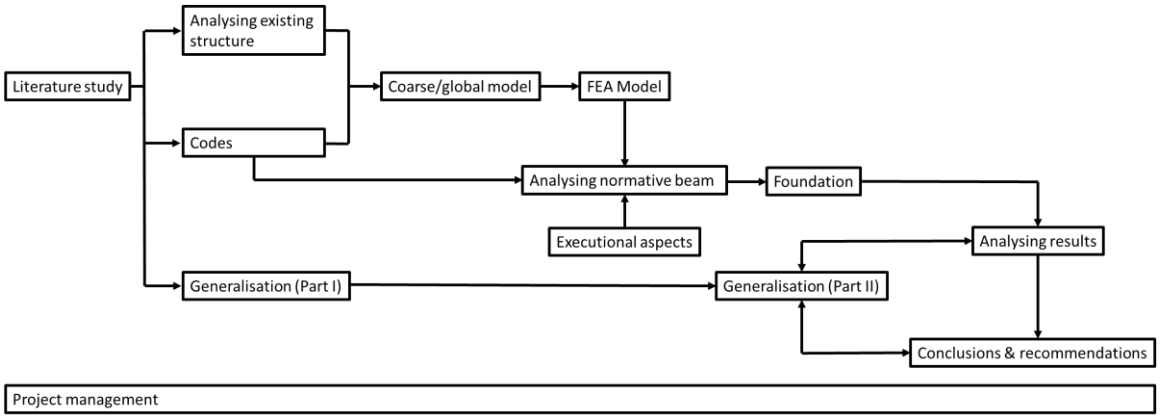

Figure 2 Flow chart of the project

The main research question has been decomposed into various sub questions. In addition, the main goals of each of these project activities have been defined. These are summarized in Table 1.

Table 1 Summary of main project activities

Part	**Goal**
Literature study I	To collect information regarding UHPC from the perspectives of both concrete science & Technology and design & execution.
Literature study II	Basic information regarding arch/prefab beam bridges (the Eefdesebrug in particular) and underlying principles of structural mechanics.
Analysing structure	To analyse available information in order to gain insight into the (current state of) the existing structure.
Codes	To collect relevant codes for design (EC), redesign (RBK) and design in UHPC in particular.
Coarse/global model	To set up a coarse/global model for the new prefab beam deck in order to gain insight into its behaviour and required dimensions.
FEA Model	To model the whole deck using FEA in order to obtain detailed information and to identify the normative beam(s).
Analysing normative beam	To analyse the normative beam(s) in accordance with the relevant codes and to optimise the design in order to reduce the amount of material whilst paying attention to the design being possible to execute in practice.
Foundation	A global assessment of the existing foundation by comparing the vertical loads on the foundation in both the old situation and new situation.
Execution	To consider two important executional aspects: (1). No overly complex shapes in the design (2). Considering different phases of the construction.
Generalisation	To illustrate the relevance of the project and to generalise the results from the redesign to other existing structures (especially those of the same type).

Each project activity is related to one or more goals and sub questions, an overview of which can be found in annex I. By achieving these goals for each individual project activity, the research questions related to this activity can be answered. Answering all sub questions leads to the final step of formulating a conclusion to answer the main research question, as well as formulating recommendations.

3

BASIC KNOWLEDGE

3.1 Twentekanaal

3.1.1 Description Twentekanaal

The Twentekanaal connects the main cities of Twente (Almelo, Hengelo and Enschede) to the main waterways in the country. The main canal starts at the IJssel river near Zutphen and runs to Enschede, passing the towns of Eefde, Almen, Lochem, Goor, Delden and Hengelo. A second branch of the canal starts just west of Delden and runs to Almelo. Figure 3 gives an overview of the location of the canal.

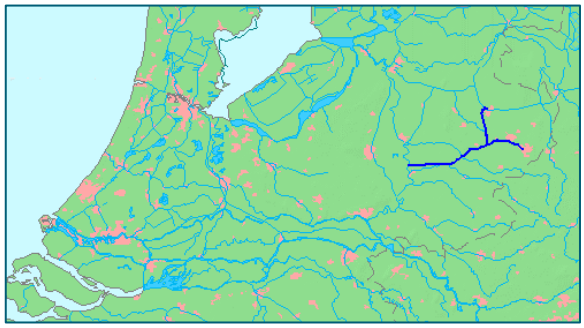

Figure 3 Location Twentekanaal – (Wikipedia, 2020)

The actual start of the construction of the canal was in 1930, it was dug for two reasons. The first reason was the transportation of goods to and from the region of Twente, especially coal and raw materials for the textile industry. The second reason was related to water management. After the required locks and bridges were constructed, the canal itself was dug. In 1936 the construction of the main canal to Enschede was finished and the construction of the side branch from Delden to Almelo started. The main canal was officially opened in 1938, the side branch in 1953.

Nowadays the canal is still intensively used for transportation, especially that of bulk cargo such as sand, gravel, salt and animal fodder. Although the economic development realised by the construction of the canal did not meet the expectations, it has proven itself as an important link in the water management system.

3.1.2 Eefdesebrug

Engineering structures Twentekanaal

The construction of the canal required the construction of a series of engineering structures. Because of the difference in elevation of 21 m between Zutphen and Enschede, three locks were constructed. From west to east one can distinguish the locks at Eefde, Delden and Hengelo. This creates three stretches of the canal with a constant water level. The water level between the IJssel river and the lock at Eefde is governed by the water level in the river.

In addition, a number of bridges was constructed to create crossing points. According to (Rijkswaterstaat, 2014) a total of twenty-nine bridges was originally built: three concrete bridges at the locks, three railroad bridges, eighteen fixed bridges spanning the main canal Zutphen – Enschede and five bridges spanning the side branch Delden – Almelo.

Of the eighteen bridges spanning the main canal fourteen were constructed in reinforced concrete. Most of the bridges were arch bridges, these were built following the same design with variations in width, span and foundations, and subsequently painted white. These bridges were a characteristic feature of the canal. One of these arch bridges was the original Eefdesebrug.

Location and function of the Eefdesebrug

The Eefdesebrug is positioned on the road between Zutphen and Eefde, its location is given in Figure 4. The bridge used to be a link in the main road (the provincial road N348) from Zutphen to Deventer until 2012. In that year the road was diverted around Zutphen and the function of the Eefdesebrug was taken over by the Polbrug, which was constructed in 2012, just west of it. The Eefdesebrug remained in service for local traffic.

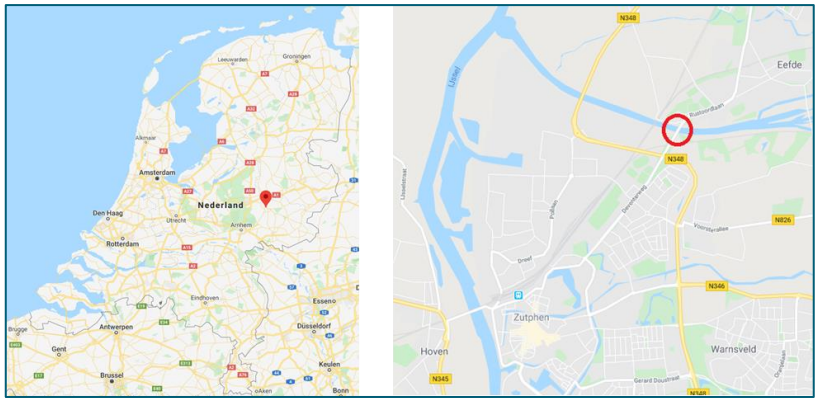

Figure 4 Location Eefdesebrug – Google Maps

History of the structure

The Eefdesebrug that can be seen today is not the first bridge to be built at this location. The first bridge was built in 1932, which was a concrete arch bridge of the design typical to the bridges crossing the Twentekanaal. Figure 5 shows one of the original design drawings on which the first bridge can be seen.

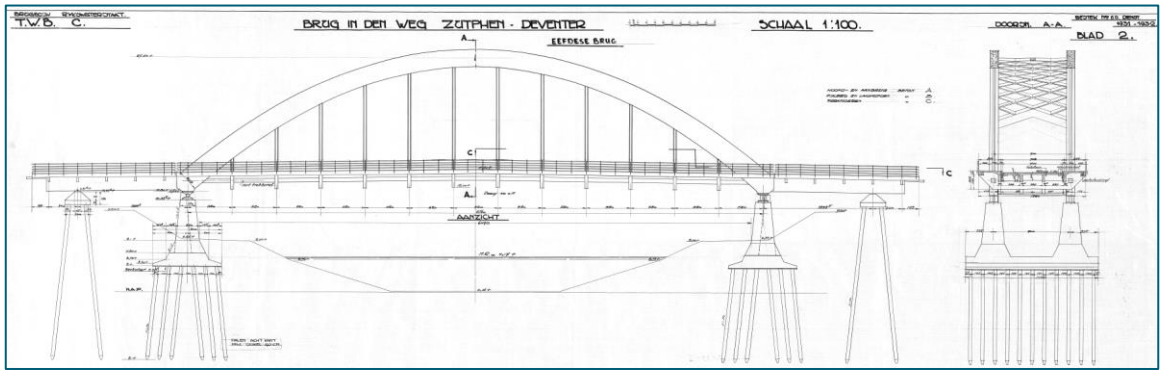

Figure 5 Design drawing of the original bridge – Part of drawing B.2790 (from Rijkswaterstaat archives)

The first bridge was destroyed in 1945. A temporary bridge was constructed in 1946, positioned directly next to the old bridge. In 1955 a new concrete arch bridge was constructed at the location of the temporary bridge. This is the bridge that can be seen today. In 2019 and 2020 maintenance work was carried out including repairs to the deck, joints, new pavement and maintenance to the railing and hangers.

General description and main dimensions

Figure 6 illustrates that different structural forms for arch bridges exist. The Eefdesebrug is an example of a tied arch bridge, this means that the horizontal support reactions due to the compression in the arch are balanced internally by using a tensile element between the ends of the arch. This way only the vertical component of the compressive force in the arch has to be transferred.

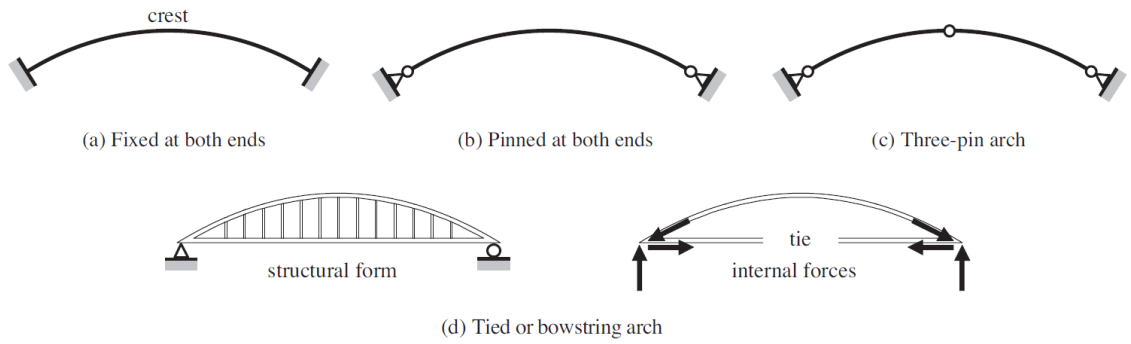

Figure 6 Different structural forms of arch bridges – (Lebet & Hirt, 2013)

The main span of the bridge is formed by two arch type girders with a span of 68,0 m and a length of 70,70 m. These are formed by a main girder with a height of 1,30 m and a width of 1,90 m. On top of these main girders the arches are constructed, their centreline intersects with the centreline of the main girders at the locations of the supports. At this location the height is increased locally.

The arches are positioned centre to centre 8,9 m in transverse direction and are supported by four stability elements. Both arches and main girders are connected by 24 sets of hangers, with two steel hangers each. The tensile tie required to complete the structural scheme of a tied arch bridge is realised using tensile cables in the main girders.

Figure 7 View of the deck from the side of Zutphen

Figure 7 gives an overview of the layout of the deck. The main carriageway is formed by a concrete deck that spans the main girders; this deck is supported by a total of 14 transverse beams between the girders. The two pedestrian lanes at outer sides of the deck structure are formed by concrete decks cantilevering outwards. Table 2 has been prepared based on original design drawings provided by Rijkswaterstaat and gives an overview of the main dimensions of the bridge.

Table 2 Main dimensions Eefdesebrug

Dimension	Value	Unit
Length deck main span	70,70	[m]
Span support to support	68,0	[m]
Height main girder	1,30	[m]
Total width	16,36	[m]
Width of deck between kerbs	7,0	[m]

The substructure of the bridge consists of box type abutments founded on piles. The decks of these abutments also form the decks of the side spans (approach bridges), which have the same width as the bridge deck.

3.2 Ultra-High Performance Concrete (UHPC)

3.2.1 Basics of UHPC

Development of concretes with higher strengths

The search to increase the concrete compressive strength and new developments for such materials has been an ongoing topic for research. In the 1950s a strength of 70 N/mm^2 was reached and by developments such as the application of silica fume and superplasticizers the limits were shifted continuously, until 120 N/mm^2 was reached at the 1980s. This was regarded as the upper limit, a further increase was deemed to be unlikely, because by following and adjusting the conventional approach to designing concrete mixtures the aggregate, which makes up the largest part of the volume, would become the weakest link of the material.

In 1981 H.H. Bache, a Danish researcher, published his findings in which he demonstrated that in fact the limit had not yet been reached. Bache was the first to develop and apply new principles for the design of concrete mixtures. This turned out to be a breakthrough, with which a new group of materials with strength values in the range of 150 – 200 N/mm^2 could be made: ultra-high strength concretes (UHSC). These concepts were embraced by others as well, resulting in further research, development of commercial products and the application of these ultra-high strength concretes in actual projects.

Definition of UHPC

The term 'ultra-high strength concrete' does not cover the full extent of the new possibilities that this type of concrete turned out to offer. The material does not only have a very high compressive strength, other properties are superior to normal strength and high strength concrete as well, for example: other mechanical properties, a higher modulus of elasticity and excellent durability because of low porosity. Therefore, the material can also be applied for reasons other than its compressive strength. For this reason, instead of using the term 'UHSC', the term ultra-high performance concrete (UHPC) is often used to denote this group of materials, despite the material still being characterised based on its 28-day compressive strength.

Characteristics of UHPC

The group of materials denoted as UHPC have various characteristics in common. A number of these characteristics offer new possibilities for the application of the material while others are inherent to the application of this type of materials and have to be kept in mind. An overview is given in this section.

Mechanical properties: The high concrete compressive strength is accompanied by other mechanical properties with values above those of normal strength and high strength concrete. UHPC therefore allows for more slender and lighter structures. Table 3 gives indicative values of various mechanical properties at different ranges of strength classes.

Durability: UHPC generally has very low porosity and as a result the microstructure of the material is very dense. The material therefore performs better with respect to durability compared to normal strength or high strength concrete.

Workability: The mixture composition of UHPC generally results in a material which is flowable and often even self-compacting. This is a useful property for prefabrication in general, but also specifically for creating complicated shapes or textures.

Brittleness and use of fibres: A higher concrete compressive strength is accompanied by more brittle behaviour. A typical UHPC mixture therefore contains fibres to increase the ductility. In addition, the steel fibres increase the tensile strength of the material. In practice the amount of reinforcement can often be reduced or even omitted due to the fibres.

Long term behaviour: Because of the mixture composition the long-term behaviour of UHPC is different than that of normal strength or high strength concrete. The creep coefficient is rather low while drying shrinkage is virtually non-existent. The autogenous shrinkage however is larger than that of normal strength or high strength concrete.

Costs: The initial costs of UHPC are significantly higher than those of conventional concrete, according to (Fehling, Schmidt, Walraven, Leutbecher, & Fröhlich, 2014) the difference can be a factor four to five per cubic meter of concrete. For this reason, optimization of the design is important. In addition, to compare the cost-effectiveness compared to conventional concrete solutions, multiple stages of the project should be taken into consideration to fully appreciate the benefits of UHPC, such as a reduction of maintenance.

Table 3 Mechanical properties of NSC, HSC and UHPC – (Betoniek, 2017)

Property	Unit	NSC	HSC	UHPC
Compressive strength	[N/mm^2]	20-65	65-105	150-200
Tensile strength	[N/mm^2]	2,3-4,3	4,5-5,0	6,0-10,0
Modulus of elasticity	[N/mm^2]	28.000-38.000	38.000-41.000	50.000-60.000
Volumetric mass	[kg/m^3]	2400	2450	2525
Drying shrinkage	[magnitude]	+++	++	+
Autogenous shrinkage	[magnitude]	+	++	+++
Creep coefficient φ	[-]	Approx. 2,0	Approx.1,0	Approx. 0,8

3.2.2 Mixture composition

Main principles of UHPC

Specific principles have to be followed to obtain a UHPC with the characteristics and performance as described in the previous section. These main principles are as follows:

Principle 1 – Low water/cement ratio: The water/cement ratio is kept low with a typical value of 0,2 to prevent that more water is present than required for the hydration, which would result in the formation of capillary pores. Such a low water/cement ratio is achieved by adding a large amount of cement to the mixture. All the water will be bonded, the remaining unhydrated cement remains and acts as a filler. Superplasticizer is required to obtain a flowable mixture.

Principle 2 – Optimization of the packing density: By optimizing the packing density the stresses at the contact surfaces of the particles are reduced. The dense and more homogeneous structure gives high durability and by limiting the stresses microcracks only start to form at higher load levels, thus increasing the strength.

The constituents are selected to optimize the packing. Different constituents with each having their own range of particle sizes are applied. From largest to smallest these are the aggregate, fillers, cement and silica fume. This results in a discontinuous grading curve, an indicative example of which can be seen in Figure 8.

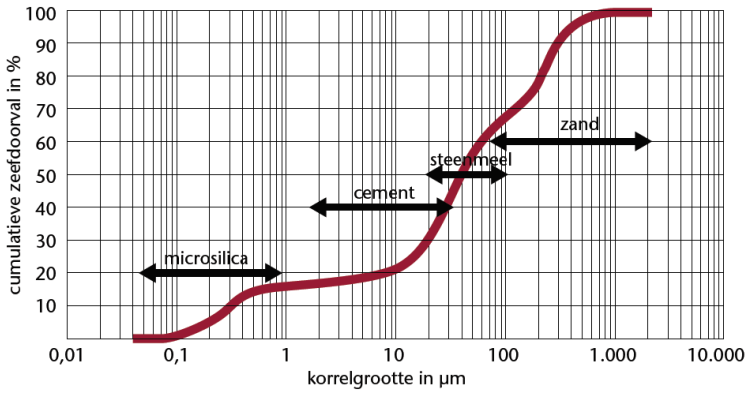

Figure 8 Grading curve of UHPC – (Betoniek, 2017)

Compared to normal strength concrete the aggregate particle size is typically chosen smaller and the amount of cement is chosen larger. Fillers (e.g. fly ash or mineral fines) are added to improve the packing between the aggregate and the cement. Silica fume is added to act as a ''microfiller'' and fill the space between the cement particles. By following this approach, the free spaces between the particles of each material are always filled by a different material with smaller particle sizes.

Principle 3 – Limiting the aggregate particle size: By reducing the maximum particle size two effects are achieved. The first effect is the reduction of the size of the porous interface zone between the aggregate and hardened cement paste. These zones are the weakest parts in the material where microcracks are formed due to a difference in properties of the paste and aggregate.

The second effect is a further homogenization of the material. This is profitable because due to the difference in properties between the aggregate and the cement paste peak stresses may occur. Further homogenization reduces these peak stresses and thus the risk of microcracking. Both of these effects subsequently result in an increase of strength.

Principle 4 – Addition of steel fibres: A higher concrete strength is accompanied by more brittle behaviour, for this reason steel fibres are added to increase the ductility. In addition, these fibres contribute to the tensile capacity of the material.

Mix design of UHPC

From the four aforementioned principles it can be seen that the composition of UHPC mixtures is different from that of conventional concrete. However, it should be noted that UHPC is not a specific mixture but rather a group of materials. Figure 9 gives an indication of the mixture composition of ordinary concrete and various UHPC mixtures.

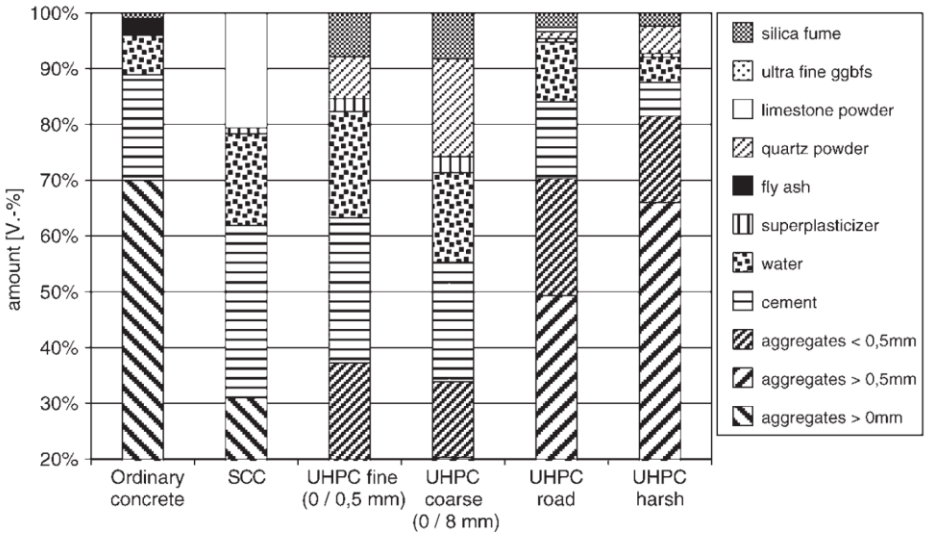

Figure 9 Mixture compositions – (Fehling, Schmidt, Walraven, Leutbecher, & Fröhlich, 2014), p.7

The constituents of typical UHPC mixtures and their requirements to meet the four aforementioned main principles of UHPC will be discussed in more detail.

Cement: In UHPC large quantities of cement are used, generally this is Portland cement, but depending on the requirements other types can be used as well, e.g. cement with fly ash or blast furnace slag. A large amount of cement remains unhydrated, because of this reason a part of the cement can be replaced by a filler such as quartz powder. On the other hand, the unhydrated cement provides the ability of self-healing.

Aggregate: The aggregate particles in UHPC are generally smaller than those in normal strength concrete to improve packing and homogenisation and to reduce the size of the interface zone. For mixtures with coarser aggregate (gravel) the maximum particle size is often in the range of 5 – 7 mm while for mixtures with only finer particles the maximum size is often in the range of 1 – 2 mm. UHPC mixtures such as reactive powder concretes contain no coarse aggregate at all.

Admixtures and additives: UHPC requires a large dosage of superplasticizer to obtain a flowable and workable material in its fresh state despite the low water/cement ratio typical for the material. Other admixtures can be added depending on the requirements of a specific project.

Fillers: Fillers are typically applied in UHPC to improve the packing density. Fillers can be reactive or inert, although the contribution of both groups is mostly physical. This physical effect is called the ''filler-effect'', which means the effect of filling up the empty space, see Figure 10. For example, smaller filler particles fill up the spaces between the cement particles, thus improving the interface zone between the paste and the aggregate. The ''filler-effect'' results in a denser structure and higher strength.

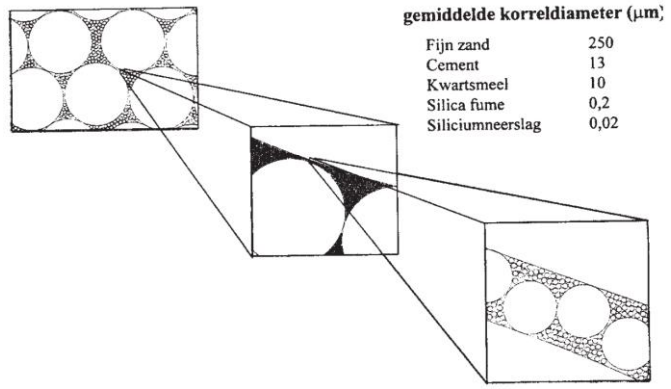

Figure 10 Optimization of packing using different particle sizes – (Kaptijn, 2002)

Examples of reactive fillers are silica fume and fly ash (pozzolanic materials) or blast furnace slag (a latent hydraulic material). Inert fillers only contribute through the physical effect by improving packing, examples are quartz powder and limestone powder.

Fibres: A typical UHPC mix contains approximately 2% of steel fibres by volume. These provide the concrete with ductility and improve the tensile strength. Fibres can differ in shape, size and materials, although for structural applications steel fibres are generally used.

The way in which the steel fibres affect the properties of the concrete partially depends on the fibres themselves, one important distinction is between short fibres and long fibres. To understand the influence of the fibre length, the fracture process of the material should be understood. First microcracks are formed at the weakest points in the concrete, being the interfaces between the paste and the aggregate. If the loads increase the number of microcracks increase and these start to propagate. In case of further load increase the microcracks grow together into macrocracks, eventually resulting in failure.

Short fibres are activated by microcracking and bridge these microcracks. Because the formation of the microcracks takes place at the initial stage of the loading these fibres mainly influence the tensile strength, the material behaves elastic for longer. Longer fibres are activated by macrocracking, which only occurs if the load becomes sufficiently large for the microcracks to propagate and widen. The fibres prevent the macrocracks from opening up further, thus mainly influence the post-peak behaviour by increasing the ductility. A combination of both fibre types can be used as well (hybrid-fibre concrete), see Figure 11.

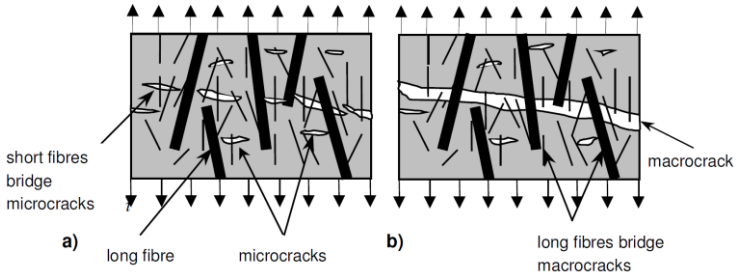

Figure 11 Hybrid fibre concrete – (Markovic, 2006), p.8

The tensile response of UHPC depends on the presence of the fibres. According to (Markovic, 2006), although the composition of different UHPC mixtures may differ, the tensile response is similar. The uniaxial stress response of plain, fibre reinforced and high performance fibre reinforced concrete (UHPC) is given in Figure 12.

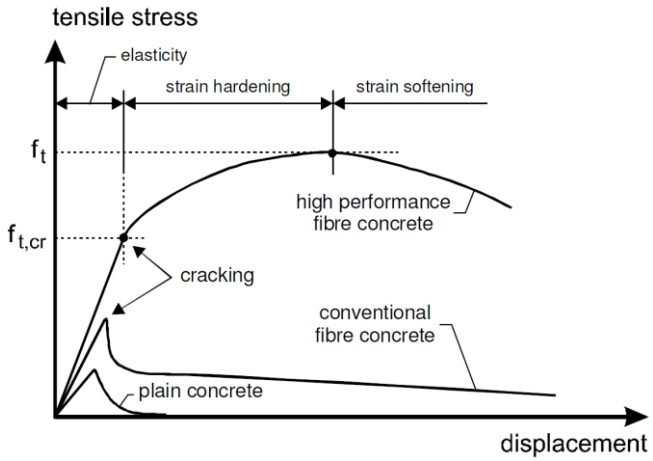

Figure 12 Uniaxial stress response of different concretes – (Markovic, 2006), p.63

From the comparison using the graph the following conclusions were drawn:

- **Pronounced microcracking**: The UHPC cracks at higher tensile loads and thus responds elastically for longer compared to the conventional fibre-reinforced concrete. This can be contributed to the presence of short steel fibres because of their effect on microcracking, especially if these are added in large quantities;

- **Occurrence of strain hardening**: The UHPC shows an increasing tensile capacity even after the first larger cracks, this is strain-hardening behaviour. This is contrary to the plain and fibre-reinforced conventional concretes of which the capacity decreases after cracking (softening);

- **Higher tensile strength**: Because of the strain-hardening the peak tensile strength of UHPC is higher than that of conventional fibre-reinforced concrete. After the peak tensile strength is reached the material starts to soften, while the crack opens further the fibres resisting this motion are pulled out until no tensile capacity is left.

The hardening behaviour of UHPC is typical behaviour of the material and important for its application. According to (Markovic, 2006) it is a decisive difference between all conventional and high-performance fibre reinforced concretes. According to (Walraven, 2006) the hardening behaviour has to be visible for a well-designed UHPC mixture.

3.2.3 Properties of UHPC

Fresh UHPC

Important properties for fresh UHPC and concrete in general are related to the consistency (firmness of form of the concrete and thus the ease with which it flows) and workability (the ease with which it can be processed). According to (Fehling, Schmidt, Walraven, Leutbecher, & Fröhlich, 2014) UHPC is generally processed in flowing consistency. In its fresh state the material is closer to self-compacting concrete than to conventional concrete. The large content of fine materials results in good consistency and the superplasticizer provides the workability. In addition, the material has often self-compacting properties.

Hardening UHPC

Strength development: The high 28-day strength of UHPC means that at earlier age already high strength values are achieved in comparison to normal strength concrete. Heat treatment can be applied to influence the hardening of the material, and thus the development of the strength.

Shrinkage: Shrinkage of UHPC is different compared to normal strength and high strength concrete. Drying shrinkage has a minimal contribution to the total shrinkage. This phenomenon is caused by a change in the moisture content of the concrete due to a difference in the relative humidity between the concrete and its surroundings. The occurrence of this effect is related to capillary pores and free water present in these pores.

After the free water evaporates, the pores contract. Because of the mixture composition of UHPC the formation of capillary pores and the presence of free water are prevented.

Contrary to drying shrinkage, autogenous shrinkage plays an important role. This phenomenon is caused by internal drying of the hardening concrete due to water consumption for the hydration. The combination of a low water/cement ratio, a large amount of fine material and the absence of coarse aggregate high autogenous shrinkage values are generally observed.

According to (Fehling, Schmidt, Walraven, Leutbecher, & Fröhlich, 2014) a total shrinkage strain of 0,6 to 0,9‰ may be assumed for UHPC of low capillary material and without heat treatment, in this context low capillary material means a water/cement ratio smaller than or equal to 0,25. Heat treatment can be applied to control the shrinkage, all shrinkage takes place during the treatment.

Hardened UHPC – Mechanical properties

Compressive strength: UHPC can, just like conventional concrete, be characterised using its 28-day compressive strength. Typical values are in the range of 150 – 200 N/mm^2 while higher values up to 800 N/mm^2 have been reported, although this requires special treatment.

Figure 13 shows the stress-strain diagram of UHPC without fibres in uniaxial compression. It can be seen that the material exhibits approximately linear behaviour until the compressive strength is reached. Small deviations from the linear curve are contributed to microcracks. According to (Fehling, Schmidt, Walraven, Leutbecher, & Fröhlich, 2014) the strain at maximum strength depends on the grading of the aggregate.

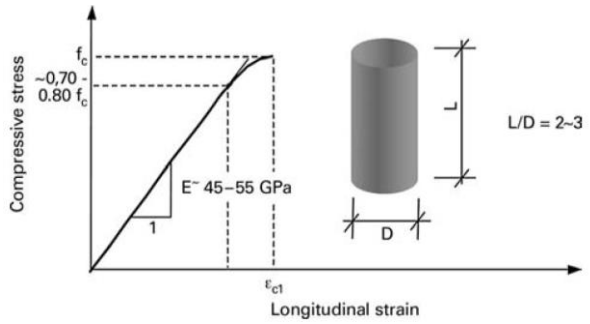

Figure 13 Stress-strain diagram UHPC without fibres in uniaxial compression (Fehling, Schmidt, Walraven, Leutbecher, & Fröhlich, 2014), p.24

The high compressive strength is explained by the microstructure of the material, which is as dense and as homogenous as possible. Because of this structure the failure mechanism of UHPC is different to that of conventional concrete. In case of the latter it is the splitting stresses between the particles that are the driving force for failure. The failure is initiated by microcracks, which grow together into macrocracks through the paste, resulting in failure. In case of UHPC however, the initiation of the crack results in propagation straight through the material, causing brittle failure.

Tensile strength: The tensile stress of UHPC is higher than that of conventional concrete, but this increase is not in proportion to the increase of the compressive strength. One of the contributing factors to the high compressive strength is the optimization of the packing density using fillers to fill up the free space between particles. This effect is more predominant to the compressive strength. According to (Fehling, Schmidt, Walraven, Leutbecher, & Fröhlich, 2014) typical values of the axial tensile strength of UHPC are in the range of 6 – 10 N/mm^2. Without fibres brittle failure is observed, cracks run through the grains and paste. For flexural tensile tests strength values in the range of 15 – 40 N/mm^2 can be found, depending on the mixture.

For both the axial and flexural tensile strength higher strength values can be achieved as well as more ductile behaviour. Depending on the amount of fibres and their orientation softening or strain-hardening may be observed after cracking. This post-cracking behaviour is governed by factors such as fibre content, geometry of the fibres and element, orientation of the fibres and bond with the matrix. Note that concrete also exhibits post-peak behaviour in compression. This means that the capacity, i.e. the compressive stress, reduces while

the compressive strain still increases. This phenomenon can also be influenced using fibres and is governed by the same factors as the factors that determine the post-cracking behaviour in tension.

Modulus of elasticity: Given the dense structure the modulus of elasticity of UHPC is higher than that of high strength and conventional concrete, although the increase is not in proportion to the increase of the compressive strength. For this reason, equations from the Eurocode should not be used. According to (Fehling, Schmidt, Walraven, Leutbecher, & Fröhlich, 2014) the common range of values for the modulus of elasticity is 45.000 – 55.000 N/mm^2. Fibres do not significantly influence this value up to 2,5% fibres by volume, while using different aggregate can have a large influence (bauxite results in an increase that can be up to 70.000 N/mm^2), as well as the size of the aggregate.

Poisson ratio: The Poisson ratio of UHPC is in the same order of magnitude as the value for conventional concrete. For example, according to (Fehling, Schmidt, Walraven, Leutbecher, & Fröhlich, 2014) the Poisson ratio is 0,18 – 0,19 for fine-grained UHPC while for coarse-grained UHPC the value is approximately 0,21.

Creep: The creep coefficient of UHPC is lower than that of high strength and conventional concrete. For a rough estimation (Fehling, Schmidt, Walraven, Leutbecher, & Fröhlich, 2014) gives a value of 0,6 – 1,4 for the final creep coefficient without heat treatment, while 0,2 – 0,4 may be used with heat treatment.

Hardened UHPC – Durability

The dense microstructure with low porosity results in better durability related performance of UHPC compared to normal and high strength concrete. Table 4 gives indicative values for normal and high strength concrete and UHPC.

Table 4 Durability of different concretes – (Betoniek, 2017)

Property	Unit	NSC	HSC	UHPC
Porosity	[% v/v]	14-20	10-13	1,5-5
Air permeability	[m^2]	10^{-16}	10^{-17}	10^{-19}
Chloride diffusion factor	[m^2/s]	$2*10^{-16}$	$2*10^{-17}$	$2*10^{-19}$
Freeze/thaw resistance	[-]	Moderate/Good	Excellent	Excellent
Carbonation after 3 years	[mm]	Approx. 7	Approx. 4	Approx. 0,2

The difference in durability related performance is contributed to the structure of the material, many deterioration mechanisms are related to the presence of larger pores in the material (porosity) and its ability to take up and transport moisture, which is related to the presence of larger pores. Figure 14 compares the pore distribution in concrete of different strength classes, it can be seen that the capillary pores are practically absent in the case of UHPC, which is explained by the low water/cement ratio and optimized packing density. This makes the material practically impermeable to harmful substances and improves the durability performance of the UHPC related to the penetration of such substances into the material.

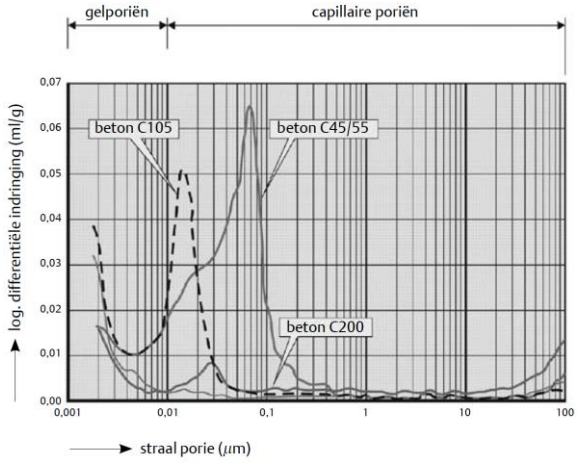

Figure 14 Comparison of pore size distribution – (Walraven, 2006)

3.2.4 UHPC and sustainability

In section 3.2.1 the characteristics of UHPC were discussed which open new possibilities for the designer, such as more slender and durable structures compared to conventional concrete. A more slender and more durable construction implies a reduction of material consumption. However, contrary to this it was discussed in section 3.2.2 that a typical UHPC mixture has a significantly higher cement content than conventional concrete.

This raises the question what results in the most sustainable solution, which is expressed by determining the solution with the lowest CO_2 footprint. If a single cubic metre of concrete is compared the conventional concrete would have a lower CO_2 footprint compared to UHPC. However, a number of benefits of solutions in UHPC over solutions in conventional concrete become apparent only after comparing all aspects a project involves, such as transportation, maintenance, etc.

In (Ng, Voo, & Foster, 2011) a comparison is made between solutions in conventional concrete, UHPC and geopolymer concrete for two structures: a traffic bridge and a retaining wall. Environmental impact calculations were performed from which it was found that the UHPC and geopolymer solutions resulted in lower material consumption, embodied energy, CO_2 emissions and global warming potential. With regard to durability these solutions also scored better than the solution in conventional concrete. It was concluded that UHPC and geopolymer concrete were greener construction materials than the conventional concrete using Portland cement.

3.2.5 Executional aspects

In this section various executional aspects are considered, namely mixing, placing and the related fibre orientation, curing and the application of heat treatment.

Mixing: A description of the mixing procedure can be found in (Fehling, Schmidt, Walraven, Leutbecher, & Fröhlich, 2014): the main prerequisite is sufficient mixing energy to intensively mix all constituents. First the dry materials are premixed. Water and superplasticizer are first mixed separately and subsequently added to the dry premix. The mixing continues until a stable and workable consistency is achieved. The final step is the mixing of fibres until these are properly mixed.

Placement and fibre orientation: With regard to the placement of the material two aspects are of prime importance. The first aspect is that the behaviour of well-designed UHPC mixtures in fresh state is close to that of self-compacting concrete, i.e. the material is flowable and self-compacting. The second aspect is the orientation of the steel fibres in the material. The latter is one of the factors determining the mechanical properties of the hardened concrete.

For optimal fulfilment of their tasks of bridging cracks fibres should be distributed through the whole concrete element. However, during casting operations various effects occur that influence the orientation of the fibres. Influencing factors are the dimensions of the concrete element and the way in which the concrete is casted and in turn the orientation of the fibres affects the behaviour of the material. This means that there is a strong relationship between properties of the UHPC used in design and the execution of the work.

The effects on fibre orientation mainly affect the post-cracking behaviour of the concrete because this is the stage at which the fibres are activated. This stage is therefore prone to more scatter in values compared to the pre-cracking behaviour. The effect on the fibre orientation can be quantified using fibre-orientation factors, which can be determined using tests on representative specimen.

Curing: The curing of concrete is the prevention of water evaporation from the fresh concrete. The curing of UHPC is, as it is for conventional concrete, governed by two parameters. Temperature controls the rate of the hydration process, an increase of temperature results in an acceleration of the process. Moisture is the second criterion. Given the low water/cement ratio the material dries quickly. Additional loss of moisture has to be prevented, measures such as covering or spraying the material can be taken as preventive measures.

The application of heat treatment is often mentioned in relation to UHPC, and because UHPC is often applied in prefab applications such treatments can be implemented in the production process relatively easily. Heat treatment can be applied at different temperatures, for UHPC a common value is 80 – 90 °C at increased moisture content for 48 hours.

Such a procedure is described in (Fehling, Schmidt, Walraven, Leutbecher, & Fröhlich, 2014). The element is left in the mould for 24 hours and covered up after which it is heated at 80 – 90 °C for 48 hours. After the treatment the elements are cooled down slowly. At these higher temperatures the silica fume reacts and additional products of hydration are formed. Benefits of the heat treatment are a denser structure, enhanced mechanical properties, a reduction of the creep and control of the shrinkage (no additional shrinkage occurs after the treatment). No further hydration takes place after the treatment.

3.2.6 Application of UHPC

Types of UHPC

As indicated in 3.2.1 UHPC is not a specific concrete mixture, but rather a group of concretes with certain characteristics in common. Therefore, in literature one may encounter different types or classes of UHPC as well as various names of commercial products. Various types and names will therefore be discussed.

DSP – Densit: The invention of H.H. Bache became known under the name 'Densified Systems containing homogeneously arranged ultrafine Particles' (DSP). This is the first example of UHPC, which has become commercially available under the name 'Densit' in 1983.

Compact Reinforced Composites (CRC): Compact Reinforced Composite (CRC) a combination of fibre-reinforced concrete and a large amount of conventional concrete, which is another invention by Bache from 1986. The fibres increase the tensile strength and controls the cracks around the rebars while the reinforcement improves the ductility of the material. This results in a material with high strength, ductility and durability. However, the material is expensive and generally only applied if it can be used to its full potential, i.e. when high mechanical properties or impact resistance are required.

Reactive Powder Concrete (RPC): Reactive Powder Concrete (RPC) is an invention from 1993 by contractor Bouygues and cement manufacturer Lafarge. This material is a further development based on the concepts found by Bache. The mixture was optimized by leaving out the coarse aggregate, increasing packing density and adding steel fibres. Curing was also optimised, which in practice often involves the application of heat treatment. A commercial name is Ductal, which is the name of the Bouygues-Lafarge product.

Commercial products: Since the first introduction of the concepts of UHPC different parties have embraced these, resulting in further research and development of commercial products. A number of commonly found commercial UHPC products are:

- Densit (nowadays part of ITW)
- Ductal (by LafargeHolcim)
- BSI/Ceracem (by Eiffage)
- BCV (by Vicat)

The list is not exhaustive and for applications one is not limited to these options. For example, in (Hunger & Spiesz, 2016) a practical experiment is described which was carried out to demonstrate the possible to design a UHPC mix using readily available constituents, produce it in a 'normal' concrete plant, transport it by a truck mixer and cast it on site. Without requiring special treatments, constituents or provisions UHPC was produced with excellent properties related to mechanical performance, self-compaction and durability.

Designing in UHPC

Given the properties of and possibilities offered by UHPC, designing using the material differs from designing with normal strength and high strength concrete. In (Van Nalta, 2015), (Hunger & Spiesz, 2016) and (Walraven, 2012), various points of attention are given, these are summarised in this section.

Validity of codes: Standard practice is to design concrete structures following Eurocode 2. However, UHPC structures fall beyond the range of validity of this code because of two reasons. The first reason is the different properties, Eurocode 2 is valid up to strength class C90/105 while the lower limit of the compressive strength of UHPC is generally taken as 150 N/mm^2. The second reason is that UHPC allows for design of slender structures, the slenderness may increase as such that elements do not longer meet the requirements regarding minimum dimensions from Eurocode 2.

In case the design does not fall within the range of validity of Eurocode 2, two options are possible. The first option is the use of additional UHPC specific codes and guidelines. Although generally accepted codes on design in UHPC are lacking, several codes and guidelines on design in UHPC are available or are in preparation. The second option is performing additional research and documentation, this means that in case deviations from Eurocode 2 are made it should be substantiated that this still results in a safe design.

Mixture: UHPC mixtures applied in practice are often commercial products delivered as premixes to the construction site. Working with such a material is not completely transparent: The composition of such UHPC mixtures is not always completely known, as are the properties or the differences with other products. In these cases, one has to rely on the documentation belonging to the product. A related complicating factor is that several available guidelines on UHPC are written for specific commercial products. One should therefore always be aware of what UHPC mixture will be applied.

Durability & long-time behaviour: UHPC allows for the design of slender structures, however, this has implications for multiple factors regarding durability and long-term behaviour. The first aspect is the concrete cover. The dense structure of UHPC suggests that a reduction of the cover compared to conventional concrete might be justified, which is also a requirement for more slender structures. However, durability requirements should still be met.

A second aspect is cracking. Slender structures loaded in bending with relatively large loads compared to the self-weight might result in microcracks that grow over time. A third aspect is the fatigue behaviour. This aspect is generally not expected to be governing for conventional concrete structures. However, it grows in importance given the increase of the variable loads relative to the self-weight of a more slender UHPC structure.

Codes and guidelines on UHPC

Although generally accepted codes on design in UHPC are lacking, several codes and guidelines are already available. Table 5 gives an overview of the codes and guidelines that have been identified in the context of the literature study.

Table 5 Codes and guidelines UHPC

Year	Country	Description
2000	Australia	Design Guidelines for Ductal Prestressed Concrete Beams
2002	France	Ultra-High Performance Fibre-Reinforced Concretes - Interim Recommendations
2006	Japan	JSCE Guidelines for Concrete No. 9 – Recommendations for Design and Construction of Ultra High Strength Fibre Reinforced Concrete Structures (Draft)
2013	France	Ultra-High Performance Fibre-Reinforced Concretes – Recommendations (Revised edition)
2016	Switzerland	SIA 2052 (Ultra-Hochleistungs-Faserbeton (UHFB) – Baustoffe, Bemessung und Ausführung)
2016-2018	France	NF P18-470 (UHPFRC – Specifications, performance, production and conformity), NF P18-710 (Design of concrete structures – Specific rules for UHPFRC) and NF P18-451(Execution of concrete structures – Specific rules for UHPFRC)

At the moment of performing the literature study other codes and guidelines are in preparation. In Germany the DAfStb is working on a guideline, as is an ACI committee in the US. On international level the fib works on a guideline for fibre-reinforced UHPC. In Canada and Spain guidelines are also in preparation.

3.3 Prefab bridges

3.3.1 Choosing for prefab solutions

Introduction to prefab concrete

In bridge construction one can distinguish different types of bridges, e.g. beam or girder bridges, arch bridges, inclined leg bridges and cable suspended bridges, and bridges of different materials, such as concrete, steel, FRP, timber and masonry. Each bridge type and material have their own fields of application. A popular bridge type in the Netherlands are the beam bridges constructed using prefabricated concrete beams.

Prefabricated concrete, or 'prefab', is a term used to denote concrete elements that are not produced on the construction site, i.e. cast in-situ, but on a different location in an industrial way and under controlled conditions. Prefab concrete is widely used because it has several specific advantages of cast in-situ solutions:

- **Quality**: Because of the controlled conditions higher concrete strength classes and lower scatter in the strength value can more easily be achieved compared to in-situ applications;
- **Optimization**: Elements can be designed as such that the material is used in the most optimal way and that the options offered by prefabrication are used to their full potential;
- **Use of moulds**: The reusable moulds used in prefabrication allow for more elaborate finishing involving shapes, texture, tolerances, etc, in a more cost-effective way;
- **Speed of construction**: The speed of the on-site construction work is high because no false or formwork is required on site. The elements only have to be placed into their final position;
- **Logistics and planning**: Because prefabrication is an industrialised process this allows for elaborate quality control and accurate planning and logistics.

Typical fields of application

The typical fields of application of prefab comprises projects with a higher degree of standardization, i.e. projects where larger numbers of the same elements are applied, and projects where the on-site construction time is to be kept as limited as possible. In projects that involves a high repetition factor benefits such as the optimization and the use of the reusable moulds are exploited to their full potential.

On the contrary the aforementioned benefits may also turn into disadvantages. Deviation from standardized elements requires additional effort, depending on the project prefab might be less suitable in such cases. If time constraints do not play a role in the project, then in-situ methods can also be economical.

The prefabrication index is a notion used to express the percentage of the work that is constructed using prefab concrete. In practice projects are almost always a combination of prefab and in-situ work because this combination minimizes costs (optimal prefabrication index). In such applications larger elements are typically prefabricated and subsequently joined together on site using in-situ concrete. Another option is to prefabricate elements at the construction site.

Prefab versus in-situ solutions

The decision to choose for prefab or in-situ solutions depends on a project-to-project basis. Criteria that may be of interest are the costs, quality, speed of construction and logistical aspects. The majority of the bridges in the Dutch infrastructure are built using precast elements because such projects are characterized

by modest spans and a demand for high speed of construction, good quality and working conditions and a minimization of costs and disturbance.

3.3.2 Design considerations for prefab bridges

Common prefab solutions in the Netherlands

In the Netherlands there are three types of prefab beam bridges that are commonly applied: the solid deck bridges (using solid slab beams or infill beams), inverted T-beam bridges and box beam bridges. All these solutions make use of prestressed beams. Each of these has their own field of application.

Solid deck bridges (infill beams): Figure 15 gives a cross section of a deck using infill beams. Using these beams a solid deck is created. After the prestressed beams are placed transverse reinforcement is placed after which in-situ concrete is cased in between and on top of the beams. This type of beams is suitable for spans from 6 – 20 m and the slenderness of the system is 20 – 25.

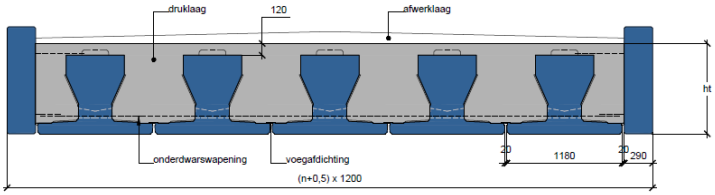

Figure 15 Cross section of prefab deck using infill beams – Spanbeton

A similar approach is applied using solid slab beams, although these can only be applied for spans of 4 – 8 m given the higher ratio of in-situ concrete versus prefabricated concrete.

Inverted T-beam bridges: T-beams offer a solution for larger spans where the construction height is not a stringent criterion. Figure 16 gives a cross section of the deck. After the prestressed beams are positioned in place in-situ reinforcement is placed for the end cross beams, which are subsequently casted. This provides the deck with the required torsional capacity (which is hardly provided by the beams) and to confine the beams in transverse direction. Subsequently reinforcement is placed and the in-situ layer is casted, which functions as a continuous slab in transverse direction.

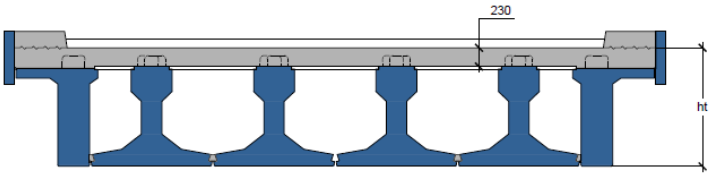

Figure 16 Cross section of prefab deck using inverted T-beams – Spanbeton

Inverted T-beams are commonly applied for decks with spans of 20 – 60 m, often in combination with edge beams to increase the resistance against collisions and for aesthetics. The slenderness is 20 – 28.

Box beam bridges: Figure 17 gives a cross section of a box beam bridge. Such a deck is formed by placing prestressed box beams, after which the longitudinal joints are filled and the deck is prestressed in transverse direction to obtain a solid deck. The use of edge beams is optional. This type of deck allows for higher slenderness and has a high prefabrication index, no in-situ layer is required. As a result, almost the full capacity can be used to carry imposed variable loads.

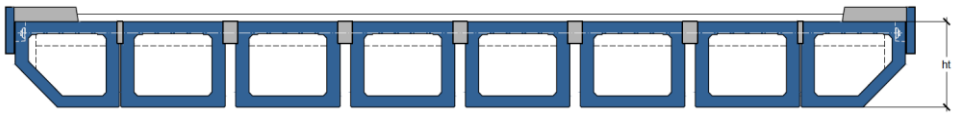

Figure 17 Cross section of prefab deck using box beams – Spanbeton

Box beams are applied for the larger spans in the range of 15 – 69 m. The slenderness is 28 – 32, which is why these beams are also suitable for situations where the height is the stringent criterion which would make inverted T-beams unsuitable. Given the high prefabrication index, the application of box beams also results in reduced construction time. In addition, box beams have high torsional stiffness, which means that cross beams are not required. The current world record of longest prefab beams is claimed by Haitsma. The firm produced 69 m long box beams with a weight of 259 tons for a project in Wanssum. The beams were placed on site in June 2020.

Overview: Although other beam types are also available and while the development of prefab products is an ongoing process, the aforementioned beams are the most commonly applied prefab solutions in the Netherlands. The following table gives an overview of typical slenderness and span for each type.

Table 6 Slenderness and span for common prefab beam types

Type of beam	**Slenderness**	**Span**
[-]	$[l/h]$	[m]
Solid deck – Solid slab with in-situ layer	20 – 25	4 – 8
Solid deck – Infill beams	20 – 25	6 – 20
Inverted T-beam	20 – 28	15 – 60
Box beam	28 – 32	15 – 69

Design considerations

For the design of prefab bridge decks the same design procedure should be followed as for any other concrete bridge type. However, in case prefabricated elements are applied several aspects require specific attention:

- **Temporary situations**: Prefab beams are subjected to several temporary situations in between the manufacturing and final use phase, e.g. manufacturing of the elements, storage, transportation, erection, etc. In each phase the forces on the beam may be different, this has to be considered;

- **Force transfer**: Prefab structures are composed of several separate prefabricated elements, often using in-situ concrete. Therefore, the force transfer between the prefab elements and in-situ concrete at interfaces for example requires specific attention;

- **Optimization**: An important aspect in practice is optimisation. By optimising the cross-section material is saved, the weight is reduced and the slenderness is increased. Although this is beneficial in all cases, it is especially important for prefabrication, because projects most suitable for prefabrication involve larger numbers of similar elements and involve storage, transportation and placement of the beams.

These three points are inherent to the application of prefabricated concrete. By paying attention to these points the benefits of prefabrication can be exploited to their full potential.

3.3.3 Applications UHPC in infrastructure

Application in the Netherlands

The first application of UHPC in the infrastructure in the Netherlands was the retrofitting of the Kaagbrug (2002). The timber deck plates of the bridge were replaced by 45 mm thick UHPC panels made of Compacted Reinforced Composite (CRC), see Figure 18.

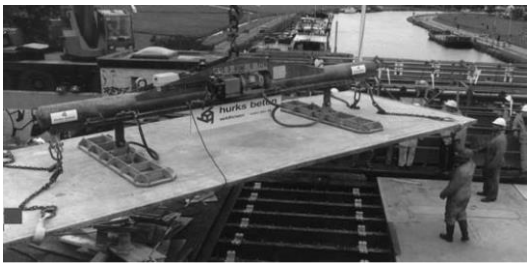

Figure 18 Replacing deck panels Kaagbrug – (Fehling, Schmidt, Walraven, Leutbecher, & Fröhlich, 2014), p.149

Since the introduction of UHPC in the Dutch infrastructural sector a limited number of smaller new bridges has been built using this material. Examples where UHPC has been used are the Brug Zwaaikom in Eindhoven (2015) and the Catharinabrug in Leiden (2016).

Applications world wide

The first worldwide application of UHPC in bridge construction was in 1997, for a pedestrian and bicycle bridge in Sherbrooke in Quebec province, Canada. The bridge was designed as a space truss, see Figure 19, with a top chord made of UHPC that serves as the deck, the lower chord constructed using two continuous prestressed UHPC girders and diagonals that consist of UHPC encased in hollow steel sections.

Figure 19 Sherbrooke pedestrian bridge

Since this first application, UHPC has been applied in different forms in many projects. Extensive lists with examples of infrastructural applications of UHPC can be found in (Russell & Graybeal, 2013) and (Fehling, Schmidt, Walraven, Leutbecher, & Fröhlich, 2014). From the examples in these references the general trend can be observed that UHPC lends itself for the following types of applications in the infrastructure:

- **Prefabricated beams**: Such beams are often prefabricated pretensioned beams with various types of cross sections (e.g. -shaped, I-shaped, T-shaped, Pi-shaped or box-type);

- **Prefabricated bridge segments**: Use of prefabricated UHPC segments that are post-tensioned on site or coupled using external prestressing allows for the construction of larger prefab structures beyond transportation limits. Various cross sections are used such as trough-type or U-shape sections;

- **In-situ joints**: Other examples are the in-situ transverse or longitudinal joints between prefabricated UHPC elements;

- **Strengthening or retrofitting**: A layer of UHPC can be added to an existing bridge deck as an overlay or new surface layer, to function as a protective layer and/or strengthening measure of the deck.

This list is not exhaustive, UHPC offers possibilities for other bridge types or applications as well. Hybrid structures are also possible, where UHPC is applied at the most exposed or most severely loaded or stressed parts of the deck while conventional concrete is used for the remainder of the structure.

4

POTENTIAL TO GENERALISATION

4.1 Generalisation of results

4.1.1 Determining potential to generalisation

In the introductory chapter of the report the Twentekanaal was introduced as the topic of the project, which comprises a large number of bridges. It was referred to in section 3.1.1 that as part of the construction of the Twentekanaal a series of bridges was built, this suggests that multiple bridges will have been constructed during the same period. In addition, one of the characteristics of canals are their set dimensions, which implies that the span and width of various bridges might very similar. As an example, Figure 20 for shows the Sint Annabrug near Delden, it can be seen that the bridge has strong similarities to the Eefdesebrug.

Figure 20 Sint Annabrug near Delden – Courtesy to R. Bril

For the elaboration of the redesign, one representative bridge was selected as a test case: The Eefdesebrug. In this chapter an analysis will be performed to investigate the potential to generalise the results of the Eefdesebrug onto the other bridges across the canal. This way it can be judged which of the bridges across the canal are of relevance to the project and the full potential of the project can thus be determined.

4.1.2 Approach of the analysis

To determine to what extent the results of the redesign of the Eefdesebrug could potentially be generalised the following approach is followed:

- **Identification of the bridges**: As a first step all bridges crossing the canal are identified, listed and categorised to set up an inventory;
- **Characterisation of the bridges**: The inventorying of the bridges is completed by further characterising all identified bridges;
- **Analysis**: By means of their characteristics the bridges are compared to determine which are relevant to the project and thus to which structures the results of the redesign of the Eefdesebrug could possibly be generalised to.

To achieve more accurate results and to draw more reliable conclusions archive material (design drawings and other documents) provided by Rijkswaterstaat has been used which was delivered along with material

regarding the Eefdesebrug. Although the information is not complete, it will provide the most reliable results. This information was supplemented by information from other publicly available sources wherever relevant or required.

4.2 Inventorying of the bridges

4.2.1 Identifying bridges

History of the bridges

The current situation regarding the number of bridges is different from the situation when the canal was dug. According to (Rijkswaterstaat, 2014) originally a total of twenty-nine bridges were originally built. Damage was done during the second world war and according to the same source all bridges across the canal were destroyed in 1945. After the war bridges were rebuilt, a large number of these following their original design. Through the decades new bridges were constructed (e.g. for the construction of highways in the 1970s) or bridges were replaced (e.g. the railroad bridge at Zutphen or Vredesbrug near Enter).

Identifying the bridges

As a starting point for the bridge inventory all bridges crossing the canal will be identified. Note that for the inventory a lock including one or more bridges or multiple bridges crossing the canal at the same location are for now denoted as a single 'bridge'. Tables have been prepared listing the different bridges and providing general information by using sources such as a list from (Wikipedia, 2020), (Rijkswaterstaat, 2014), (Rijkswaterstaat, 2020) and Maps. The following general information is provided for each bridge:

- **Numbering** – All bridges have been numbered corresponding to their location from west (start of the canal) to east (end of the canal);
- **Location** – The position of the bridge is given measured from the start of the canal at the IJssel river;
- **Name** – If given the name of the bridge was included. If no name was identified a descriptive name was used;
- **Road/railroad** – Distinction is made between roads and railroads. Distinction is also made between road bridges in highways ('A-roads'), provincial roads ('N-roads') or roads for local traffic;
- **Road section** – Additionally the bridges for road traffic are further classified by denoting the start and endpoint of the road crossing the bridge;
- **Bridge type** – A classification between bridge types is introduced by distinguishing girder bridges (concrete or steel), truss bridges (steel), arch bridges (concrete or steel), locks and a remaining category.

Reference is made to annex IV for the overview of all bridges.

Current situation

Following the aforementioned approach, a total of 37 bridges or bridges part of larger engineering structures (lock or multiple bridges) crossing the Twentekanaal has been identified. Figure 21 gives an overview of the location of the different bridges. Note that this figure, which is published in 2014b is partially dated, but it suffices for providing an overview of the situation.

Figure 21 Bridges across the Twentekanaal – (Rijkswaterstaat, 2014), p.30

4.2.2 Characterising bridges

After identifying the bridges and providing basic information, the bridges were characterised using the available sources. This information is required for the subsequent analysis. Within limits of what can be found in the available sources, the main points of the characterisation are:

- **Coordinates**: Coordinates are provided for referencing using maps;
- **Span and width**: Preferably the span and width are determined or estimated based on original design drawings. If these are not available, the dimensions are determined or estimated using other sources;
- **Year of construction**: The year of construction is preferably determined based on original design documents. If no such sources are available, an estimation is made based on other sources or, if nothing is known, a comparison is made with similar bridges that have been identified;
- **Pictures and general information**: Pictures are added to provide an overview of the overall structure and deck layout. In addition, general information about the bridge is added, obtained from local news for example;
- **Additional information**: If available additional information based on design documents were added to supplement the aforementioned information.

Using these points, the bridge inventory is further elaborated on. Reference is made to annex IV for the descriptions of all bridges as well as a summarizing table.

4.3 Analysis and conclusions

4.3.1 Analysis of bridges in inventory

Approach

With the characterisation of all bridges as complete as possible, the collected information is analysed to determine which bridges are relevant to the project. This indicates to what extent the solutions for the redesign of the Eefdesebrug could be generalised and thus gives the full extent of the potential of the project. This analysis is performed in three steps during which the characteristics of the different bridges are compared based on the bridge category, year of construction and dimensions. Those with characteristics similar to the characteristics of the Eefdesebrug will remain in the inventory while those with larger differences will be left out.

Analysis – Bridge category

The first step in the analysis is the classification of the bridges according to a number of categories. A distinction is made between bridges for highway traffic, bridges for provincial or local traffic, railroad bridges, bridges part of a lock and a remaining category. Figure 22 presents the results of this comparison.

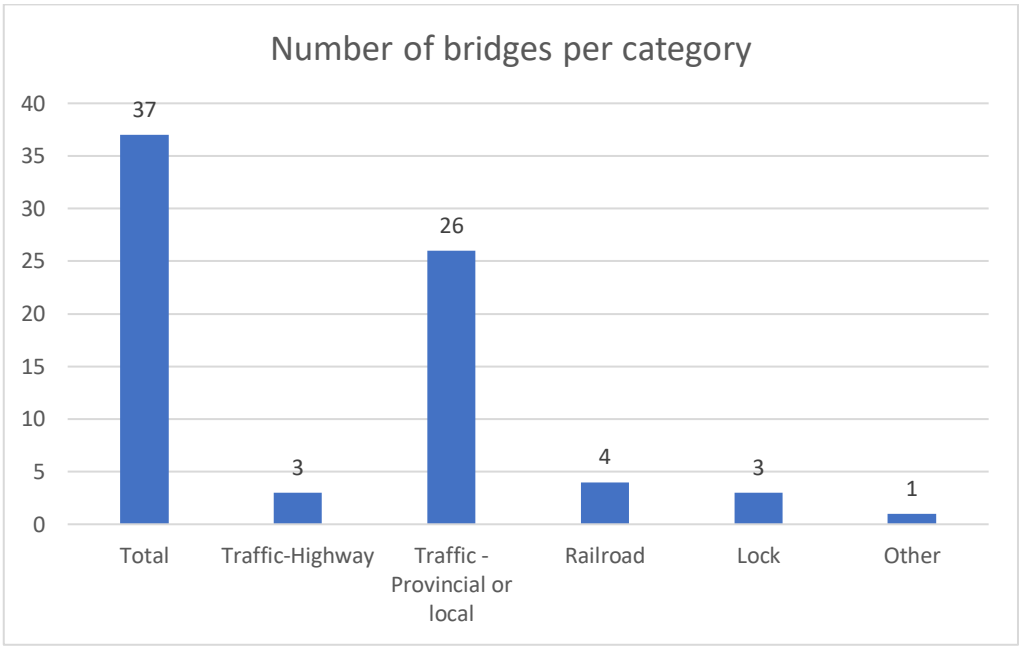

Figure 22 Bridges per category

Of these bridges only the bridges for provincial or local traffic (26 of the 37 bridges) will be included in the remainder of the analysis, which is the category which also includes the Eefdesebrug. The bridges within the other categories are excluded for the following reasons:

- **Bridges highway traffic**: The identified bridges for highway traffic typically have larger dimensions and are typically subjected to a larger total load and number of vehicles compared to bridges for provincial or local traffic.

- **Railroad bridges**: The characteristics of railroad traffic are different than those of road traffic, e.g. higher variable loads on fixed locations, high demand for stiffness because of the sensitivity of railroad tracks to deformations and dynamic effects. This has implications for design and therefore a solution for a road traffic bridge should not automatically be assumed to provide a solution for railroad bridges as well.

- **Locks**: Bridges near or part of a lock are excluded because these are regarded as a part of the lock infrastructure, which might impose additional boundary conditions to the design.

- **Other**: The final category contains a cable stayed pedestrian bridge. Design procedures for cable stayed bridges and pedestrian bridges require a different approach than arch or beam bridges for road traffic. Therefore, this bridge is excluded.

Analysis – Year of construction

The next phase in the analysis is to compare the year of construction of the remaining 26 bridges to determine which bridges are potential candidates for replacement or redesign in the nearer future. Figure 23 gives an overview of the year of construction of the remaining bridges. The horizontal axis gives the numbering of the bridges as introduced for inventorying purposes while the vertical axis denotes the year of construction.

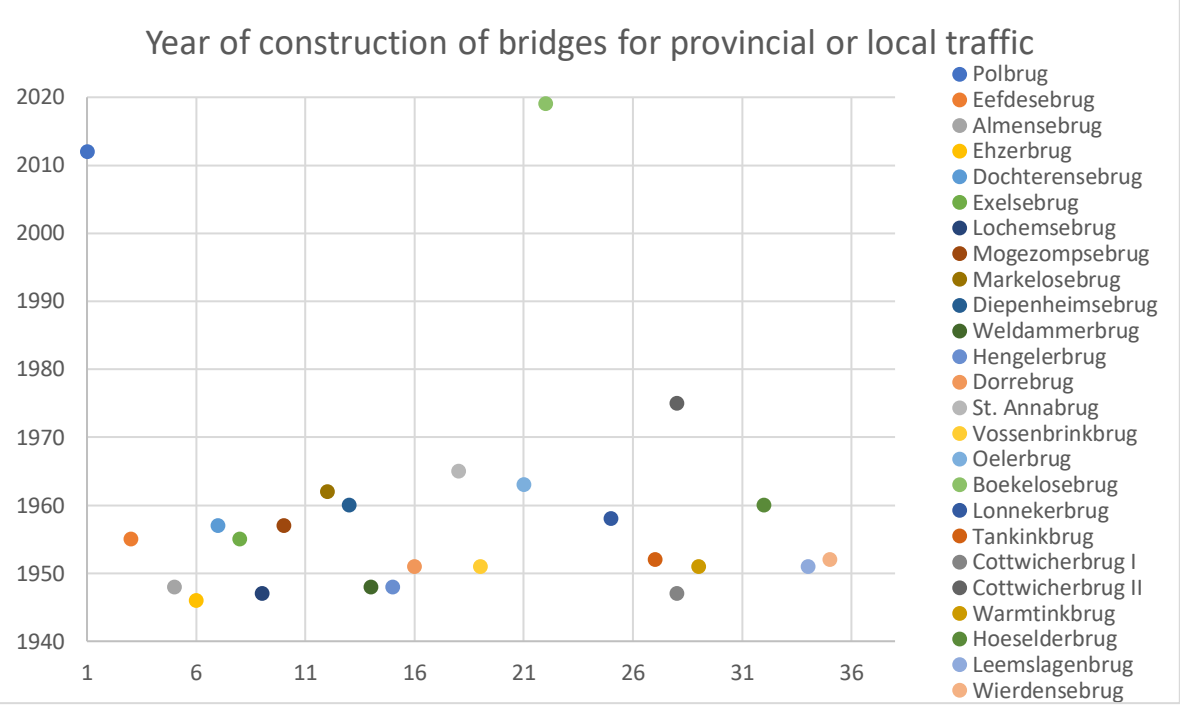

Figure 23 Year of construction of bridges for provincial or local traffic

Note that only 24 of the 26 bridges that have been categorised as bridges for provincial or local traffic are represented in the graph. Because of uncertainty in the year of construction certain bridges have been left out from the figure while others are represented by an estimated value:

- The year of construction of the Grensbrug is unknown but estimated to be built ≤ 1950s. Given the large uncertainty it is left out from the graph;

- According to (Rijkswaterstaat, 2014), the Vredesbrug is constructed in the 1960s or 1970s, replacing an older bridge with the same name. Because specific information is lacking the bridge is left out from the graph;

- The year of construction of the Sint Annabrug is also unknown, but given its similarities with other bridges (Eefdesebrug and Exelsebrug for example), it is estimated to be constructed in the same period with 1965 as upper limit. This year is therefore given in the graph.

- The Cottwicherbrug is plotted twice because it has two decks from 1947 and 1975, respectively.

Figure 23 and the two bridges not given in the figure indicate that a rough distinction can be made between bridges from before and after 1970. The older group comprises mostly bridges built as replacements of those destroyed during the second world war or their temporary replacements. Bridges constructed after 1970 are either parts of new projects (e.g. the Polbrug as part of the new provincial road) or replacements of the pre-1970 bridges.

The bridges of constructed pre 1970 are included in the remainder of the analysis while the other bridges are excluded. The older category comprises bridges of roughly the same generation, these will be the first candidates for replacement or redesign in the nearer future. The Polbrug (2012), Boekelosebrug (2019) and the newer span of the Cottwicherbrug (1975) are therefore excluded. The number of bridges is thus reduced from 26 to 23.

Analysis – Dimensions

In a number of steps, the remaining bridges are compared based on their dimensions, which will implicitly take differences in loads on the bridges into account as well.

Distinction larger and smaller bridges: First the bridges are grouped into two categories, one for larger bridges for provincial/local traffic and one for the smaller bridges. This distinction is based on the number of traffic lanes, the smaller bridges having one lane and the larger bridges having two. Figure 24 gives the results, note that larger bridges can be subdivided in those of concrete and those of steel.

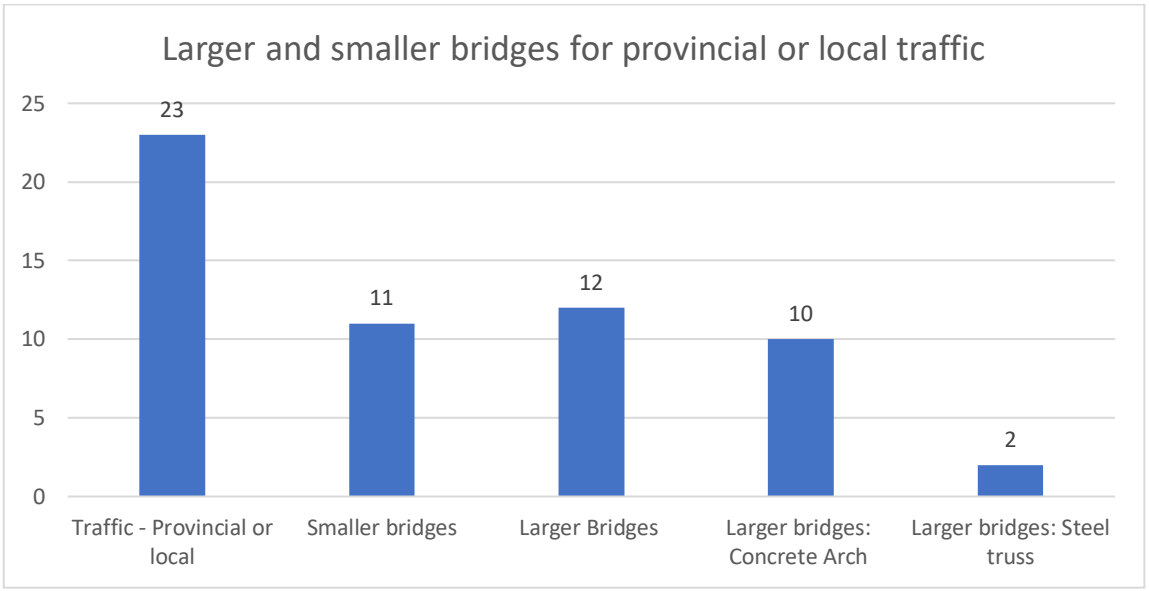

Figure 24 Larger and smaller bridges for local traffic

Making a distinction between larger and smaller bridges is implicitly related to the type of traffic that may be expected to cross the bridges. From these remaining 23 bridges in the inventory the general impression is obtained that the smaller bridges are lighter steel structures, constructed at the locations where only local traffic and agricultural machinery were expected. At the locations where more traffic was expected, larger bridges were built. This is confirmed by (Rijkswaterstaat, 2014), in which it is mentioned that there are large similarities between the bridges and that the concrete arch and truss bridges are applied for crossings of larger roads while local roads cross the canal using smaller steel bridges. The Eefdesebrug is one of these larger bridges.

Because the already slender and light steel decks of the smaller bridges are supported by a lighter sub structure, it is not expected that solutions for the larger deck of the Eefdesebrug can be applied to the smaller existing bridges. Hence these smaller bridges are excluded from the remainder of the analysis and from the 23 bridges 12 larger bridges remain. These remaining bridges are all expected to be loaded by approximately the same category of traffic, which corresponds to (busy) local traffic and agricultural machinery or traffic corresponding to provincial roads.

Span and width: Subsequently a more quantitative comparison is made between the 12 remaining bridges by comparing their dimensions, i.e. spans and width. Figure 25 gives an overview of the spans of the remaining bridges. The horizontal axis denotes the bridge number, the vertical axis denotes the span.

From the comparison of the spans, it can be seen that the Eefdesebrug has the largest span of the remaining set of bridges. This implies that in terms of span the Eefdesebrug can be regarded as an upper limit in terms of the feasibility of designing a UHPC beam deck with a larger span. If the span of the Eefdesebrug is not a limiting factor to obtain a solution, then based on the span as the only criterion this solution will be applicable to other bridges as well.

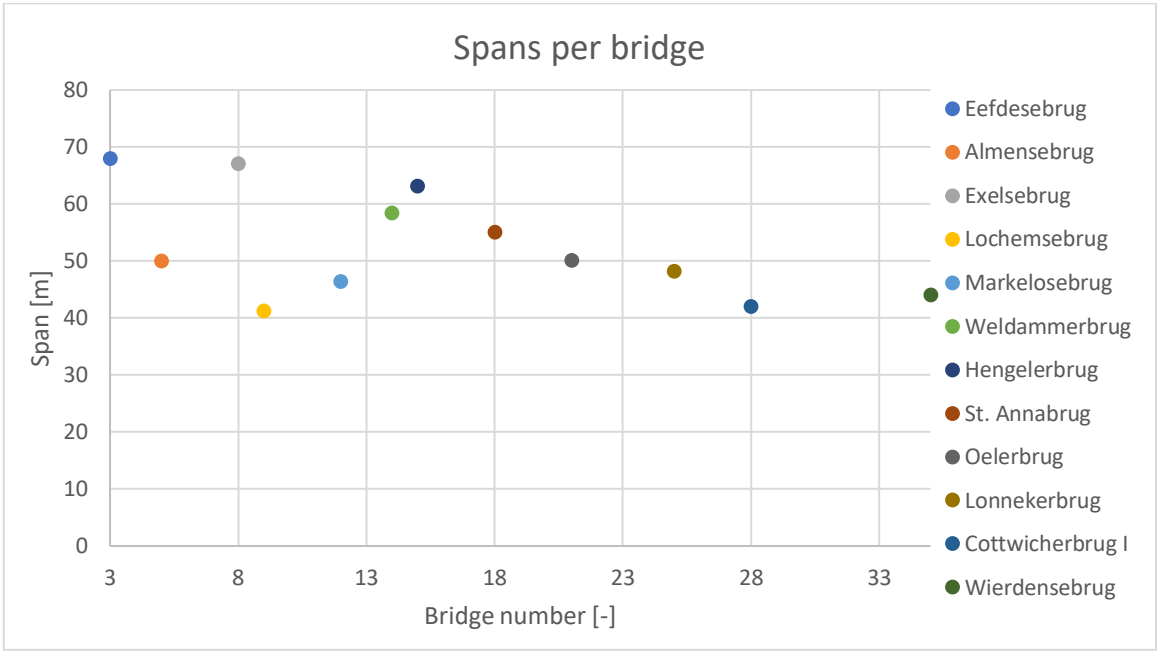

Figure 25 Span comparison of the remaining bridges

Figure 26 gives the width of the remaining bridges. Based on the width there are roughly two groups of bridges. The first group has a width in the range of approximately 10 – 12 m, these bridges were reconstructed at the end of the 1940s following their original design, which is similar to that as presented in Figure 5. The other bridges are wider and are constructed in the 1950s or 1960s, following different designs.

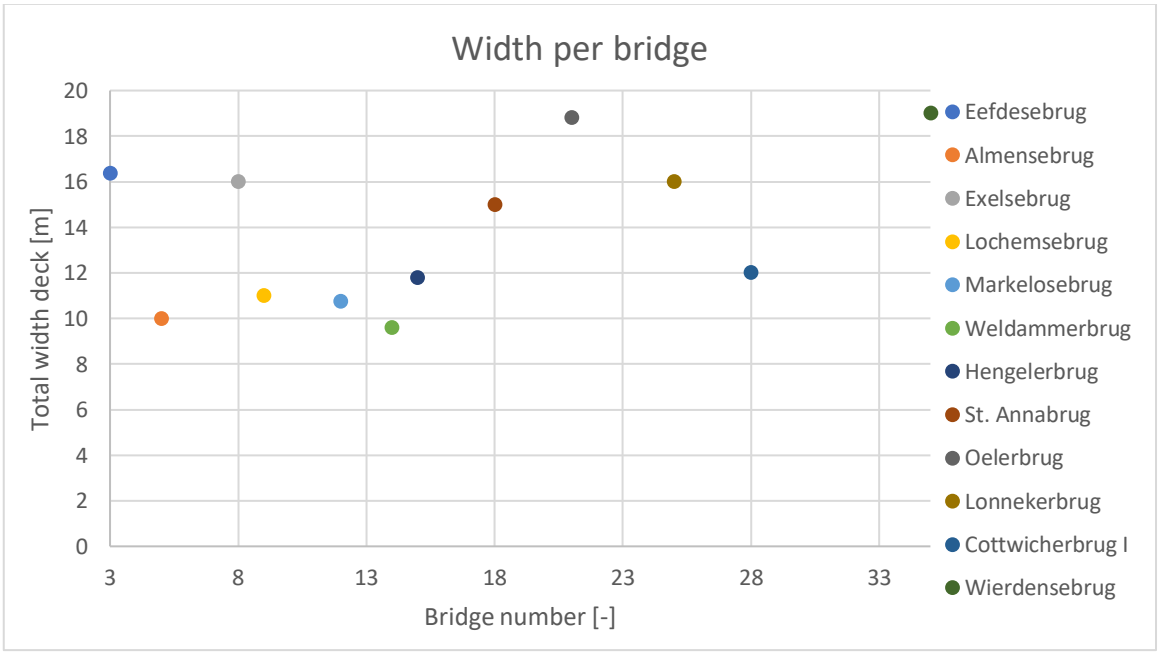

Figure 26 Width comparison of the remaining bridges

It can be observed that the Eefdesebrug does not have the largest width, but this does not have to be a limiting factor to the optimisation potential. All remaining bridges roughly follow the same deck layout with a two-lane carriageway in the middle and separate lanes for pedestrians or cyclists at the outer sides. Loads for the main carriageway are higher than those for the pedestrian lanes. If beams can be designed that are suitable for the main carriageway, additional beams can be added or left out for each individual bridge to obtain the desired width. In addition, the redesign will no longer include an arch, resulting in more efficient use of the area of the deck. Hence it is concluded that a solution for the Eefdesebrug can be generalised to bridges with both smaller and wider decks.

Remark – Substructure

A final point to consider is the substructure of the bridges. Although not included in the scope of the project it is still the case that the designed concrete deck has to be supported. In practice capping beams are often applied to support prefab beams. Because the design of the substructures of the remaining bridges are different, the construction of such a supporting element is a point of attention.

Although the actual weight of a new UHPC deck might not be a problem for these bridges, some of the bridges might require more modifications to their substructure than others to enable the placement of a new prefab UHPC deck. This is not a reason to exclude some of the remaining bridges but it is a point that one should be aware of, which is why this remark has nonetheless been made in this section.

A final remark related to the substructure is that two of the remaining twelve bridges are steel truss bridges while the others are concrete arch bridges. Typically speaking a steel deck is lighter than a concrete deck with equal capacity. Replacing a steel deck with a concrete deck might not be possible in all cases because of insufficient capacity of the foundation. However, from the inventory it is concluded that originally these bridges were constructed as concrete arch bridges following a similar design as other bridges on the list. After the bridges were damaged during the second world war these were replaced by truss bridges, but these were constructed on the original foundations of the arch bridges. This suggests that replacing a steel deck by a concrete deck might still be plausible for these two bridges.

4.3.2 Conclusions

A total of 37 bridges or bridges part of larger engineering structures (lock or multiple bridges) crossing the Twentekanaal has been identified. An inventory was set up in which the characteristics of these bridges were described. Subsequently an analysis was performed in which the bridges in the inventory were based on three characteristics: bridge category, year of construction and their dimensions. The latter implicitly accounted for traffic loads as well.

By following this procedure, the total of 37 bridges was reduced to 12 bridges that have comparable characteristics to those of the Eefdesebrug and are therefore relevant for the project. Given these characteristics it is concluded that there is the potential to generalise the solution for the redesign of the Eefdesebrug to this group of 12 bridges. Table 7 summarizes the names of the bridges along with basic information.

Table 7 Basic information bridges Twentekanaal relevant to the project

Nr.	km	Bridge name	Road	Section from-to	Bridge type	Year
3	2,05	Eefdesebrug	Local road	Zutphen-Eefde	Arch bridge (concrete)	1955
5	7,43	Almensebrug	N826	Zutphen-Laren	Arch bridge (concrete)	1948
8	14,38	Exelsebrug	N346	Zutphen-Hengelo	Arch bridge (concrete)	1955
9	16,23	Lochemsebrug	N346	Zutphen-Hengelo	Truss Bridge	1947
12	23,71	Markelosebrug	N754	Markelo-Stokkum	Truss Bridge	1962
14	29,04	Weldammerbrug	Local traffic	Goor-Diepenheim	Arch bridge (concrete)	1948
15	30,71	Hengelerbrug	N346	Zutphen-Hengelo	Arch bridge (concrete)	1948
18	37,88	St. Annabrug	N740	Delden-Markvelde	Arch bridge (concrete)	1965
21	42,57	Oelerbrug	Local traffic	Hengelo-Haaksbergen	Arch bridge (concrete)	1963
25	48,21	Lonnekerbrug	Local traffic	UT-Havengebied	Arch bridge (concrete)	1958
28	1,46	Cottwicherbrug I	N346	Zutphen-Hengelo	Arch bridge (concrete)	1947
35	13,28	Wierdensebrug	Local traffic	Almelo-Wierden	Arch bridge (concrete)	1950

Key points with regard to the elaboration of the project and obtaining more certainty with regard to generalising the solutions of one representative bridge (the Eefdesebrug) to the total of twelve relevant bridges are:

- **Dimensions of the bridges**: In terms of span the Eefdesebrug is regarded as an upper limit of the remaining bridges, therefore it is expected that if it is feasible to find a solution for the Eefdesebrug, it will also be possible to obtain a solution for the bridges with smaller spans;

- **Variable loads**: The remaining bridges are expected to be loaded by approximately the same category of traffic. Taking the upper limit by designing for traffic loads corresponding to provincial roads will improve the reliability of the solution if this is to be generalised to all bridges of the group. This is especially important for the number of vehicles for fatigue verifications. If a solution for the Eefdesebrug can be designed under these loads, it is expected to hold for all twelve bridges;

- **Substructure**: Although excluded from the project scope awareness is required regarding the fact that a new prefab deck has to be supported. Given the weight of the decks of the existing bridges there is a large potential for reusing the existing foundation and, depending on the solution, (a part of) the substructure. However, certain bridges might require more effort to modify their substructure as such that a new prefab deck can be placed.

Figure 27 gives an overview of the remaining twelve bridges relevant to the project.

Eefdesebrug

Almensebrug

Exelsebrug

Lochemsebrug

Markelosebrug

Weldammerbrug

Hengelerbrug

Sint Annabrug

Oelerbrug

Lonnekerbrug

Cottwicherbrug I

Wierdensebrug

Figure 27 Overview bridges Twentekanaal relevant to the project

5

CODES AND DESIGN VERIFICATIONS

5.1 Codes and guidelines

5.1.1 General design codes

Introduction

In this section the general codes and guidelines that can be used for the elaboration of the redesign are listed. In the subsequent section, guidelines on design in UHPC are covered and the most appropriate code is selected to be used in further elaboration of the project. Note that the codes and guidelines mentioned in this chapter hold for the total project. Not all documents are used during the same design stages.

General codes and guidelines – Eurocode

For the redesign of the Eefdesebrug the following codes are consulted:

- Basis of structural design (Eurocode 0): NEN-EN 1990
- Actions on structures (Eurocode 1): NEN-EN 1991-series
- Design of concrete structures (Eurocode 2): NEN-EN 1992-1-1 and NEN-EN 1992-2

The mentioned documents are the Dutch translations of the Eurocode and these are applied in combination with the Dutch national annexes.

General codes and guidelines – Guidelines Rijkswaterstaat

In addition to the Eurocode, two guidelines from Rijkswaterstaat may be of relevance:

- Richtlijnen Ontwerp Kunstwerken ROK 1.4
- Richtlijnen Beoordeling Kunstwerken RBK 1.1

If these documents are applied, then this will be explicitly mentioned in the relevant sections.

5.1.2 Guideline UHPC

Identified codes and guidelines on design UHPC

Table 5 in section 3.2.6 gave an overview of the currently available guidelines on UHPC that have been identified in the literature study. From the different documents in the table, the following were acquired:

- Design guidelines for Ductal Prestressed concrete Beams (2000)
- AFGC-SETRA 2002 interim recommendations (2002)
- AFGC-SETRA 2013 recommendations (2013)
- SIA 2052 (2016)
- NF P18-710 (2016)

One of these guidelines will be selected to be applied in the elaboration during the design phase of the project. To make a substantiated comparison and selection, in addition to the content of the guidelines, one should be aware of the following points:

- **Developments**: Given the rapid developments within the field of UHPC more recent guidelines are expected to be more comprehensive and up-to-date compared to the older guidelines;

- **Completeness**: A single code or guideline is typically part of a larger framework. The selected guideline is preferably applicable within the framework of the Dutch versions of the Eurocodes and if additional information is required, this should be available.

Comparing the guidelines

Table 5 and the list of guidelines that have been acquired indicate that two 'generations' of UHPC guidelines can be distinguished. The first set of guidelines dates from the early 2000s. These documents commonly make use of the same sources and are the first attempt to provide guidance on the application of UHPC in structural design.

The second 'generation' of guidelines is more comprehensive compared to the first generation and is founded on more experience and research. From the AFGC-SETRA 2013 guideline it can be seen that the experience from the use of UHPC in practice since the publication of the interim guideline in 2002 as well as the results on ongoing research are included in the document. In addition, this guideline is written as such that it can be used within the framework of the Eurocode, the layout of the part of the guideline relevant for design follows the layout of Eurocode 2-1-1 and Eurocode 2-2.

In 2016 and 2018 a total of three French codes have been published which are another step up in the standardization effort of UHPC. In (Toutlemonde, et al., 2017) the relation between these codes and the AFGC-SETRA 2013 recommendations are clarified. The NF P18-470 is a separate code which follows the French version of the EN 206 and gives the material requirements that UHPC has to comply to. The aforementioned NF P18-710 is a national complement to Eurocode 2-1-1 and Eurocode 2-2 and focuses on the design of UHPC with metallic fibres. The NF P18-451 complements the standard for execution of concrete structures with provisions for the execution of UHPC structures.

In the article it is mentioned that these three codes are based on the AFGC-SETRA 2013 recommendations. However, provisions have been clarified further or complemented to further stimulate the application of the UHPC in practice. The added value of the new set of codes compared to the guideline is in particular their formal status and the fact that the codes fit within the French system of codes, which is in turn derived from the European system. In the article the expectation is expressed that by publishing standards for product, design and execution will turn out to be a milestone to widen the use of UHPC.

The Swiss SIA 2052 code fits within the framework of SIA standards. Given the contents of the code which involves general principles, mechanical properties, structural analysis and execution of UHPC structures as well as the description of tests or references to other codes to determine these, the code is expected to fulfil a similar role as the aforementioned set of French codes.

Selecting a guideline

The 'second generation' of guidelines is more comprehensive and up-to-date compared to the 'first generation', which is why one of the more recent documents will be applied. The set of French codes (P18-470, P18-710 and P18-451) are comprehensive and applicable directly in combination with Eurocode 2. However, of this set of codes only the P18-710 is acquired. Given the references made to the P18-470 for determining parameters, the P18-710 is not deemed useable as a standalone document and thus will not be applied.

The French version of the SIA 2052 was also acquired, but in comparison with the AFGC-SETRA 2013 this code was found to be less comprehensive and will therefore not be used for design either. The remaining option is the AFGC-SETRA 2013 guideline. This is deemed to be a good option because this document formed the basis for further standardization and contains experience and research results that have been obtained since the first introduction of the interim guideline in 2002.

Conclusion

The AFGC-SETRA 2013 guideline will be used for the elaboration of the design. Although this is not the most recent document it is deemed to be comprehensive and up to date compared to the interim guideline from 2002 given the experience and research results that have been included. In addition, the use of this guideline

provides all required information because it can be used directly in combination with Eurocode 2 without requiring additional codes or guidelines.

All codes and guidelines required for the design have now been collected. In the remaining paragraphs of this chapter material parameters and constitutive laws of the different materials applied in the design will be covered: conventional concrete, prestressing steel and UHPC will be discussed. Subsequently the calculation procedures for various verifications of UHPC elements in the ultimate limit state will be covered. The basis for determining the parameters and verifications are the aforementioned codes and guidelines. Use will be made of other sources from literature wherever relevant and this will be clearly indicated.

5.2 Material parameters and constitutive laws conventional concrete

5.2.1 Conventional concrete – Eurocode 2

Definitions

The properties of concrete are discussed in 3.1 of Eurocode 2-1-1. Concrete is characterised by its compressive strength using the following notation: CX/Y. In this notation 'X' denotes the characteristic value of the cylindric compressive strength and 'Y' denotes the characteristic value of the cube compressive strength. The Eurocode 2 is applicable for strength classes C12/15 up to and including C90/105.

Compressive strength

The compressive strength of concrete is determined by means of compression tests on specimen stored under controlled conditions, from test results the characteristic strength is deduced. According to Eurocode 2-1-1, the mean value of the cylinder compressive strength is related to the characteristic value through the following relationship:

$$f_{cm} = f_{ck} + 8 \text{ [N/mm}^2\text{]} \qquad \text{Equation (1)}$$

The design value of the compressive strength is calculated from the characteristic strength using the following equation:

$$f_{cd} = \frac{\alpha_{cc} * f_{ck}}{\gamma_c} \qquad \text{Equation (2)}$$

The factor α_{cc} accounts for long-term effects on the compressive strength and unfavourable effects caused by the way in which loads are applied. According to the national annex the factor $\alpha_{cc} = 1{,}0$.

Tensile strength

The mean axial tensile strength of the material for strength classes up to and including C50/60 can directly be calculated from the characteristic compressive strength using the following relationship:

$$f_{ctm} = 0{,}30 * f_{ck}^{\left(\frac{2}{3}\right)} \qquad \text{Equation (3)}$$

For high strength concrete, i.e. strength classes from C50/60 up to and including C90/105, a different relation is to be used:

$$f_{ctm} = 2{,}12 * \ln\left(1 + \frac{f_{cm}}{10}\right) \qquad \text{Equation (4)}$$

The lower bound value of the tensile strength, the 5% fractile, can subsequently be calculated from the mean value of the axial tensile strength using the following relationship:

$$f_{ctk,0,05} = 0{,}7 * f_{ctm} \qquad \text{Equation (5)}$$

Using this lower bound value, the design value of the tensile strength is calculated as follows:

$$f_{ctd} = \frac{\alpha_{ct} * f_{ctk,0,05}}{\gamma_c}$$ Equation (6)

In a similar way as α_{cc} for compression, the factor α_{ct} accounts for long-term effects on the tensile strength and unfavourable loading. Conforming the national annex, the value for α_{ct} should be taken equal to 1,0.

Modulus of elasticity

The modulus of elasticity E_{cm} can also be determined from the mean value of the compressive strength:

$$E_{cm} = 22.000 * \left[\frac{f_{cm}}{10}\right]^{0,3}$$ Equation (7)

Overview for various strength classes

By applying the aforementioned equations for compressive and tensile strength values and the modulus of elasticity, the numerical values of various quantities can be calculated for all strength classes covered by Eurocode 2.

Table 8 Material properties concrete in accordance with Eurocode 2

	Strength class	f_{ck}	f_{cm}	f_{cd}	f_{ctm}	f_{ctd}	E_{cm}
		[N/mm^2]	[N/mm^2]	[N/mm^2]	[N/mm^2]	[N/mm^2]	[N/mm^2]
NSC	C12/15	12	20	8,0	1,57	1,05	27.000
	C16/20	16	24	10,7	1,90	1,27	29.000
	C20/25	20	28	13,3	2,21	1,47	30.000
	C25/30	25	33	16,7	2,56	1,71	31.000
	C30/37	30	38	20,0	2,90	1,93	33.000
	C35/45	35	43	23,3	3,21	2,14	34.000
	C40/50	40	48	26,7	3,51	2,34	35.000
	C45/55	45	53	30,0	3,80	2,53	36.000
	C50/60	50	58	33,3	4,07	2,71	37.000
HSC	C55/67	55	63	36,7	4,21	2,81	38.000
	C60/75	60	68	40,0	4,35	2,90	39.000
	C70/85	70	78	46,7	4,61	3,07	41.000
	C80/95	80	88	53,3	4,84	3,23	42.000
	C90/105	90	98	60,0	5,04	3,36	44.000

Constitutive law in compression

Stress-strain diagram: The stress-strain diagrams of concrete obtained from experiments are non-linear curves that are close to a parabola. However, for calculations this is not suitable. Eurocode 2 prescribes that simplified stress-strain diagrams may be used, such as a curve consisting of a parabolic and rectangular part (left part Figure 28) or a more simplified relation (right part Figure 28). The only prerequisite is that the relation should be equivalent to or more conservative than the parabolic-rectangular curve. The most widely used curve is the bi-linear stress-strain diagram.

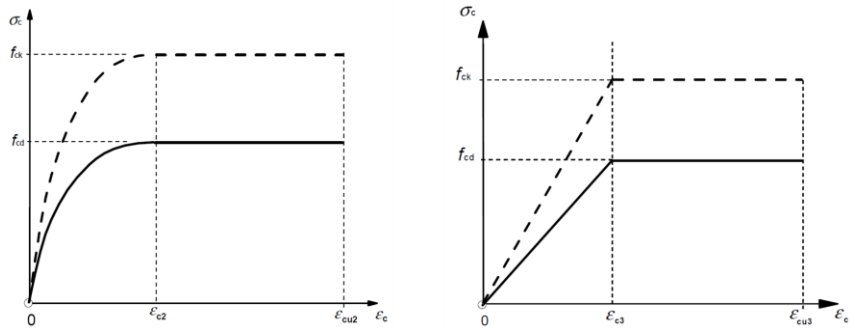

Figure 28 Stress-strain diagrams concrete in compression - after Eurocode 2-1-1 p.36-37

The bi-linear stress-strain diagram consists of two branches; the first branch is the elastic part following Hooke's law up to a strain value ε_{c3}. The second part is the plastic branch, the stress is $\sigma_c = f_{cd}$ and the strains increase to an ultimate strain for concrete under compression with value ε_{cu3}.

Brittleness of the material: The parameters α and β are commonly used in design to describe the shape of the bi-linear stress-strain diagram. The parameter α is the 'shape factor' and describes the shape of the compressive zone, which differs from a rectangle. The parameters β is used to determine the location of the centre of gravity of the compressive zone. Both parameters can be derived by considering the cross-sectional area and centre of gravity of the diagram representing the concrete compressive zone. Table 9 summarizes the values for ε_{c3}, ε_{cu3}, α and β for all strength classes covered by the Eurocode.

Table 9 Parameters concrete compressive zone in accordance with Eurocode 2-1-1

	α	β	ε_{c3}	ε_{cu3}
	[-]	[-]	[‰]	[‰]
≤C50/60	0,75	0,39	1,75	3,5
C55/67	0,71	0,37	1,8	3,1
C60/75	0,67	0,36	1,9	2,9
C70/85	0,62	0,35	2,0	2,7
C80/95	0,58	0,34	2,2	2,6
C90/105	0,56	0,34	2,3	2,6

Figure 29 gives the stress-strain diagrams for concrete in compression of all strength classes covered by the Eurocode. It can be seen that above C50/60 the elastic branch becomes larger while the plastic branch becomes smaller, this implies more brittle behaviour of concrete in compression, which occurs at higher strength classes.

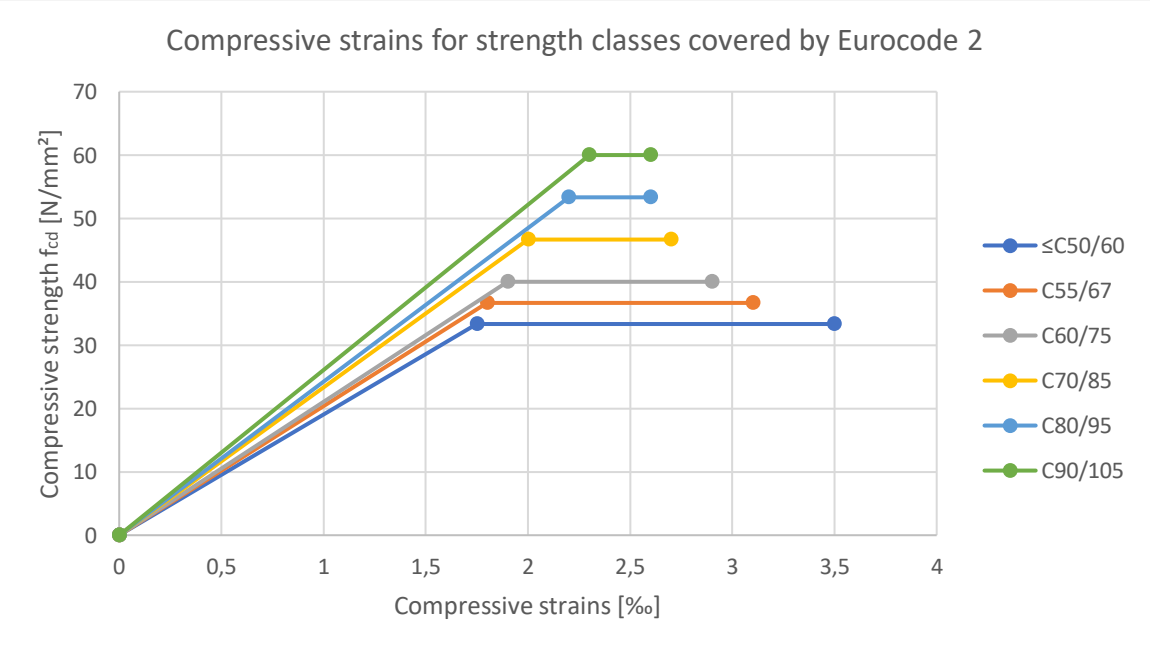

Figure 29 Maximum compressive strains for all strength classes covered by Eurocode 2

High strength concrete in Eurocode 2: The increase in brittleness that can be observed if the strength class increases has to be accounted for in design, this is included in the code. Figure 30 gives another example of a stress distribution allowed by the code: a rectangular stress block. Two factors are introduced to describe the compressive zone: the factor λ defines the effective height of the compressive zone and factor η defines the effective strength. Eurocode 2 does not use the term 'high strength concrete' explicitly but through the factor η the increase in brittleness of the concrete above strength class C50/60 up to and including strength class C90/105 (these strength classes are commonly classified as 'high strength concrete') is accounted for.

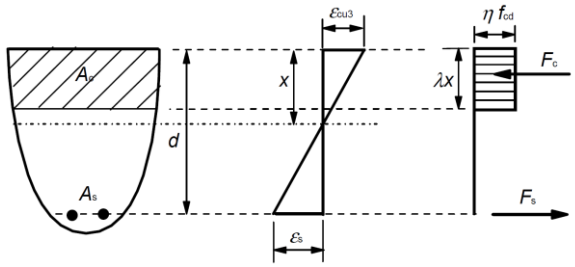

Figure 30 Rectangular stress distribution - Eurocode 2-1-1, p.37

For $f_{ck} \leq 50$ N/mm^2 the values for λ and η are 0,8 and 1,0, respectively, while for strength classes from f_{ck} of 50 N/mm^2 up to and including 90 N/mm^2:

$$\lambda = 0{,}8 - \frac{f_{ck} - 50}{400}$$

$$\eta = 1{,}0 - \frac{f_{ck} - 50}{200}$$

5.2.2 Prestressing steel – Eurocode 2

Material properties

The properties of prestressing steel are discussed in section 3.3 of Eurocode 2-1-1. Prestressing elements can be wires, strands or bars. Prestressing elements can be classified based on properties such as strength, relaxation classes, dimensions and properties of the surface.

In order to classify the prestressing steel based on strength, three characteristics are required: the characteristic tensile strength f_{pk}, the characteristic value of the 0,1%-strain limit $f_{p0,1k}$ and the strain at maximum loading ε_{uk}. To provide sufficient ductility the ratio of f_{pk} divided by $f_{p0,1k}$ should be at least 1,05. If this requirement is met, it may be assumed that the prestressing element has sufficient ductility in tension.

Other values defined in the code are the modulus of elasticity E_p, this may be taken equal to 205.000 N/mm^2 for wires and bars and 195.000 N/mm^2 for strands. The average volumetric mass of the elements is 7850 kg/m^3. The following table, from (Walraven & Braam, 2019), gives an overview of various characteristics of frequently used types of prestressing elements.

Table 10 Mechanical properties of prestressing steel - (Walraven & Braam, Prestressed Concrete, 2019), p.2-21

steel type	type	tensile strength		fracture strain	0,1% proof-stress	maximum tensile stress			slope discontinuity in the σ-ε diagram (ULS)	modulus of elasticity
						during pre-stressing	during pre-stressing with accurate jack	initial stress		
		f_{pk}	f_{pk}/γ_s	ε_{pu}	$f_{p0,1k}$	$\sigma_{p,max}$	$\sigma_{p,max}$	σ_{pm0}	f_{pd}	E_p
		MPa	MPa	‰	MPa	MPa	MPa	MPa	MPa	GPa
Y1030H	bar	1030	936	35	927	773	773	773	843	205 or 170
Y1670C	wire	1670	1518	35	1503	1336	1428	1253	1366	205
Y1770C	wire	1770	1609	35	1593	1416	1513	1328	1448	205
Y1860S7	strand	1860	1691	35	1674	1488	1590	1395	1522	195

Constitutive law

Calculation procedure: Figure 31 gives the simplified curve for design calculations as given in the code, as well as the required equations. The calculations are performed using the characteristic values f_{pk}, $f_{p0,1k}$ and ε_{uk}. Both the ascending upper branch and horizontal upper branch may be used, but in the first case the strain has to be limited to ε_{ud}. According to the annex this is $\varepsilon_{ud} = 0{,}9 * \varepsilon_{uk}$. In case the horizontal branch is used no maximum strain value is prescribed.

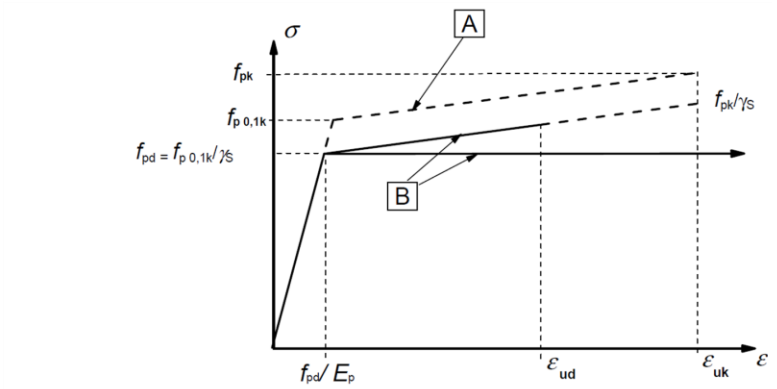

Equations:

$$f_{pd} = \frac{f_{p0,1k}}{\gamma_S}$$

$$\varepsilon_{ud} = 0{,}9 * \varepsilon_{uk}$$

$$\varepsilon_{pd} = \frac{f_{pd}}{E_p}$$

Verklaring

A geschematiseerd
B berekening

Symbols:
f_{pk}: Characteristic tensile strength
$f_{p0,1k}$: Characteristic stress value at 0,1% strain
f_{pd}: Design value of the steel stress
ε_{uk}: Characteristic strain at maximum load
ε_{ud}: Design value of the maximum strain
E_p: Modulus of elasticity
γ_S: Partial safety factor

Figure 31 Schematized stress-strain diagram and equations prestressing steel - Edited, after Eurocode 2-1-1, p.46

Relaxation

The code defines three relaxation classes: class 1 for wires or strands with normal relaxation, class 2 for wires and strands with low relaxation and class 3 for hot rolled bars. Relaxation losses can be determined using certificates of manufacturers or, alternatively, using equations given in the code. For relaxation classes 1 and 2 these are:

$$\frac{\Delta\sigma_{pr}}{\sigma_{pi}} = 5{,}39 * \rho_{1000} * e^{6{,}7\mu} * \left(\frac{t}{1000}\right)^{0{,}75(1-\mu)} * 10^{-5} \qquad \text{Equation (8)}$$

$$\frac{\Delta\sigma_{pr}}{\sigma_{pi}} = 0{,}66 * \rho_{1000} * e^{9{,}1\mu} * \left(\frac{t}{1000}\right)^{0{,}75(1-\mu)} * 10^{-5} \qquad \text{Equation (9)}$$

In these equations $\Delta\sigma_{pr}$ denotes the absolute value of relaxation loss. Stress σ_{pi} is the absolute value of the initial prestressing ($\sigma_{pi} = \sigma_{pm0}$) in case of post-tensioned steel, or the maximum tensile stress in the element minus the direct losses during stressing in case of pretensioned steel. The factor 't' denotes the time after stressing, which may be taken as 500.000 hours to determine the final relaxation loss for $t \to \infty$. The factor 'μ' is the ratio σ_{pi}/f_{pk}. The factor 'ρ_{1000}' is the value of the relaxation loss (in %) at 1000 h after stressing at an average temperature of 20 °C. For class 1 this value can be taken as 8% while for class 2 this value can be taken as 2,5%.

Maximum stresses

In Eurocode 2-1-1 various provisions are given regarding the maximum allowable stress due to prestressing, an overview is given in this section.

Maximum prestressing stress (5.10.2.1 (1)): During stressing the maximum allowable stress applied to the prestressing element is:

$$\sigma_{p,max} = \min\{0{,}8 * f_{pk}; 0{,}9 * f_{p0,1k}\}$$

Maximum concrete compressive stress (5.10.2.2 (5)): During stressing the concrete compressive stress due to prestressing and other loads should not exceed $0{,}60 * f_{ck}(t)$ in case of post-tensioned steel and $0{,}70 * f_{ck}(t)$ in case of pretensioned steel.

Initial prestressing stress (5.10.3 (2)): Directly after stressing and anchoring (post tensioned steel) or relaxing the strands (pretensioned steel) the maximum value of the prestressing stress should not exceed:

$$\sigma_{pm0} = \min\{0{,}75 * f_{pk}; 0{,}85 * f_{p0{,}1k}\}$$

5.3 Material parameters and constitutive laws UHPC

5.3.1 Review AFGC-SETRA 2013

Outline of the AFGC-SETRA 2013 guideline

The AFGC-SETRA 2013 guideline is the revised version from 2002. It is complemented with experience on the application of UHPC in projects as well as research results, and no longer has an interim status. The guideline comprises four parts:

- Part 1. UHPFRC material characterisation – Covers the characterisation of the material, mechanical properties and quality control;
- Part 2. Design of UHPFRC structures – Covers the design of UHPFRC structures, following the layout of Eurocode 2 with modifications wherever relevant to account for the differences between UHPFRC compared to conventional concrete;
- Part 3. Durability of UHPFRC – Covers the durability of UHPFRC;
- Part 4. Sustainable development – Comprises feedback on the use of material from a sustainable development point of view.

For a more detailed discussion of the outline of the guideline, reference is made to annex V.

Definition UHPC

In the AFGC-SETRA 2013 guideline Ultra High Performance Fibre-Reinforced Concrete (UHPFRC) is defined as follows:

- *"UHPFRC are materials with a cement matrix and a characteristic compressive strength of more than 150 MPa and a maximum of 250 MPa."*

In the guideline it is stated that this material sets itself apart from high-performance and very-high performance concrete because of a number of reasons. First there is the high post-cracking tensile strength of the material due to the high percentage of steel fibres, which are added to achieve ductile behaviour in tension. Secondly, good durability is achieved (also of the fibres) due to the high binder content, which results in the elimination of capillary porosity. Thirdly the material possesses self-healing capacity, which means that the tensile strength of the material could be retained for long-term provided that crack widths remain limited. The final reason is the direct tensile strength of the matrix, which is greater than 7 N/mm^2.

For the design of the structure the guideline is used together with Eurocode 2-1-1 and Eurocode 2-2, and in essence this means the guideline replaces provisions from the Eurocode wherever required, to account for the properties of the UHPFRC. The most important difference is the fibre contribution of the material to the ductility and tensile capacity. This capacity can be considerable and may result in not having to provide conventional reinforcement to the structure.

Note that in the guideline the term 'UHPFRC' is used instead of 'UHPC'. In the remainder of this report the material will remain to be denoted as UHPC.

Validity of the guideline

The AFGC-SETRA 2013 guideline is developed in collaboration with the concrete and construction industry in France and is based on the research and application of certain commercial products. Therefore, the guideline only covers certain specific types of UHPC, mentioned are:

- Ductal mixtures (including Reactive Powder Concrete)
- BSI/CERACEM mixtures
- BCV mixtures

In section 5.3.2 of this chapter the constitutive laws of UHPC will be formulated in accordance with the guideline and other sources if required, followed by determining the material parameters in section 5.3.3. In section 5.4 UHPC design verifications will be discussed based on the constitutive laws and properties from the aforementioned sections.

5.3.2 Constitutive laws

Constitutive law compression – AFGC-SETRA 2013 guideline

Figure 32 gives the constitutive laws for concrete in compression in the serviceability limit state (left) and ultimate limit state (right) according to the AFGC-SETRA 2013 guideline. In addition, equations are given that are required to fully define the graphs.

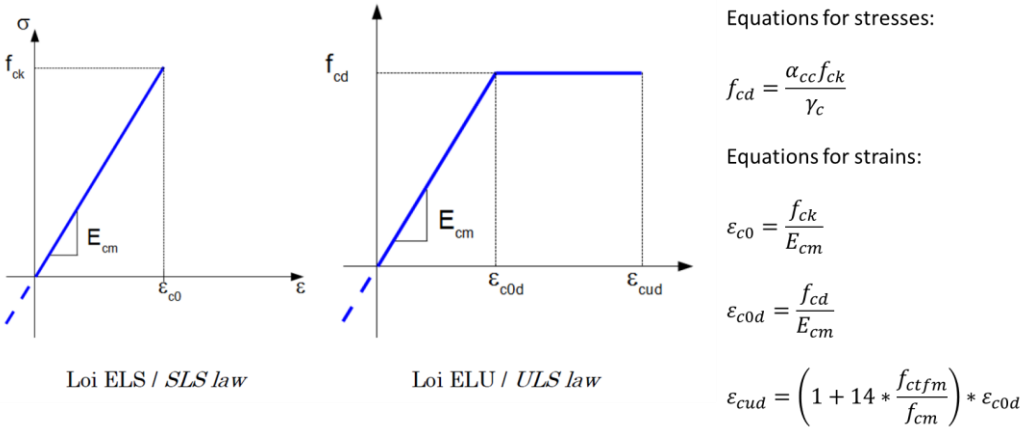

Figure 32 Constitutive laws and equations for concrete in compression - Edited, after (AFGC-SETRA 2013), p.83

In the equations f_{ctfm} denotes the mean value of the maximal post-cracking stress in tension, ε_{c0} denotes the strain corresponding to reaching the characteristic compressive strength, ε_{c0d} denotes the strain corresponding to reaching the design compressive strength and ε_{cud} denotes the maximum compressive strain in the ultimate limit state. The factors α_{cc} and γ_C will be discussed in more detail in section 5.3.3.

Constitutive laws tension – AFGC-SETRA 2013 guideline

Types of material: From experiments different types of behaviour of UHPC in tension can be observed and for this reason the guideline distinguishes different constitutive laws of concrete in tension. Which class is applicable depends on the material itself and on how the material is placed. The three different types of materials are distinguished in the guideline:

- **Strain-softening material (Type 1)**: UHPC for which both the average and characteristic laws are strain-softening. If for such a material the tensile strength of the matrix is reached, cracking occurs and the crack localises. Examples of such materials are those with either a low fibre content or in case the fibres are used inefficiently.

- **Low strain-hardening material (Type 2)**: UHPC for which the average law is hardening, but the characteristic law is softening. For characterisation and design these materials are analysed as strain-softening materials. According to the guideline most of the UHPC on the market falls within this category.

- **Strain hardening material (Type 3)**: UHPC for which both the average and characteristic laws are strain-hardening. If for such a material the tensile strength of the matrix is reached, a large number of fine cracks develop. This type of behaviour occurs for materials with a high fibre content.

The material type influences the type of law applied to describe the post-cracking behaviour. For type 1 and type 2 materials a stress-crack width law is applied to describe this, while for type 3 materials a stress-strain type of constitutive law is applied because the micro-cracks that develop may be treated as strain for calculation purposes. Table 11 summarizes the information from the AFGC-SETRA 2013 guideline.

Table 11 Overview of constitutive laws for different material types

	Average law	**Characteristic law**	**Design law**	**Type post-cracking law**
Type 1 – Strain-softening	Softening	Softening	Softening	$\sigma_f - w$
Type 2 – Low strain-hardening	Hardening	Softening	Softening	$\sigma_f - w$
Type 3 – Strain-hardening	Hardening	Hardening	Hardening	$\sigma_f - \varepsilon$

Thin and thick elements: In addition to the three material types, a distinction is also made between thin and thick elements. A structure is considered to be thin if $e \leq 3 * l_f$, in this expression e denotes the thickness of the element and l_f denotes the length of an individual fibre.

The fibre orientation has a more predominant effect in case of thin members compared to thick members and as a result their constitutive law is similar to that of type 3 material. Given the expected fibre length and dimensions of the elements of the bridge deck that is to be designed, the focus is on thick elements. No further provisions from the guideline on thin elements will be discussed in the remainder of this report.

Strain softening or low strain hardening law: Figure 33 gives the stress-strain diagrams in the serviceability limit state and ultimate limit state for softening or low strain-hardening materials. In addition, the equations required to fully define the graphs have been given.

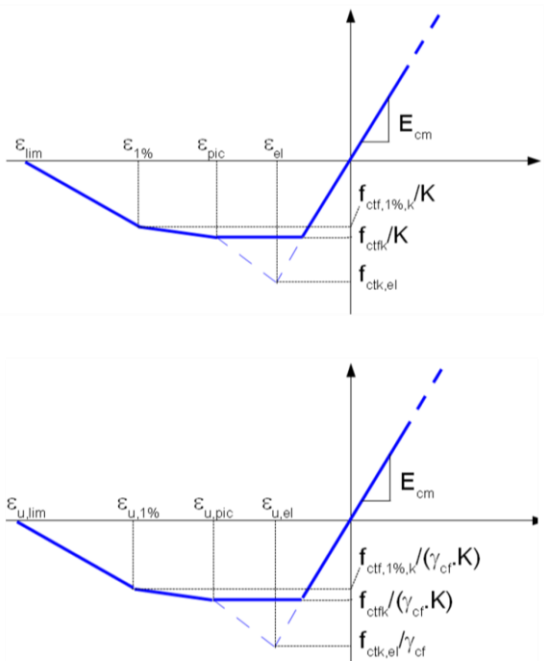

Serviceability limit state

$$\varepsilon_{lim} = \frac{l_f}{4l_c}$$

$$\varepsilon_{1\%} = \frac{w_{1\%}}{l_c} + \frac{f_{ctk,el}}{E_{c,eff}}$$

$$\varepsilon_{peak} = \frac{w_{peak}}{l_c} + \frac{f_{ctk,el}}{E_{c,eff}}$$

With: $w_{1\%} = 0{,}01 * H$ and $l_c = 2/3 * h$

Ultimate limit state

$$\varepsilon_{u,lim} = \frac{l_f}{4l_c}$$

$$\varepsilon_{u1\%} = \frac{w_{1\%}}{l_c} + \frac{f_{ctk,el}}{\gamma_{cf} E_{c,eff}}$$

$$\varepsilon_{u,peak} = \frac{w_{peak}}{l_c} + \frac{f_{ctk,el}}{\gamma_{cf} E_{c,eff}}$$

With: $w_{1\%} = 0{,}01 * H$ and $l_c = 2/3 * h$

Figure 33 Constitutive law and equations of type 1 and 2 materials in tension – Edited, after (AFGC-SETRA 2013), p.85

In practice the tensile strength of the material is generally determined using tests, after which the required relationships can be established. For calculation purposes the simplified stress-strain diagram is truncated to form a plateau. The curve is clipped at a value of f_{ctfk} divided by the fibre-orientation factor (SLS) or the multiplication of a partial factor and fibre-orientation factor (ULS). The guideline prescribes a similar way of clipping the actual curves of softening or low-strain hardening materials.

Strain hardening law: Figure 34 gives the stress-strain diagrams in the serviceability limit state and ultimate limit state for strain hardening material.

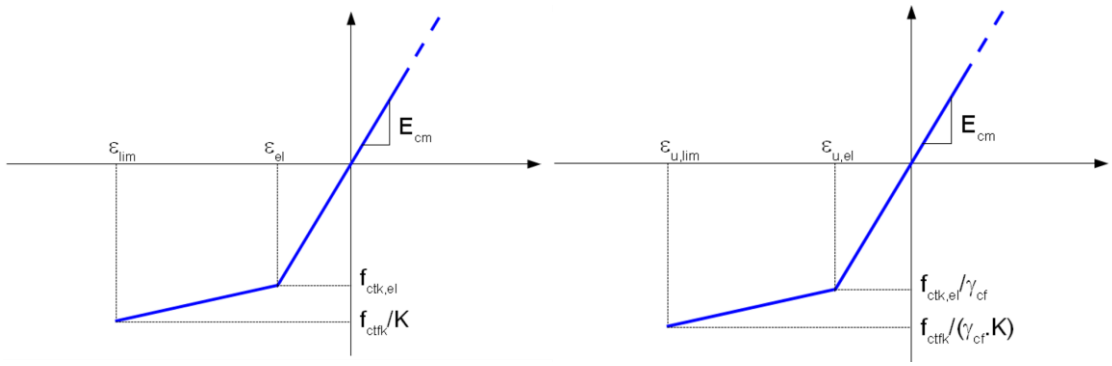

Figure 34 Constitutive law and equations of type 3 material in tension – (AFGC-SETRA 2013), p.85

Applied constitutive law

An appropriate constitutive law (stress-strain diagram) is required for design verifications. Laws from the AFGC-SETRA 2013 have been given and in literature one can find other diagrams as well that are often simplified for more practical application. Figure 35 gives a simplified stress-strain diagram that is assumed for use in further ultimate limit state verifications, as well as all relationships required to define all quantities in the figure. The diagram is not to scale.

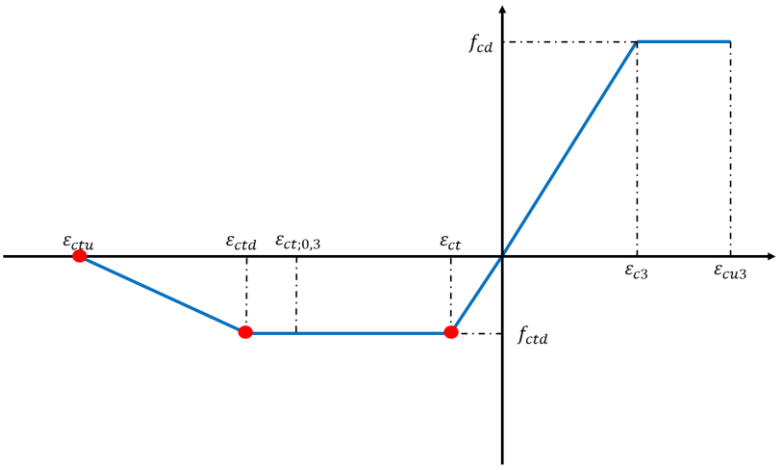

Calculating stresses:

$$f_{cd} = \frac{\alpha_{cc} * f_{ck}}{\gamma_C}$$

$$f_{ctd} = \frac{\alpha_{ct} * f_{ctk,el}}{\gamma_C}$$

Calculating strains:

$$\varepsilon_{ct} = \frac{f_{ctd}}{E_{cm}} = \frac{f_{ctk,el}}{\gamma_c * E_{cm}}$$

$$\varepsilon_{ct;0,3} = \frac{w_{0,3}}{l_c} + \varepsilon_{ct}$$

$$\varepsilon_{ctd} = \varepsilon_{ctu} - \frac{f_{ctd}}{f_{ctd;2}} * (\varepsilon_{ctu} - \varepsilon_{ct;0,3})$$

$$\varepsilon_{ctu} = \frac{l_f}{4 * l_c} \leq 2{,}5\ ‰$$

Figure 35 Adopted simplified stress-strain relationship and equations for the ULS verifications

The given stress-strain diagram is taken from (Ketel, Willemse, Van Rijen, & Koolen, Rekenmodel VVUHSB (1), 2011) and an example of its application can be found in (Van Geffen & Attahiri, 2016). This law is applied because it allows for a practical approach. To obtain the curve a number of simplifications are made to the graph from the guideline.

A linear declining line is drawn between the strain at $w = 0{,}30$ and the ultimate strain value. Subsequently the graph is truncated above the tensile strength of the matrix f_{ctd}, above this value no tensile contribution is taken into consideration. This results in a simplified calculation, neglecting the contribution above f_{ctd} is justified by the relatively small area under the graph that will be neglected when following this approach.

A strain value ε_{ctd} is introduced to describe the point where the horizontal line at tensile stress value f_{ctd} intersects the declining branch of the diagram. This strain value can be calculated by considering the geometry of the stress-strain diagram. Note that the values of $f_{ctk,el}$ and f_{ctfk} can be as such that their respective design values f_{ctd} and $f_{ctd;2}$ are equal, in that case the strain values ε_{ctd} and $\varepsilon_{ct;0,3}$ will also be equal.

$$\varepsilon_{ctd} = \varepsilon_{ctu} - \frac{f_{ctd}}{f_{ctd;2}} * \left(\varepsilon_{ctu} - \varepsilon_{ct;0,3}\right) \qquad \text{Equation (10)}$$

The simplified diagram was originally derived based on constitutive laws for strain hardening material in accordance with the AFGC-SETRA 2002 guideline. To apply the diagram the characteristic maximal post-cracking stress divided by the fibre orientation factor has to be above the or at least be equal to the characteristic elastic tensile strength of the matrix. The model is unsuitable for softening material. In accordance with the AFGC-SETRA 2013 guideline, for strain-hardening material a maximum of 2,5 ‰ is imposed upon the ultimate strain for fibre participation. This means that the use of the graph is on the conservative side for high strain-hardening material as depicted in Figure 34, because the increase in capacity (hardening) above f_{ctd} is neglected.

Note that the symbols between the AFGC-SETRA 2013, the Eurocode 2 and the aforementioned article are not always consistent. Table 12 gives an overview of symbols according the AFGC-SETRA 2013 and Eurocode 2, as well as the symbols that will be adopted. With the constitutive law established and the fundamentals of the guideline discussed, the material properties will be determined in section 5.3.3.

Table 12 Symbols according to AFGC-SETRA, Eurocode 2 and adopted symbols

Definition	**Symbol**		
	AFGC	EC2	Adopted
Strain at reaching design compressive strength	ε_{c0d}	ε_{c3}	ε_{c3}
Maximum compressive strain at ULS	ε_{cud}	ε_{cu3}	ε_{cu3}
Characteristic value compressive stress	f_{ck}	f_{ck}	f_{ck}
Design value compressive strength	f_{cd}	f_{cd}	f_{cd}
Modulus of elasticity	E_{cm}	E_{cm}	E_{cm}
Characteristic elastic (5% percentile value) tensile strength	$f_{ctk,el}$	$f_{ctk;0,05}$	$f_{ctk,el}$
Design value of tensile strength (tensile strength 1st crack)	-	f_{ctd}	f_{ctd}
Characteristic maximal post-cracking stress (stress at w=0,30)	f_{ctfk}	-	f_{ctfk}
Design value maximal post-cracking stress (stress at $w = 0{,}30$)	$f_{ctfk}/(\gamma_{cf}*K)$	$f_{ctd;2}$	$f_{ctd;2}$
Elastic strain (strain at the first crack)	$\varepsilon_{u,el}$	ε_{ct}	ε_{ct}
Strain corresponding to local peak or crack width $w = 0{,}30$ mm	$\varepsilon_{u,peak}$	-	$\varepsilon_{u,peak}$
Strain corresponding to crack width of $0{,}01 * H$	$\varepsilon_{u,1\%}$	-	$\varepsilon_{u,1\%}$
Ultimate strain for fibre participation	$\varepsilon_{u,lim}$	ε_{ctu}	$\varepsilon_{u,lim}$
Characteristic length	l_c	-	l_c
Fibre length	l_f	-	l_f

5.3.3 Material parameters

UHPC in compression

According to the guideline the design value of the compressive strength is calculated from the characteristic strength through the following relationship.

$$f_{cd} = \frac{\alpha_{cc} * f_{ck}}{\gamma_C} \qquad \text{Equation (11)}$$

Similarly to the Eurocode, the factor α_{cc} is included in the calculation. However, the AFGC-SETRA 2013 recommends a value of 0,85 compared to the factor of 1,0 as given in the Eurocode. For the partial factor γ_c reference is made to the Eurocode, which prescribes the value of 1,5.

UHPC in tension

The design value of the tensile strength of the matrix is calculated from the characteristic tensile strength value of the matrix through the following relationship.

$$f_{ctd} = \frac{\alpha_{ct} * f_{ctk,el}}{\gamma_C}$$ Equation (12)

According to the guideline the factor α_{ct} may be taken equal to 1,0. Note that although the AFGC-SETRA 2013 guideline prescribes f_{ctd} to be calculated by dividing $f_{ctk,el}$ over γ_{cf} (partial safety factor for fibre-reinforced concrete in tension, with a value equal to 1,3) instead of γ_c (equal to 1,5), the latter has been applied to be consistent with the concrete tensile strength calculation according to Eurocode 2.

The design value of the maximum post-cracking strength can be calculated using the following expression.

$$f_{ctd;2} = \frac{f_{ctfk}}{\gamma_{cf} * K_{global}}$$ Equation (13)

In this equation f_{ctfk} denotes the characteristic value of the maximum post-cracking strength, which is the stress value corresponding to a crack width of $w = 0{,}30$ mm.

According to (Fehling, Schmidt, Walraven, Leutbecher, & Fröhlich, 2014), equations (14) and (15) can be used to determine the axial tensile strength of UHPC. These equations are identical to those for conventional concrete, see equations (3) and (5). According to the aforementioned source, the application of these equations for UHPC is justified by experimental results and these equations can be applied to determine the strength of the matrix.

$$f_{ctm} = 0{,}3 * f_{ck}^{\frac{2}{3}}$$ Equation (14)

$$f_{ctk,0{,}05} = 0{,}7 * f_{ctm}$$ Equation (15)

Modulus of elasticity

Equation (7) from the Eurocode cannot be applied to UHPC to determine the modulus of elasticity. In (Fehling, Schmidt, Walraven, Leutbecher, & Fröhlich, 2014) two equations are given to determine the modulus of elasticity, which is influenced by the aggregate size and type. For fine grained UHPC:

$$E_c = 8800 * f_c^{\frac{1}{3}}$$ Equation (16)

For coarse-grained UHPC with basalt chipping:

$$E_c = 10.200 * f_c^{\frac{1}{3}}$$ Equation (17)

In both equations $f_c = f_{ck} + 8$ [N/mm²], in which f_c is the cylinder compressive strength.

To determine time dependent effects the AFGC-SETRA 2013 guideline states that creep effects can be accounted for by calculating an effective modulus of elasticity from the mean modulus E_{cm}:

$$E_{c,eff} = \frac{E_{cm}}{1 + \varphi}$$ Equation (18)

Fatigue

The design value of the fatigue compressive strength of UHPC can be calculated in accordance with the following equation, which is from (Fehling, Schmidt, Walraven, Leutbecher, & Fröhlich, 2014):

$$f_{cd,fat} = 0{,}85 * \beta_{cc}(t) * f_{ck} * \left(1 - \frac{f_{ck}}{40 * f_{ck0}}\right) * \frac{1}{\gamma_c}$$ Equation (19)

In this equation f_{cto} denotes a reference strength value of 10 N/mm^2 and $\beta_{cc}(t)$ is a factor to account for the increase of strength as the hydration progresses, the latter can be calculated in accordance with section 3.1.2. of Eurocode 2-1-1, for a value of 28 days this results in a value of 1,0.

$$\beta_{cc}(t) = \exp\left\{s\left[1-\left(\frac{28}{t}\right)^{\frac{1}{2}}\right]\right\}$$

5.4 Design verifications of UHPC in the ultimate limit state

Using the material properties and constitutive laws of the various materials as defined in the previous sections, calculation procedures will be formulated for the required design verifications for UHPC. During the design stage of the project, reference will be made to the relevant verifications that will be described in this section.

5.4.1 General verifications

The AFGC-SETRA 2013 guideline prescribes a number of general verifications that have to be performed and effects that have to be considered. These are covered first, followed by other design verifications in the subsequent sections.

Scatter in fibre distribution

Fibre orientation: The importance of fibres for the behaviour and mechanical properties of UHPC is especially predominant for the non-linear branch of UHPC in tension because this is when the fibres become effective. It is not only the amount of fibres in the mix that affects the mechanical properties of UHPC in tension, there is a strong relationship between properties used in design and execution.

During execution different factors occur that influence the fibre distribution and orientation, which in turn affects the mechanical properties of the material. Examples of such effects are given in (Simon, Corvez, & Marchand, 2013) and are:

- Shape of formwork
- Method of casting UHPC
- Viscosity of the UHPC

This list is not exhaustive, other factors affect the distribution and orientation of the fibres as well, such as the dimensions of the element.

Fibre-orientation factor: In the ideal theoretical model the fibres are distributed perfectly random through the concrete element, i.e. there is a homogenous 3D distribution of the fibres and the mechanical properties are thus isotropic. Due to the aforementioned effects this will never be the case in reality. In the AFGC-SETRA guidelines the 'fibre orientation factor' $1/K$ is introduced as a practical and robust way of accounting in the design for the fact that in reality the distribution and orientation of the fibres deviate from the perfectly random and homogeneous distribution. The application of the factor could already be seen from, for example, Figure 33 and equation (13).

Determining factor: Although initial assumptions have to be made for the K-factors during design, procedures are given in the guideline to determine the K-factors experimentally, which is an essential step in the design process because the assumed value and the actual value have to be in accordance with one another. For thick elements this procedure can summarized as follows:

- First, full-scale mock ups representative of the structure and the method of production that will be used are made. Test specimen are sawn from the mock up to be able to perform tests (bending or tensile test) to determine the maximum bending moment or tensile force;

- The dimensions of the specimen depend on the fibre length and type of test. The location of the samples depends on the main tensile stresses in the structure, at the regions where the tensile capacity and thus a high contribution of the fibres and high fibre efficiency is required. Figure 36 gives an example of this;

- At the same time specimen (prisms) are casted using the same material and subjected to bending or tensile tests to determine the maximum moment or tensile force. Using the results for the casted prims and the sawn prims, the K-factor can be determined.

Given the many effects that influence the fibre distribution and orientation, the K-factors varies from project to project and different values can be determined for different parts of the same structure as well (e.g. different values for the web or top flange of a box beam). Accurately predicting the behaviour of UHPC flowing through the formwork is not possible, which makes that testing is required. In case the K-factors found by performing tests are different from the initially assumed values, modifications are required to the method of execution and/or to the design until both are in accordance.

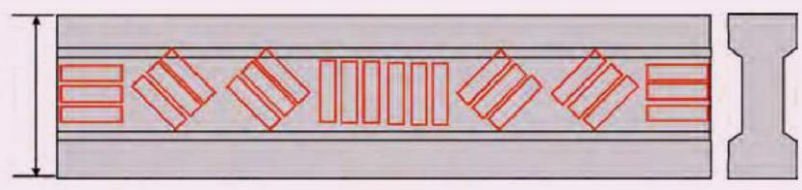

Figure 36 Example of taking sawn specimen to determine the K-factor – (AFGC-SETRA 2013), p.27

Local and global factors: In the AFGC-SETRA 2013 guideline a distinction is made between a global coefficient K_{global} for verifications involving the general stress distribution, for example a shear verification of a cross section, and a local coefficient K_{local} for verifications involving smaller components or specific situations, for example a tensile tie in a strut and tie model. The guideline recommends the use of $K_{global} = 1{,}25$ and $K_{local} = 1{,}75$ as default values for the preliminary design if no additional information is available.

Minimum ductility condition

For strain softening or low strain hardening material it has to be verified that sufficient ductility in bending is provided, which is done using the ductility requirement. For elements showing strain hardening behaviour this verification is not required.

$$\frac{1}{w_{lim}} \int_0^{w_{lim}} \frac{\sigma(w)}{K_{global}} dw \geq \max\left(0{,}4 * f_{ctm,el}; 3\ MPa\right) \qquad \text{Equation (20)}$$

Where:
w_{lim}: Crack width that can be chosen equal to 0,3 mm
$f_{ctm,el}$: Mean limit of elasticity in tension
$\sigma(w)$: Characteristic post-cracking stress

Non-brittleness condition

The non-brittleness condition has to be verified, which prescribes that the ULS loads are higher than the loads resulting in cracking. In practical terms for bending this means that it has to be verified that the elastic bending moment in the uncracked cross section is smaller than the ultimate bending moment capacity, to prevent brittle failure in case the section cracks. This replaces the conventional verification of the minimum amount of reinforcement in conventional concrete structures conforming Eurocode 2.

5.4.2 Bending moment capacity

Prestressed cross section

Determining the bending moment capacity of a prestressed cross section is an iterative process and comprises a number of steps. Figure 37 gives an overview of the calculation procedure. The approach for prestressed cross sections of conventional concrete is modified to include the tensile capacity of UHPC.

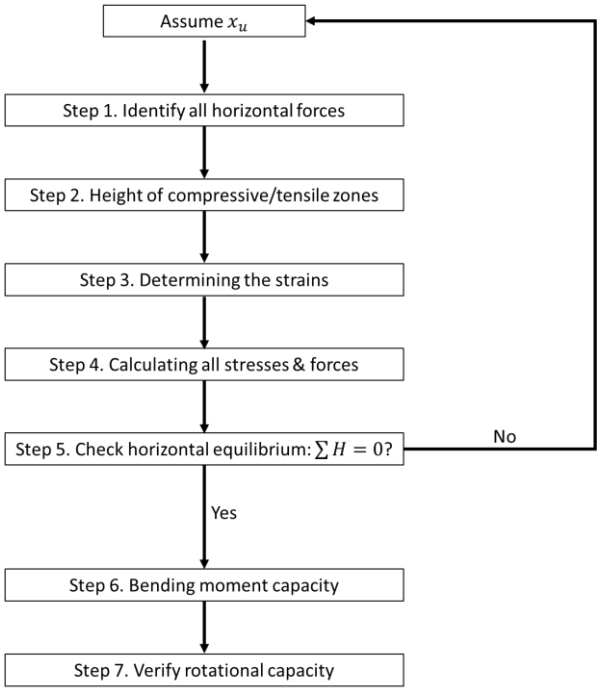

Figure 37 Calculating the bending moment capacity

Figure 38 gives the stress-strain diagram that has been assumed for the verification of the bending moment capacity of a prestressed UHPC beam, the figure is not to scale.

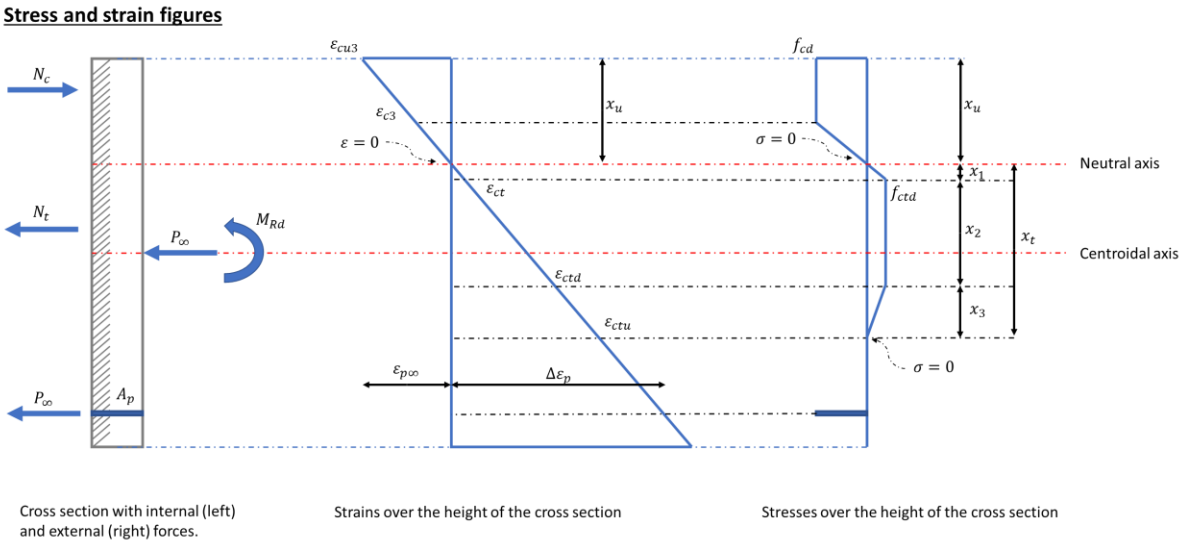

Figure 38 Schematic stress and strain diagrams of prestressed UHPC cross section in the ULS

By following the procedure as given in Figure 37 the capacity can be calculated. To calculate the capacity of a prestressed cross section of conventional concrete, the same procedure is used but the contribution of concrete in tension is neglected. Reference is made to annex V for more elaborate derivations of the approach as presented in this paragraph.

Unreinforced UHPC with or without external compressive force

Given its relatively high tensile strength, UHPC can in certain cases be applied without conventional reinforcement. In annex VI derivations are given to obtain expressions to determine the bending moment capacity of such a cross section. The maximum bending moment is reached at the situation where the outermost tensile fibre of the cross section in bending has reached a strain value of ε_{ctd}.

By adding an external compressive force, the bending moment can be increased because a higher external bending moment is required to achieve the strain value ε_{ctd} in the fibre with the highest tensile strain. Figure 39 gives the assumed schematic stress-strain diagram for the verification of such elements in bending in the ultimate limit state.

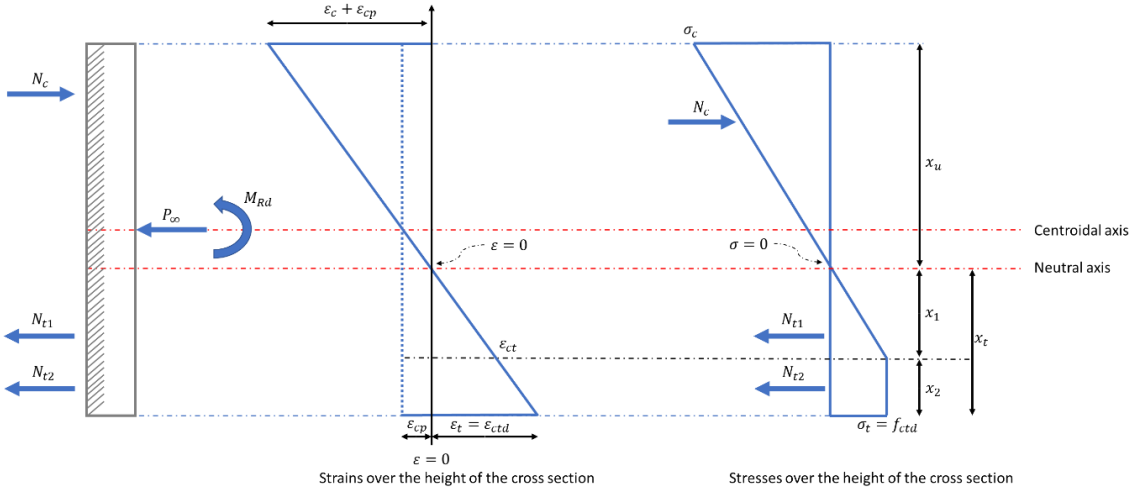

Figure 39 Schematic stress and strain diagrams of unreinforced UHPC with external compressive force in the ULS

The compressive force is assumed to result in a uniform strain of ε_{cp}. If no such compressive force would be present and the strain at the most tensioned fibre is ε_{ctd}, then the compressive strain in the most compressed fibre is ε_c. The total compressive strain is thus $(\varepsilon_c + \varepsilon_{cp})$, which may be determined as follows:

$$(\varepsilon_c + \varepsilon_{cp}) = \varepsilon_{cp} + \sqrt{\varepsilon_{cp}^2 + \frac{2 * f_{ctd} * \varepsilon_{ctd} - f_{ctd} * \varepsilon_{ct}}{E_{cm}} + 2 * \varepsilon_{cp} * \varepsilon_{ctd}} \qquad \text{Equation (21)}$$

Using the total strain value at the most compressed fibre and the strain diagram, it can be derived that the height of the compressive zone x_u is:

$$x_u = \frac{f_{ctd} * t_{ft} + \varepsilon_{cp} * E_{cm} * t_{ft}}{\frac{1}{2} * (\varepsilon_c + \varepsilon_{cp}) * E_{cm} + \frac{1}{2} * f_{ctd} * \frac{\varepsilon_{ct}}{\varepsilon_c + \varepsilon_{cp}} + f_{ctd}} \qquad \text{Equation (22)}$$

By considering the strain diagram of the cross section, the height of the tensile zones x_1 and x_2 can be calculated as well, followed by calculating the compressive force N_c and the tensile forces N_{t1} and N_{t2}. The bending moment capacity subsequently follows from:

$$M_{Rd} = -N_c * \frac{1}{3} * x_u + N_{t1} * \left(x_u + \frac{2}{3} * x_1\right) + N_{t2} * \left(x_u + x_1 + \frac{1}{2} * x_2\right) + P_{m,\infty} * \frac{1}{2} * t_{ft} \qquad \text{Equation (23)}$$

If no compressive force is present, then ε_{cp} is set equal to zero after which all aforementioned equations in this section can still be applied to determine the bending moment capacity.

5.4.3 Shear force capacity

General equation

According to the AFGC-SETRA 2013 guideline the shear capacity is to be calculated as follows:

$$\min(V_{Rd}; V_{Rd,max})$$ Equation (24)

In this equation the term V_{Rd} denotes the tensile resistance of the ties in the concrete while $V_{Rd,max}$ denotes the resistance of the concrete compressive strut. The tensile resistance of the concrete ties is determined as the summation of three individual components:

$$V_{Rd} = V_{Rd,c} + V_{Rd,s} + V_{Rd,f}$$ Equation (25)

In this equation $V_{Rd,c}$ denotes the concrete contribution, $V_{Rd,s}$ denotes the shear reinforcement contribution and the term $V_{Rd,f}$ denotes the fibre contribution.

Individual contributions concrete, reinforcement and fibres

Concrete: For a prestressed concrete cross section, the concrete contribution is:

$$V_{Rd,c} = \frac{0{,}24}{\gamma_{cf}\gamma_E} * k * f_{ck}^{\frac{1}{2}} * b_w * z$$ Equation (26)

In this equation k is a factor that accounts for the presence of an axial force, d is the effective height and z is the lever arm. In the guideline the values $z = 0{,}9 * d$ and $d = 7/8h$ are given.

Steel fibres: The design value for the fibre contribution to the shear capacity is:

$$V_{Rd,f} = \frac{A_{fv} * \sigma_{Rd,f}}{tan\theta}$$ Equation (27)

In this expression A_{fv} is the area of the fibre effect, which is $A_{fv} = b_w * z$ for rectangular or T-sections, the factor θ is the angle between the principal compression stress and the beam axis ($\theta \geq 30^o$) and $\sigma_{Rd,f}$ is the residual tensile strength of the fibre-reinforced cross-section.

Following the AFGC-SETRA 2013 guideline the latter should be calculated using an integral. However, according to (Ketel, Willemse, Van Rijen, & Koolen, Dwarskracht- en kolomberekening VVUHSB, 2011), a safe approximation is obtained by setting the residual tensile strength equal to the stress value corresponding to a crack width of 0,30 mm. Therefore, equation (27) can be rewritten to:

$$V_{Rd,f} = \frac{A_{fv} * \sigma_{Rd,f}}{tan\theta} \approx \frac{A_{fv} * f_{ctd;2}}{tan\theta}$$ Equation (28)

Reinforcement: If vertical reinforcement is provided, then its contribution can be calculated as follows:

$$V_{Rd,s} = \frac{A_{sw}}{s} * z * f_{ywd} * cot\,\theta$$ Equation (29)

In this equation A_{sw} denotes the cross-sectional area of the shear reinforcement, s denotes the spacing of the stirrups and f_{ywd} is the design yield strength of the shear reinforcement. By adding up the results of equations (26), (28) and (29), the total capacity V_{Rd} of the tensile resistance of the ties in the concrete is obtained.

Ultimate strength of the concrete compressive strut $V_{Rd,max}$

The concrete compressive strut determines the upper limit of the shear capacity, its capacity is calculated as follows:

$$V_{Rd,max} = 2 * 1{,}14 * \frac{\alpha_{cc}}{\gamma_c} b_w * z * f_{ck}^{\frac{2}{3}} * \frac{1}{cot\theta + tan\theta}$$ Equation (30)

5.4.4 Torsion

General provisions

Provisions required for the verification of the torsion capacity and capacity under the combination of shear and torsion can be found in Eurocode 2-1-1, Eurocode 2-2 and the AFGC-SETRA 2013 guideline. The latter modifies equations as such that the fibre contribution can be taken into consideration while the first two give various general provisions, of which of relevance are:

- Effects of torsion and shear for hollow elements may be superimposed, after which the maximum capacity of an element subjected to the combined effect is determined, provided that the same angle for the compressive strut is applied in both calculations;

- For box type cross sections the section has to be divided in separate segments after which the individual capacity of each segment to the combined effect of shear and torsion is assessed, see Figure 40.

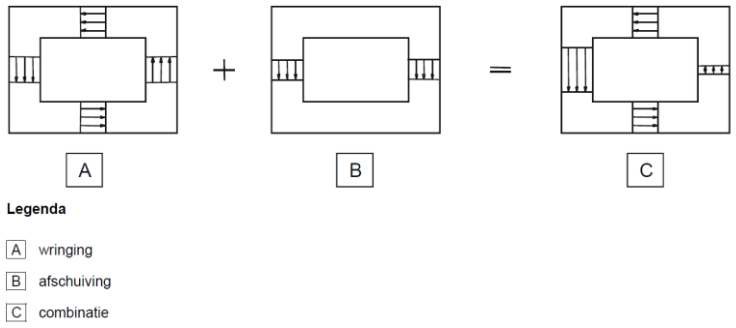

Figure 40 Combined effect shear and torsion - Eurocode 2-2, p.32

Torsional moment capacity

The torsional cracking moment can be found by taking the shear stresses equal to the tensile capacity of the material, $\tau_{t,i} = f_{ctd}$, which results in:

$$T_{Rd,c} = f_{ctd} * t_{ef} * 2 * A_k \qquad \text{Equation (31)}$$

In this equation A_k denotes the area enclosed by the centre lines of the connected walls, including enclosed hollow parts and the term t_{ef} denotes the effective wall thickness.

Combined effect of torsion and shear

After the effects of torsion and shear have been superimposed it has to be verified whether each segment 'i' has sufficient capacity to withstand this combined effect. The AFGC-SETRA 2013 guideline gives the following equation to verify the capacity of each segment:

$$V_{Rd,c} + V_{Rd,f} + V_{Rd,s} \geq V_{Ed,i} + \frac{T_{Ed}}{2 * A_k} * Z_i \qquad \text{Equation (32)}$$

The righthand side denotes the equivalent shear force in segment 'i'due to the combined effect of shear and torsion, while the rightmost term denotes the shear force in the segment due to torsion. The capacity of the segment is calculated following the procedures for shear capacity. However, the dimensions plugged into these equations have to be in accordance with the dimensions of the segment 'i' under consideration.

The upper limit of the resistance to this combined effect is determined by the failure of the compressive strut. For solid or open profiles, the capacity of the compressive strut is verified by satisfying the condition:

$$\frac{T_{Ed}}{T_{Rd,max}} + \frac{V_{Ed}}{V_{Rd,\max}} \leq 1{,}0 \qquad \text{Equation (33)}$$

In this equation T_{Ed} is the design value of the acting torsional moment and V_{Ed} is the design value of the acting shear force. $T_{Rd,max}$ and $V_{Rd,\max}$ denote the design value of the torsional resistance and the shear resistance, these are calculated as follows:

$$T_{Rd,max} = 2 * 1{,}14 * \frac{\alpha_{cc}}{\gamma_C} * 2 * A_k * t_{ef,i} * sin\theta * cos\theta \quad \text{Equation (34)}$$

$$V_{Rd,max} = 2 * 1{,}14 * \frac{\alpha_{cc}}{\gamma_C} * b_w * z * f_{ck}^{\frac{2}{3}} * \frac{1}{cot\theta + tan\theta} \quad \text{Equation (35)}$$

Note that equation (33) holds for solid or open profiles while for box beams a different procedure is to be applied. Each segment is verified separately as a beam element loaded by an equivalent shear force to confirm that the equivalent shear force due to the combination of torsion and shear is smaller than $V_{Rd,max}$:

$$V_{Ed,i} + \frac{T_{Ed}}{2 * A_k} * z_i \leq V_{Rd,max,i} \quad \text{Equation (36)}$$

In this equation the capacity of the concrete compressive strut of the segment 'i' is calculated in accordance with equation (30), where the terms b_w and z should correspond to the dimensions of the segment under consideration by taking $b_w = t_{ef,i}$ and $z = z_i$.

5.4.5 Fatigue

UHPC in compression

The verification of UHPC in compression is performed following provisions from Eurocode 2-1-1 and Eurocode 2-2, no additional provisions are given in the AFGC-SETRA 2013 guideline. Eurocode 2-2 prescribes that for the verification of concrete under fatigue Miner's rule has to be applied, the fatigue capacity is sufficient if:

$$\sum_{i=1}^{m} \frac{n_i}{N_i} \leq 1 \quad \text{Equation (37)}$$

The number of cycles to failure at constant amplitude 'i', N_i, is conforming Eurocode 2-2 calculated as follows:

$$N_i = 10^{14 * \frac{1 - E_{cd,max,i}}{\sqrt{1 - R_i}}} \quad \text{Equation (38)}$$

In this equation:

$$R_i = \frac{E_{cd,min,i}}{E_{cd,max,i}}$$

$$E_{cd,min,i} = \frac{\sigma_{cd,min,i}}{f_{cd,fat}}$$

$$E_{cd,max,i} = \frac{\sigma_{cd,max,i}}{f_{cd,fat}}$$

The design value of the fatigue strength is calculated using equation (19), this gives more appropriate results compared to the expression in the Eurocode, because the latter results in a reduction of the fatigue strength within the range of very high and ultra-high strength concretes.

UHPC in tension

The AFGC-SETRA 2013 guidelines gives an additional requirement for elements subjected to fatigue that are loaded in tension under service conditions. In persistent design situations under the frequent load combination in the serviceability limit state, the tensile stress should be limited to:

$$\sigma_{t,max} = \min(f_{ctm,el}; f_{ctfm})$$ Equation (39)

Where:
$f_{ctm,el}$: The mean value of the tensile strength of the matrix
f_{ctfm}: The mean value of the maximal post-cracking stress.

This rule is clarified further in annex 12 of the guideline, in which it is stated that by means of bending tests with cyclic loads resulting in alternating compressive and tensile stresses it was proven that no irreversible damage occurs if the tensile stress remains below the value $f_{ctm,el}$.

6

OUTLINE OF THE DESIGN STAGE

6.1 Outline of the design stage

6.1.1 Overview of the design stage

Various activities within the project comprise design work. Collectively these are denoted as the ''design stage'' of the project, as indicated in Figure 41. During the design stage and the subsequent assessment of the foundation and analysis of the results, the focus is placed on the Eefdesebrug.

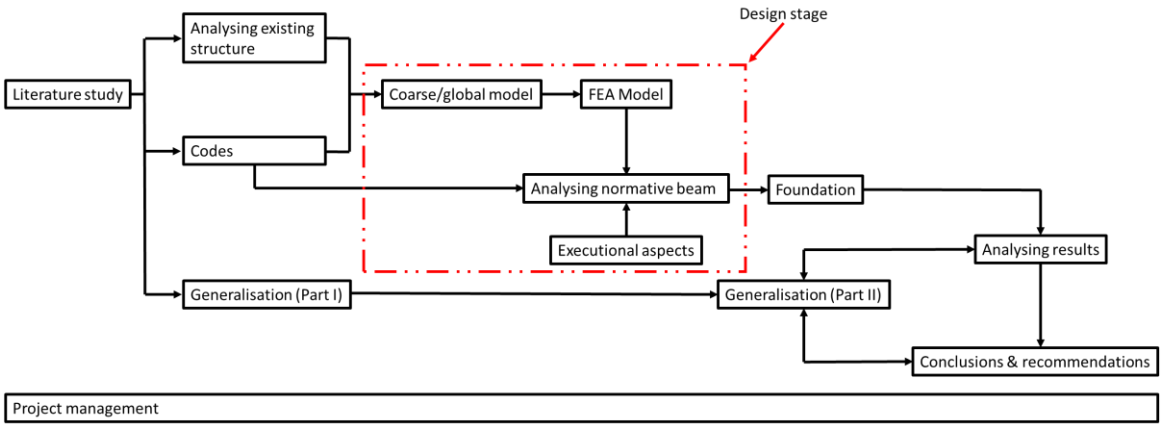

Figure 41 Design stage

6.1.2 Design phases

To organize the design stage of the project in a structured manner it is further decomposed into four design phases. Figure 42 gives an overview of the phases as well as the order in which these will be covered in the elaboration of the new design for the Eefdesebrug.

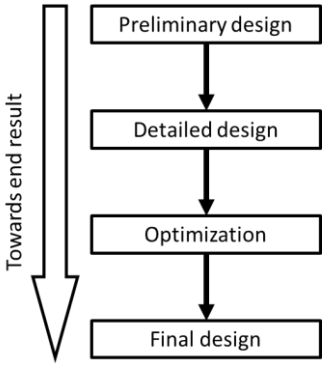

Figure 42 Design phases

By decomposing the design stage into the four aforementioned phases, a more stepwise and coherent approach to the design work is possible, by formulating the goals and identifying the limitations of the results of each step.

6.1.3 Goals and limitations

During the elaboration of each of the design phases specific goals are to be achieved. These are as follows:

- **Preliminary design**: The goals of the preliminary design are to gain insight into the required dimensions of the structure and to determine the feasibility of the project goal based on the self-weight of the structure;

- **Detailed design**: The goals of the detailed design are to perform a more complete and accurate analysis to obtain better insight into the structural behaviour of the bridge, and to identify the best options for optimization;

- **Optimization phase**: The goals of the optimization phase are to investigate the effect of varying different parameters and to determine the most optimal design based on the structures self-weight and the limiting executional aspects;

- **Final design**: The goal of the final design is to finalize the design with which the optimization phase was concluded.

Given the goals for each design phase and the approaches selected to achieve these, there are certain limitations that should be kept in mind during the interpretations of the results of each phase:

- **Limitations preliminary design**: The preliminary design is set up only to obtain the first impressions required to achieve the aforementioned goal. Therefore, only the most basic global verifications are included, i.e. bending moment capacity, shear force capacity and deflections;

- **Limitations detailed design**: Although the detailed design includes a more complete and elaborate set of verifications, no additional optimizations of the design are included;

- **Limitations optimization phase**: While investigating the effect of variation of different parameters, simplifications are made to the approach: not all possible methods of optimizing the design are included;

- **Limitations final design**: In the final design a number of verifications that are not expected to be governing remain only to be mentioned instead of being elaborated completely. Examples are local verifications of ship collision or vibrations.

The final design is the final version of the design as formulated during the optimization phase in which all verifications are satisfied and with which the design stage is concluded. Subsequently the results will be analysed and interpreted during the subsequent phases of the project, as indicated in Figure 41.

6.2 Framework of the design stage

6.2.1 Assumptions

A number of assumptions, boundary conditions and requirements are formulated that will hold for all design phases. For the elaboration of the design a number of assumptions is made to simplify the calculation or to rule out aspects that are not relevant or of lesser importance for the design stage of the project:

- **Horizontal levelling**: Although in reality the bridge deck is not levelled, which is caused by differences in the vertical height of the abutments, this is not considered and the deck is assumed to be levelled in the horizontal plane.

- **Span and width**: For the design the span of the beams is assumed to be equal to the span of the existing bridge deck, the option of moving the supports is not considered. In addition, the total width of the deck has to be equal to the width in the existing situation.

- **Minimum clearance and beam height**: Minimum clearance for shipping is guaranteed by assuming that the bottom side of the deck in the new situation is identical to the existing situation. The numerical value of the beam height is not of relevance for the project, the goal is to optimize the deck. Possible implications and solutions in case the height of the deck in the final design is different compared to the current situation will be discussed in chapter 11.

If additional assumptions have to be made during the further elaboration of the project, these will be clearly mentioned and substantiated.

6.2.2 Boundary conditions and requirements

A number of boundary conditions and requirements will be imposed upon the design. These resulted from the scope of the project as formulated in section 2.2, the findings from the analysis of the existing bridges across the Twentekanaal as formulated in section 4.3.2 and the fact that it is an existing structure that is being considered. The boundary conditions and requirements are:

- **Substructure**: Although the substructure is excluded from the scope it cannot be neglected completely because in reality a new prefab beam deck has to be supported. Therefore, the substructure will be considered if this is required to illustrate that a new beam deck can be constructed, e.g. by constructing a capping beam to support the prefab UHPC elements. The substructure will be considered only up to the extent that is necessary for achieving this purpose.

- **Bridge layout**: For the redesign the existing layout of the bridge deck, i.e. traffic lanes and lanes for pedestrians and cyclists, have to be retained. This requirement is imposed because the new deck is part of an existing road. A sudden change in road alignment is unwanted and potentially dangerous.

- **Positioning of the loads**: The main carriageway and pedestrian lanes are separated by a sufficiently high kerb, as such the traffic load only has to be positioned in between the kerbs. In design codes the positioning of traffic loads is based on the principle of ''future-proof'' design, if the layout of the lanes is changed in the future the structure still has to function. However, because the Eefdesebrug has been in service for decades without such a change it is deemed sufficient to apply the existing alignment, complying to the ''future-proof'' design concept is unnecessarily conservative.

- **Number of vehicles**: For the design traffic loads should be applied corresponding to traffic on provincial roads. This requirement is based on the conclusions from section 4.3.2 and affects the number of vehicles to be considered, which is relevant for fatigue verifications.

7

PRELIMINARY DESIGN

7.1 Outline of the preliminary design

7.1.1 Scope preliminary design

The goal of the preliminary design is twofold, namely to gain insight into the required dimensions of the structure and to determine the feasibility of the project goal. Given these goals the scope of the preliminary design is, in addition to the points mentioned in the previous chapter, defined as follows:

- **Verifications**: Only the most basic global verifications are included, i.e. bending moment capacity, shear force capacity and deflection because these contribute the most to the achievement of the goals of this design phase;

- **Governing beam**: For the same reason only a single beam type will be considered, the governing beam of the deck, and no optimizations are carried out;

- **Loads and situations**: Only the situations of $t = 0$ (manufacturing or placing the beams) and the final situation (bridge during use phase) are considered. Only the permanent loads and vertical traffic loads are included, this is deemed sufficient to achieve the goals of the current design phase.

Other assumptions will be made during the elaboration of the preliminary design wherever required, these will be clearly indicated and substantiated.

7.2 Design of the deck

7.2.1 Main dimensions bridge deck

Conforming 6.2.1 the span of the beams is taken equal to $l = 68{,}0$ m and the total width of the deck is taken equal to $b_{tot} = 16{,}36$ m.

7.2.2 Dimensioning the main beams

Selecting beam type

As discussed in section 3.3.2. there are several types of prefab beams that are commonly applied in the Netherlands. Given the span of 68 m, the Eefdesebrug is at the upper limit of what has been achieved with conventional prefab beams, which means that a beam type has to be selected which is suitable for larger spans. In this regard, box beams are a suitable solution because of their characteristics:

- High slenderness
- High prefabrication implies reduction of construction time
- Large torsional stiffness means that additional cross beams are not required
- Edge beams are not required

Given the span and the characteristics of the box type cross section, applying box beams is the only viable option from the beam types that have been considered.

Height of the beam

Before all other dimensions of the beam are established, the required height is estimated using a rule of thumb. For box beams the slenderness is typically in the range of 28 – 32, the height is estimated as follows:

$$\frac{l}{h} = 30 \qquad \text{Equation (40)}$$

In this equation l denotes the span and h the height of the beam. This results in a height h of approximately 2,3 m.

Type of box beam

It has been established that box beams will be designed. However, within this class of beam types different options are available. As a starting point box beams with widened top flanges ('top hat beams') are assumed. Because of the mechanical properties of UHPC compared to conventional concrete it is expected that this results in a reduction of the material required for the webs and bottom flanges compared to 'conventional' rectangular box beams as seen in Figure 17. Note that in the remainder of the report the beams are simply denoted as 'box beams'.

Cross sectional dimensions

As a starting point it is assumed that five box type beams are applied, this assumed number of beams is based on capacity (i.e. bending moment capacity, shear capacity and bending stiffness), execution (practical dimensions for execution) and material reduction given the excellent material properties of UHPC. Figure 43 gives a sketch of the cross-section with all relevant definitions.

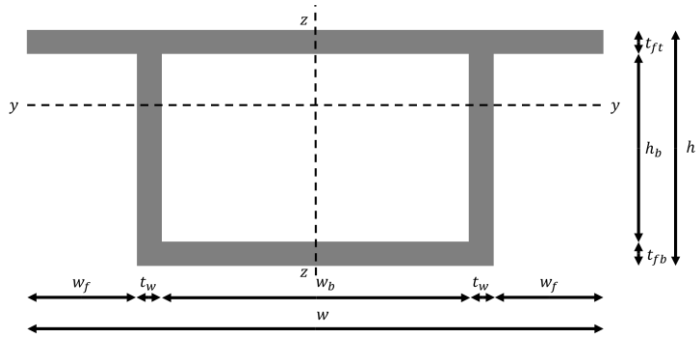

Figure 43 Definitions cross-sectional dimensions

After a value for the total height was assumed, values for the individual parts of the cross section were determined. The internal width w_b and height h_b were subsequently calculated. The assumptions that have been made were based on the requirement of accommodating prestressing strands in the bottom flange and possibly in the webs, the overall stability of the beam, limiting the length of the outstand parts of the top flanges to limit bending moments and to achieve practical dimensions. Table 13 gives an overview of the designed and calculated values.

Table 13 Assumed dimensions box beam

Symbol	Definition	Value [mm]
t_{ft}	Thickness of the top flange	250
t_{fb}	Thickness of bottom flange	150
t_w	Thickness of the web	150
$w_b = w - 2 * t_w - 2 * w_f$	Width of the box	1900
w_f	Width of a single flange	500
$h_b = h - t_{ft} - t_{fb}$	Internal height of the box	1900
w	Total width of the beam	3200
h	Total height of the cross section	2300

With these assumed values four joints with a width of 90 mm are present in between the beams of the deck, for design purposes later on the beams and joints are numbered as depicted in Figure 44.

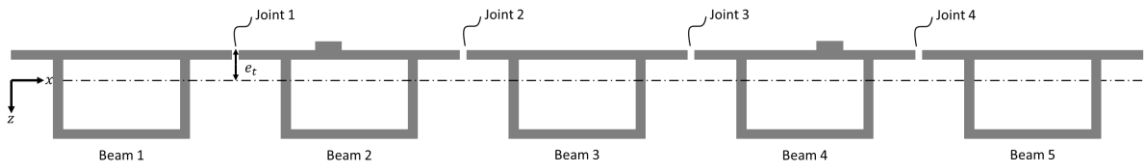

Figure 44 Numbering of beams and joints

7.2.3 Description of the deck

Figure 45 gives a cross section of the proposed preliminary bridge design, which is based on the assumed dimensions of the beam as established in sections 7.2.1 and 7.2.2. The prefab beam deck consists of five UHPC box beams with four longitudinal joints in between.

The beams are supported by a capping beam which is positioned on the existing buttresses that carry the supports of the existing bridge. On top of both of these beams five bearings are placed on which the prefab beams are placed. Once the beams are in place post tensioning is applied through the top flanges in transverse direction. In addition, end cross beams are constructed in-situ and post tensioned. These measures result in a solid deck structure.

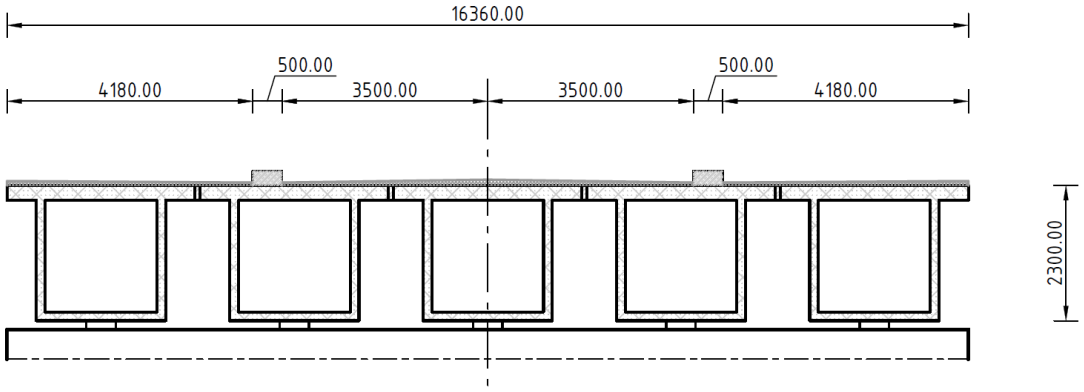

Figure 45 Cross section with the assumed main dimensions

Figure 45 also gives an indication of the layout of the deck. Positioned centrically on the deck is the main carriageway comprising two traffic lanes, one lane for each direction. At the edges of the carriageway concrete kerbs are positioned. On both outer sides a separate pedestrian or bicycle lane is positioned.

For the preliminary design calculation an asphalt layer is assumed on top of the deck with a thickness of 140 mm, which is a value prescribed by the ROK 1.4 of Rijkswaterstaat. This material is assumed to be present over the full width of the deck and accounts for different situations that could be realised in practice, such as creating a profiled cross section (cross slope for dewatering). Conforming the national annex to EN 1991-2, the kerbs that are to be used as traffic obstacle have to be at least 200 mm. Taking into account the height of the pavement, a height of 340 mm is assumed for the kerbs.

7.3 Loads

7.3.1 Load cases

Identifying relevant load cases

For the preliminary design only a limited number of loads is taken into consideration, these are the loads assumed to contribute most to the goal of the design phase. Permanent loads considered are the self-weight of the prefab beams, concrete kerbs and asphalt layer. Variable loads are the vertical traffic loads on the main carriageway and those on the pedestrian/bicycle lanes. These loads are determined according to Eurocode 1. Another load is the prestressing, which will be designed in later sections of the chapter.

Permanent loads – Self-weight of UHPC beams

For the volumetric weight of UHPC different ranges of values can be found in literature. For the preliminary design an upper limit is taken by taking the value $\gamma_{UHPC} = 28{,}0$ kN/m^3 from annex 9 of the AFGC-SETRA 2013 recommendations. The self-weight of the beam as a line load is:

$$G_{k,beams} = A_c * \gamma_{UHPC} \text{ [kN/m]}$$

Permanent loads – Asphalt surfacing

According to table A.6 of Eurocode 1991-1-1 the volumetric weight for hot rolled asphalt is $\gamma_{asphalt} = 23{,}0$ kN/m^3. The asphalt surfacing represented as a line load is:

$$G_{k,asphalt} = t_{asphalt} * \gamma_{asphalt} * b_{eff} \text{ [kN/m]}$$

In this equation b_{eff} equals the beam width plus one times the width of a longitudinal joint (for beams 2 to 4) or the beam width plus half the width of the joint (for beams 1 and 5).

Permanent loads – Kerbs

The kerbs are assumed to be made of reinforced concrete; therefore, a volumetric weight is assumed of $\gamma_{kerbs} = 25{,}0$ kN/m^3. The kerbs represented as a line load are:

$$G_{k,kerbs} = w_{kerbs} * h_{kerbs} * \gamma_C \text{ [kN/m]}$$

Variable loads – Traffic on main carriageway (LM1)

Traffic load models are given in Eurocode 1-2 and for the traffic on the main carriageway load model 1 (LM1) is applied. For the application of this model the deck has to be divided into a number of theoretical lanes. With the deck width w between the kerbs equal to 7,0 m this results in $n_1 = 2$ theoretical lanes with a width $w_1 = 3{,}0$ m and a remaining area with a width of 1,0 m.

Load model 1 is described in 4.3.2 and consists of tandem axles with a load per axle $\alpha_Q Q_k$ and a uniformly distributed load $\alpha_q q_k$. The values for Q_k and q_k depend on the traffic lane 'i' considered. The α_Q and α_q are correction factors to account for the expected type of traffic crossing the bridge. For the preliminary design phase these are taken equal to 1,0. Table 14 gives the values of load model 1 that will be applied.

Table 14 Application of LM1

Lane	$\alpha_Q Q_k$ **[kN/axle]**	$\alpha_q q_k$ **[kN/m^2]**
Theoretical lane 1	300	9,0
Theoretical lane 2	200	2,5
Remaining area	-	2,5

The load model is subsequently applied onto the deck. This should be done in such a way that the most unfavourable situation is obtained. In transverse direction the theoretical lanes can be shifted over the width of the deck. Three different load configurations are possible:

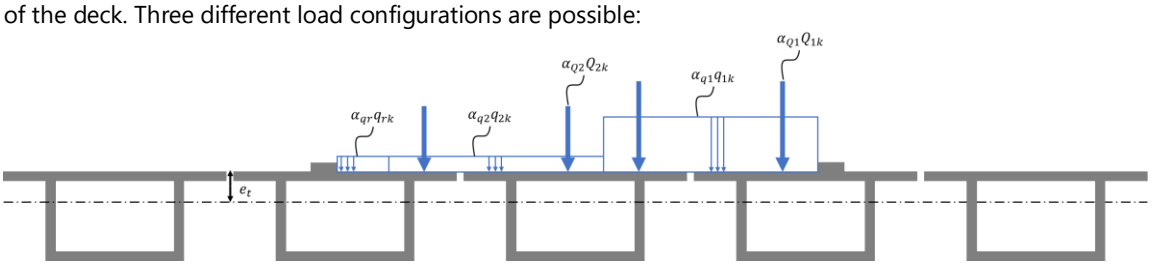

Figure 46 LM1 configuration 1 – Lane 1 next to the kerb

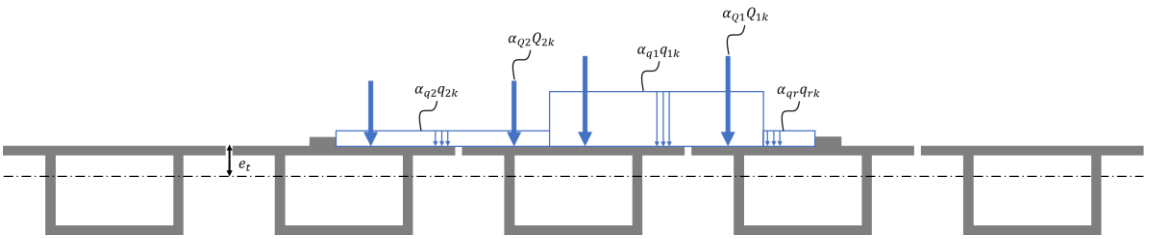

Figure 47 LM1 configuration 2 – Lane 2 next to the kerb

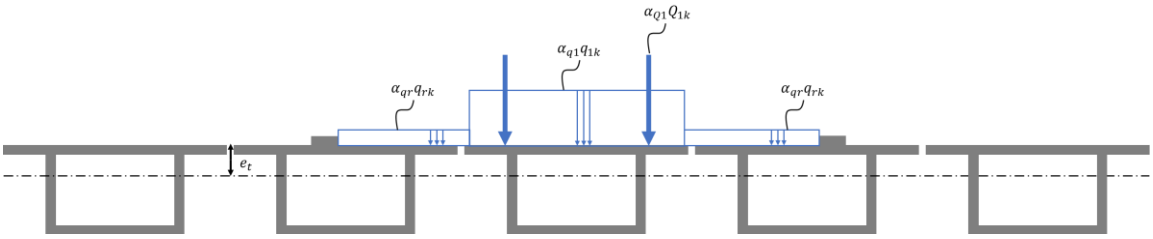

Figure 48 LM1 configuration 3 – Lane 1 centred on middle beam

In addition to shifting the loads in transverse direction, the axle loads can be moved in longitudinal direction, while the axle loads are always centred on their respective theoretical lane. In accordance with the code in transverse direction the axle loads are 2,0 m apart while in longitudinal direction the distance is 1,2 m.

Variable loads – Load on bicycle/pedestrian lanes (LM4)

This load model is described in 4.3.5 and it represents a crowd loading, the basic value is 5 kN/m^2 and the national annex allows for a reduction for bridges longer than 10 m, according to:

$$q_{fk} = 2{,}0 + \frac{120}{L+3}, 2{,}5 \leq q_{fk} \leq 5{,}0\ kN/m^2$$

Assuming L equals the span of the bridge, this results in:

$$q_{fk} = 2{,}0 + \frac{120}{68+3} = 3{,}7\ kN/m^2$$

Prestressing

The prestressing actions are calculated in later sections of this chapter.

7.3.2 Load combinations

Ultimate limit state

Bending moment and shear force capacity are verified in the ultimate limit state (ULS STR). According to 6.4 of Eurocode 0 it has to be verified that:

$$E_d \leq R_d$$

To determine the design values of the effects of actions, load combinations have to be formulated. According to 6.4.3.2, for the STR-limit state the least favourable of the following two expressions (equations 6.10a and 6.10b in the code) should be applied:

$$E_d = \sum_{j\geq 1} \gamma_{G,j} G_{k,j} + \gamma_P P + \gamma_{Q,1}\psi_{0,1} Q_{k,1} + \sum_{i>1} \gamma_{Q,i}\psi_{0,i} Q_{k,i} \qquad \text{Equation (41)}$$

$$E_d = \sum_{j\geq 1} \xi_j \gamma_{G,j} G_{k,j} + \gamma_P P + \gamma_{Q,1} Q_{k,1} + \sum_{i>1} \gamma_{Q,i}\psi_{0,i} Q_{k,i} \qquad \text{Equation (42)}$$

The partial factors γ and the combination factors ψ can be found in annex A of Eurocode 0 and Eurocode 1-2 as well as the corresponding national annexes. The results are:

- $\gamma_G = 1{,}40$ for equation 6.10a, see table NB.16 – A2.4(B) of NA to NEN-EN 1990
- $\gamma_G * \xi = 1{,}25$ for equation 6.10b, see table NB.16 – A2.4(B) of NA to NEN-EN 1990
- $\gamma_G = 1{,}50$, see table NB.16 – A2.4(B) of NA to NEN-EN 1990
- $\psi_0 = 0{,}8$, see table NB.12 – A2.1 of NA to NEN-EN 1990

In addition, it is prescribed in the national annex to Eurocode 1-2 (see table NB.3 – 4.4a) that the characteristic values of LM1 are to be combined with those of LM4 and that the latter is multiplied with a factor of 0,4. Together, these loads form the load group ''gr1a''. This load group can be written as:

$Q_k = 1{,}0 * Q_{k,LM1} + 0{,}4 * Q_{k,LM4}$.

With these provisions, the load combinations from equations (41) and (42) can be written as:

$$E_d = 1{,}40 * \left(G_{k,beams} + G_{k,asphalt} + G_{k,kerbs}\right) + \gamma_P P + 0{,}8 * 1{,}5 * Q_k \quad \text{Equation (43)}$$

$$E_d = 1{,}25 * \left(G_{k,beams} + G_{k,asphalt} + G_{k,kerbs}\right) + \gamma_P P + 1{,}5 * Q_k \quad \text{Equation (44)}$$

Serviceability limit state

Deflections are verified in the serviceability limit state. According to 6.5 of Eurocode 0 it has to be verified that:

$E_d \leq C_d$

The code distinguishes between three different combinations for the serviceability limit state: the characteristic combination, the frequent combination and the quasi-permanent combination. These are applied for irreversible situations (e.g. plastic deformation), reversible situations (e.g. elastic deformation to verify deflections) or long-term effects (e.g. increase of deflection due to creep), respectively. Therefore, the frequent combination is applied:

$$E_d = \sum_{j \geq 1} G_{k,j} + P + \psi_{1,1} Q_{k,1} + \sum_{i>1} \psi_{2,i} Q_{k,i} \quad \text{Equation (45)}$$

In the serviceability limit state, the γ-factors for the loads are set equal to zero while $\psi_1 = 0{,}8$ for the load group gr1a of the variable loads. By plugging in all relevant symbols, equation (45) can be rewritten as:

$$E_d = G_{k,beams} + G_{k,asphalt} + G_{k,kerbs} + P + 0{,}8 * Q_k \quad \text{Equation (46)}$$

7.4 Determining force distribution

7.4.1 Model

Principles & assumptions

To determine the governing beam, internal forces and deflections a simple model is used in which the transverse and longitudinal direction are studied separately. Using the following approach, the deck can be analysed using standard engineering formulas, which is a conservative but justifiable approach for the preliminary design stage.

- **Transverse direction**: First the transverse direction is analysed and the variable loads are positioned as such that the most unfavourable situation is obtained and the governing beam is determined;

- **Longitudinal direction**: Subsequently the longitudinal direction is considered. The axle loads are positioned along the beam, positioned centrically onto their respective lanes in transverse direction, as such that the most unfavourable results are obtained.

After the loads have positioned following this approach the internal forces and deflections are calculated using load combinations in accordance with equations (43), (44) and (46).

The main assumption on which the calculation will be based is that there is no interaction between the different beams. That means that if a concentrated load or an (part of an) uniformly distributed load is placed on a beam, the beam carries this entire force. In reality there is an interaction between the beams which is obtained via post-tensioning of the box beams in transverse direction. However, this effect is neglected at this stage because for a simple model mainly based on hand calculations it cannot be quantified what the contribution of this effect is. Given the relatively slender cross section it is decided to apply a conservative approach. For the preliminary design this approach is justifiable, because the goals are to obtain an impression of the required dimensions and the feasibility of the project.

Transverse direction

The loads are positioned on the deck to determine the internal forces. The only load case of which the positioning has to be determined is the variable load LM1, in section 7.3.1 three different load configurations are presented. Under the assumption that there is no interaction between the beams the most unfavourable situation is obtained when applying configuration 3, see Figure 48, because the full load of lane 1 is carried by a single beam. Given the magnitude of the loads of LM1 with respect to the other load cases, this makes beam 3 into the governing beam. The other beams will therefore not be considered.

The different permanent loads acting on the beams can be converted to line loads. For the middle beam only the self-weight of the beam and the asphalt layer are of relevance. The line load on beam 3 due to the uniformly distributed load is as follows:

$$Q_{k,UDL,LM1} = w_1 * \alpha_{Q1} Q_{1k} + \left(b_{eff,i} - w_1\right) * \alpha_{qr} q_{rk}$$

In this equation $b_{eff,i}$ is the width of the beam increased with twice half the width of the joint, to take into consideration the full width over which the load is applied onto the beam. Two sets of axle loads are also present, these have to be positioned in the most unfavourable position in longitudinal direction.

Longitudinal direction

In longitudinal direction of beam 3 the permanent loads due to the self-weight, asphalt layer and uniformly distributed load are schematized as line loads over the full span of the bridge, see Figure 49.

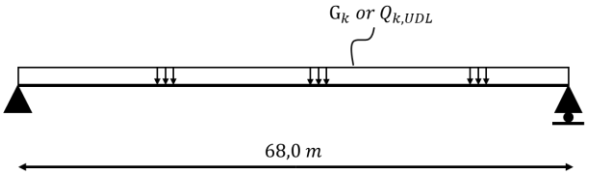

Figure 49 Line loads due to permanent loads or UDL of variable load

The axle loads of load model 1 have to be positioned as such that the most unfavourable situation is obtained. By centring the axle loads around midspan, the maximum bending moment and maximum deflection are obtained, these occur at this location, see Figure 50. To obtain the most unfavourable situation for the shear forces the axle loads should be positioned close to one of the supports. The conservative assumption is made that the support then carries the full load of the set of axles.

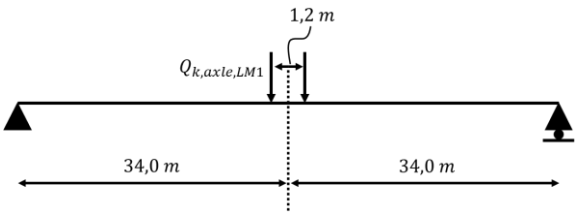

Figure 50 Axle loads positioned to obtain maximum bending moment

7.4.2 Calculation and results ULS

Design values of the loads

The characteristic values of the loads as determined in section 7.3.1 are multiplied with the appropriate factors as determined in section 7.3.2 to obtain the design values of the loads. The internal design forces are subsequently calculated for each individual load, after which these are combined in accordance with the load combinations in equations (43) and (44). The governing values are used as input for the verifications. The equations to determine the internal forces in the governing beam are briefly summarized.

Design values bending moments

The design value of the bending moment at the governing location, which is mid span, for all relevant line loads (q_d may denote the line load accounting for self-weight, the asphalt layer or the uniformly distributed variable load of LM1) is calculated as follows:

$$M_{Ed,UDL} = \frac{1}{8} * q_d * l^2$$

The design value of the bending moment at mid span in case the axle loads are centred around this position are calculated as follows, note the factor '2' to account for the fact that two axles are present:

$$M_{Ed,axle} = \frac{1}{4} * 2 * Q_{d,axle,LM1} * l$$

Design values shear forces

The design value for the shear forces at the governing location, which is at either one of the supports, due to all relevant line loads (q_d may denote the line load accounting for self-weight, the asphalt layer or the uniformly distributed variable load of LM1) is calculated as follows:

$$V_{Ed,UDL} = \frac{1}{2} * q_d * l$$

The design value of the shear force due to the axle loads is calculated by placing the axles close to one of the supports. The conservative assumption is made that:

$$V_{Ed,axle} \approx 2 * Q_{d,axle,LM1}$$

Serviceability limit state

For the calculation of the load effects in the serviceability limit state information regarding the prestressing is required. Therefore, this aspect will be discussed in a later section of this chapter.

7.5 Design calculations and verifications

7.5.1 Material parameters

Concrete

Because no specific UHPC mixture has been chosen at this stage, substantiated assumptions have to be made for the parameters of the UHPC. Table 15 gives an overview of all assumed values. Most parameters are recommended values from the AFGC-SETRA 2013 guideline, which are given as values that can be used

for the first preliminary design calculations if no additional information is available. For concrete in tension these recommended values correspond to a low strain-hardening material. For the maximum compressive strain ε_{cu3} the recommended value from the guideline is taken, while the value ε_{c3} is calculated as follows:

$$\varepsilon_{c3} = \frac{f_{cd}}{E_{cm}} = \frac{85}{50.000} = 1{,}7\ [‰]$$

Note that these strain values result in a shape factor α of 0,69 and a factor β of 0,37. Also required for the calculations is the length of the steel fibres. Based on values from the literature study, a length l_f of 30 mm is taken as a first assumption. In addition, the creep factor is taken equal to 0,8, which is a typical value for UHPC without heat treatment, in the AFGC-SETRA 2013 guideline this is given as an indicative value. For all details regarding establishing these parameters reference is made to annex V.

Table 15 Material parameters – UHPC

Parameters concrete compression			
Definition	**Symbol**	**Value**	**Unit**
Characteristic value compressive stress	f_{ck}	150	[N/mm^2]
Design value compressive strength	f_{cd}	85	[N/mm^2]
Modulus of elasticity	E_{cm}	50.000	[N/mm^2]
Maximum compressive strain at ULS	ε_{cu3}	2,7	[‰]
Strain at reaching concrete compressive strength	ε_{c3}	1,7	[‰]
Parameters concrete tension			
Definition	**Symbol**	**Value**	**Unit**
Characteristic elastic (5% percentile value) tensile strength	$f_{ctk,el}$	9	[N/mm^2]
Design value of tensile strength (tensile strength 1st crack)	f_{ctd}	6,0	[N/mm^2]
Design value maximal post-cracking stress (stress at $w = 0{,}30$)	$f_{ctd;2}$	6,0	[N/mm^2]
Fibre orientation factor (global)	K_{global}	1,25	[-]
Fibre orientation factor (local)	K_{local}	1,75	[-]
Parameters concrete other			
Definition	**Symbol**	**Value**	**Unit**
Factor for shape of concrete compressive zone	α	0,69	[-]
Factor for position centre of gravity of concrete compressive zone	β	0,37	[-]
Factor for long term effects and unfavourable loading (compression)	α_{cc}	0,85	[-]
Factor for long term effects and unfavourable loading (tension)	α_{ct}	1,0	[-]
Fibre length	l_f	30	[mm]
Creep	φ	0,8	[-]

Prestressing steel

For the prestressing steel grade Y1860 is assumed. Table 16 gives an overview of the steel parameters.

Table 16 Material parameters – Prestressing steel

Parameters prestressing steel			
Definition	**Symbol**	**Value**	**Unit**
Characteristic value tensile strength	f_{pk}	1860	[N/mm^2]
Design value steel stress	f_{pd}	1522	[N/mm^2]
Maximum allowed stress directly after tensioning	σ_{pm0}	1395	[N/mm^2]
Modulus of elasticity	E_p	195.000	[N/mm^2]
Characteristic value strain at failure	ε_{uk}	35	[‰]

It is assumed that the beams are prestressed using pretensioned strands with a diameter Ø15,2 mm, with a cross section of $A_p = 140$ mm^2 per strand.

7.5.2 Design of the prestressing

Approach and assumptions

The first calculations that are performed comprise the design of the prestressing. The prestressing is designed under the following assumptions:

- The prestressing is designed in the serviceability limit state, all partial load factors are set equal to 1,0. The requirement that has been formulated is that no tensile stresses are allowed over the cross section, i.e. full prestressing. Although this is conservative, no specific UHPC mixture has been selected. The exact tensile capacity is therefore unknown, making this into a justifiable assumption;

- The prestressing consists of straight prestressing strands positioned in the bottom flange. The centre of gravity of the prestressing strands is at half the thickness of the bottom flange;

- It is assumed that the steel stresses directly after tensioning are equal to the maximum allowable stress (σ_{pm0}) and that the total prestress losses at $t \rightarrow \infty$ equals 20 %.

Determining the required prestressing force

Under the aforementioned assumptions and approach the prestressing force required to keep the cross section in compression in the SLS is calculated, the governing cross section is at mid span. Figure 51 gives the bending moments over the length of the governing beam.

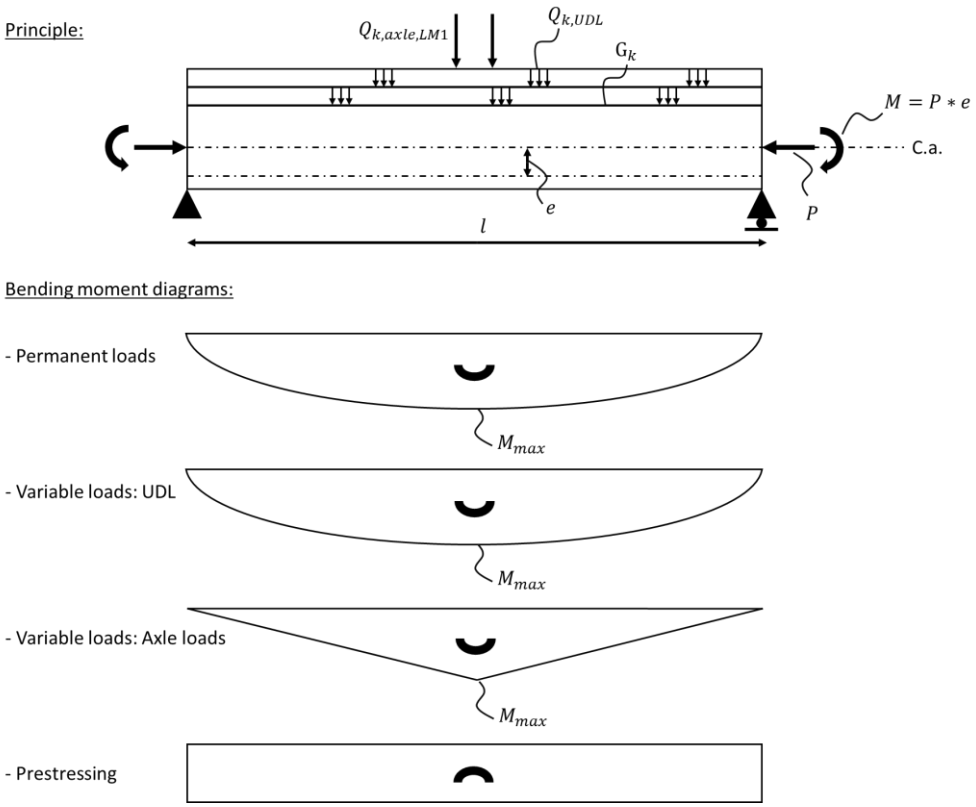

Figure 51 Bending moment distributions

To determine the required prestressing force the stresses in the outer fibres of the cross section at mid span are calculated. Two situations are analysed and in both situations the stresses at the outer fibres should be smaller than or equal to the maximum tensile stress of $\sigma_{max} = 0$ N/mm^2.

The first situation only includes the permanent load and prestressing and is calculated at $t = 0$, which resembles the situation where the beams are just manufactured or just placed at their final position and no variable loads are applied yet. The second situation also includes variable loads and is calculated at $t \rightarrow \infty$, this resembles the use phase.

Figure 52 gives the stresses over the height of the cross section in the first situation. Note that the prestressing causes both a compressive force and an upward bending moment due to the eccentricity between the group of strands and the centroidal axis.

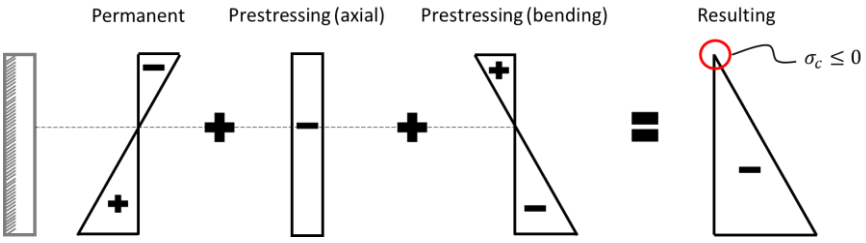

Figure 52 Stresses over the cross section – Situation 1

The stresses at the top and bottom fibre are respectively calculated as follows:

$$\sigma_{c,t} = -\frac{M_G}{W_t} - \frac{P_0}{A_c} + \frac{P_0 * e}{W_t} \quad \text{Equation (47)}$$

$$\sigma_{c,b} = +\frac{M_G}{W_b} - \frac{P_0}{A_c} - \frac{P_0 * e}{W_b} \quad \text{Equation (48)}$$

Figure 53 gives the stresses over the height of the cross section in the use phase. The variable loads are also included and it is assumed that the maximum value of time dependent losses has been reached, thus from the initial prestressing force only the working prestressing force remains. Under the assumption that the losses are 20%, the working prestressing force is $P_\infty = 0{,}8 * P_0$.

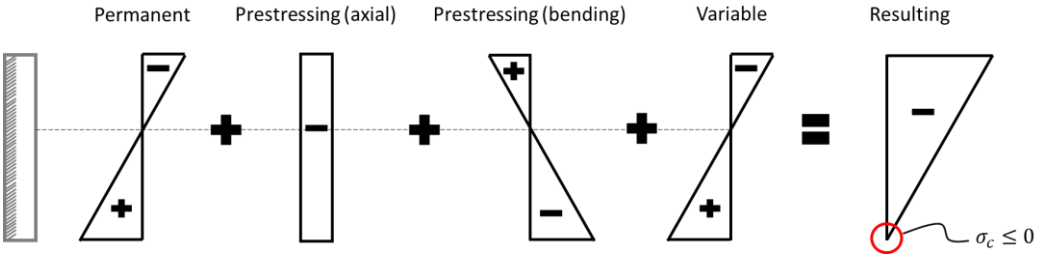

Figure 53 Stresses over the cross section – Situation 2

The stresses at the top and bottom fibre are respectively calculated as follows:

$$\sigma_{c,t} = -\frac{M_G}{W_t} - \frac{0{,}8 * P_0}{A_c} + \frac{0{,}8 * P_0 * e}{W_t} - \frac{M_Q}{W_t} \quad \text{Equation (49)}$$

$$\sigma_{c,b} = +\frac{M_G}{W_b} - \frac{0{,}8 * P_0}{A_c} - \frac{0{,}8 * P_0 * e}{W_b} + \frac{M_Q}{W_b} \quad \text{Equation (50)}$$

The number of prestressing strands is adjusted until the criterion is satisfied that for both situations the tensile stresses at the top and bottom fibre are smaller than or equal to $\sigma_{max} = 0$ N/mm^2. This is an iterative calculation which has been performed using Excel. The result is a required number of 214 strands of Ø15,2 mm.

Concrete cover and spacing

The required strands have to be distributed over the cross section of the bottom flange while providing sufficient concrete cover onto and spacing between the strands. Given the mechanical properties of UHPC compared to conventional concrete, it is expected that the minimum cover and spacing is less than that of conventional concrete.

The AFGC-SETRA 2013 and Eurocode 2 are not considered for these design aspects yet, and the minimum values will be based on values found in literature, see (Russell & Graybeal, 2013) and (Bertram & Hegger,

2012). These sources refer to a cover of $2{,}5 * d$ and a spacing between $2{,}0 - 2{,}5 * d$. Sufficient spacing is required because of force transfer onto the concrete, a value of $2{,}0 * d$ is assumed to be sufficient.

Positioning the tendons turned out the be the stringent criterion for the preliminary design of the beams, with the aforementioned number of strands, dimensions and cover and spacing the required number of strands cannot be accommodated in the bottom flange. Therefore, a number of measures were taken:

- **Strands**: The diameter of the strands is reduced from Ø15,2 mm to Ø13,0 mm. Although this increases the absolute number of strands from 214 to 332 strands, the spacing and cover is reduced, thus a larger cross section of the prestressing steel can be accommodated at the same area;

- **Dimensions**: The dimensions of the beam are adjusted. The total height is increased to 2325 mm, the thickness of the bottom flange is increased to 273 mm. The internal height of the box becomes 1802 mm. The other dimensions are kept equal to those defined in 7.2.2.

Figure 54 gives an overview of the positioning of the strands in the bottom flange of the beam. Note that the centre of gravity of the strand group coincides with the centre of gravity of the bottom flange.

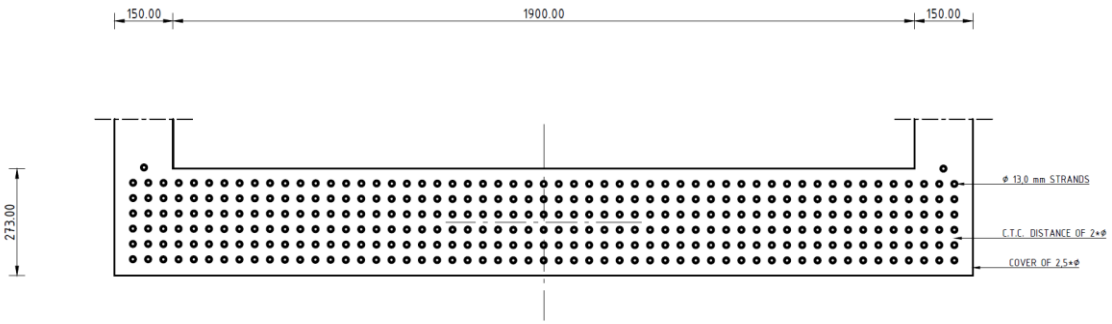

Figure 54 Positioning of prestressing strands in bottom flange

Introduction of prestressing forces

The aforementioned design of the prestressing is based on the mid span cross section. However, near the supports the downward bending moment due to the self-weight is smaller than the upward bending moment due to prestressing. This may cause cracking at the top of the beam if the tensile stresses exceed the maximum value. Although not elaborated on in detail two options are briefly described that can be implemented if measures are to be taken to prevent cracking near the supports.

The first option is that near the supports a number of strands can be bend upwards. The second option is to prevent the bond of a number of strands near the supports, this way the zone over which these strands transfer their forces onto the concrete is moved more inwards towards mid span. Both measures have the result that the upward bending moment near the supports is decreased, the bending moment diagram is 'smoothened' at this region, see Figure 55. As a result the tensile stresses at the top of the beam are reduced.

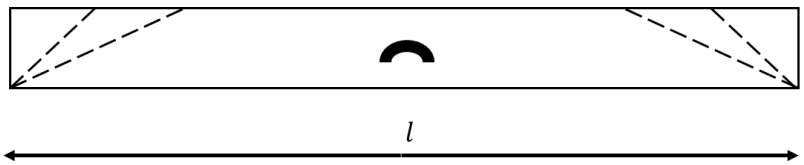

Figure 55 Principle of 'smoothening' the bending moment distribution

7.5.3 ULS verifications – Bending moment capacity

To verify the bending moment capacity in the ULS the following equation has to be satisfied:

$$M_{Ed} \leq M_{Rd}$$

In this equation M_{Ed} is the design value of the bending moment, which is calculated in accordance with section 7.4. If both the permanent and variable loads are considered, then the load combination as given in equation (44) gives the governing value. The bending moment due to the permanent load is 46.924 kNm while the bending moments due to the variable uniformly distributed load and axle load are 24.038 kNm and 15.300 kNm.

The upward bending moment due to the prestressing is 42.086 kNm and is calculated as follows:

$$M_{p,\infty} = P_{\infty} * e_p$$

The design value of the bending moment is:

$$M_{Ed} = M_{Ed,G} + M_{Ed,Q,UDL} + M_{Ed,Q,Axle} - M_{p,\infty}$$

The design value of the bending moment capacity is calculated following the procedure as given in 5.4.2, but with modifications to account of a box type cross section instead of a rectangular cross section. In accordance with 5.3.2.1 of Eurocode 2-1-1 the full width of the top flange may be regarded as part of the effective width, see Figure 56.

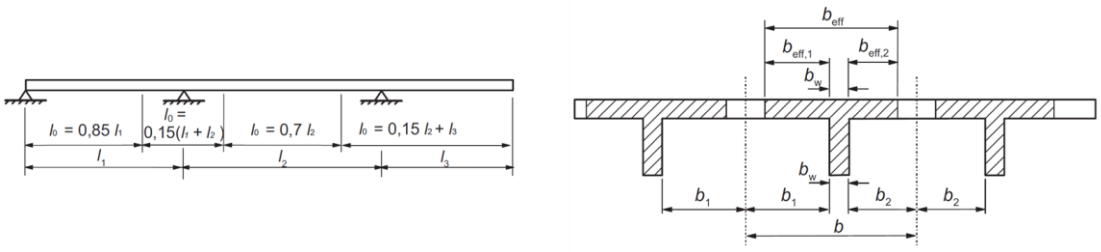

Figure 56 Determining effective flange width – NEN-EN 1992-1-1, p.61-62

In addition, it should be included in the calculation that if the compressive height x_u is larger than the thickness of the top flange, the width of the section is variable. Figure 57 gives the three cases that can be distinguished, these are accounted for in the calculations. Note that the contribution of concrete in tension is calculated only by considering the width of the webs, if a part of the top flange contributes to the tensile concrete capacity this will only be a small value.

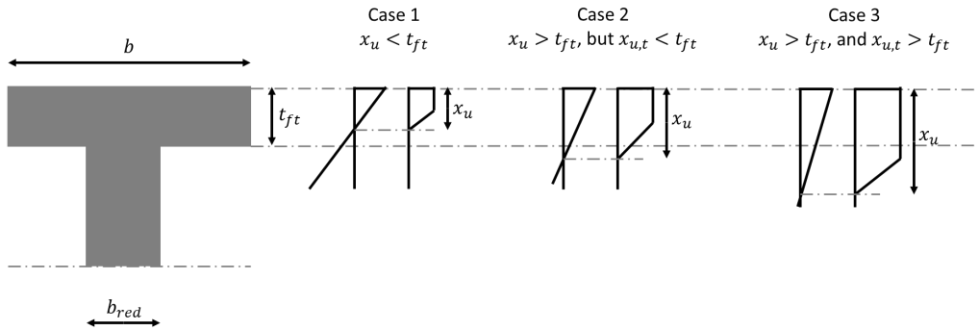

Figure 57 Height of concrete compressive zone and variable width of the cross section

By following the procedure from chapter 5.4.2 with the additional provisions for effective width of the top flanges and variable width over the height of the beam the bending moment capacity can be calculated and the unity check can be performed:

$$UC = \frac{M_{Ed}}{M_{Rd}} \leq 1{,}0 \rightarrow \frac{44.176}{69.130} = 0{,}64$$

In addition, the rotational capacity is verified. Note that the effective height of the strand group, d_p, is taken equal to $d_p = h - 0{,}5 * t_{fb}$.

$$\frac{x_u}{d_p} \leq \frac{\varepsilon_{cu} * 10^6}{\varepsilon_{cu} * 10^6 + 7f} \rightarrow 0{,}14 < 0{,}40$$

The criteria regarding bending moment capacity and rotational capacity are therefore satisfied.

7.5.4 ULS verifications – Shear force capacity

To verify the shear force capacity in the ULS the following equation has to be satisfied:

$$V_{Ed} \leq V_{Rd}$$

In this equation V_{Ed} is the design value of the shear force, which is calculated in accordance with section 7.4, as for the bending moment capacity the load combination as given in equation (44) gives the governing value. The shear force due to the permanent load is 2760 kN, the shear force due to the variable uniformly distributed load is 1414 kN while the shear force due to the axle loads is conservatively taken as 900 kN. The total shear force V_{Ed} therefore is 5074 kN.

The shear force capacity is calculated following the procedure as given in 5.4.3. The width of the shear cross section is taken equal to the summation of both webs: $b_w = 2 * t_w$. The angle of the concrete compressive strut with the beam axis, the angle θ, is taken equal to the minimum angle: 30^o. This results in:

$$UC = \frac{V_{Ed}}{V_{Rd}} \leq 1{,}0 \rightarrow \frac{5074}{7739} = 0{,}66$$

The criteria regarding shear force capacity are therefore satisfied.

7.5.5 SLS verifications – Deflection

Approach

The deflection of the deck is verified in the serviceability limit state using the frequent load combination as given in equation (46). The increase of the deformation due to long term effects is accounted for by applying the effective modulus of elasticity, as given in equation (18). The reduction is applied both to the permanent loads and the variable loads, therefore also covering the potential reduction of stiffness due to effects that occur or may occur over time, such as creep or cracking of the concrete.

The deflections are calculated for the governing beam and the axle loads are positioned at mid span to obtain the largest deflection. Standard engineering formulas are applied to calculate the deflection for each load case separately, after which these results are superimposed to obtain the total deformation. This approach is used because the deflection of the deck is a reversible situation, which is why the frequent combination is applied, and the prestressing is designed as such that the cross section does not crack, implying no reduction of the stiffness after unloading (except for creep effects).

No requirements regarding the maximum allowable deformations are given in the codes because these are defined on a project-to-project basis. Therefore, δ_{max} is taken equal to:

$$\delta_{max} = \frac{l}{300}$$

Calculating the deflection

The deflection of the governing beam is calculated by determining the deflection due to the individual load cases and superimposing the results. The individual contributions are the downward deflection due to self-weight and permanent loads δ_G, the upward deformation due to the prestressing δ_P, the downward deflection due to the uniformly distributed variable loads $\delta_{Q,UDL}$, and downward deflection due to the concentrated variable loads $\delta_{Q,axle}$. The total deflection is:

$$\delta_{tot} = \delta_G - \delta_P + \delta_{Q,UDL} + \delta_{Q,axle}$$

If the expressions for the individual contributions are plugged into the equation, the result is:

$$\delta_{tot} = \frac{5 * G_{k,total} * l^4}{384 * E_{c,eff} * I} - \frac{P_\infty * e * l^2}{8 * E_{c,eff} * I} + \frac{5 * 0{,}8 * Q_{k,UDL,tot} * l^4}{384 * E_{c,eff} * I} + \frac{2 * 0{,}8 * Q_{k,axle,LM1} * l^3}{48 * E_{c,eff} * I}$$

The upward deformation due to the prestressing is denoted as a negative value. When plugging the numerical values into the equation, the result is:

$$\delta_{tot} = 401 - 540 + 137 + 70 = 68 \text{ [mm]}$$

Including all loads, the resulting downward deflection is 68 mm at mid span. The maximum deflection is 227 mm, the deflection criterion is therefore satisfied.

7.5.6 Results of the preliminary design

Based on the cross-sectional dimensions as assumed in 7.2.2 and the loads and load combinations as determined in 7.3.1 and 7.3.2, the preliminary design calculations and verifications have been performed. First the prestressing was designed, this resulted in the conclusion that the initially assumed bottom flange could not accommodate the required prestressing strands.

After modifications to the assumed dimensions and varying the strand diameter, this criterion was satisfied. The bending moment and shear force capacity and deflections were calculated for the governing beam at its governing cross sections (i.e. mid span, support and mid span, respectively). All criteria were satisfied, and the most stringent criterion of those considered in the preliminary design turned out to be accommodating the prestressing strands at the bottom flange. Figure 58 gives the resulting cross section, the full elaboration of the preliminary design and drawings of the results can be found in annex V.

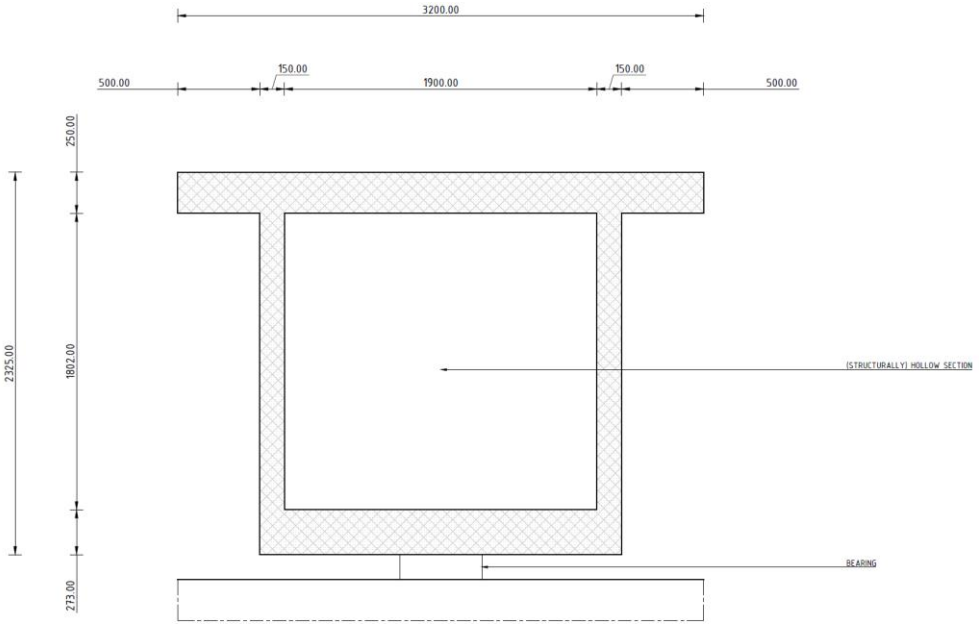

Figure 58 Result of the preliminary design

7.6 Weight comparison

7.6.1 Importance of weight comparison

With the result of the preliminary design an indication has been obtained of the dimensions of the main beam required to satisfy the most basic ULS and SLS verifications, this was the first goal of the preliminary design. The second goal is to determine the feasibility of the project goal, which will be done by comparing the self-weight of the existing bridge with the results of the preliminary design. If the preliminary design results in a significantly larger self-weight, the project goal and approach will have to be reconsidered. If the increase is limited or if the weight of the preliminary design is smaller than that of the existing bridge, the reuse of the foundation of the Eefdesebrug and thus the project goal is deemed to be feasible based on the criterion of self-weight.

7.6.2 Approach

A calculation is made in which the self-weight of the bridge as designed in this chapter and the self-weight of the existing bridge are roughly calculated and compared. The weight of the existing bridge is calculated based on information given in 3.1.2 and original design drawings. The weight of the new design is based on the dimensions in Figure 58 and the permanent loads in 7.3.1.

The preliminary design calculations only involved the design of the main beams while in reality the deck also comprises two end cross beams and capping beams to support the deck. As these are expected to significantly influence the result, dimensions are assumed for these elements as well.

For the end cross beams, it is assumed that post tensioned solid beams are applied over the full width of the deck and that the height and width of the beams is equal to the height of the main beams. This results in a beam with dimensions 2,325 by 2,325 by 16,36 m (height, width, length). A volumetric weight of 25 kN/m^3 is assumed, which corresponds to reinforced and prestressed concrete.

For the capping beam it is assumed that prestressed beams are applied with a volumetric weight of 25 kN/m^3. The length is taken equal to that of the width of the deck, the height is assumed to be 1,0 m and the width is taken equal to 0,75 m. The result is a beam with dimensions 1,0 by 0,75 by 16,36 m (height, width, length).

As a simplification, elements such as bearings, railings, joints and hangers of the existing bridge are not considered. It is not expected that such elements are decisive factors in the calculation. In addition, except for the hangers, these elements are present at both the existing and new bridge. Hence their contributions can be cancelled out of the comparison.

7.6.3 Elaboration and comparison

Estimation self-weight preliminary design and existing bridge

Table 17 gives the results of the weight calculation of the preliminary design as discussed in this chapter.

Table 17 Estimation self-weight preliminary design

	Length	Height/depth	Width	Cross-section	Number	Weight	Result
	[m]	[m]	[m]	[m^2]	[-]	[kN/m^3]	[kN]
Prefab UHPC beams	70,70			1,94	5	28	19.214
In-situ UHPC joints	70,70	0,25	0,09		4	28	178
Cross beams	16,36	2,325	2,325		2	25	4422
Asphalt layer	70,70	0,14	16,36			23	3724
Kerbs	70,70	0,34	0,50		2	25	601
Capping beam	16,36	1,00	0,75		2	25	614
Total							28.753

Table 18 gives the results of the weight calculation of the existing bridge.

Table 18 Estimation self-weight existing bridge

	Length	Height/depth	Width	Number	Weight	Result
	[m]	[m]	[m]	[-]	[kN/m^3]	[kN]
Arches	75,0	1,80	0,90	2	25	6075
Supports arches	8,0	0,36	1,60	4	25	461
Main girders	70,70	1,30	1,90	2	25	8731
Cross beams	7,0	0,80	0,80	12	25	1344
end cross beams	7,0	1,20	1,30	2	25	546
Main deck	70,70	0,25	7,00		25	3093
Deck pedestrian lanes	70,70	0,20	2,78	2	25	1965
Asphalt layer	70,70	0,05	7,00		23	569
Total						22.785

Comparison

According to the results in Table 17 and Table 18 the new design results in a weight increase of 26% compared to the existing bridge. This raises the question where these differences come from and what the implication of this result is on the goal of the project. A number of remarks can be made to these results.

First it is remarked that the comparison is incomplete and is simply a rough estimation. Aspects such as potentially reducing the height of the existing buttresses to place the capping beam or overlap of the cross section of the cross beams and main girders are not considered.

Secondly different principles should be applied to use the UHPC more to its potential, an example is the application of the asphalt layer. Its application is prescribed in the ROK 1.4 while at the same time this is not required from a structural point of view, as illustrated in (Braam, Kaptijn, & Buitelaar, 2003), or in examples in (Fehling, Schmidt, Walraven, Leutbecher, & Fröhlich, 2014). Reducing such a load implies a reduction of the imposed permanent loads and the possibility to design lighter beams.

Thirdly a remark is made on the way in which the design is elaborated. The dimensions are selected and adjusted using rules of thumb, the material parameters are mostly taken from the AFGC-SETRA 2013 guideline and in determining the force distribution and prestressing various conservative assumptions were made. Furthermore, dimensions of for example the end cross beams are solely based on assumptions.

The first two remarks indicate that without extensive further design calculations the weight increase can be reduced considerably. For example, by leaving out the asphalt layer the weight increase is only 10% compared to the current 26%. The third remark indicates that although a well substantiated starting point of the design has been formulated, many possibilities are open to refine and optimize the design.

To summarize, there is a large potential to reduce the weight of the new bridge design by optimizing and refining the design. This potential is deemed to be sufficiently large to obtain a design with a self-weight equal to or lower than the self-weight of the existing bridge. The project goal is therefore deemed to be feasible based on the comparison of the self-weight.

It has to be noted that in realty the self-weight is not the only factor that is of relevance to determine the feasibility of the project. For example, optimisation of the design is also required with regard to the number of prestressing strands. The design resulted in a large number of prestressing strands which might prove to be a challenge in later design stages. The first reason for this is that a large number of strands is required while in reality there are limits to the number of strands can be applied at a prefab concrete factory. The second reason is that casting the concrete, especially if larger fibres are present, might become problematic if the spacing of the strands is limited. Such 'practical' aspects also have to be included in the design.

7.7 Conclusion and prospects

7.7.1 Conclusion preliminary design phase

This chapter covered the preliminary design phase of the project. The goals of this design phase were to gain insight into the required dimensions of the structure and to determine the feasibility of the project goal, based on the self-weight of the structure.

After the type of cross section was selected and, based on rules of thumb, the dimensions were determined, the loads were calculated. A simple model was chosen to calculate the internal forces. Although this was a conservative approach, it enabled the deck to be schematized and analysed using standard engineering formulas.

During the calculation process, the accommodation of the prestressing turned out to be the stringent criterion. Dimensions had to be changed and different strands were applied to satisfy the requirement. Subsequently the bending moment capacity, shear force capacity and deflections were calculated and these criteria were satisfied. This concluded the preliminary design calculations, with which the first goal of the preliminary design was achieved.

Using the designed and verified cross section, a brief weight calculation was performed for the new design and the existing bridge. The results were subsequently compared and interpreted. Although the preliminary design results in a weight increase, there is a large potential to reduce the weight of the new design. Therefore, the main goal of the project is deemed to be feasible, with which the second goal of the preliminary design was also achieved.

7.7.2 Prospects towards later design phases

In addition to the achievement of the aforementioned project goals, the preliminary design phase has also provided insight into opportunities to refine and optimize the design. To conclude this chapter, an overview of possible improvements is given. These will be implemented or taken into consideration in the later design phases.

Material parameters: The assumption of more accurate parameters corresponding to a specific UHPC mixture to be able to use the material to its full potential.

More accurate model: Using a FEM model instead of more practical but conservative approaches contributes to a more optimized design.

Beam design: The number and shape of the beams provides potential to optimization, as those in the preliminary design are only based on rules of thumb, practical values and reference projects.

Prestressing: The design of the prestressing offers possibilities, for example, calculating the actual losses instead of using assumed values might contribute to more economical solutions.

Adjusting requirements: The conservative assumption was made that the beams would have to be prestressed as such that these are in compression over their full height, i.e. 'full prestressing'. However, UHPC has a large tensile capacity. By allowing a limited tensile stress to occur, the required prestressing force will decrease.

Evaluating the loads: By critically evaluating the applied loads the actions on the beams can be reduced, which will result in a more economical design. An example is the asphalt layer, which is not required from a structural point of view.

8

DETAILED DESIGN

8.1 Outline of the detailed design

8.1.1 Setup of the design phase

In the previous chapter the preliminary design was covered. The goals of this first design were to gain insight into the required dimensions of the structure and to determine the feasibility of the project goal based on self-weight. Based on this criterion, it was concluded that the project goal is feasible. Although this was justifiable for this design phase, the remark has to be made that the preliminary design did not cover all relevant aspects and criteria of a design and that it was on the conservative side.

This means that the preliminary design only gives a 'rough estimation' and that further elaboration and optimization is required. This leads to the detailed design as will be discussed in this chapter, the goals of this design are to obtain better insight into the structure and its behaviour and to identify options for optimization.

The detailed design may be regarded as a continuation of the preliminary design. Various options for the improvement and optimization of the design as given in section 7.7.2 are already implemented. The detailed design sets itself apart from the preliminary design because of the following four factors:

- **More accurate assumptions**: More accurate and substantiated input is used compared to the preliminary design. For example, in terms of cross-sectional dimensions, material parameters and design requirements.

- **More complete and accurate model**: All relevant loads are identified, critically assessed and determined in accordance with Eurocode 1. A FEA package is used to determine the global force distribution.

- **More elaborate verifications**: The detailed design covers a more elaborate set of design calculations and verifications.

- **Boundary conditions from practice**: Executional aspects may impose additional boundary conditions upon the project and therefore these are discussed as well.

The implementation of these points results in a more complete overview of the structure, which is required for the achievement of the goals of the detailed design phase. The chapter will be finalized with a weight calculation to compare the results to the results of the preliminary design and to the existing structure.

8.1.2 Scope of the design

Figure 59 gives an overview of all calculations and design verifications included in the detailed design phase. All other assumptions made for the preliminary design and not changed by the points in 8.1.1 also hold for the detailed design phase.

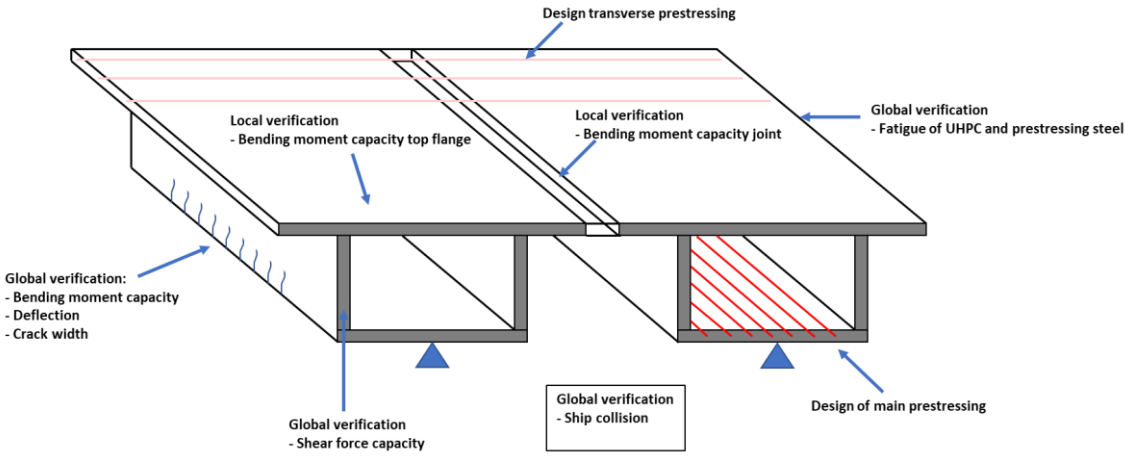

Figure 59 Calculations and design verifications of the main beams

8.2 Design of the deck

8.2.1 Geometry of the structure

The main geometry of the deck is identical to what is described in 7.2.3, except for newer features implemented to improve on the design and the dimensions of the elements required to satisfy the design requirements. However, the dimensions of the main beams and end cross beams have changed, Figure 60 gives the cross section of the deck with the final dimensions as established in the detailed design phase.

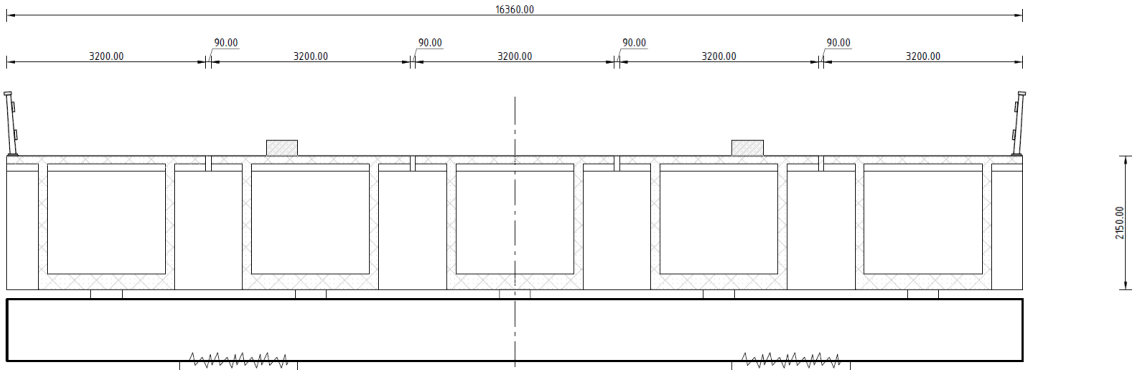

Figure 60 Cross section of the deck

8.2.2 Dimensioning the structural elements

Main beams

The cross section is of the similar type to the section used in the preliminary design. However, the exact dimensions differ and a new feature is the application of prestressing ribs at the top flange. To save material and reduce the weight, the height of the top flange is made variable in transverse direction. Prestressing ribs are applied with a certain centre-to-centre distance to accommodate the post-tensioning cables. In between the ribs, the thickness of the top flange is reduced. Figure 61 shows one such prestressing ribs.

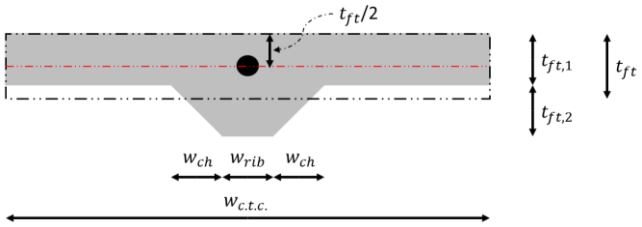

Figure 61 Prestressing rib with variable thickness

To take the variable thickness of the top flange into consideration in a practical way, the mean value of the thickness of the top flange t_{ft} is introduced, see equation (51). In all calculations where the thickness of the top flange is one of the parameters, this mean value will be used. This approach is deemed to be justifiable given the small centre to centre distance between the prestressing ribs.

$$t_{ft} = \frac{w_{c.t.c.} * t_{ft,1} + w_{rib} * t_{ft,2} + 2 * 0{,}5 * w_{ch} * t_{ft,2}}{w_{c.t.c.}} \qquad \text{Equation (51)}$$

For the detailed design the values $t_{ft,1}$ and $t_{ft,2}$ are both taken equal to 125 mm. The values w_{rib} and w_{ch} are taken equal to 250 mm. The centre-to-centre distance $w_{c.t.c.}$ is taken equal to 1000 mm. Table 19 gives the final dimensions of the main beams in the detailed design that resulted from the design verifications.

Table 19 Final dimensions main beams detailed design

Symbol	Definition	Value [mm]
t_{ft} (*weighted average value*)	Thickness of the top flange	187,5
t_{fb}	Thickness of bottom flange	250
t_w	Thickness of the web	150
$w_b = w - 2 * t_w - 2 * w_f$	Width of the box	1900
w_f	Width of a single flange	500
$h_b = h - t_{ft} - t_{fb}$	Internal height of the box	1712,5
w	Total width of the beam	3200
h	Total height of the cross section	2150

The prefab beams are designed with solid end sections at locations coinciding with the locations where the in-situ end cross beam will be constructed after placing the beams. The width of the solid segments is taken equal to the height of the beams.

End cross beams

End cross beams are positioned at the ends of the deck. These are constructed in-situ by casting concrete in between the solid end parts of the beams, and are subsequently post tensioned after sufficient hardening of the concrete. The beams obtained in this manner have a length equal to the deck width. The centre of the beams is assumed to be coinciding with the centre of the supports of the main beams. The height and width of the cross beams are taken equal to the height of the main beams, hence: $h_{cb} = w_{cb} = 2150$ mm.

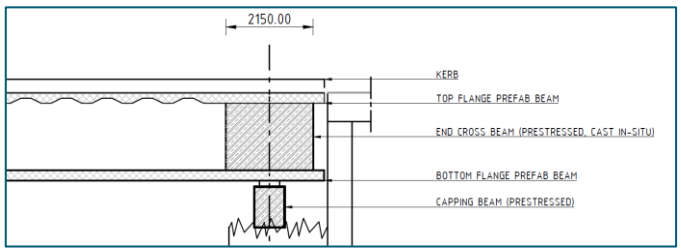

Figure 62 Cross section end cross beam

For calculation purposes it is assumed that the beams are solid over their full length, which is equal to the width of the deck. The overlap with the solid ends of the main beams is neglected in the design calculations.

Longitudinal joints

Figure 63 gives the main dimensions of the joint, it is assumed that the main beams are provided with small 25 mm high cantilevering edges onto which the in-situ concrete of the joints can be casted. The width w_j of the joints is 90 mm while the height t_j of the joint is thus 162,5 mm. For the local verifications of the joints two main assumptions are made in the analysis of the joint. First it is assumed that all dimensions are related to the mean value t_{ft} of the top flange. Second it is assumed that the transverse prestressing is positioned as such that the centre of the tendons coincides with half the mean value of the top flange. Because of the latter assumption the prestressing tendon is positioned centrically with respect to the top flange but always eccentric with respect to the centre of the joint.

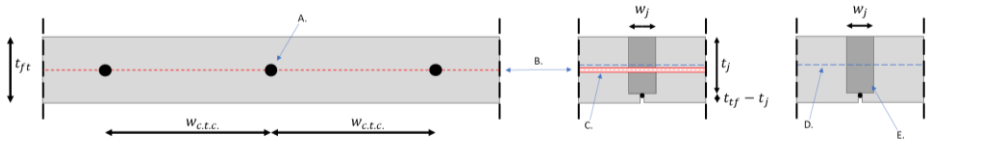

Side view part of the deck | Cross section joint with tendon | Cross section joint without tendon

Symbols:
A. Position prestressing tendon
B. Centre of gravity of prestressing tendon
C. Prestressing tendon
D. Centre of gravity of the joint
E. In-situ concrete (joint)

Figure 63 Longitudinal joint

Capping beam

Although the capping beams are beyond the scope of the design calculations, these are included in the weight calculations. The dimensions are assumed to be identical to those in the preliminary design, hence the dimensions are 16,36 by 1,0 by 0,75 m (length by height by width).

8.2.3 Materials

Overview of different materials

Different types of concrete are applied in the design, as well as different types of prestressing. Table 20 gives an overview of the various materials used, after which each will be covered in more detail.

Table 20 Different materials

Element	Material	Description
Main beams	UHPC	Prefabricated pretensioned elements. Material properties are based on heat treated Ductal FM.
End cross beams	Conventional concrete	In situ elements made of conventional C30/37 concrete, post tensioned.
Longitudinal joints	UHPC	Joints filled using in situ UHPC (based on Ductal JS1000) and subsequently post tensioned.
Prestressing elements	Steel grade Y1860	Prestressing elements are used for the pretensioned and post tensioned elements. Steel quality is Y1860.

Main beams

Defining unambiguous parameters for UHPC is not straightforward. Although commercial products are available there is no specific formulation because mixtures are generally adjusted on a project-to-project basis to optimally meet the requirements for each specific project. As a result, one therefore usually encounters a range of values instead of specific values, which is contrary to conventional concrete with specific values defined in Eurocode 2-1-1. However, for design purposes specific values have to be determined for the required parameters and in order to do so the following approach is used:

- First a number of requirements of the material are listed as well as a description on how the material will be applied.

- Subsequently the parameters of a ''fictitious mixture'' are formulated and substantiated based on literature, while accounting for these conditions and requirements.

Requirements are that the mechanical properties should be at least equal to the recommended values of the AFGC-SETRA 2013 guideline. Higher values for the compressive and tensile strength result in more slender cross sections because less material is required and because passive reinforcement may be omitted. A more slender structure in turn translates into a reduction of the self-weight, and thus into a further contribution to the achievement of the project goal. With regard to application, the use of heat treatment is prescribed. This contributes to achieving a denser microstructure, further enhancing the mechanical properties, but also to a reduction of creep and control of the shrinkage. The latter two are important with regard to the time dependent behaviour of the structure and the calculation of prestress losses.

With these requirements formulated the actual numerical values of the parameters can be established, these will be based on a range of commercial products called Ductal FM. Parameters are based on this range of products because it is covered by the AFGC-SETRA 2013 guideline and supporting information, describing its main features such as high strength, durability and its strain-hardening behaviour, is widely available. In addition, many reference projects can be found that give examples of successful application of the material, where its application resulted in slender structures.

References used to determine the main parameters are (Behloul & Acker, 2004), (Behloul, Durukal, Batoz, & Chanvillard, 2004) and (Behloul & Batoz, 2008). In addition, relationships from the AFGC-SETRA 2013 were applied to determine the design values and values related to time dependent behaviour, while the strain values of the UHPC in compression and the corresponding α and β factors were are based on (Ketel, Willemse, Van Rijen, & Koolen, Rekenmodel VVUHSB (1), 2011). Table 21 gives an overview of the adopted values for the material parameters. For the full elaboration of the table, reference is made to annex VI.

Table 21 Assumed parameters heat treated Ductal FM

Parameters mixture composition				
Definition	**Symbol**		**Value**	**Unit**
Density	ρ		2500	[kg/m^3]
Fibre length	l_f		13	[mm]
Parameters concrete in compression				
Definition	**AFGC**	**Symbol**	**Value**	**Unit**
Characteristic value compressive strength	f_{ck}	f_{ck}	200	[N/mm^2]
Design value compressive strength	f_{cd}	f_{cd}	113	[N/mm^2]
Strain at reaching concrete compressive strength	ε_{c0d}	ε_{c3}	2,3	[‰]
Maximum compressive strain at ULS	ε_{cud}	ε_{cu3}	2,6	[‰]
Parameters concrete in tension				
Definition	**AFGC**	**Symbol**	**Value**	**Unit**
Characteristic elastic (5% percentile value) tensile strength	$f_{ctk,el}$	$f_{ctk,el}$	9	[N/mm^2]
Design value of tensile strength (tensile strength 1st crack)	-	f_{ctd}	6,0	[N/mm^2]
Characteristic value maximal post-cracking stress ($w = 0{,}30$)	f_{ctfk}	-	10,0	[N/mm^2]
Design value maximal post-cracking stress (at $w = 0{,}30$)	f_{ctfk}/(Y *K)	$f_{ctd;2}$	6,15	[N/mm^2]
Fibre orientation factor (global)	K_{global}	K_{global}	1,25	[-]
Fibre orientation factor (local)	K_{local}	K_{local}	1,75	[-]
Parameters stiffness and deformations (temperature, creep and shrinkage)				
Definition	**Symbol**		**Value**	**Unit**
Modulus of elasticity	E_{cm}		50.000	[N/mm^2]
Shear modulus	G		20.833	[N/mm^2]
Poisson ratio	v		0,2	[-]
Coefficient of thermal expansion	α		12*10^{-6}	[K^{-1}]
Creep	φ		0,3	[-]
Autogenous shrinkage (during HT)	ε_{shr}		0,8	[‰]
Parameters concrete other				
Definition	**Symbol**		**Value**	**Unit**
Factor for shape of concrete compressive zone	α		0,56	[-]
Factor position centre of gravity concrete compressive zone	β		0,34	[-]
Long term effects and unfavourable loading (compression)	α_{cc}		0,85	[-]
Long term effects and unfavourable loading (tension)	α_{ct}		1,0	[-]

Note that some of these values are on the more favourable side of the range that can be found in the literature considered. The decision to deliberately assume more optimistic values might seem demanding for mix design and execution, but it is also justified by the following two arguments:

1. Technological advancement: The ranges of values found in the literature are sometimes based on partially dated information. Upper values reached with difficulty some years ago might have become more common over time due to technological advancements in the construction industry;

2. Challenging the industry: Formulating requirements that may provide a challenge to manufacturers and contractors may function as an incentive to innovate. This results in shifting boundaries of what is possible, thus contributing to further technological advancements in the construction industry.

The challenge for execution lies in the fact that the behaviour and performance of UHPC are directly influenced by it. An example is the post-cracking stage behaviour of the material. Reference was made to strain hardening behaviour of Ductal FM, however, this does not only require a high fibre content but also appropriate execution methods because this affects the fibre orientation.

A single fibre should be aligned with the direction of the tensile stress to contribute in the most optimal way and in the ideal theoretical situation the orientation of the fibres is random and thus the material behaviour is isotropic. In practice this is not the case, the orientation and distribution are affected by execution aspects and in calculations this is accounted for by the fibre orientation factor 'K', which is established experimentally. This makes the project demanding with regard to for execution in order to eventually meet the fibre orientation factors assumed for the design and thus the assumed mechanical properties. This may result in having to revise the methods for execution (e.g. casting method or modifications to formwork) to come to the right result.

End cross beams

Given the large cross-sectional dimensions and function of the beams the use of conventional normal strength concrete is deemed to be sufficient for the end cross beams. This results in a more economical solution compared to the application of UHPC given the considerably higher costs of the latter that cannot be justified with a technical reason. The concrete is applied in-situ and the beams are post-tensioned after hardening.

Concrete strength class C30/37 is assumed, this is a common strength class for in-situ concrete which can be achieved without requiring additional measures or provisions. Material parameters are deduced from table 3.1 of Eurocode 2-1-1 (concrete in compression and tension and modulus of elasticity) and calculated in accordance with section 3.14 (creep and shrinkage).

Longitudinal joints

Given the required capacity the longitudinal joints will also be made of UHPC. However, different material properties will be applied than those of the main beams. This is because the concrete of the joints is applied under in-situ conditions, which are usually not as optimal as those in a prefab factory. In addition, it is unlikely that heat treatment can be applied. This results in lower performance compared to the material of the main beams, and thus applying the parameters from Table 21 would be too optimistic.

Table 22 gives the adopted properties for the material of the main joints. These properties are mainly based on the product sheet of Ductal JS1000, which is a material developed for connections and joints in prefab structures. For more detailed information on determining the properties in the table, reference is made to annex VI.

Table 22 Material properties longitudinal joints

Parameters mixture composition – Joint filling				
Definition	**Symbol**		**Value**	**Unit**
Density	ρ		2500	[kg/m^3]
Parameters concrete in compression				
Definition	**AFGC**	**Symbol**	**Value**	**Unit**
Characteristic value compressive strength (4 days)	f_{ck}	f_{ck}	100	[N/mm^2]
Maximum compressive strain at ULS	ε_{cud}	ε_{cu3}	2,6	[‰]
Parameters stiffness and deformations (temperature, creep and shrinkage)				
Definition	**Symbol**		**Value**	**Unit**
Modulus of elasticity (28 days)	E_{cm}		45.000	[N/mm^2]
Creep	φ		0,8	[-]
Shrinkage (long term)	ε_{shr}		0,8	[‰]
Parameters concrete other				
Definition	**Symbol**		**Value**	**Unit**
Factor for shape of concrete compressive zone	α		0,56	[-]
Factor position centre of gravity concrete compressive zone	β		0,34	[-]
Long term effects and unfavourable loading (compression)	α_{cc}		0,85	[-]

Prestressing elements

For the prestressing of the main beams and end cross beams 7-wire strands Ø15,2 of steel quality Y1860 will be applied, the material properties corresponding to this steel grade are given in Table 16. For the pretensioned prestressing these strands are applied individually while for the post-tensioning several strands are combined into tendons.

Main prestressing: Two groups of pretensioned strands are applied. One group provides centric prestressing by means of 10 strands divided over the webs. The centre of gravity of this strand group coincides with the centre of gravity of the cross section. In addition, 120 strands are applied in the bottom flange, the strands are positioned as such that their centre of gravity coincides with half the thickness of the bottom flange.

Transverse prestressing: In transverse direction one tendon comprising five strands is positioned in each prestressing rib.

End cross beam: The end cross beams are prestressed using four tendons consisting of five strands each and these are positioned as such that the centre of gravity of the tendons coincides with that of the beam. This way the resulting prestressing force acts centrically. By dividing the strands over four tendons, the force per tendon is kept limited which allows for the use of smaller anchors and thus for a lower value for the wedge set.

Parameters prestress losses: To calculate the loss due to relaxation it is assumed that all prestressing strands are of relaxation class 2 (low relaxation). For the post-tensioned prestressing (both the top flange and the end cross beams) it is assumed that the friction coefficient μ is 0,23 while the value k for the unintentional rotation due to the Wobble-effect is 0,009 rad. These values are based on those given in 5.10.5.2 of the ROK 1.4. The value of the wedge set depends on the type of anchor used. Under the assumption that smaller anchors are used to limit this contribution to the direct losses, a value of 3 mm is assumed for w_{set}.

8.2.4 Basis of design

Aspects not explicitly covered in the preliminary design phase but nonetheless relevant are notions such as consequence classes and the design service life. These are covered in Eurocode 0 (basis of design) and these notions are related to the basic requirement that a structure should be designed and executed as such that

during its intended service life all actions and influences that may occur can be withstood while satisfying the requirements regarding the use of the structure.

This basic requirement is met by providing sufficient reliability. Structures are classified according to consequence classes and corresponding reliability classes. The main load bearing structure of the Eefdesebrug is classified as a structure in consequence class CC3, given the large potential consequences if the structure would fail.

In addition, the intended design service life has to be specified. During this period the structure has to function in a safe and durable way. The Eefdesebrug will be designed for a minimum design service life of 100 years, which corresponds to consequence class CC3.

8.3 Loads

8.3.1 Load cases

Identifying relevant loads

In the preliminary design only the most basic load cases were considered, being the self-weight of the structure, imposed permanent loads and vertical traffic loads (LM1 and LM4 combined as gr1a). In practice different load cases can be distinguished as well. The following loads are taken into consideration in the detailed design phase:

- Permanent action (G):
    - Self-weight of the structure: The self-weight of the main beams, end cross beams and longitudinal joints;
    - Imposed permanent loads: The imposed permanent loads include a road surface layer, kerbs and a railing;
- Variable action (Q):
    - Vertical traffic loads: Different load models are used for global verifications (LM1 and LM4 combined as gr1a) and local verifications (LM2);
    - Fatigue loads: For the fatigue verification fatigue load model 1 (FLM1) is included;
- Accidental actions (A): Two categories of accidental actions are distinguished. First, traffic accidents due to road traffic may occur, resulting in heavy vehicles being positioned outside the traffic lanes, which is modelled by wheel loads at the edges of the bridge deck. Given the location of the bridge spanning a main shipping route, another possible scenario is ship collision, which is therefore also accounted for.
- Prestressing action (P): This load case comprises the action on the beam due to the prestressing, this will be covered in section 8.5.1.

Loads that are not considered are imposed deformations (settlements, shrinkage and creep), horizontal traffic loads, actions due to rain, wind and snow and imposed deformations due to temperature. Imposed deformations are not of relevance because the structure is statically determinate, thus these deformations are not restrained and do not cause stresses. The only exception is the inclusion of shrinkage and creep into the calculation of the prestress losses. Horizontal traffic loads are not considered because these are especially relevant for the substructure of the bridge instead of the deck. The substructure is excluded from the scope of the project. Loads such as those due to rain, wind and snow are neglected given the small characteristic value in comparison with other loads considered.

Permanent loads – Self-weight of the beams

The self-weight of the main beams and end cross beams is calculated in the same way as given in 7.3.1, the dimensions and values for the volumetric weight are given in 8.2.

Permanent loads – Longitudinal joint

The joints result in line loads along the length of the deck. The cross section of the joint is calculated by multiplying the mean value of the thickness of the top flange with the width of the joint:

$G_{k,j} = t_{ft} * w_j * \gamma_{UHPC}$ [kN/m]

Permanent loads – Surface layer

An asphalt layer is not required from a structural point of view, its thickness is therefore reduced to 10 mm, to account for the presence of a protective or finishing layer. A volumetric weight $\gamma_{asphalt}$ of 23 kN/m^3 is assumed, the surface load is:

$G_{k,surf} = t_{surf} * \gamma_{asphalt}$ [kN/m^2]

Permanent loads – Kerbs

The calculation of the imposed permanent loads is identical to the calculation performed in 7.3.1, no alterations have been made to the dimensions of the kerbs.

Permanent loads – Railing

An estimation of the imposed permanent load due to the railing is made based on the original design values of the existing bridge, after which the value was rounded off to a line load of 0,50 kN/m, hence:

$G_{k,rail} = 0{,}50$ [kN/m]

Variable loads – Traffic on main carriageway – Global verifications (LM1)

For the application of LM1 the deck is divided into theoretical lanes, the exact approach is followed as described in 7.3.1 including the three different load configurations in transverse direction. The application of the load model is the same to that of the preliminary design. The only difference is the application of the reduction factors α_Q and α_q. Given the expected number of vehicles passing the bridge a reduction is deemed to be justified. Based on the national annex to Eurocode 1-2 these values are $\alpha_{Qi} = \alpha_{qi} = 0{,}97$ (to be applied onto all lanes) and $\alpha_q = 0{,}90$. Table 23 gives the resulting characteristic values for the loads after application of the reduction factors.

Table 23 Application of LM1 – Detailed design

Lane	$\alpha_Q Q_k$ **[kN/axle]**	$\alpha_q q_k$ **[kN/m^2]**
Theoretical lane 1	291	8,73
Theoretical lane 2	194	2,424
Remaining area	-	2,25

Variable loads – Traffic on main carriageway – Local verifications (LM2)

For local verifications Eurocode 1-2 prescribes LM2, which consists of a single axle with value $\beta_Q Q_{ak}$ and which can be applied at any point of the carriageway. The contact area represents double tires and is 0,6 m in transverse direction and 0,35 m in longitudinal direction. In accordance with the national annex β_Q is taken equal to α_{Q1}, which is 0,97 in this case. The value of Q_{ak} is 400 kN, this results in an axle load of:

$\beta_Q Q_{ak} = 0{,}97 * 400 = 388$ [kN]

Variable loads – Bicycle/pedestrian lanes – Global verifications (LM4)

The characteristic value of LM4 is calculated in the same way as described in 7.3.1.

Variable loads – Load on railing

Variable loads acting on railings are covered in Eurocode 1-2 and these comprise a horizontal and a vertical line load. Given the presence of the kerbs the railing is assumed to be protected against collision with vehicles from the main traffic lanes. According to the national annex the loads transferred by the railing onto the bridge deck are line loads. These have to be considered once both horizontally and vertically, as a variable load acting at the upper side of the railing. The appropriate value for the Eefdesebrug is a line load of 3,0 kN/m.

$$Q_{k,rail,h} = Q_{k,rail,v} = 3 \text{ [kN/m]}$$

Note that the application of the horizontal load is not expected to give governing results. Therefore, only the variable load is applied in further calculations.

Variable loads – Fatigue loads (FLM1)

Eurocode 1-2 distinguishes a total of five different fatigue load models. At this design stage FLM1 is used to determine the maximum and minimum stresses that occur in the bridge to determine whether the fatigue life can be regarded as infinite or not.

The number of heavy vehicles (N_{obs}) is determined by consulting the following table from the national annex to the code. The values corresponding to provincial roads are used, which is in accordance with the findings summarized in section 4.3.2.

	Verkeerscategorie	$N_{obs,a,sl}$ per jaar en per rijstrook voor zwaar verkeer
1	Autosnelwegen (A-wegen) en wegen met twee of meer rijstroken per rijrichting en met intensief vrachtverkeer	$2{,}0 \times 10^6$
2	(Auto)wegen met gemiddeld vrachtverkeer (zoals N-wegen)	$0{,}5 \times 10^6$
3	Wegen met weinig vrachtverkeer	$0{,}125 \times 106$
4	Wegen met weinig vrachtverkeer en bovendien uitsluitend bestemmingsverkeer	$0{,}05 \times 10^6$
OPMERKING	De aantallen zware voertuigen per jaar en per rijstrook voor zwaar verkeer $N_{obs,a,sl}$ zijn inclusief de trend.	

Figure 64 Number of heavy vehicles – NA to Eurocode 1-2, p.17

The configuration of Fatigue load model 1 is identical to that of LM1. However, the difference is that the numerical values of the loads of FLM1 are only a percentage of those of LM1. The axle loads are equal to $0{,}7 * Q_{ik}$, the uniformly distributed loads are equal to $0{,}3 * q_{ik}$ and the remaining area is $0{,}3 * q_{rk}$. This results in axle loads of 210 and 140 kN for lanes 1 and 2 respectively. The uniformly distributed loads for lane 1 are 2,7 kN/m^2 and 0,75 kN/m^2 for lane 2. The load on the remaining area is also 0,75 kN/m^2. The fatigue loads will be modelled in a similar fashion as configuration 2 of load model 1 with the axle loads at mid span (the governing location for this criterion), as this results in the largest bending moments, see Figure 65.

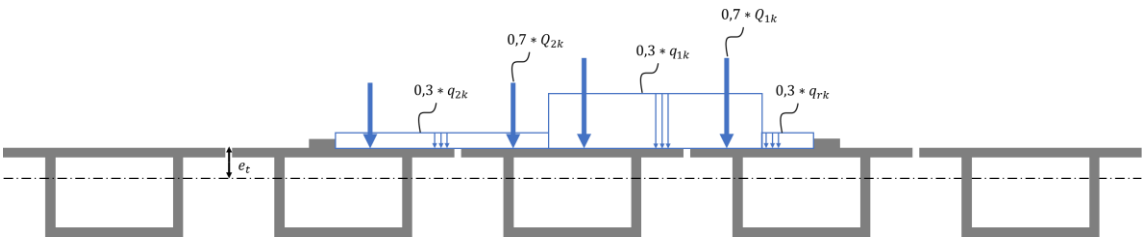

Figure 65 Load configuration FLM1

Accidental actions – Accidental actions due to road traffic

Accidental situations may result in heavy vehicles being present outside the main carriageway. According to the ROK 1.4 this is considered by assuming the outer wheels of the heaviest concentrated loads $2 * Q_{1k}$ to be positioned at the outer edge of the bridge while the remainder of the bridge is loaded by a load with the magnitude of the representative value of the traffic load. Figure 66 indicates how this is modelled: lane 1 is

positioned at the edge of the bridge while the remainder of the main carriageway is loaded by the load corresponding to the remaining area.

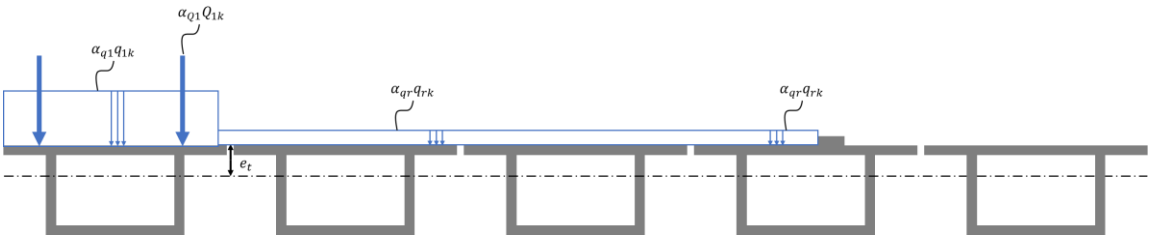

Figure 66 Load configuration traffic accident

Another possible accidental situation is a collision with a kerb, which is covered in Eurocode 1-2 and the ROK 1.4. Given the magnitude of this loads, this load case is not expected to be governing and therefore omitted.

Accidental actions – Accidental actions due to shipping

Load models for collisions with ships are described in Eurocode 1-1-7. It is prescribed that, if this situation is of relevance, the deck of the bridge should be designed as such that it can withstand the equivalent static load due to ship impact in the direction perpendicular to the axis of the deck. According to the national annex the equivalent static force has a magnitude of 1 MN.

8.3.2 Load combinations

Ultimate limit state – STR

The load combinations for the verification of the capacity of the structural components of the deck are formulated as given in 7.3.2, using equations (41) and (42), these are the fundamental combinations for permanent or transient design situations. For the sake of completeness all required factors are listed:

- $\gamma_G = 1{,}40$ for equation 6.10a, see table NB.16 – A2.4(B) of NA to NEN-EN 1990
- $\gamma_G * \xi = 1{,}25$ for equation 6.10b, see table NB.16 – A2.4(B) of NA to NEN-EN 1990
- $\gamma_G = 1{,}50$, see table NB.16 – A2.4(B) of NA to NEN-EN 1990
- $\psi_0 = \psi_1 = 0{,}8$, see table NB.12 – A2.1 of NA to NEN-EN 1990

In addition to the fundamental combinations a number of load combinations is formulated to account for accidental load situations. According to Eurocode 0 these include an accidental action while the other variable loads are reduced by applying factors $\psi_{1,1}$ and/or $\psi_{2,1}$:

$$E_d = \sum_{j\geq 1} G_{k,j} + P + A_d + (\psi_{1,1} \text{ or } \psi_{2,1})Q_{k,1} + \sum_{i>1} \psi_{2,i} Q_{k,i} \qquad \text{Equation (52)}$$

With the application of the appropriate factors and values equation (52) can be written as:

$$E_d = \sum_{j\geq 1} G_{k,j} + P + A_d \qquad \text{Equation (53)}$$

In equation (53) the symbol A_d represents the accidental load, which can be one of the different accidental loads, it is not combined with any other variable load. For the accidental actions due to traffic the accidental action already includes a variable load over the full area of the deck. In case of ship collision other variable loads are left out to obtain the most unfavourable situation with regard to static equilibrium.

Ultimate limit state – FAT

In addition to the ultimate limit state 'STR', the ultimate limit state 'FAT' (fatigue) will be verified as well. Provisions on formulating load combinations for this limit state are found in Eurocode 2-1-1. The code prescribes that the loads have to be divided into non-cyclic and cyclic loads. Two load combinations are formulated:

$$E_d = \sum_{j\geq 1} G_{k,j} + P + \psi_{1,1} Q_{k,1} + \sum_{i>1} \psi_{2,i} Q_{k,i}$$ Equation (54)

$$E_d = \sum_{j\geq 1} G_{k,j} + P + \psi_{1,1} Q_{k,1} + \sum_{i>1} \psi_{2,i} Q_{k,i} + Q_{fat}$$ Equation (55)

The first combination only contains non-cyclic loads and is equal to the frequent combination for the SLS while the second combination includes the cyclic load Q_{fat} and is combined with the most unfavourable combination of non-cyclic loads. These load combinations are subsequently used to determine the stress range required for the fatigue analysis. After substituting the appropriate values and factors the equations (54) and (55) can be written as:

$$E_d = \sum_{j\geq 1} G_{k,j} + P + 0{,}4 * Q_{k,2}$$ Equation (56)

$$E_d = \sum_{j\geq 1} G_{k,j} + P + 0{,}4 * Q_{k,2} + Q_{fat}$$ Equation (57)

Serviceability limit state

The frequent combination in the serviceability limit state is required to verify the deflections. The formulation of this limit state is discussed in 7.3.2, see equation (45). After substituting the appropriate values and factors this equation may be written as:

$$E_d = \sum_{j\geq 1} G_{k,j} + P + 0{,}8 * Q_{k,1} + 0{,}4 * Q_{k,2}$$ Equation (58)

In this equation $Q_{k,1}$ represents load group gr1a of the variable loads and $Q_{k,2}$ represents the variable load acting on the railing of the bridge.

8.4 Determining global force distribution

8.4.1 FEA model

The global force distribution in the bridge deck is calculated using the finite element programme RFEM. Because such a model considers the interaction between different structural elements, this will contribute to obtaining a more economical design compared to the conservative hand calculations as applied in the preliminary design.

The bridge deck is modelled as a beam structure consisting of the five prefab beams and two end cross beams, one at each side. All beams are rigidly connected. The total span of the deck is 68,0 m and the total width is 16,36 m. In addition, a surface element is added, this acts as a 'distribution element' and allows for the interaction between the beams to be taken into account. On one side the beams are supported by hinges while on the other side sliding supports are modelled, the coordinate parallel to the longitudinal axis of the beam is released.

To model the cross sections of the beams, the values as given in 8.2.2 are used. For the distribution element the mean value of the top flange, t_{ft}, is used. The material parameters as given in 8.2.3 are used to define the materials in the programme. Linear elastic isotropic material models are used for both beam types and the surface element. This implies that that the linear elastic behaviour defined using the values in the table is independent from the directions. This resembles the situations in the serviceability limit state where the concrete is uncracked, which is reasonable because the prestressing in longitudinal and transverse direction will be designed as such that cracking will not occur. Figure 67 gives an overview of the RFEM model.

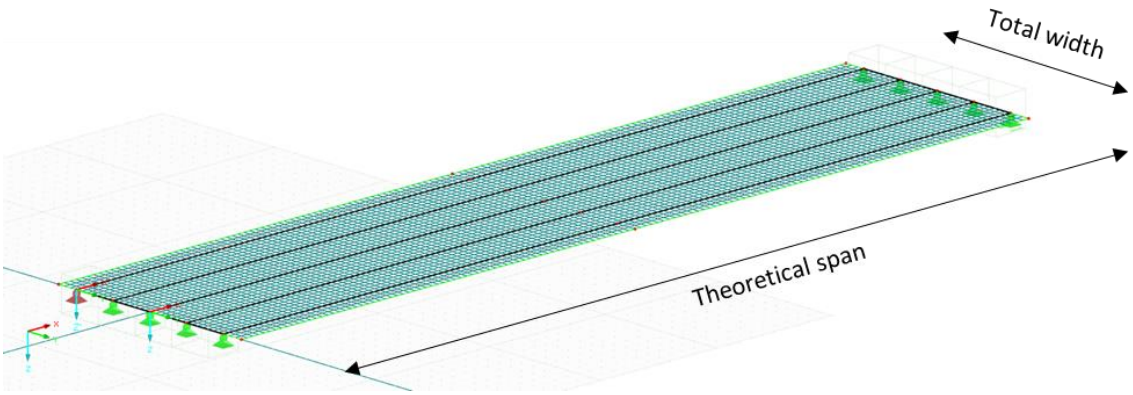

Figure 67 Finite element model in RFEM

The different loads and load combinations as defined in section 8.3 are modelled in the programme. For more details on the input of the loads reference is made to annex VI. A geometrically linear analysis is performed, equilibrium is thus based on the undeformed structure. For the mesh of the surface element the default values of RFEM are used, which is a mesh with target length of 0,5 m for the finite elements. Given the dimensions of the deck this is deemed to be an appropriate value.

8.4.2 Calculation and results

After performing the calculations, the various load combinations are combined into result combinations to determine the various governing values that are required. These values will be used to design the prestressing and to perform the verifications.

Main beams

Beam 3, see Figure 44, is the governing beam. For the ultimate limit state, the design value of the bending moment M_{Ed} is 48.426 kNm, the shear force V_{Ed} is 4090 kN and the torsional moment T_{Ed} is 1222 kNm. The shear force is determined conservatively by taking the shear force equal to the support reaction. At beam 2 a torsional moment was found which is larger than the value at beam 3. However, with the combination of shear and torsion beam 3 turned out to be governing and is thus mentioned in this verification.

For the fatigue verification the bending moment at mid span for the combination without cyclic load is 27.183 kNm while the value for the combination including the cyclic load is 31.539 kNm.

To design the prestressing the characteristic combination in the serviceability limit state is applied, which at mid span resulted in a bending moment $M_{E,G,perm}$ of 1727 kNm due to all imposed permanent loads and $M_{E,Q}$ is 9694 kNm due to the variable loads.

To verify the deflections of the beam the frequent load combination in the serviceability limit state is applied, this results in a maximum deflection δ_{max} is 344,4 mm at mid span of beam 3. Note that this value does not yet include the upward bending due to the prestressing.

End cross beam

For the ultimate limit state of the end cross beam the design value of the hogging bending moment $M_{Ed,hog}$ is 1212 kNm, the sagging bending moment is $M_{Ed,sag}$ is 436 kNm and the shear force is V_{Ed} is 837 kNm.

To design the prestressing the characteristic combination in the serviceability limit state is applied, which resulted in a maximum hogging bending moment $M_{E,hog}$ of 469 kNm and a maximum sagging bending moment $M_{E,sag}$ of 298 kNm.

Top flange – Local verifications

The internal forces of the top flange for the local verifications will be calculated manually in section 8.6.

8.4.3 Validation of the RFEM model

Validation

A validation of the RFEM model has been performed to confirm that the results used for the design are in a realistic order of magnitude. To perform the validation the following load cases in RFEM were compared with hand calculations: self-weight of the prefab beams, permanent loads due to the surface layer, uniformly distributed load with lane 1 positioned on the middle beam and the axle loads at mid span.

Qualitative validation

First the results are judged qualitatively by means of the boundary conditions. Because of the supports the displacements at the edges of the deck should be equal to zero. Figure 68 gives the results for the axle loads for example. It can be seen that the results are as to be expected. The deflection is zero at the edges and at is maximum at mid span. The other load cases confirm this impression and based on the qualitative aspects the results from the model are correct.

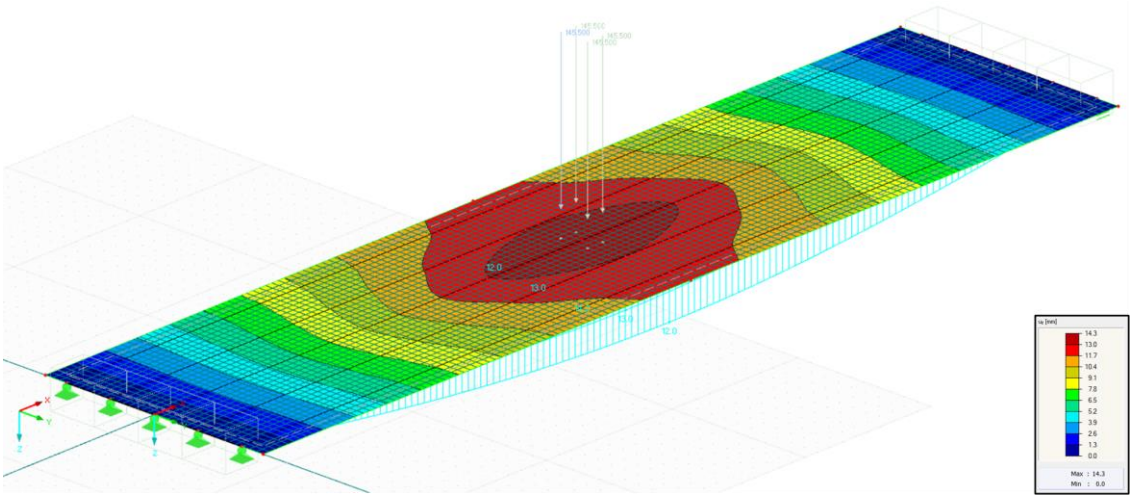

Figure 68 Deflections bridge deck due to axle loads at midspan

Quantitative validation

Subsequently a brief quantitative validation is performed by comparing a hand calculation and comparing the results with RFEM. An important part of this calculation is to quantify the effect of the beam interaction due to the 'distribution element'.

The bending moments at midspan calculated using RFEM are 23.997 kNm due to the self-weight of the prefab beams, 434 kNm due to the self-weight of the road surface, 5465 kNm due to the uniformly distributed variable load and 2769 kNm due to the variable axle loads (total bending moment due to variable loads thus is 8234 kNm). The total bending moment at mid span is 32.665 kNm.

To calculate the bending moments manually the initial assumption is made that, given the thickness of the top flange, approximately 50% of the variable loads is redistributed. The bending moment due to the self-weight of the beams and the road surface layer is:

$$M_G = \frac{1}{8} * \left(G_{k,beams} + b_{eff,i} * G_{k,surf}\right) * l^2 \rightarrow M_G = \frac{1}{8} * (41{,}59 + 3{,}29 * 0{,}23) * 68{,}0^2 = 24.476\ [kNm]$$

The bending moment due to the variable load is:

$$M_Q = \frac{1}{8} * 50\% * \left(\alpha_{q1} q_{1k} * w + \left(b_{eff,1} - w\right) * \alpha_{rk} q_{rk}\right) * l^2 + \frac{1}{4} * 50\% * 2 * \alpha_{Q1} Q_{1k} * l$$

$$M_Q = \frac{1}{8} * 50\% * (8{,}73 * 3{,}0 + (3{,}29 - 3{,}0) * 2{,}25) * 68{,}0^2 + \frac{1}{4} * 50\% * 2 * 291 * 68{,}0 = 12.705\ [kNm]$$

The total bending moment M_{tot} is 37.181 kNm. The difference between the hand calculation and RFEM is approximately 14%. Although this is deemed to be an acceptable difference when comparing a hand calculation with a FEA model, the question is what explains the difference.

Given the results for the self-weight and road surface layer, the difference should be sought for in the variable loads. If only the variable loads are considered, the difference between the hand calculation and the RFEM results is:

$$\Delta = \frac{(12.705 - 8234)}{8234} * 100\% \approx 54\%$$

Although the difference may be partially explained by the fact that the hand calculation does not include all the loads that are modelled in RFEM, the largest contributor is expected to be an underestimation of the effect of the beam interaction. If it is assumed that only the axle loads are present at mid span without a reduction, then theoretically the bending moment would be:

$$M_Q = \frac{1}{4} * 100\% * 2 * 291 * 68 = 9894\ [kNm]$$

The RFEM model results in a bending moment of 2769 kNm, this means that the reduction due to the force redistribution is approximately 70%. Thus, only approximately 30% of the variable load remains at the main beams. If the hand calculation is performed once more using this value, the bending moment at midspan due to the variable loads is:

$$M_Q = \frac{1}{8} * 30\% * (8{,}73 * 3{,}0 + (3{,}29 - 3{,}0) * 2{,}25) * 68{,}0^2 + \frac{1}{4} * 30\% * 2 * 291 * 68{,}0 = 7622\ [kNm]$$

This value is closer to the RFEM result. The differences between the RFEM model and the hand calculation are therefore explained. As a part of the preliminary design report, see annex V, the effect of the redistribution was studied in a sensitivity analysis. In this analysis a similar value for the redistribution was found. The results in this calculation are of the same order of magnitude and therefore the deck is considered to be modelled correctly in RFEM and to produce results in the correct order of magnitude.

8.5 Global design calculations and verifications

8.5.1 Design main prestressing

Approach

The prestressing is designed and detailed using the following procedure:

- A number of strands is assumed (see section 8.2.3);
- The prestress losses are calculated to determine the initial and working prestressing force;
- Stresses over the height of the cross section are verified at mid span;
- Various aspects of the detailing are covered.

Positioning and assuming number of strands

As discussed in 8.2.3 two groups of strands are applied. One group of 10 strands is applied centrically while one group of 120 strands is applied eccentrically, with the centre of gravity of the group coinciding with that of the bottom flange. The eccentricity with respect to the centre of gravity of the cross section is:

$$e_p = e_b - \frac{1}{2} * t_{fb} \qquad \text{Equation (59)}$$

Figure 69 shows the positioning of the strands over the cross section.

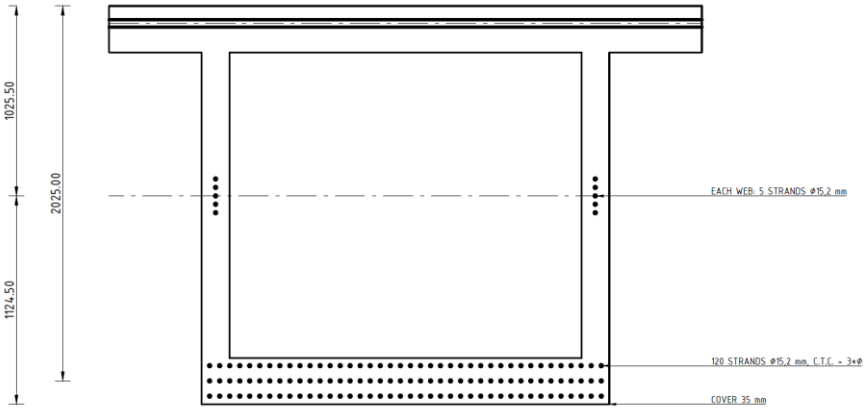

Figure 69 Positioning of the pretensioned strands in the prefab beams

Calculating prestress losses

The prestressing is designed for the governing cross section: mid span of the governing beam. The prestress losses of both strand groups are calculated separately, and are only related through the compressive force in the concrete. The direct loss is caused by elastic losses while for the time dependent losses shrinkage, creep and relaxation are considered. The elastic loss of both strand groups is calculated as:

$$\Delta P_{el} = \frac{\alpha_e \rho_p f}{1 + \alpha_e \rho_p f} * P_{max}$$ Equation (60)

In this equation $\alpha_e = E_p/E_c$, $\rho_p = A_p/A_c$ and $f = (1 + A_c e_p^2/I_c)$. The initial prestressing force is subsequently calculated as $P_{m0} = P_{max} - \Delta P_{el}$. The total time dependent loss is calculated following the simplified expression given in the Eurocode, see equation (61):

$$\Delta P_{c+s+r} = A_p * \Delta\sigma_{p,c+s+r} = A_p * \frac{\varepsilon_{cs} E_p + 0{,}8\Delta\sigma_{pr} + \frac{E_p}{E_{cm}}\varphi(t,t_0)\sigma_{c,QP}}{1 + \frac{E_p}{E_{cm}}\frac{A_p}{A_c}\left(1 + \frac{A_c}{I_c} z_{cp}^2\right)[1 + 0{,}8 * \varphi(t,t_0)]}$$ Equation (61)

During this calculation the stresses in the steel and concrete are also verified. Note that in this equation three terms can be distinguished in the numerator. From left to right one can identify the term for shrinkage of the concrete, relaxation of the prestressing steel and creep of the concrete. The expression for relaxation follows from equation (9).

Heat treatment is assumed to be applied and this will affect the phenomena of creep, shrinkage and relaxation. The effect on creep is accounted for by assuming an appropriate value for the creep factor φ. Common values for heat treated UHPC are in the range of 0,2 to 0,4 whereas for UHPC without heat treatment the values are higher. As can be seen in Table 21, a value of 0,3 was assumed.

Although the magnitude of the shrinkage does not change, it is affected by the heat treatment in the sense that all shrinkage occurs during the application of the treatment. A strain value ε_{cs} of 0,8 ‰ is assumed, which is based on the values for Ductal as given in the AFGC-SETRA 2013 guideline. Calculating the time dependent loss due to shrinkage of a pretensioned and heat-treated beam involves uncertainty. As a conservative approach the upper limit of the loss is calculated by fully including the shrinkage strain in equation (61), while in reality a certain reduction of the shrinkage losses may occur due to the treatment.

The effect of the heat treatment on the relaxation loss of the prestressing steel can be quantified by following the provisions from Eurocode 2-1-1, which prescribes calculating the equivalent time 't_{eq}', see equation (62), and subsequently adding up this value to the prescribed $t = 500.000$ hours from equation (9).

$$t_{eq} = \frac{1{,}14^{T_{max}-20}}{T_{max} - 20} * \sum_{i=1}^{n} \left(T_{(\Delta t_i)} - 20\right)\Delta t_i$$ Equation (62)

In the equation t_{eq} is the equivalent time, $T_{(\Delta t_i)}$ the temperature during time interval Δt_i and T_{max} the maximum temperature during the treatment. One interval is considered, the elements are heated up to approximately 90 °C for a period of 48 hours. Hence $\Delta t_1 = 48$ h, $T_{(\Delta t_1)} = 90$ °C and $T_{max} = 90$ °C, resulting in:

$$t_{eq} = \frac{1{,}14^{90-20}}{90-20} * (90-20) * 48 = 461.935\ h$$

The stress $\sigma_{c,QP}$ in the concrete surrounding the tendons is calculated by considering the permanent loads, imposed permanent loads and prestressing actions. Note that both strand groups are coupled through this equation because they influence the compressive stresses at the centre of the other strand groups. The working prestress forces are subsequently calculated as:

$$P_{m,\infty} = P_{m0} - \Delta P_{c+s+r} \qquad \text{Equation (63)}$$

Table 24 summarizes the results of the calculation. For more detailed information on the calculation of the prestress losses or the design of the prestressing reference is made to annex VI.

Table 24 Summary of results calculating prestressing forces and losses

Strand group	**Prestressing forces**			**Prestress losses forces**			
	$\boldsymbol{P_{max}}$	$\boldsymbol{P_{m0}}$	$\boldsymbol{P_{m,\infty}}$	$\boldsymbol{\Delta P_i}$	$\boldsymbol{\Delta P_{c+s+r}}$	$\boldsymbol{\Delta P_{tot}}$	$\boldsymbol{\Delta P_{\%}}$
Prestressing:	[kN]	[kN]	[kN]	[kN]	[kN]	[kN]	[%]
Centric	1946	1940	1615	6	325	331	17,0
Eccentric	24.360	22.269	18.581	2091	3688	5779	23,7

Stresses over the height of the cross section

The prestressing forces are subsequently used to calculate the stresses over the height of the cross section in two different situations. This way it can be verified whether the prestressing force is sufficiently large to meet the stress limit criterion that will be formulated. Two 'limit cases' are considered, if the prestressing force is sufficient for these cases, it will also be sufficient for all intermediate situations:

- The first case only includes the self-weight and prestressing at time $t = 0$ and covers all situations where only the self-weight and prestressing are present, e.g. the beam after demoulding, in storage or when hoisting the beam into position.

- The second case is calculated at $t \to \infty$ and covers the situation where the bridge has been in service for a considerable time. The prestressing force is reduced to the working prestress $P_{m,\infty}$ and combined with the maximum value of the loads.

Self-weight and prestressing only ($t = 0$): For the first case the stresses at the outer fibres are calculated as follows:

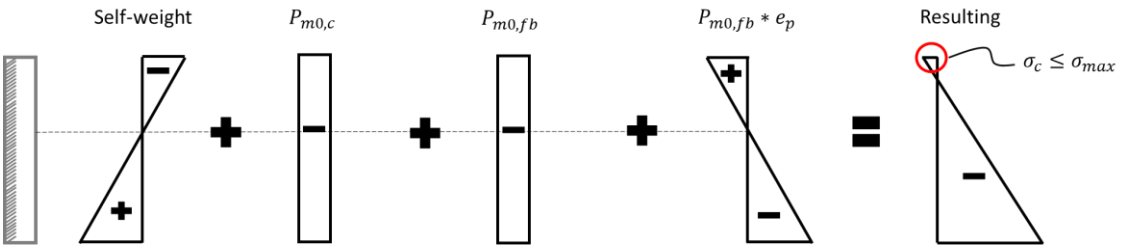

Figure 70 Stresses over the height of the cross section - Situation 1

$$\sigma_{c,t} = -\frac{M_{G,sw}}{W_t} - \frac{P_{m0,c}}{A_c} - \frac{P_{m0,fb}}{A_c} + \frac{P_{m0,fb} * e_p}{W_t} \leq \sigma_{max} \qquad \text{Equation (64)}$$

$$\sigma_{c,b} = +\frac{M_{G,sw}}{W_b} - \frac{P_{m0,c}}{A_c} - \frac{P_{m0,fb}}{A_c} - \frac{P_{m0} * e_p}{W_b} \leq \sigma_{max} \qquad \text{Equation (65)}$$

Use phase ($t \rightarrow \infty$): For the second case the stresses at the outer fibres are calculated as follows:

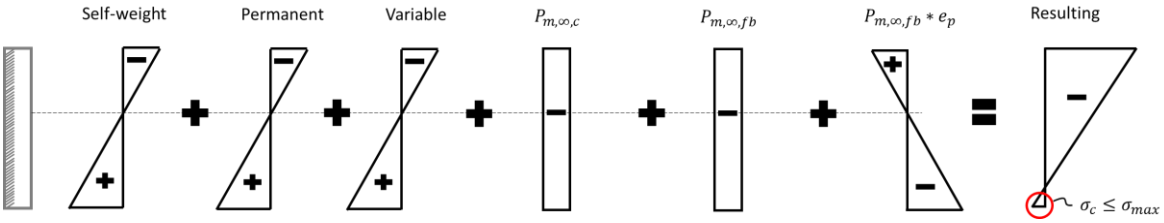

Figure 71 Stresses over the height of the cross section - Situation 2

$$\sigma_{c,t} = -\frac{M_{G,sw}}{W_t} - \frac{M_{G,perm}}{W_t} - \frac{M_Q}{W_t} - \frac{P_{m,\infty,c}}{A_c} - \frac{P_{m,\infty,fb}}{A_c} + \frac{P_{m,\infty,fb} * e_p}{W_t} \leq \sigma_{max} \quad \text{Equation (66)}$$

$$\sigma_{c,b} = +\frac{M_{G,sw}}{W_b} + \frac{M_{G,perm}}{W_t} + \frac{M_Q}{W_b} - \frac{P_{m,\infty,c}}{A_c} - \frac{P_{m,\infty,fb}}{A_c} - \frac{P_{m,\infty,fb} * e_p}{W_b} \leq \sigma_{max} \quad \text{Equation (67)}$$

In these equations the subscript 'c' is used to denote the centric strand group and the subscript 'fb' is used to denote the eccentric group. $M_{G,sw}$ is the bending moment due to the self-weight of the beams only, $M_{G,perm}$ is the bending moment due to superimposed permanent loads and M_Q is the bending moment due to variable loads. The latter two are calculated using RFEM.

Verification: Using equations (64) to (67) the stresses in the outer fibres are determined and the following graphs show the stresses due to permanent loads, variable loads and the total stresses. The blue lines indicate the stresses due to the self-weight (left graph) or all permanent loads (right graph), the orange lines denote stresses due to the variable loads and the green lines indicate the total stresses after the addition of the stresses due to the prestressing.

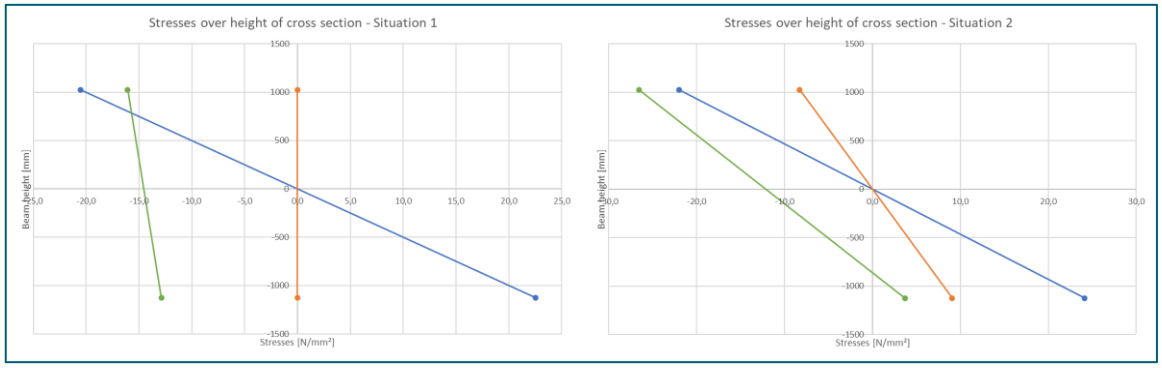

Figure 72 Calculated stresses over the beam height

The maximum tensile stress is 3,7 N/mm^2, which is smaller than the maximum value of 6,7 N/mm^2, the criterion is therefore satisfied. The maximum value follows from provisions given in the AFGC-SETRA 2013 guideline, see section 8.5.8.

Detailing of the beam ends

Various calculations and verifications have been performed with respect to the detailing of the beam ends, an overview is given in this section and for a more detailed discussion reference is made to annex VI.

- **Transmission length**: Pretensioned prestressing steel transfers its forces onto the concrete via bond, which requires a certain transmission length. The bond stress and transmission length has been calculated for both strand groups.

- **Tensile stresses at the top fibre**: As discussed in 7.5.2 The design of the prestressing is based on the mid span cross section while near the supports tensile stresses may occur due to the upward prestressing in combination with a limited bending moment due to the self-weight. The stresses

have been calculated from which it was found that, although tensile stresses occur, the tensile stresses remain below the limit value. See Figure 73 for the results.

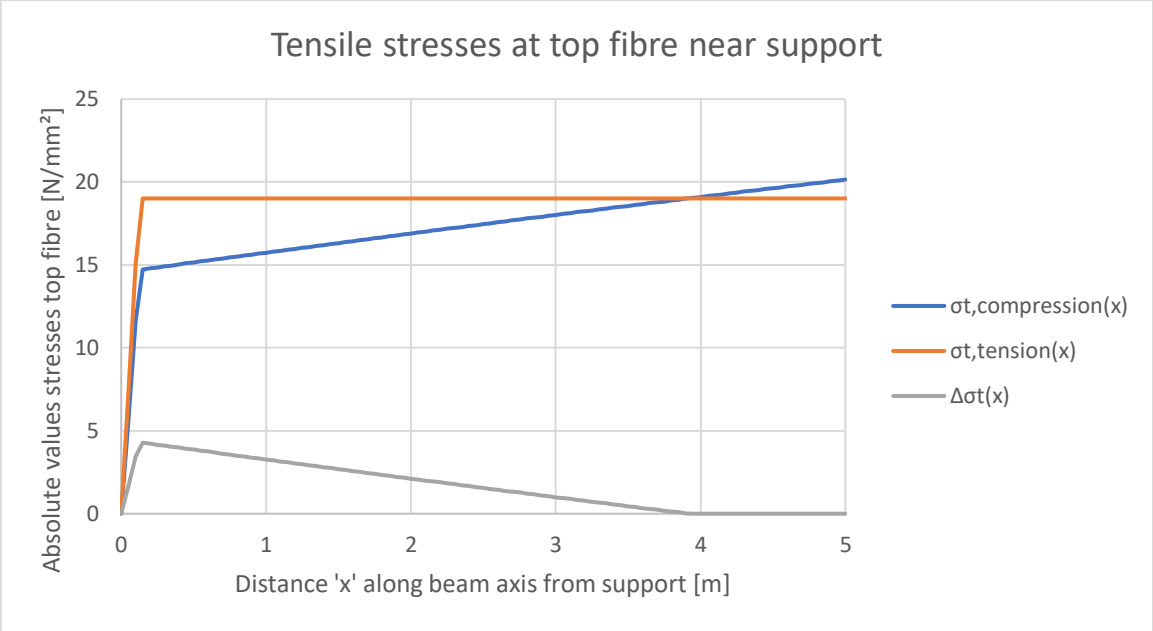

Figure 73 Tensile stresses at top fibre near the support

- **Positioning of strands**: In addition, the positioning of the strands has been analysed, which resulted in the positioning as can be seen in Figure 69. These positioning has been determined while considering the minimum spacing and concrete cover in between and onto the pretensioned strands.

- **Splitting action**: At the anchorage zone various tensile stresses occur, these may result in different types of cracking (splitting action). One can distinguish bursting, spalling and splitting. The introduction of the prestressing forces was analysed in vertical and horizontal direction.

  In vertical direction the spalling and bursting stresses remained below the tensile capacity of the material while splitting was accounted for implicitly, splitting is prevented by applying the minimum required spacing and concrete cover. In horizontal direction the forces were determined using a strut and tie model. Although UHPC has a relatively high tensile capacity, it was still expected that reinforcement would be required, which was therefore calculated.

8.5.2 Bending moment capacity

The bending moment capacity has been verified following largely the same procedure as described in 5.4.2 and applied in 7.5.3. Only the differences with these sections are discussed in this chapter. The design value of the bending moment is calculated using the RFEM output and the eccentricity of the eccentric strand group in the bottom flange:

$$M_{Ed} = M_{Ed,RFEM} - P_{m,\infty,fb} * e_p$$

The bending moment capacity has been calculated using the assumed distribution of strains and stresses over the height of the cross section as schematically given in Figure 74. A linear concrete compressive zone is applied instead of the typical bi-linear curve. During the elaboration of the calculation the strain in the prestressing strands turned out to be governing over the strains in the concrete because of the limited height x_u in the concrete compressive zone in combination with the large total height of the beam.
As a result, the plastic branch of the concrete cannot be reached, with the given design this would require a tensile strain in the prestressing steel which exceeds the maximum value ε_{ud}. Therefore, the assumed stress and strain distribution was been modified and the strain in the concrete was limited to ε_{c3} instead of ε_{cu3}.

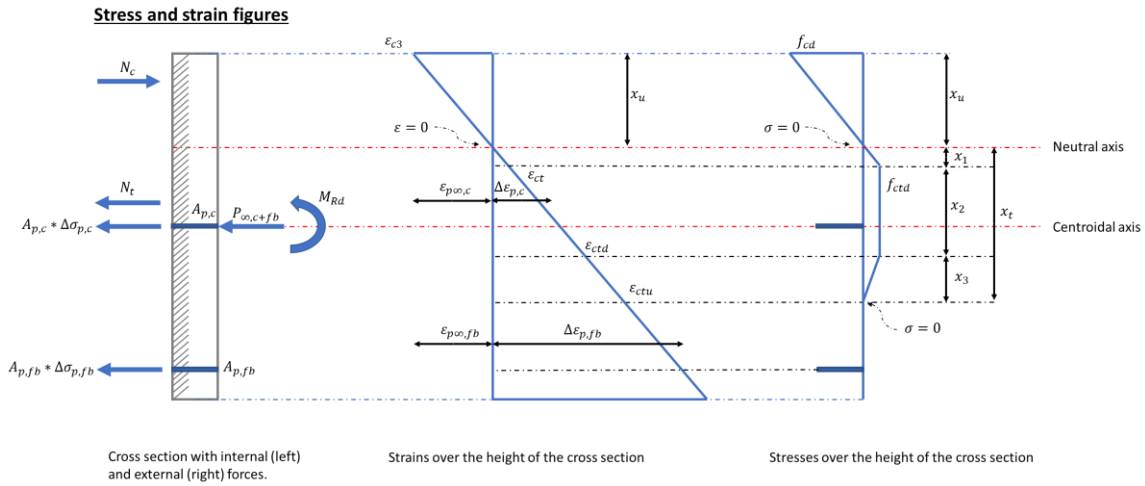

Figure 74 Assumed stress and strain distributions in the ULS

The following unity check is performed to verify the bending moment capacity:

$$UC = \frac{M_{Ed}}{M_{Rd}} \leq 1{,}0 \rightarrow \frac{29.855}{38.756} = 0{,}77$$

The rotational capacity is also verified. Because both centric and eccentric prestressing is applied, weighted average values of the effective height and working prestressing stress have been used to verify this criterion.

$$\frac{x_u}{d_{p,ave}} \leq \frac{\varepsilon_{cu} * 10^6}{\varepsilon_{cu} * 10^6 + 7f} \rightarrow \frac{0{,}09}{0{,}36} = 0{,}24$$

Both the criterion of the bending moment capacity and rotational capacity are satisfied.

8.5.3 Shear force capacity

The shear force capacity at the beam ends has been verified following the same procedure as in 7.5.4. This resulted in a unity check of:

$$UC = \frac{V_{Ed}}{V_{Rd}} \leq 1{,}0 \rightarrow \frac{4090}{7290} = 0{,}56$$

The verification of the shear force capacity is therefore satisfied.

8.5.4 Torsion

To verify the torsional capacity of the cross section, the beam has been simplified into the cross section as given in Figure 75.

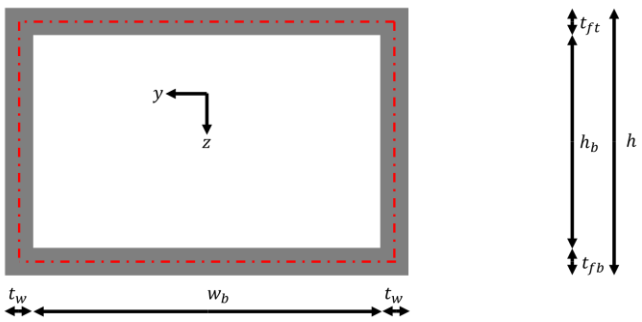

Figure 75 Simplified cross section for torsion design

Two verifications have been performed. First the torsional moment capacity of the beam as a whole has been verified by calculating the torsional cracking moment and comparing this value with the RFEM output, this verification is given in 5.4.4, see equation (31). This resulted in a unity check of:

$$UC = \frac{T_{Ed}}{T_{Rd,c}} \leq 1{,}0 \rightarrow \frac{1222}{7126} = 0{,}17$$

The second verification involved the combination of torsion and shear, see equation (32) in 5.4.4. The cross section has been divided into four segments (the top and bottom flange and both webs) after which the equivalent shear force due to the combined effect shear and torsional moment was calculated. The capacity of each segment was subsequently verified by applying the following equation:

$$V_{Ed,i} + \frac{T_{Ed}}{2 * A_k} * z_i \leq V_{Rd,c,i} + V_{Rd,f,i} \qquad \text{Equation (68)}$$

One of the webs (denoted as segment 1) turned out to be governing with a unity check of 0,61. In addition the failure of the concrete compressive strut of each segment was verified by applying equation (36) and calculating the capacity of each segment using equation (35). The same web (segment 1) turned out to be governing with a unity check of 0,42. Based on these results it is concluded that the verification of the resistance to the combined effect of shear and torsion is satisfied.

8.5.5 Ship collision

A global verification was performed to verify the static equilibrium of the deck in case of ship collision. The ROK 1.4 prescribes that for such a situation it has to be verified that:

$$F_{eq} \leq \mu * F_{sw} \qquad \text{Equation (69)}$$

In this equation F_{eq} denotes the equivalent static force caused by the ship collision of 1000 kN, μ is the friction coefficient for friction between the concrete beams and its supports and F_{sw} denotes the self-weight of the deck. For the friction coefficient a value of 0,5 is applied, which is a value found in the older versions of the ROK for friction between supports and concrete. For simplicity the self-weight of the deck was approximated by only considering the weight of the UHPC beams: $F_{sw} = n_{beams} * l_{tot} * A_c * \rho$. Equation (69) results in the following verification, from which it can be seen that the requirement of static equilibrium in case of ship collision has been satisfied:

$$UC = \frac{F_{eq}}{\mu * F_{sw}} \leq 1{,}0 \rightarrow \frac{1000}{0{,}5 * 14.703} = 0{,}14$$

In practice the situation of ship collision is not only verified by performing a global verification, but also a series of local verifications to ensure that the different relevant sections of the box beam have sufficient capacity to withstand the static equivalent load due to ship collision. Detailed elaborations of these verifications are not considered in the design, but their importance has to be acknowledged.

In practice such local verifications will involve extensive detailing but such structural problems can be solved very well, for example by reinforcing the edge beams by applying diaphragms (transverse stiffening walls within the box beam) placed with a certain centre to centre distance. Using these elements, the effects of ship collision can be mitigated, because these elements increase the stiffness and restrain and redistribute the impact force.

It is expected that the application of such a solution would have a negligible effect on the results of the project. Even the application of very slender diaphragm elements to the edge beams will already have large effects on the force distribution, while the overall increase of the self-weight of the structure is kept to an absolute minimum.

8.5.6 Fatigue

General approach

In case of a typical concrete structure of conventional concrete fatigue is not expected to be the governing failure mode because the stress cycles are relatively small. This is because of the self-weight, which is relatively large compared to the variable loads that cause the stress cycles. Because during the project the goal is to design a slender deck and reduce the self-weight as much as possible, fatigue verifications have been included because by reducing the self-weight the relative contribution of the variable loads to the total loads acting on the structure increases.

The RFEM model was applied to determine the force distribution required for the fatigue analysis, after which the maximum and minimum stresses in the steel of the eccentric prestressing and the concrete in the top and bottom fibres have been calculated. The cross section under consideration is mid-span of the middle beam because at this location the largest bending moments and thus the largest stresses due to the cyclic fatigue loads are found. Note that strictly speaking fatigue in shear also has to be verified, but this is not expected to be governing for the given structure and therefore not considered in this report.

Based on the design service life of 100 years, see section 8.2.4, and the number of heavy vehicles per year of $N_{obs} = 0{,}5 * 10^6$, see section 8.3.1, the number of cycles that has to be designed for equals:

$$n = N_{obs} * n_{years} = 100 * 0{,}5 * 10^6 = 5 * 10^7 \text{ [-]}$$

Prestressing steel

The maximum and minimum stresses in the eccentric strands are calculated using the maximum and minimum bending moments found in RFEM. The stresses in the concrete adjacent to the tendons are:

$$\sigma_{c,max} = \frac{M_{fat,max} * e_p}{I_c} - \frac{P_{m,\infty,c}}{A_c} - \frac{P_{m,\infty,fb}}{A_c} - \frac{P_{m,\infty,fb} * e_P}{I_c}$$

$$\sigma_{c,min} = \frac{M_{fat,min} * e_p}{I_c} - \frac{P_{m,\infty,c}}{A_c} - \frac{P_{m,\infty,fb}}{A_c} - \frac{P_{m,\infty,fb} * e_P}{I_c}$$

By multiplying with $\alpha_e = E_p/E_c$ the maximum and minimum stresses in the prestressing strands are found, after which the stress range is calculated using $\Delta\sigma_p = \sigma_{p,max} - \sigma_{p,min}$. The minimum stress value in the steel is -19,4 N/mm^2 while the maximum value is -5,2 N/mm^2. The range $\Delta\sigma_p$ in absolute values is 14,1 N/mm^2.

The fatigue verification of the steel is performed following the provisions from Eurocode 2-1-1. Using the S-N curve for pretensioned strands, the number of cycles and the stress range can be related. The parameters belonging to the curve are presented in the following figure and table.

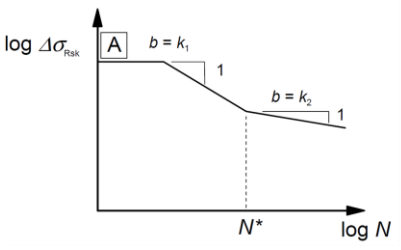

Tabel 6.4N — Parameters voor S-N-curven van voorspanstaal

S-N-curve van voorspanstaal gebruikt voor	N*	Spanningsexponent		Δσ_Rsk (MPa)
		k_1	k_2	bij N* wisselingen
voorgerekt staal	10^6	5	9	185
nagerekt staal				
— enkelvoudige strengen in kunststofkanalen	10^6	5	9	185
— rechte of gebogen spanelementen in kunststofkanalen	10^6	5	10	150
— gebogen spanelementen in stalen kanalen	10^6	5	7	120
— koppelingen	10^6	5	5	80

Figure 76 S-N curve and corresponding parameters for prestressing steel – Eurocode 2-1-1, p.122 and p.123

The stress $\Delta\sigma_{Rsk}$ is 185 N/mm^2 and corresponds to of N^* cycles $(1 * 10^6)$ cycles, because $n > N^*$ the stress until failure at the actual number of cycles 'n' can be determined as follows:

$$\Delta\sigma_{Rsd} = \frac{\Delta\sigma_{Rsk}}{\gamma_{S,fat}} * \left(\frac{N^*}{n}\right)^{\frac{1}{k_2}} \rightarrow \frac{185}{1{,}1} * \left(\frac{1 * 10^6}{100 * 0{,}5 * 10^6}\right)^{\frac{1}{9}} = 108{,}9\ [MPa]$$

Using this result the verification of the fatigue capacity can be performed:

$$\Delta\sigma_p * \gamma_{F,fat} \leq \Delta\sigma_{Rsd} \rightarrow 14{,}1 * 1{,}0 < 108{,}9$$

The fatigue capacity of the prestressing steel is therefore sufficient.

Concrete

Using the maximum and minimum bending moments calculated using RFEM the stress amplitude in the top and bottom fibres of the concrete are calculated. In the calculation $\sigma_{cd,max}$ is the largest compressive stress value while $\sigma_{cd,min}$ is the smallest compressive stress value (i.e. closest to zero). If $\sigma_{cd,min}$ is a tensile stress, it is set equal to zero and additional verifications will have to be applied instead to consider the more unfavourable case of fatigue under alternating compressive and tensile stresses. For the top fibre the results are:

$$\sigma_{cd,max} = -\frac{M_{fat,max}}{W_t} - \frac{P_{m,\infty,c}}{A_c} - \frac{P_{m,\infty,fb}}{A_c} + \frac{P_{m,\infty,fb} * e_P}{W_t} = -23{,}2\ [MPa]$$

$$\sigma_{cd,min} = -\frac{M_{fat,min} * e_p}{W_t} - \frac{P_{m,\infty,c}}{A_c} - \frac{P_{m,\infty,fb}}{A_c} + \frac{P_{m,\infty,fb} * e_P}{W_t} = -19{,}5\ [MPa]$$

For the bottom fibre the results are:

$$\sigma_{cd,max} = \frac{M_{fat,min}}{W_b} - \frac{P_{m,\infty,c}}{A_c} - \frac{P_{m,\infty,fb}}{A_c} - \frac{P_{m,\infty,fb} * e_P}{W_b} = -4{,}1\ [MPa]$$

$$\sigma_{cd,min} = \frac{M_{fat,max} * e_p}{W_b} - \frac{P_{m,\infty,c}}{A_c} - \frac{P_{m,\infty,fb}}{A_c} - \frac{P_{m,\infty,fb} * e_P}{W_b} = 0{,}0\ [MPa]$$

The lowest compressive stress in the latter case was approximately equal to zero.

Subsequently the number of cycles to failure at these two constant amplitudes are calculated by means of equation (38). This results in $4{,}41 * 10^{20}$ cycles for the top fibre and $9{,}85 * 10^{12}$ for the bottom fibre. Eurocode 2-2 prescribes that for the fatigue verification of concrete Miner's rule has to be applied. Because there is only one stress amplitude for the top and bottom fibre this results in the criterion that $n/N \leq 1{,}0$ for both verifications. For both cases a value for the fatigue damage factor D_{Ed} was found which is by approximation equal to zero, this criterion has therefore been satisfied for both the top and bottom fibre.

8.5.7 Deflection

Approach

The deflections are calculated using the frequent load combination in the serviceability limit state, the calculation is performed in two different ways. An upper limit of the deflections is calculated using standard engineering formulas and the conservative assumption that there is no interaction between the beams. This approach is similar to the approach given in section 7.5.5 and meant solely to obtain a first impression of the deflections and to verify the RFEM results. A second calculation is performed by calculating the deflections using RFEM.

Upper limit of deflections

Using the approach as given in section 7.5.5 the total deflection may be expressed as:

$$\delta_{tot} = \delta_G - \delta_P + \delta_{Q,UDL} + \delta_{Q,axle} \rightarrow 255{,}3 - 232{,}4 + 129{,}5 + 66 = 218{,}4\ [mm]$$

In this equation the downward deflection is positive while the upward deflection is negative. The maximum deflection is taken equal to $\delta_{max} = l/300$. This results in a maximum of 226,7 mm, the upper limit therefore satisfies the requirement.

Comparison with RFEM

To determine the deflections in RFEM the frequent load combinations have been modelled after which a result combination was used to determine the maximum deflection. This occurred at midspan of beam 3 and has a magnitude of 344,4 mm. Note that the modulus of elasticity of the main beams in these combinations were reduced by multiplication with a factor of 0,77 to account for the effective modulus of elasticity.

The value of the deflection found using RFEM does not include the upward deflection due to prestressing yet. The total deflection is calculated as follows:

$$\delta_{tot,RFEM} = \delta_{max} - \delta_P \leq \delta_{max} \rightarrow 344{,}4 - 232{,}4 = 112{,}0 < 226{,}7 \text{ [mm]}$$

This value is smaller than the maximum value and therefore it satisfies the requirement.

8.5.8 Crack width

According to the AFGC-SETRA 2013 guideline it is not required to verify the crack widths of elements made of UHPC of which both the average and characteristic constitutive laws are strain hardening. This is assumed to hold for the material of the main beams and therefore the verification of the crack width may be omitted.

However, provisions of the guideline on crack width can be used to define a limit for the tensile stresses that can be allowed without the risk of negative effects on the durability of the UHPC. Figure 77 gives a table from the guideline in which for different exposure classes limitations are given to the crack width to ensure the durability of the steel fibres and reinforcement and/or prestressing.

Classe d'exposition *Exposure class*	Eléments en BFUP armé et éléments en BFUP précontraint à armatures non adhérentes *Reinforced UHPFRC members and prestressed UHPFRC members with unbonded tendons*	Eléments en BFUP précontraint à armatures adhérentes *Prestressed UHPFRC members with bonded tendons*	Eléments en BFUP non armé et non précontraint *Non-reinforced and non prestressed UHPFRC members*
AN de l'EC2 NA of EC2	Combinaison quasi-permanente des charges *Quasi-permanent load combination*	Combinaison fréquente des charges *Frequent load combination*	Combinaison caractéristique des charges *Characteristic load combination*
X0, XC1	0,3	0,2	0,3 combinaison caractéristique et 0,3 combinaison fréquente *0.3 characteristic load combination and 0.3 frequent load combination*
XC2, XC3, XC4	0,2 (*) (**)	0,1 (*)	0,2 (*) combinaison caractéristique et 0,05 combinaison fréquente *0.2 (*) characteristic load combination 0.05 frequent load combination*
XD1, XD2, XS1, XS2, XS3	0,1 (*) (**)	Limitation traction à $2/3.\min(f_{ctm,el}, f_{ctfm}/K)$ *Limitation of tensile stress to* $2/3.\min(f_{ctm,el}, f_{ctfm}/K)$	0,1 (*) combinaison caractéristique et 0,05 combinaison fréquente *0.1 (*) characteristic load combination 0.05 frequent load combination*

Figure 77 Recommended values w_{max} - AFGC-SETRA 2013, p.119

Given the exposure classes that have been determined (XC4 and XD3, see annex VI) and the type of structure (prestressed UHPC with bonded strands and tendons) the requirement is imposed that under the frequent load combination the tensile stresses should be limited to a value of:

$$\sigma_{t,max} = \frac{2}{3} * \min\left\{f_{ctm,el}; \frac{f_{ctfm}}{K}\right\}$$

The value $f_{ctm,el}$ is the mean value of the elastic tensile strength, i.e. the tensile strength of the matrix, while f_{ctfm} is the mean value of the maximum post-cracking stress. The value of $f_{ctm,el}$ can be calculated following equation (14), which results in a value of approximately 10 N/mm^2. Because the material is strain hardening, it is assumed that f_{ctfm}/K is at least equal to the mean value of the elastic tensile strength. Therefore:

$$\sigma_{max} = \frac{2}{3} * 10 = 6{,}7\ [N/mm^2]$$

This stress value was applied in various calculations where the limitation of tensile stresses was involved. Note that instead of the frequent combination in the SLS, the characteristic combination was used to design the prestressing, which is more stringent.

8.5.9 Vibrations

In bridge design vibrations also play a role, which is especially of importance for very slender or light bridges. Although the importance of vibrations has to be acknowledged, it is not expected that this criterion would be a governing criterion for the design presented in this report, because the slenderness of the beam deck is relatively low and its weight is relatively large compared to structures such as slender steel decks or pedestrian bridges, in which vibrations do play a predominant role. For this reason, this criterion has not been included in the design.

8.5.10 Calculations and verifications of the end cross beams

Design approach end cross beam

The function of the end cross beams is to restrain the ends of the prefab beams and in combination with the transverse post tensioning in the top flange this results in a solid deck structure. The goals of the calculations and verifications of the end cross beam as presented in this report are to determine the required prestressing and to demonstrate that the cross section of the beam in combination with the prestressing results in sufficient bending moment and shear capacity. No other verifications are included. The end beams are post-tensioned using four prestressing tendons, Figure 78 gives a schematic overview of the beam and the positioning of the tendons.

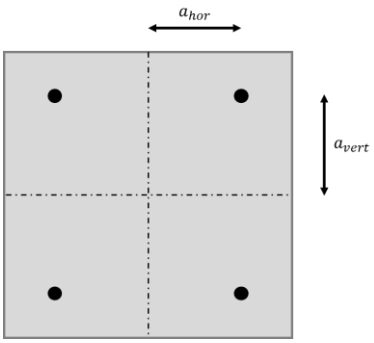

Figure 78 Position of the prestressing ducts in the end cross beams

In the analysis of the beam the following assumptions are made:

- The beam has a rectangular cross section and it is analysed as if it is a solid cross section over its full width of the deck (the presence of the prefab beams is neglected);
- It is assumed that the height is equal to the width, and that the height of the end cross beam is equal to that of the prefab beams;
- An equal number of prestressing tendons is positioned at both sides of the beam. Therefore, the resultant of the prestressing force is assumed to act centrically on the beam;

- No tensile stresses are allowed to occur in the cross section, that means that full prestressing has to be achieved.

The latter requirement is formulated to prevent cracking of the beam, by imposing a more stringent criterion compared to that of the UHPC by applying a sufficiently large prestressing force, the durability of the end cross beams is ensured.

Design of the post-tensioned prestressing

Given the positioning of the tendons at both halves of the beam the prestressing losses are calculated assuming a resulting prestressing force acting centrically. For this post-tensioned beam, the following prestress losses are included in the calculation:

- Direct losses:
  - Elastic shortening
  - Friction
  - Wedge set
- Time dependent losses:
  - Shrinkage
  - Creep
  - Relaxation

The applied value of the working prestressing force P_{m0} is the mean value calculated over the length of the beam. This value was subsequently used to determine the time dependent losses and to perform subsequent verifications. The following figure summarizes the results of the calculation. The symbol P_{max} denotes the maximum prestressing force, $P_{m0}(x)$ denotes the initial prestressing force as a function of the coordinate 'x', P_{m0} is the mean value of the initial prestressing force and $P_{m,\infty}$ is the working prestressing force, which is calculated using the mean value of the initial prestressing force over the width of the deck.

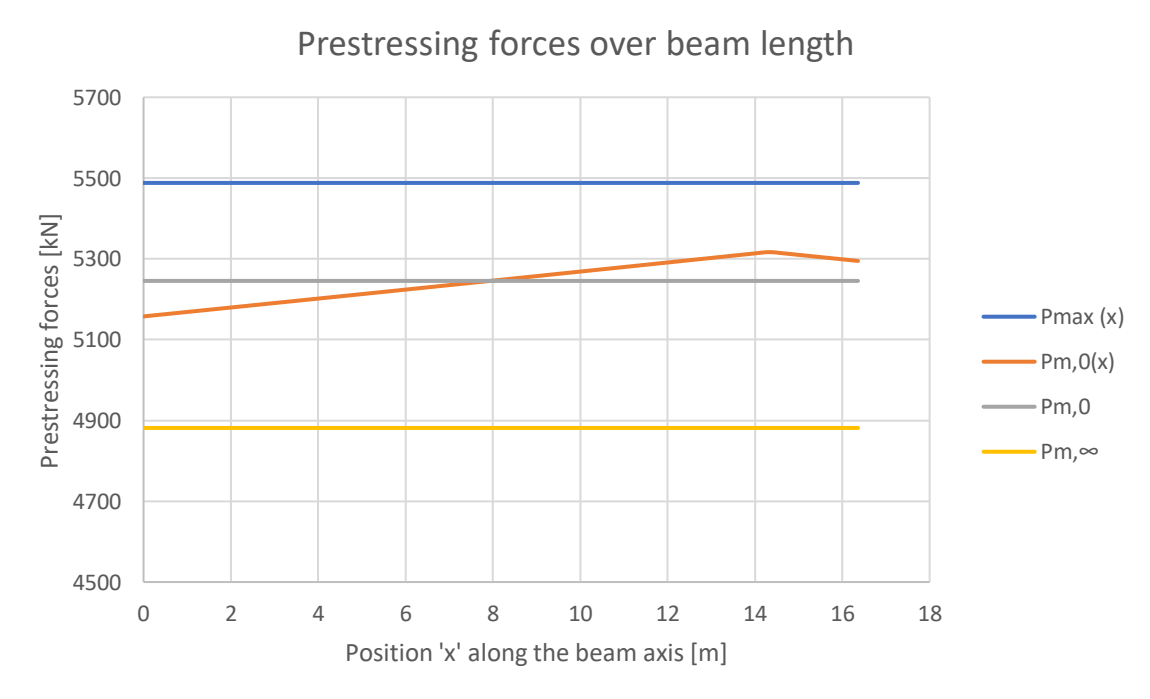

Figure 79 Prestressing forces along the length of the end cross beam

Using the hogging and sagging bending moments found using RFEM it was subsequently verified that the working prestressing force is sufficiently large to keep the beam under compression.

Bending moment capacity

The bending moment capacity in the ultimate limit state is calculated following largely the same procedure as applied for the main beams, however, the contribution of the concrete in tension is neglected because the end cross beams will be made of conventional concrete. The following simplified strain and stress distributions are assumed to occur over the height of the end cross beam in the ULS.

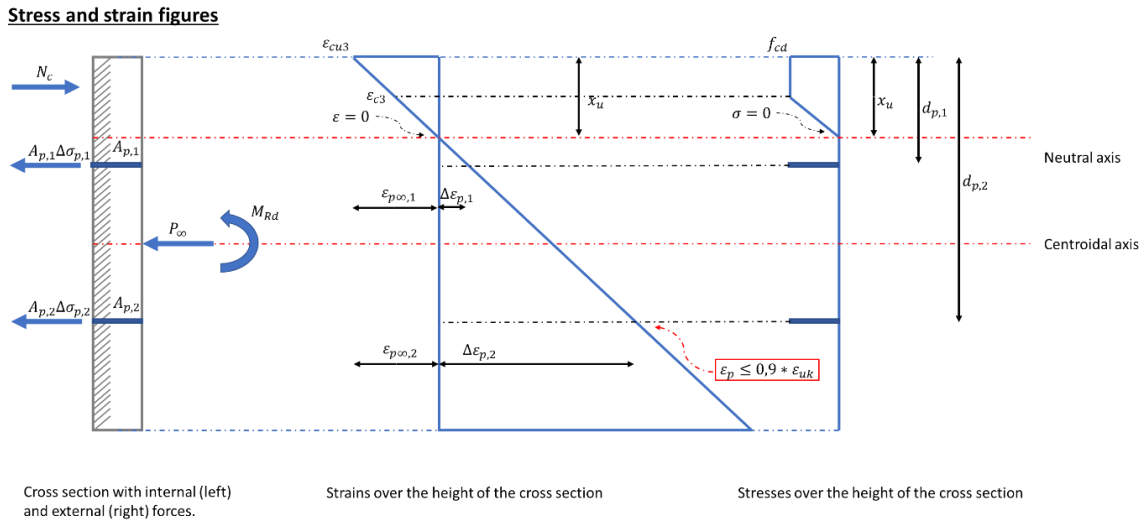

Figure 80 Assumed stress and strain distributions over the beam height in the ULS

The design value of the bending moment is the maximum of the hogging and sagging bending moments found using RFEM. The following criterion had to be satisfied:

$$UC = \frac{M_{Ed}}{M_{Rd}} \leq 1{,}0 \rightarrow \frac{1212}{6416} = 0{,}19$$

In addition, the rotational capacity is satisfied, for which the effective height is taken as the average value of the upper and lower prestressing strands. This results in:

$$\frac{x_u}{d_{p_{ave}}} \leq \frac{500}{500 + f} \rightarrow 0{,}18 \leq 0{,}53$$

It is concluded that the bending moment capacity and rotational capacity are sufficient.

Shear force capacity

The capacity of the cross section is calculated using the following equation:

$$V_{Rd,c} = \left(v_{min} + k_1 * \sigma_{cp}\right) * b_{cb,nom} * d_{p,2} \qquad \text{Equation (70)}$$

This is the minimum value of the equation from Eurocode 2-1-1 for elements without shear reinforcement and for which it is assumed that no longitudinal reinforcement is present. In addition, it has to be verified that the upper limit, which is governed by failure of the concrete compressive strut, is not exceeded:

$$V_{Rd,max} = \alpha_{cw} * b_{cb,nom} * z * v_1 * f_{cd} * \frac{1}{\cot(\theta) + \tan(\theta)} \qquad \text{Equation (71)}$$

The shear resistance of the cross section can be written as $V_{Rd} = \min\{V_{Rd,c}; V_{Rd,max}\}$. The capacity of the concrete compressive strut is not reached and $V_{Rd,c} = 1562$ kN. This results in a unity check of:

$$UC = \frac{V_{Ed}}{V_{Rd}} \leq 1{,}0 \rightarrow \frac{837}{1562} = 0{,}54$$

It is concluded that the shear force capacity is sufficient.

Force introduction

Although not considered in detail in this report, in practice the transition between the solid end beam and the slender cross section of the prefab beam requires adequate detailing. The direct fixed connection between a large element with high stiffness and a more slender element may cause local failure due to high local stresses.

The verification of such details involves more extensive calculations which are not included in the design. However, their importance has to be acknowledged. If more detailed verifications would indicate that measures have to be applied, then the thickness of the elements of the prefab cross section could be increased locally. This results in a more gradual transition between the solid end beam and the slender cross section of the box beam.

If such measures would have to be applied, then it is not expected that this would influence the results of the project. From an executional point of view these measures can be realised by adjustments of the formwork. At the same time the effect on the total weight of the structure is expected to be negligible because such measures would only be applied over a limited length, which implies only a minimal increase of the weight of the prefab beams.

8.6 Local design calculations and verifications

8.6.1 Analysis top flange of the main beams

Local verifications

In this section the design of the transverse prestressing and the local verification of the top flange are discussed. The following calculations and verifications are included:

- **Design of transverse prestressing**: Contrary to the preliminary design the interaction between the beams is taken into consideration. As a result of this, transverse bending moments occur in addition to the longitudinal bending moments. To enable the transfer of these bending moments between the beams, continuity is required which is achieved by applying transverse prestressing. This prestressing is designed with the requirement that no tensile stresses may occur at the joints.

- **Capacity of longitudinal joint**: It will be verified whether the prestressed longitudinal joints have sufficient capacity to transfer the transverse bending moments caused by the interaction between the beams.

- **Capacity of top flange – transverse direction**: In addition, the prestressed top flanges should also be able to transfer these transverse bending moments. Therefore, their bending moment capacity at the beam webs and in between the webs will be verified.

- **Capacity of top flange – longitudinal direction**: The top flanges of the beams are provided with prestressing ribs in order to decrease the thickness of the top flange. These ribs act as supports to the segments of the top flange spanning these ribs. The bending moment capacity of these parts of the top flange will be verified as well.

Design approach local verifications

The local verifications in this paragraph are carried out almost separately from the global verifications. Different load models are applied and in addition the force distribution is determined using standard engineering equations instead of a finite element model: parts of the top flange will be schematized as beams with clamped or hinged supports.

8.6.2 Design transverse prestressing of the top flange

Assumptions

The first step in the analysis of the top flange is the design of the transverse prestressing. The analysis is based on the following points:

- A strip of the top flange is analysed with width $w_{c.t.c.}$ and average thickness t_{ft}, the strip is centred in horizontal direction around the centre of the prestressing duct;
- The prestressing tendon is positioned in vertical direction at a height $0{,}5 * t_{ft}$, the top flange is therefore prestressed centrically;
- The joint has a thickness t_j which is smaller than the thickness t_{ft}. As a result, an upward bending moment is caused in the joint because of an eccentricity of:

$$e_j = 0{,}5 * t_{ft} - 0{,}5 * t_j$$

Calculating prestress losses

The prestress losses are calculated in a similar fashion as done for the post-tensioned end cross beams. The following figure summarizes the results of the calculation. The symbol P_{max} denotes the maximum prestressing force, $P_{m0}(x)$ denotes the initial prestressing force as a function of the coordinate 'x', P_{m0} is the mean value of the initial prestressing force over the width of the deck and $P_{m,\infty}$ is the working prestressing force calculated using the mean value of the initial prestressing force.

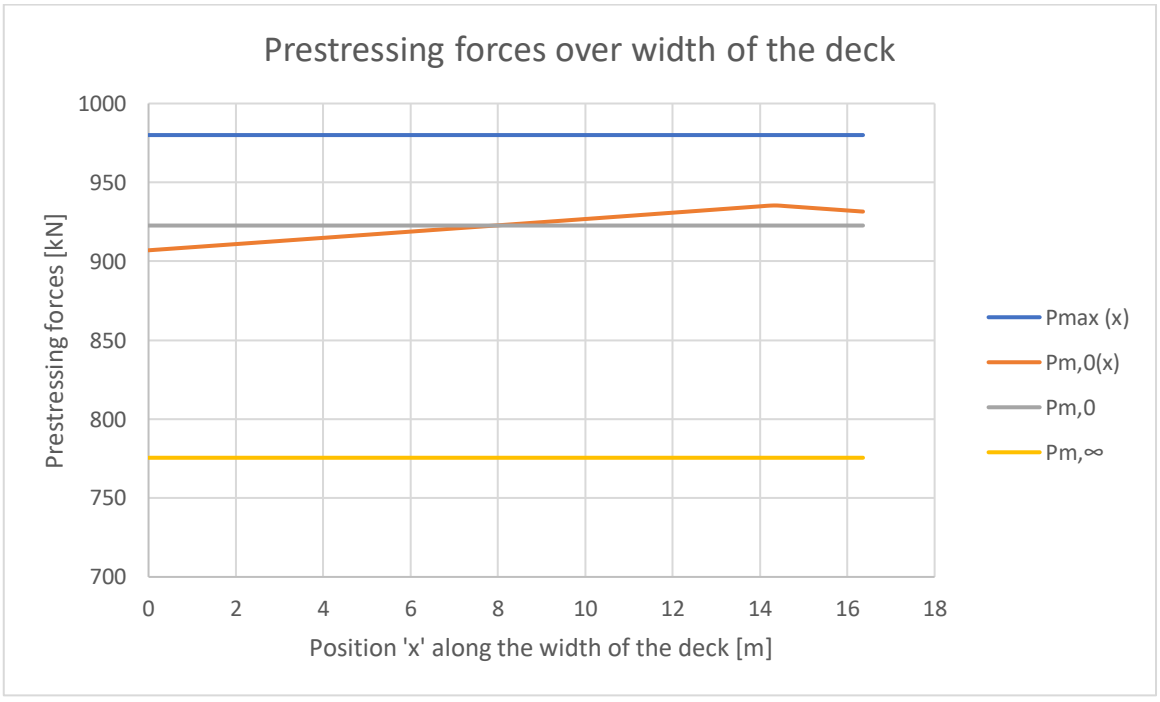

Figure 81 Prestressing forces over the width of the deck

Loads acting on the top flange and the joint

Subsequently it has to be verified that the prestressing force is sufficient to keep the joints under compression. A strip of the deck with a unity width (1,0 m) is considered. Different load models are used compared to the global verifications. The following loads are included:

Self-weight & permanent load: This load includes the self-weight of the concrete top flange and the asphalt layer. For a strip of 1,0 m width this results in a line load of:

$$G_k = t_{tf} * \rho_{UHPC} + t_{asphalt} * \gamma_{asphalt} \text{ [kN/m]}$$

Variable load: LM2 as described in 8.3.1 is applied. It consists of a single axle but given the beam dimensions only a single wheel load is applied, which is positioned at mid span. This way the most unfavourable situation is obtained.

$Q_k = 194$ [kN]

Prestressing forces: The prestressing force $P_{m,\infty}$ causes an upward bending moment at the location of the joint due to the eccentricity between the tendon and centre of the joint:

$$M_P = \frac{P_{m,\infty} * e_j}{w_{c.t.c.}} \text{ [kNm]}$$

Calculation model

To determine the values of the bending moments the top flange is schematized as a beam with clamped supports loaded by concentrated or uniformly distributed loads. Figure 82 gives the model used in the calculation. The joint is positioned at mid span of the beam and the clamped edges represent the centre of the webs of the adjacent beams. The span follows from: $l = 2 * w_f + w_j + t_w$.

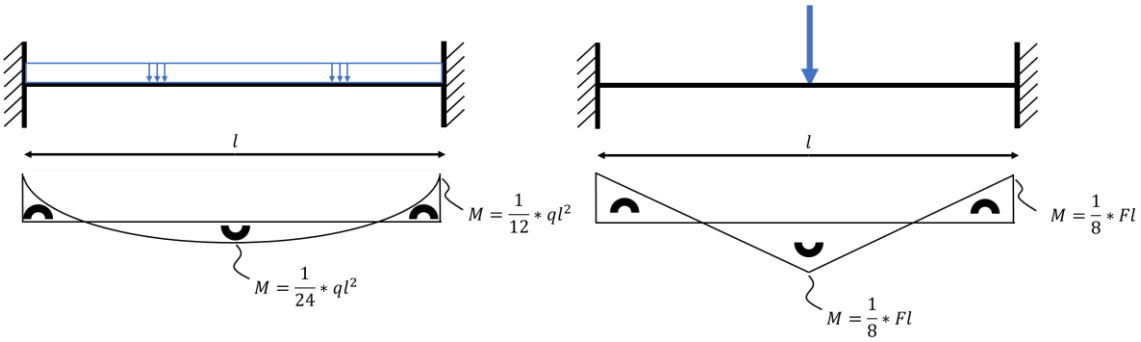

Figure 82 Calculation model top flange

Verifying stresses over the joint height

With the working prestressing force and the actions on the joints the stresses at both the top fibre and bottom fibre of the joint can be calculated. Two situations are considered, one without variable load (i.e. only permanent loads and prestressing) and one including the variable load. The results are given in Figure 83.

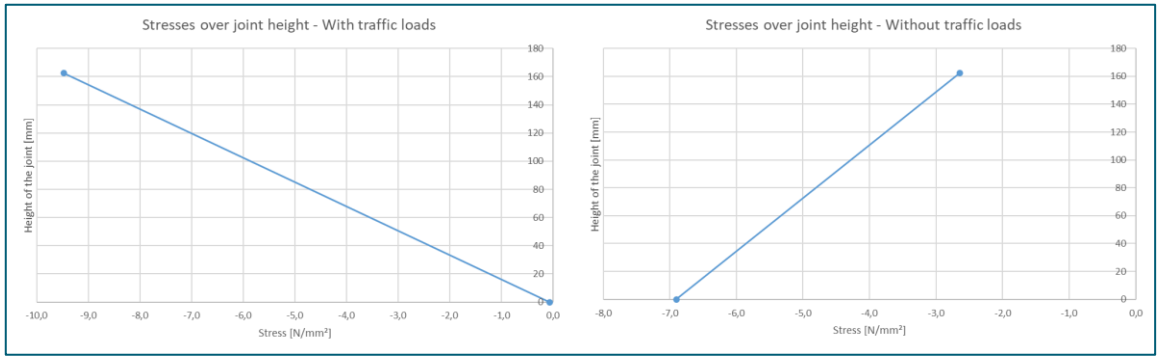

Figure 83 Stresses over the joint height for both situations

The results indicate that the working prestressing force is sufficient to keep the joints under compression, this criterion is therefore satisfied.

Detailing – Introduction of prestressing forces

In addition to the calculation of the prestressing force and the verification of the stresses over the joint height, the introduction of the prestressing forces at the position of the anchors has been analysed using strut and tie models.

Using these models, the distribution of the prestressing force over the height and width of the top flange is analysed, from which the tensile splitting forces in both directions were calculated. For the full elaboration reference is made to annex VI. For both situations splitting reinforcement was calculated under the assumption that the UHPC does not contribute to the capacity of the tensile ties.

This is a conservative assumption and the calculated amount of reinforcement should therefore be interpreted as an upper bound value. Nonetheless this assumption has been implemented because of the uncertainty in the available cross section of the tensile tie and because the capacity of the steel fibres cannot be mobilised for this purpose along the full length of the beam. The latter is caused by the fact that the stresses in the top flange are not constant along the length of the beam, which means that the available capacity from the UHPC is also not constant.

8.6.3 Local verifications top flange

Transverse direction – Joint and top flange

Three local verifications are performed. The verification of the bending moment capacity of the longitudinal joint and the top flange in transverse direction are similar. Both make use of the loads and load models as given in 8.6.1, although for the latter the value of the span is different. Using the aforementioned loads, load combinations are formulated following equations (41) and (42), after which the most unfavourable result is applied for the bending moment verifications. For the longitudinal joints this results in:

$$UC = \frac{M_{Ed}}{M_{Rd}} \leq 1{,}0 \rightarrow \frac{35{,}8}{78{,}8} = 0{,}45$$

For the sagging bending moment of the top flange in between the webs the unity check is:

$$UC = \frac{M_{Ed,sag}}{M_{Rd}} \leq 1{,}0 \rightarrow \frac{75{,}6}{97{,}1} = 0{,}78$$

For the hogging bending moment at the webs the bending moment is:

$$UC = \frac{M_{Ed,hog}}{M_{Rd}} \leq 1{,}0 \rightarrow \frac{76{,}7}{97{,}1} = 0{,}79$$

It is concluded that the bending moment capacity of the longitudinal joint and the webs in transverse direction are sufficient. Reference is made to annex VI for the full elaboration of these verifications.

Longitudinal direction – Top flange between prestressing ribs

The final local verification is the bending moment of the top flange in longitudinal direction, spanning the prestressing ribs. Figure 85 gives the model applied in the calculation. The flange is modelled as a 1,0 m wide beam and is prestressed by the external axial force in the top flange, which is caused by the prestressing and self-weight of the beams.

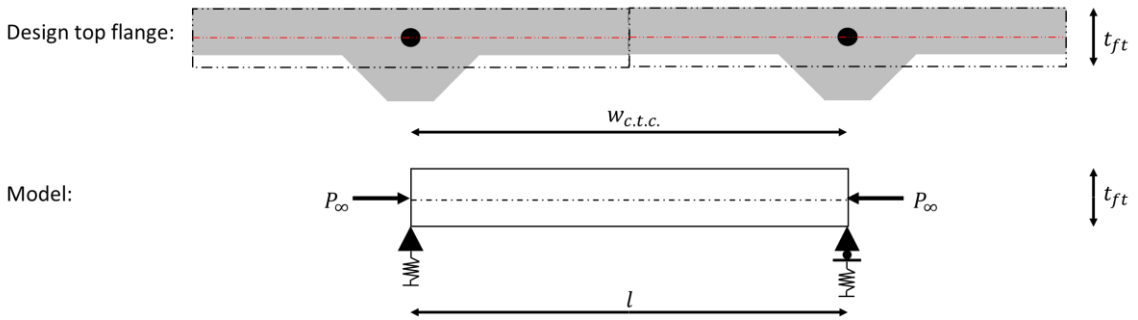

Figure 84 Model local verification top flange in longitudinal direction

The beam is assumed to be unreinforced; no conventional longitudinal reinforcement is provided. However, an external prestressing force P_∞ is present and is assumed to act centrically on the top flange. The

prestressing force is not constant along the beam length because it is a function of the bending moment due to the self-weight and the prestressing. It is at its maximum at midspan and at its minimum near the supports. If a tensile force is present, the value P_∞ is taken equal to zero.

The design value of the bending moments is calculated by applying the actions given in 8.6.1 and the load combinations from equations (41) and (42). The beams are assumed to be simply supported by the prestressing ribs. The capacity of the cross sections is calculated by following the equations as discussed in section 5.4.2. Using equations (21) to (23), the capacity has been calculated for a large number of interval points along a beam segment near the support, which is the governing region. Figure 85 summarizes the results of the calculation. In the graph both the design value of the bending moment and the capacity are plotted.

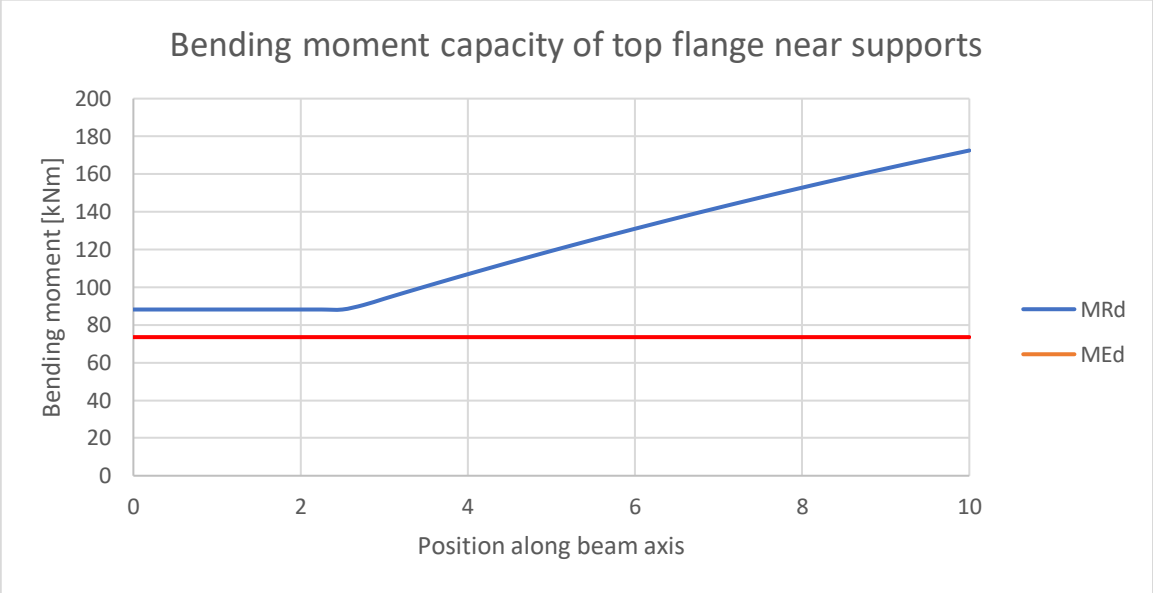

Figure 85 Bending moment capacity top flange in longitudinal direction near the support

Because the curve denoting the capacity envelopes the graph of the design values of the actions, the capacity of the top flange is sufficient over the full length of the beam. At the most unfavourable region the unity check is $73{,}5/88{,}2 = 0{,}83$. Reference is made to annex VI for the full elaboration of the calculations.

8.7 Executional aspects

8.7.1 Phased description of the main beams

To determine how the deck would be constructed in practice and to identify possible limitations that should be regarded as boundary conditions of the project, a phased description is given of the main beams of the bridge deck from the production to the use phase.

Production of the beams

The beams are produced in the prefab factory using pretensioned steel which is a process that consists of a number of clearly distinguishable steps. In addition, heat treatment is applied, which is a technique that is very suitable for application in the prefab industry. The production of the beam could take place according to the following steps:

- **Phase 1**. The first elements of the formwork (the frames required for the prestressing) are placed after which the strands are guided through and fixated on one end using a supporting structure and on the other side using jacks. The strands are stressed after which the remaining elements of the formwork are placed to close the mould. Note that the prestressing capacity might be a possible limitation;

- **Phase 2**. The concrete is placed and while hardening it bonds with the concrete over the full length of the strands in the formwork;

- **Phase 3**. While the element is still in the mould heat treatment is applied. The element is taken to 80 – 90 °C for a period of 48 hours, after which the element is allowed to cool down slowly;

- **Phase 4**. After parts of the formwork that may restrain the deformation are removed, the prestressing strands are gradually released. The element is now prestressed and the self-weight is activated.

Storing the beams
After the beams are finished these are typically stored at the storage area. For this stage the elements should at least be able to carry their own weight, which allows them to be hoisted and stored.

Transport to and placement on site
At a certain moment in time the beams are moved from the storage location at the prefab factory to the construction site. In general transportation can take place via land or water, depending on the size and weight of the element. Once taken to the construction site the elements are hoisted into their final position. The transportation or hoisting of the elements might be a possible limitation.

On site construction work
Once the prefab box beams are placed on their bearings the remaining work is carried out to finalize the structure. The remaining structural work involves the construction of the end cross beams, filling the longitudinal joints and applying the post tensioning of the top flanges. The end cross beams are constructed by casting concrete in between the solid ends of the box beams with in situ concrete. After hardening, prestressing tendons are guided through the ducts and these are subsequently post tensioned. The joints are filled with UHPC and after sufficient hardening the prestressing force is applied. After finalizing the main load bearing structure, the deck is finished by applying the surface layer, placing railings and barriers, etc.

Use phase
After aforementioned construction work the use phase starts during which the bridge should be able to function without requiring excessive repairs or maintenance under the anticipated use.

8.7.2 Boundary conditions

Identifying boundary conditions
In the phased description of the previous sub paragraph two possible limitations were identified. The first possible limitation is the maximum prestressing capacity that can be applied in the prefab factory using pretensioned steel. The second possible limitation is the transportation and placement of the beams. To determine where the limits are regarding these two factors more details on both factors are given, after which the implications on the project will be discussed.

Prestressing capacity
Prestressing using pretensioned steel is applied using wires or strands. Because the forces are transferred onto the concrete via bond the force per element can only be relatively small. It is possible to apply larger prestressing forces onto elements, providing that the minimum spacing and cover is respected to limit the tensile stresses around the elements, by applying a larger number of wires or strands. However, there is an upper limit in terms of the prestressing force, which is a boundary condition for the design of the beams if the beam is required to be constructable.

The value of the upper limit has been established by contacting a firm that produces prefab concrete elements. According to the received information the limit for prestressing using pretensioned steel is approximately 2500 tons (i.e. about 25.000 kN). This corresponds to 120 strands with diameter Ø15,7, each loaded with 21 tons (i.e. about 210 kN).

Transportation and placement of the beams
Prefab elements have to be moved from the factory or storage site to the construction site to be placed onto their final position. Transportation and hoisting can be limiting factors for prefab structures and therefore

two reference projects will be discussed. These are examples of prefab projects involving larger beam elements. One example involves transportation via road while the other involves transportation via water. Using these examples an indication can be obtained of where the upper limits are regarding the transportation and placement of larger prefab beams.

Transportation over road – Vervoersknooppunt Bleizo (August 2017): The first example covers the interchange at Bleizo, which is formed by four fields spanned using prefab box beams. The main span crosses the A12 and no intermediate support was allowed to be constructed. Box beams with a length of 61 m, a height of 2,20 m and a weight of approximately 200 tons each would be required for this solution. However, such dimensions and weight are a challenging in terms of logistics.

Figure 86 Placement of beams at Bleizo – Spanbeton

Spanbeton produced 31 box beams for the main span which were optimised to reduce the weight. The height was kept at 2,20 at mid span, but reduced to 1,60 towards the ends of the beam and once in place the beams would be brought up to the 2,20 m height over their full length using in-situ concrete. This optimization reduced the weight from 200 to 172 tons.

The time frame in which the beams would have to be placed was only a single weekend, in which the highway would be closed down for traffic. The beams were temporarily stored at a storage site nearby and at the weekend of the placement the beams were taken to the construction site one by one and hoisted into position using two cranes, see Figure 86. The beams were transported via road using special road transport, which requires additional provisions.

Transportation via water – Lienebrug (June 2020): The second example covers transportation over water. The Lienebrug was constructed in 2020 as a part of the new alignment of the provincial road around the town of Wanssum. The application of long beams was beneficial for this project, because this would maximize the free space underneath the bridge. This resulted in a solution involving box beams for which the manufacturer, Haitsma Beton, claims the record of the longest prefabricated beams.

The bridge consists of eight box beams, each beam is 1,48 m wide, 2,25 m high and 69,0 m long, resulting in a weight of 256 tons per beam. At the ends the beams have a solid cross section over a length of 2,25 m and the beams are prestressed using 112 strands, each stressed with a force of 210 kN. To keep the dimensions as limited as possible, concrete of strength class C90/105 was applied.

Figure 87 Transportation and placement of beams Lienebrug – Haitsma Beton

Given the dimensions and weight of the beams transport via road was not an option, which is why the beams were transported from the prefab factory to the construction site via water using pontoons and

pusher boats, see Figure 87. On site the beams were hoisted into position using floating sheerlegs because there was no space for the use of cranes.

8.7.3 Implications for structural design

The two identified limiting factors for the execution of the work have been discussed in the previous subparagraph. These limiting factors have implications for the design, which will be discussed in this section.

Prestressing capacity
In the detailed design a total of 130 strands Ø15,2 is applied, with a maximum prestressing force of approximately 26.300 kN (2630 tons) while the maximum capacity is approximately 120 strands Ø15,7, which is approximately 2500 tons. Strictly speaking the maximum capacity is therefore exceeded.

However, if the total area of the maximum number of strands and the maximum force are compared with the applied total area and maximum prestressing force, the difference is relatively small. The maximum value of 120 strands Ø15,7 (or equivalent) will be imposed as a boundary condition for the optimisation phase. Given the small difference it is expected that after the optimisation phase the required prestressing force and number of strands can be reduced to or below this maximum value.

Transportation and placement
The weight of an individual prefab beam as designed in the detailed design is calculated as follows:

$$W_{beam} = A_c * l_{tot} * \gamma \rightarrow 1{,}66 * 70{,}7 * 25 \approx 2940 \text{ kN}$$

$$W_{end} = 2 * h_b * w_b * w_{cb} * \gamma \rightarrow 2 * 1{,}71 * 1{,}9 * 2{,}15 * 25 \approx 350 \text{ kN}$$

This results in a total weight of approximately 329 tons, which is compared to the weight of the beams from the reference projects in subparagraph 8.7.2. The viaduct at Bleizo consisted of beams with a length of 61 m and a weight of 172 tons. This proved to be a challenge with respect to transportation, optimization was required to reduce the weight. The beams for the detailed design are even longer and heavier, it is therefore deemed unlikely that road transport would be possible.

The second reference project is more promising. For the Lienebrug beams with a length of 69 m and a weight of 256 tons were transported via water and hoisted onto place using floating sheerlegs. The beams required for the Eefdesebrug are approximately as long with a total length of 70,7 m while the weight difference is approximately 73 tons.

Given the position of the Eefdesebrug at a main waterway, the Twentekanaal, with a connection to the IJssel river, transportation and placement of the beams via water is deemed to be a plausible solution, with the remark that further weight reduction would be an additional benefit. By means of a reference project it is demonstrated that it is possible to transport and place bridge elements with comparable dimensions.

8.8 Weight calculation

8.8.1 Approach

The final part of the detailed design phase is an estimation of the weight of the structure and the subsequent comparison with the results of the preliminary design. This way the effects of the improvements as mentioned in 8.1.1 can be quantified and furthermore the reference point for the optimization phase is established.

The approach of the weight calculation is similar to the approach described in 7.6. The weight of the main structural components of the deck are calculated, for the capping beam the estimated dimensions from the preliminary design are reused. Elements such as bearings, railings and joints are neglected and the weight calculation of the existing bridge is also taken from the calculation in 7.6.

8.8.2 Results and comparison

Results of the weight calculation

The full elaboration of the detailed design and drawings of the result can be found in annex VI. Table 25 summarizes the results of the weight calculation of the deck designed in the preliminary design and detailed design. Note that the given weight of the cross beam of the detailed design includes a correction for the overlap of the cross beams and prefab beam ends. For a solid cross beam, the weight is 3781 kN while accounting for the overlap results in a reduction of 894 kN to the end result of 2887 kN.

Table 25 Different contributions to weight reduction

	Preliminary design	**Detailed design**	**Difference**
Element	[kN]	[kN]	[kN]
Prefab UHPC beams	19.214	14.703	-4511
In-situ UHPC joints	178	119	-59
Cross beams	4422	2887	-1535
Asphalt layer	3724	266	-3458
Kerbs	601	601	0
Capping beam	614	614	0
Total	28.753	19.190	-9563

Comparison

According to the weight calculation the deck as designed in the preliminary design has a weight of 19.190 kN compared to the 22.785 kN of the existing bridge and the 28.753 kN of the preliminary design. This implies a weight reduction of 16% compared to the existing bridge and 33% compared to the preliminary design. This confirms the expectation as formulated in 7.6.3 that there would be the potential to reduce the weight as such that this would be equal to or lower than the weight of the existing bridge.

Analysis of the results

The remaining question is what the different factors are that contribute to the reduction of the weight. Based on Table 25 the following observations are made:

Main contributions: The largest contributions to the reduction are contributable to the main beams and the asphalt layer. Related are the contributions such as those of the end cross beams.

Contribution asphalt layer: During the elaboration of the preliminary design, it was expected that a large weight reduction could already be realised by reducing the thickness of the asphalt layer. The results indicate that indeed this is a large contribution which accounts for approximately 45% of the weight reduction.

Contribution main beams: The main beams contribute for approximately half of the total weight reduction, making the prefab beams the largest contributor. The weight reduction of the beams is the combined result of various improvements implemented in the detailed design, for example the different material properties such as specific weight, using a FEM model to determine the force distribution, etc., and changes made to the dimensions to satisfy the various verifications that have been performed.

Contribution end cross beams & joints: The adjustment of the dimensions of the main beams also resulted in a reduction of the dimensions of the end cross beams. These are directly related given the assumption that the height and width of the end beams are equal to the height of the end cross beam. The contribution of the cross beams is $1535 - 894 = 641$ kN. In addition, the dimensions of the joints also changed because of the alterations in the thickness of the top flange, resulting in a contribution of 59 kN.

Conclusion weight comparison

The results of the detailed design have confirmed the expectations formulated during the preliminary design that there would be the potential to reduce the weight of the new bridge down to or even below that of the existing bridge. The result of the detailed design is approximately 16% lower than that of the existing bridge.

8.9 Conclusion and prospects – Detailed design

8.9.1 Conclusion detailed design phase

The goal of the detailed design was to perform a more complete and accurate analysis to obtain more insight into the behaviour of the structure and to identify the best options for optimization. The first goal was achieved through the modelling and analysis of a finite element model and performing verifications of the structure under different loads and load combinations. The second goal was achieved by performing the various verifications. The various unity checks can be interpreted as an indication of where the potential to further optimisation is the largest. Table 26 summarizes the results of the verifications that have been performed.

Table 26 Summarizing table unity checks

Verification	**Element**	**Value unity check**
Bending moment capacity	Main beams (global)	0,77
Shear force capacity	Main beams (global)	0,56
Torsional moment capacity	Main beams (global)	0,17
Combination shear and torsion	Main beams (global)	0,61
Combination shear and torsion – Compressive strut	Main beams (global)	0,42
Ship collision – Static equilibrium	Whole deck (global)	0,14
Bending moment capacity joint	Longitudinal joints (local)	0,45
Bending moment capacity transverse direction	Top flange (local)	0,78 and 0,79
Bending moment capacity longitudinal direction	Top flange (local)	0,83
Fatigue verification – Prestressing steel	Main beams (global)	0,13
Fatigue verification – Concrete	Main beams (global)	≈0
Deflection	Main beams (global)	0,50
Bending moment capacity	End cross beams (global)	0,19
Shear force capacity	End cross beams (global)	0,54

From the table it can be seen that the room for optimisation can be sought for in the bending moment capacity while the capacity of the webs and top flange is more limited. However, the verification does not only include ULS verifications. SLS verifications such as the deflections and the tensile stress criterion of the beam have to be considered as well.

In addition, various executional aspects were covered to identify possible limitations from practice that should be imposed onto the design as boundary conditions. The two identified limiting factors were the prestressing capacity and the transportation and placement. The current design exceeds the maximum prestressing capacity though it is expected that this can be compensated for in the optimization phase because the difference is only limited. Transportation and placement of the beams via waterways is deemed to be feasible, which was illustrated by means of a reference project.

Apart from the verifications a weight calculation has been performed as well, which confirmed the expectations from the preliminary design that substantial weigh reduction could be achieved. The detailed design results in a weight value that is approximately 33% lower than that of the preliminary design and 16% lower than that of the existing bridge. This total reduction is a combined result of various improvements of the design and changes to the dimensions that have been implemented during the elaboration of the detailed design.

8.9.2 Prospects optimization phase

In this chapter the elaboration of the detailed design has been discussed. With a weight reduction of 16% compared to the weight of the existing bridge, another step is taken towards achieving the goal of the project. However, various remarks can still be made which have to be considered in the optimisation phase. These are as follows:

- **Maximum prestressing force**: It was found that the required prestressing force for the pretensioned steel exceeds the maximum value that can be applied in practice. In the subsequent design phase, the design should be modified as such that only a smaller number of strands per beam is required, or as such that an alternative prestressing method is used to work around this limitation.

- **Further weight reduction**: Another remaining question is whether the weight of the deck can be reduced further while satisfying the relevant requirements. Answering this question is the main objective of the optimization phase and also affects the number of prestressing strands required.

During the optimisation phase a study will be carried out in which various dimensions are varied, while other factors such as material parameters are kept identical to those of the detailed design. By following this approach, the influence of varying different dimensions can be identified and the most optimal design, within the boundaries of the project scope and of what is required to meet the goal of the project, can be determined.

9

OPTIMIZATION AND FINAL DESIGN

9.1 Approach to the optimization

With the detailed design finished, the design stage continues with the optimization phase to investigate the effect of varying different dimensions in order to determine the most optimal design in terms of self-weight of the structure. Executional aspects, specifically the aspect of number of strands, will be accounted for as well. This will eventually result in the final design, with which the design stage will be concluded.

9.1.1 Results from detailed design phase

The results of the detailed design are used as the starting point for the optimization phase. The results in Table 26 are interpreted as a first indicator of potential to optimization. From the results it can be observed that the in case of the top flange there is little room to reduce the dimensions. The webs, predominantly providing capacity to shear and torsion, indicate that a reduction of the thickness is possible. The dimensions of the end cross beam also indicate that the cross section is sufficiently large to provide the required capacity.

However, these ULS and SLS verifications are not the only criteria, especially if the dimensions are to be kept as minimal as possible. Aspects such as the accommodation of the pretensioned strands in the webs and bottom flange and the prestressing ducts in the top flange have to be included as well. In addition, the webs require sufficient thickness for overall stability and the resistance to ship collision.

9.1.2 Different approaches to optimization phase

Different approaches are possible to achieve the self-weight of the deck by reducing the cross-sectional dimensions. Based on the results from and approach to the detailed design phase, three approaches can be formulated that can be applied separately or combined:

- Option 1: The first option is to vary the dimensions of the cross section designed in the detailed design phase, as such that the cross section is reduced as much as possible.

- Option 2: The second option involves variation in box beam type as well as a variation with the number of beams.

- Option 3: The third option is to exploit the high compressive strength of the UHPC to a higher degree by applying prestressing forces using a combination of pretensioned strands and post-tensioned prestressing elements. By introducing a higher compressive force, the material is exploited to a higher degree and this contributes to more slender structures.

9.1.3 Selected approach to optimization

Selecting an approach for the optimization

The first option is selected as the approach to reducing the cross section of the deck. The second option is not expected to yield a reduction at this point unless the height of the beams is reduced significantly. This option involves a larger number of smaller beams without outstand flanges, which would result in more

material being required for webs and bottom flanges. Although the third option may result in significant reduction of the cross section, it comprises a different design approach which may not be required to achieve the goal of the project, and is therefore not applied.

Optimization procedure

The procedure of the optimization phase using the first approach, variation with the dimensions to reduce the cross section, can be decomposed into three steps:

Step 1 – Establish new dimensions: The first part of the optimization procedure is to establish new dimensions in a substantiated way, the starting point is the cross section from the detailed design;

Step 2 – Verifications: After the new dimensions have been determined a full verification is carried out to determine whether all included requirements are met. If this is not the case, modifications are made to the design. Figure 88 gives an overview of all verifications of the optimization phase.

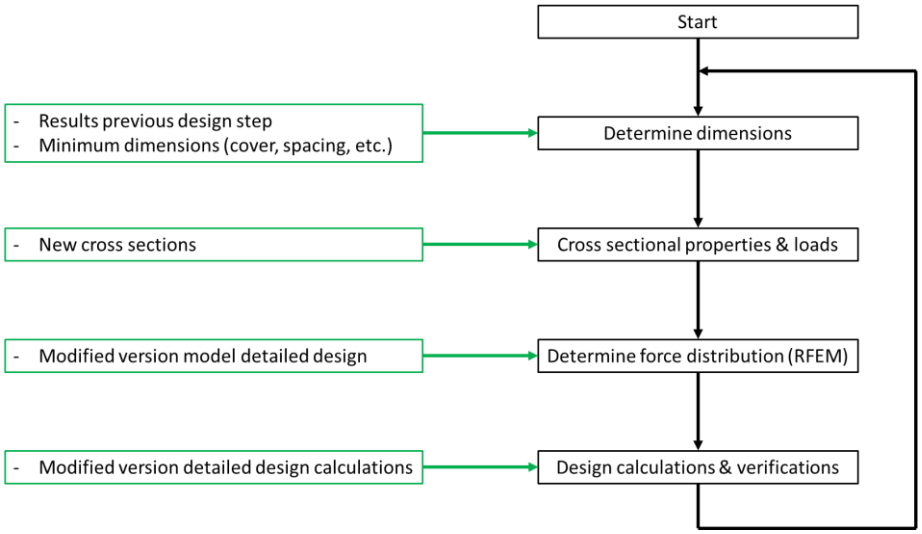

Figure 88 Verifications of the optimization phase

Step 3 – Analysis of results: Subsequently the results of the verifications are analysed, if the achieved weight reduction is deemed to be satisfactory, then the optimization phase is concluded. The resulting design is denoted as the final design. If not, then the aforementioned steps are repeated. In the remainder of this chapter the optimization will be carried out as described in this paragraph.

9.2 Establishing new dimensions

In section 9.1.1 it was concluded based on the results from the detailed design that there are options to reduce the cross section of the beams. In addition, the remark was made that there are two types of 'limitations' or 'constraints' for the optimization which determine the minimum dimensions. The first aspect are constraints related to aspects such as cover, spacing and overall stability. The second aspect is the capacity of the beams. In this section information is collected to determine the minimum dimensions based on these aspects.

9.2.1 Constrains related to cover and spacing

Figure 89 gives an overview of the aspects that are relevant in determining the dimensions of the cross section other than the capacity.

Figure 89 Constraints of the design other than capacity

The top flange, webs and bottom flange will subsequently be discussed to determine the minimum dimensions for each of these elements based on the aspects given in the figure.

Top flange

The dimensions of the top flange are governed by the prestressing ducts for transverse post-tensioned prestressing, which requires sufficient cover. Prestressing anchors have to be accommodated as well.

Minimum cover on the tendon: Exposure classes and the corresponding nominal cover are determined in accordance with the AFGC-SETRA 2013 guideline, this resulted in exposure classes XC4 and XD3 for the top flange. With an assumed diameter of the duct of 45 mm this results in a nominal cover of 50 mm.

In the detailed design, see Figure 61 and Table 19, the centre of the duct was assumed to be positioned at 94 mm from the top of the top flange. With the assumed diameter of the duct and the calculated value for cover, the requirement of sufficient cover would be met.

Anchorage elements: Expected to be a more stringent criterion is the application of a prestressing anchor. Not only should this anchor be able to provide the required prestressing force (based on the detailed design P_{max} is 980 kN), it should also be possible to accommodate the anchor within the prestressing ribs, which have a total height of 250 mm with the prestressing tendon positioned at 94 mm from the top.

In construction practice different types of anchorage systems are available for different applications and purposes. One example of anchors that might are suitable for post-tensioned prestressing are the plate anchorage type 'SD' manufactured by Dywidag. Figure 90 gives the dimensions of the anchors of the aforementioned type.

The figure is added to give an indication of the order of magnitude of the anchors that should be expected, it confirms that indeed the possibility of applying the anchorage is more stringent than the dimensions required to provide sufficient cover on the prestressing ducts.

It also indicates that anchors that can provide the required force are available with dimensions that are as such that these can be accommodated in the prestressing ribs. However, it also indicates that it would be beneficial from the prestressing point of view to move the anchor downwards to create to create more room accommodate the anchor. Attention will be paid to this aspect during the optimization.

Webs

The minimum dimensions of the web are determined by three aspects: the accommodation of prestressing strands with sufficient cover, the overall stability of the beam and the capacity to withstand accidental ship collision.

Minimum cover on the strands: With the exposure classes XC4 and XD3 and a strand diameter of 15,2 mm, the minimum cover onto the strands is 35 mm. If the same cover is applied at the inner and outer side of the webs, then based on these criteria the minimum thickness of the web is:

$$t_{min} = 2 * c_{nom} + \emptyset \approx 85 \text{ mm}$$

Plate Anchorage SD

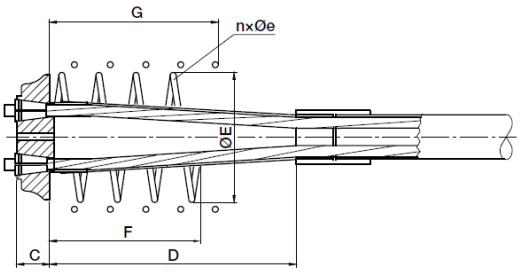

Technical Data

Type 0.5" f_{pk} 1860 [N/mm²]	Ultimate Load Ø 12.9mm (186kN per strand) [kN]	Type 0.6"/0.62" f_{pk} 1860 [N/mm²]	Ultimate Load Ø 15.7mm (279kN per strand) [kN]	A [mm]	B [mm]	C [mm]	D [mm]
5904	744	6803	837	125	140	41	200
5905	930	6804	1,116	135	160	41	200
5907	1,302	6805	1,395	150	180	40	300
5909	1,674	6807	1,953	170	215	44	270
5912	2,232	6809	2,511	190	245	48	325

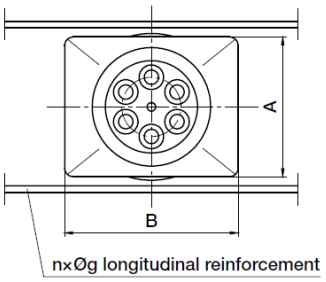

Figure 90 Example of anchorage system for post-tensioned transverse prestressing – DYWIDAG, p.24

Stability & ship collision: The webs of the box beams have an important role in the overall stability of the beams and the capacity to withstand ship collision. Sufficient thickness of the webs is therefore required, even if slender diaphragm elements are applied to reinforce the beams. As mentioned in the detailed design no detailed calculations are made, which is why an estimation has to suffice. A minimum thickness of 100 mm is deemed to be sufficient to provide the required overall stability and capacity to withstand impact loads, this value will be applied to all beams.

Bottom flange

For the bottom flange the stringent criterion is the accommodation of the prestressing strands, sufficient cover and spacing has to be provided. In addition, reinforcement might have to be provided onto which sufficient cover has to be provided as well.

Minimum cover on strands: The cover onto the strands is calculated in the same way as done for the pretensioned strands in the web. The result is therefore the same: $c_{nom} = 35$ mm.

Minimum cover onto reinforcement: If tensile reinforcement is applied because of splitting forces, sufficient cover has to be provided to the strands as well. Assuming rebars Ø10 and exposure classes XC4 and XD3, then the cover is 30 mm.

The cover requirement has to be met both for the strands and reinforcement. The cover onto the strands is, in case reinforcement is provided, equal to the summation of the cover onto the rebars and the bar diameter.

Spacing of strands: The AFGC-SETRA 2013 prescribes that the provisions from Eurocode 2 should be satisfied, see Figure 91. In addition, the guideline adds the requirement that, to enable flow of the UHPC which is influenced by the fibres in the mixture, the spacing between the strands should be at least $1{,}5 * l_f$.

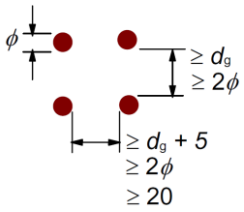

Figure 91 Minimum spacing between prestressing elements - Eurocode 2-1-1, p.156

Because the strand diameter is larger than the fibre length and because the dimension of the grains in UHPC is small, the requirements can be rewritten into:

$$s_{min,hor} = s_{min,vert} = s_{min} = 2 * \emptyset$$

9.2.2 Constraints related to capacity

Capacity as a function of beam height

The dimensions of the cross section are partly determined by the required load bearing capacity. To give a first indication of the required dimensions of the beam, different values and properties of the beam are plotted as a function of the total height of the beam. Graphs have been prepared for the following aspects:

- Stresses at mid span at the outer fibres
- Bending moment capacity
- Shear force capacity
- Torsional capacity
- Capacity under combined effect of shear and torsion.

The graphs are prepared following the calculation procedure of the detailed design. The only differences are the height, which is made variable, and the thickness of the web. The aforementioned aspects are determined for a web thickness of 150 mm and of 100 mm. All other parameters are identical.

Stresses in outer fibres at midspan

The first verification for a prestressed beam is usually the stresses over the cross section in the serviceability limit state, to verify the maximum stress values. After this verification is satisfied the ultimate limit state verifications are considered. For this reason, the stresses in the outer fibres at mid span are considered first.

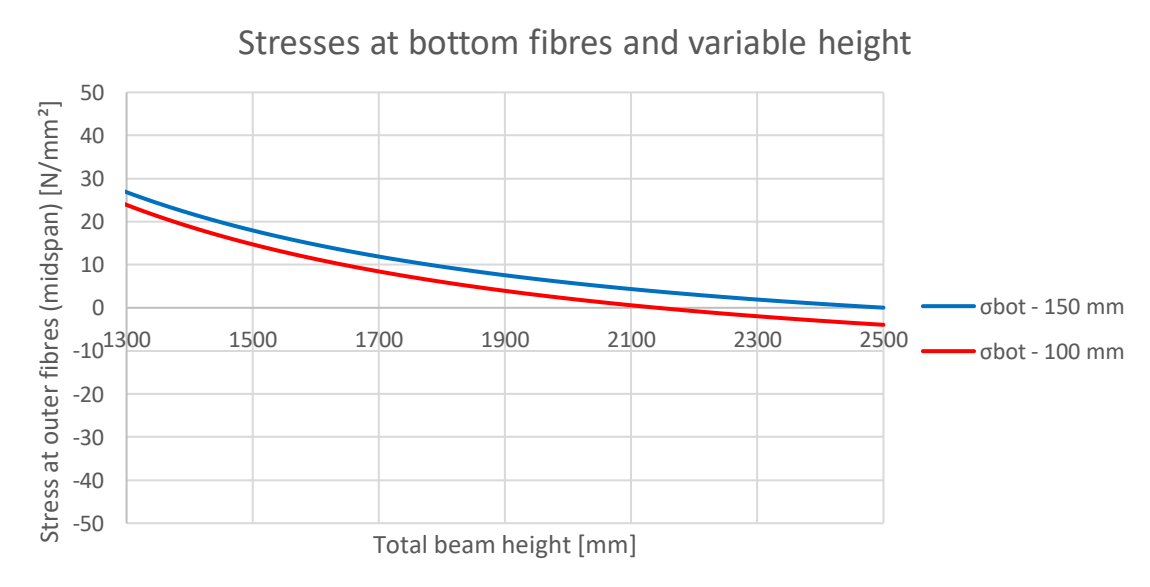

Figure 92 Stresses in top and bottom fibres at midspan as a function of the beam height

Figure 92 gives the graphs of the stresses at the bottom fibres at midspan of the beams for a web thickness of 150 mm and 100 mm. The graphs are plotted for the situation $t \to \infty$ and full loading, i.e. permanent and variable loads, because this was the governing situation in the detailed design. The stresses in the bottom fibre are tensile and therefore governing over those in the top flange.

Bending moment capacity

Figure 93 gives the graphs of the bending moment capacity as a function of the beam height. The graphs are by approximation linear and it can be observed that the variation in thickness has a negligible effect on the bending moment capacity, this is due to the fact that the contribution of the webs is mainly through the tensile zone of the concrete. Given the limited height over which the concrete contributes in tension the contribution is limited and the effect of a reduction of the web thickness is therefore limited as well.

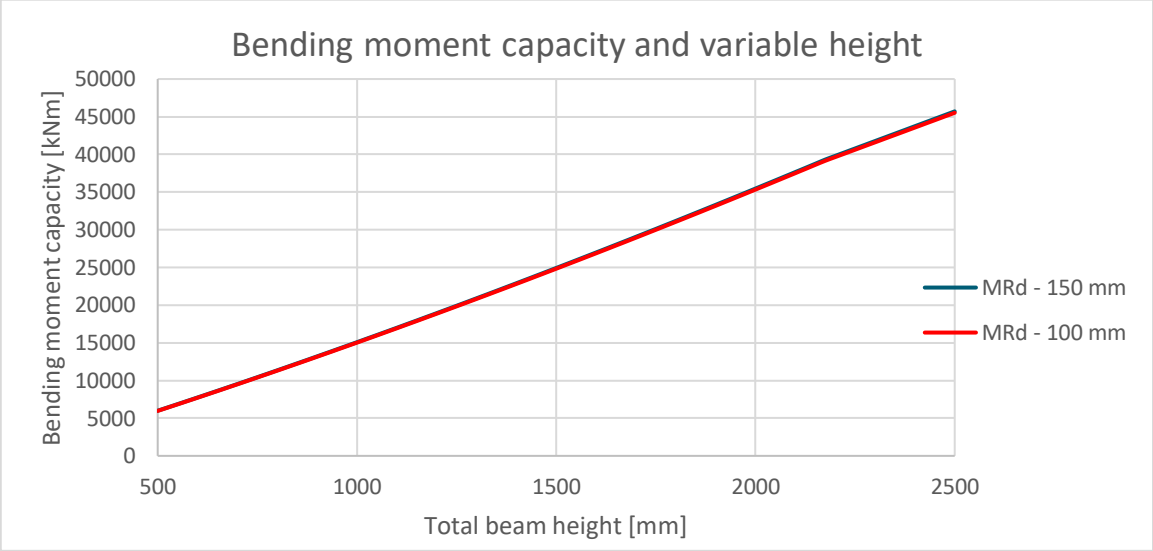

Figure 93 Bending moment capacity as a function of the beam height

Shear force and torsional moment capacity

Figure 94 gives the graphs of the shear capacity as a function of the beam height. It can be observed that reducing the thickness of the web by a third results in a reduction of the shear force capacity of equal proportion. The shear capacity is directly proportional to the dimensions of the cross section, as can be seen from equations (26) and (27).

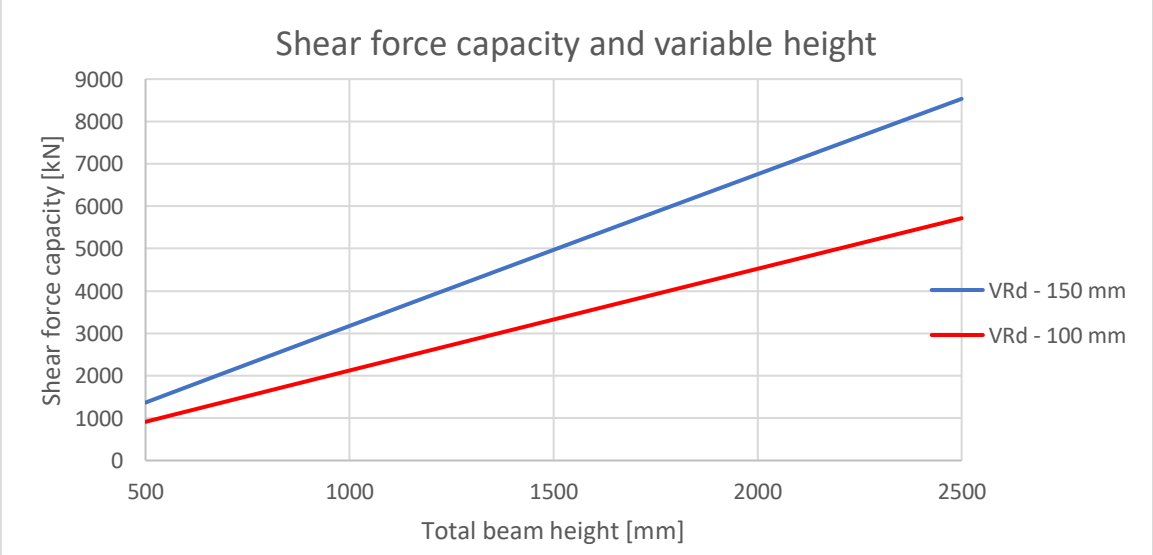

Figure 94 Shear force capacity as a function of the beam height

For the torsional moment capacity and the resistance to the combined effect of shear and torsion similar trends can be observed in the graphs, this is explained by contribution of the webs to these capacities. These graphs are not included in the report but can be found in annex VII.

9.2.3 Dimensioning the beams

With the discussions from sections 9.2.1 and 9.2.2 all information has been required to formulate new design assumptions. New dimensions will be determined for the segments of the cross section based on the capacity (graphs from section 9.2.2) and the minimum dimensions regarding cover and spacing (see sections 9.2.1). To use the graphs the design values of the bending moment, shear force, torsional moment and combined effect of shear and torsion are used as determined in the detailed design. These are 29.855 kNm, 4090 kN, 1222 kNm and 2343 kN (occurring in one of the webs), respectively.

Beam height: The first dimension to be newly established is the total height of the beams. With the maximum tensile stress in the concrete of 6,7 N/mm^2, Figure 92 indicates that the minimum value of the height is approximately 1900 mm. The stresses at midspan turn out to be the stringent criterion: according to the graphs the ultimate limit state verifications are also satisfied at this beam height.

Web thickness: The web is the significant contributor to shear and torsional moment capacity. The design graphs for shear, torsional moment and the combined effect of shear and torsion indicate that at a beam height of 1900 mm the capacity will be sufficient and that the thickness of the webs can be reduced. Because for the optimized design the permanent loads will be lower compared to the detailed design, it is expected that a reduction of the thickness from 150 mm to the minimum of 100 mm will be possible.

Bottom flange: The most stringent criterion for the bottom flange is accommodating the large number of prestressing strands. Based on the results of the detailed design, it is expected that three rows of Ø15,2 mm strands will have to be applied. If, because of splitting action, reinforcement Ø10 is applied, then the cover on the strand would have to be 40 mm and the minimum theoretical thickness of the bottom flange is:

$$t_{fb,min} = 2 * c + 3 * \emptyset_s + 2 * 2 * \emptyset_s \rightarrow 2 * 40 + 3 * 15{,}2 + 2 * 2 * 15{,}2 = 186{,}4 \text{ mm}$$

This value is rounded off to 200 mm to obtain a practical value that also allows for variation with the diameters of the strands and passive reinforcement.

Top flange: The results from the detailed design indicated that no substantial further optimization can be made in the top flanges, these dimensions are therefore not changed. The only modification is that centre of the prestressing tendons in the prestressing ribs are moved downwards.

The tendons will be positioned at half the height of the prestressing rib, instead of the fictitious top flange with height t_{ft} as was done for the detailed design, this way more space is created to accommodate the anchor. The additional eccentricity is calculated as follows:

$$\Delta e_{ft} = 0{,}5 * \left(t_{ft,1} + t_{ft,2}\right) - 0{,}5 * t_{ft}$$

This results in a value of 31,25 mm.

9.3 Elaboration of optimization phase

9.3.1 Dimensioning of the structure

In section 9.2.3 new dimensions have been established, these are summarized in Table 27.

Table 27 New dimensions for optimization phase

Symbol	Value	Units	Definition
w	3200	[mm]	Total width
h	1900	[mm]	Total height
t_{fb}	200	[mm]	Thickness of the bottom flange
t_w	100	[mm]	Thickness of the web
w_f	500	[mm]	Width of the outstand flanges
w_b	2000	[mm]	Internal width of the box

The parameters of the transverse prestressing ribs are summarized in Table 28.

Table 28 New dimensions for optimization phase – Prestressing ribs

Symbol	Value	Units	Definition
$w_{c.t.c.}$	1000	[mm]	Centre to centre distance of the transverse prestressing ribs/ducts
$t_{ft,1}$	125	[mm]	Continuous thickness of the top flange
$t_{ft,2}$	125	[mm]	Local increase thickness top flange at transverse rib
w_{rib}	250	[mm]	Width of the transverse prestressing rib
w_{ch}	250	[mm]	Width of chamfer next to the transverse prestressing rib

9.3.2 Loads

With the new dimensions being established, the RFEM model of the detailed design is modified to determine the global force distribution. Before this can be determined, the self-weight of the main beams and end cross beams are adjusted. All other loads and load combinations are kept identical to those of the detailed design.

9.3.3 Determining global force distribution

In addition to the loads, the cross sections of the main beams and end cross beams also have to be adjusted in the RFEM model. The global force distribution can subsequently be determined. Before the results are summarized, expectations are formulated:

- Because the self-weight of the beams is reduced while the superimposed permanent loads and variable loads are kept the same, it is expected that the maximum forces of the internal forces will be smaller than those found in the detailed design.

- Because all beams have the same stiffness value which is lower than the value of the detailed design while the distribution element is unchanged, a (limited) increase of distribution of variable loads over the beams is expected to occur.

- Despite the small expected increase, the same beams and locations and load combinations are expected to be governing for the main beams as those in the detailed design. Should a different location or load combination become governing, then it is expected that the difference will only be small.

Table 29 summarizes the results from the calculation. The results from the detailed design are added in grey to compare the results.

Table 29 Results from RFEM model

ULS verifications of main beams				
Definition	**Symbol**	**Value**	**Units**	**Description**
Governing bending moment value (mid span)	M_{Ed}	41.753 (48.426)	[kNm]	Beam 3, CO3, config. 2, eq. 6.10a and axles at mid-span (Beam 3, CO3, config. 2, eq. 6.10a and axles at mid-span).
Governing shear force value (near supports)	V_{Ed}	3632 (4090)	[kN]	Beam 3, CO10, config 2, eq. 6.10b and axles at support (Beam 3, CO10, config. 2, eq. 6.10b and axles at supports).
Governing torsional moment	T_{Ed}	1268 (1222)	[kNm]	Beam 3, CO13, accidental situation with axles at mid-span (Beam 3 for combination CO13).
Prestressing main beams – Characteristic combination of the SLS				
Bending moment imposed permanent loads in SLS at midspan	$M_{E,G,perm}$	1725 (1727)	[kNm]	Value of beam 3 is applied (approximately equal values for all beams, value of beam 3 was applied).
Bending moment variable loads in SLS at midspan	$M_{E,Q}$	9553 (9694)	[kNm]	Governing value is beam 3, which is found for config 2 (Maximum found at beam 3 for configuration 2).
Deflections main beams – Frequent combination of the SLS				
Maximum deflection at midspan in the SLS (frequent combination)	δ_{max}	440,9 (344,4)	[mm]	Value of beam 3 is applied, which is found for config 2 (Maximum found at mid span of beam 3 for configuration 2).
Fatigue analysis main beams				
Maximum bending moment at midspan (found using RFEM)	$M_{fat,max}$	26.812 (31.539)	kNm	Value for beam 3 is applied (Value for beam 3 is applied).
Minimum bending moment at midspan (found using RFEM)	$M_{fat,min}$	22.543 (27.183)	kNm	Value for beam 3 is applied (Value for beam 3 is applied).
ULS verification end cross beams				
Maximum hogging bending moment (all loads considered)	$M_{Ed,hog}$	1271 (1212)	[kNm]	Support of beam 1, found for CO13 with axle loads at mid-span (Support of beam 1 for CO13).
Maximum sagging bending moment (all loads considered)	$M_{Ed,sag}$	396 (436)	[kNm]	Span between supports of beams 3 and 4, for CO8 (span between supports of beams 3 and 4, for CO8).
Maximum shear force (all loads considered)	V_{Ed}	846 (837)	[kN]	Support of beam 1, found for CO14 with axle loads near supports (At support of beam 1 for CO14).
Prestressing end cross beams – Characteristic combination of the SLS				
Maximum hogging bending moment SLS	$M_{E,hog}$	453 (469)	[kNm]	Support of beam 3, found for CO27 (Found at support of beam 3 for CO24).
Maximum sagging bending moment SLS	$M_{E,sag}$	270 (298)	[kNm]	Span between supports of beams 3 and 4, for CO27 (Found at span between supports of beams 3 and 4 for CO27).

From the results it can be observed that for the main beams the same beams and load combinations remained governing. The imposed permanent loads, which are required for the design of the prestressing, are close to the results of the detailed design. However, the bending moments due to the variable loads decreased which is contributable to the relative increase of the distributing effect of the distribution element.

The results for the deflections and bending moments for the fatigue analysis are also in accordance with the expectations that were formulated. The deflection increased due to the reduction of the bending stiffness while both the maximum and minimum bending moments for the fatigue analysis decreased due to the reduction of the self-weight.

For the end cross beams, the design values of the bending moments and shear forces are found at the same location as those in the detailed design. This was also observed for the bending moments calculated using the characteristic combination of the SLS. However, a different load combination became governing, though the difference with the load combination in the detailed design is minimal. The difference is contributable to the decrease of the value of the self-weight compared to the variable load.

9.3.4 Design verifications

Calculation procedure and results

With the global force distribution found using RFEM the design verifications can be performed. The calculations are performed using Excel. The setup of the calculation of the detailed design is identical to that of the detailed design except for a number of modifications that are included to allow for optimization or for a more accurate analysis. See annex VII for the details regarding the modifications. Table 30 gives an overview of all verifications that have been performed during the verification procedure.

Table 30 Results calculations optimization phase – Set I

Verification	Element	Unity check
Bending moment capacity	Main beams (global)	0,75
Shear force capacity	Main beams (global)	0,84
Torsional moment capacity	Main beams (global)	0,29
Combination shear and torsion	Main beams (global)	0,93
Combination shear and torsion – Compressive strut	Main beams (global)	0,65
Ship collision – Static equilibrium	Whole deck (global)	0,17
Bending moment capacity joint	Longitudinal joints (local)	0,04
Top flange transverse - Sagging moment	Top flange (local)	0,45
Top flange transverse - Hogging moment	Top flange (local)	0,82
Bending moment capacity longitudinal direction	Top flange (local)	0,83
Fatigue verification – Prestressing steel	Main beams (global)	0,18
Fatigue verification – Concrete at top fibre	Main beams (global)	≈0
Fatigue verification – Concrete at bottom fibre	Main beams (global)	≈0
Deflection	Main beams (global)	0,52
Bending moment capacity	End cross beams (global)	0,23
Shear force capacity	End cross beams (global)	0,60

Results that are not included in the table are the maximum tensile stresses at the bottom fibre for $t \rightarrow \infty$ and the maximum stresses in the longitudinal joints. The maximum tensile stress in the bottom fibre is 3,0 N/mm^2, this is below the maximum allowable tensile strength and leaves margin to reduce the prestressing force.

The stress in the joint turns out to be 4,16 N/mm^2, because the design criterion for the joints is that tensile stresses are not allowed, this is the only verification that has not been satisfied. This therefore turns out to be the governing design criterion with the selected dimensions.

9.3.5 Modifications to the design

Required modifications to the design

The results from the first set of verifications indicates that measures are required because the stress criterion of the longitudinal joints has not been satisfied. In addition, other adjustments have to be made to satisfy the boundary condition of the maximum number of prestressing strands. Furthermore, reducing the transverse prestressing results in more economical solutions, provided such a reduction is possible. This will also be investigated.

Summary of modifications

The different modifications that have been made as well as several points of attention are summarized. The full elaboration can be found in annex VII.

Top flange: The cause of the tensile stresses in the longitudinal joint is the eccentricity Δe_{ft} of 32,5 mm, this eccentricity was provided to create more room for the prestressing anchors. The eccentricity had to be decreased to satisfy the stress criterion while at the same time being kept as large as possible for the accommodation of the prestressing anchors.

Trial and error resulted in a value for Δe_{ft} of 8,0 mm, in this case the joint is just kept under compression. Figure 90 suggests this could be sufficient for the accommodation of the prestressing anchors. In addition, the number of strands per tendon can be reduced from 5 to 4.

Pretensioned strands: The number of prestressing strands in the bottom flange is reduced from 120 strands to 105 strands. With an initial stress $\sigma_{max,fb}$ in the strands of 1488 N/mm^2. The number of centrically positioned strands remains 10 and the initial stress $\sigma_{max,c}$ is 1400 N/mm^2. This results in a stress in the bottom fibre of 6,2 N/mm^2. These adjustments reduce the number of strands to well below the maximum value.

Fatigue of concrete: After applying the aforementioned changes to the prestressing, it was observed during the fatigue verification of the concrete at the bottom fibre that the maximum stress $\sigma_{cd,max}$ was compressive with a value of -4,5 N/mm^2 while the minimum stress $\sigma_{cd,min}$ was tensile with a value of 1,1 N/mm^2. The calculation procedure employed to verify the fatigue capacity of the concrete follows from Eurocode 2-2 and is to be used only for concrete under compression. A combination of compressive stresses and tensile stresses is more unfavourable and therefore a different approach is required.

In section 7.4.1.4 of the fib Model Code a procedure is given which does allow for verifying stress cycles in concrete that result in alternating compressive and tensile stresses. This approach is added to the report to allow for a comparison with the Eurocode approach. Following the symbols in the fib Model Code, $\sigma_{ct,max}$ is 1,1 N/mm^2 and $\sigma_{c,max}$ is 4,5 N/mm^2. Because $\sigma_{ct,max} > 0{,}026 * |\sigma_{c,max}|$, the number of resisting cycles 'N' has to be determined as follows:

$$S_{td,max} = \frac{\gamma_{Ed} * \sigma_{ct,max}}{f_{ctd,fat}} \rightarrow \frac{1{,}1 * 1{,}1}{6{,}0} = 0{,}20\ [-]$$

$$\log(N) = 12 * \left(1 - S_{td,\max}\right) \rightarrow N = 10^{12*(1-0{,}20)} = 3{,}8 * 10^9$$

The design value $f_{ctd,fat}$ of the fatigue tensile strength can be calculated by dividing the lower bound value of the tensile strength $f_{ctk,0,05}$ (which is 9,0 N/mm^2) by the partial factor $\gamma_{c,fat}$ for concrete under fatigue, which equals 1,5. When comparing the number of resisting cycles with the number of cycles due to the loads, which is $5 * 10^7$ cycles, a value for the fatigue damage factor is found of $D = 0{,}01$, which is indeed more unfavourable than the result from the Eurocode expression for fatigue under compression.

In section 6.8 of the AFGC-SETRA 2013 guideline additional provisions are given for elements subjected to fatigue that are loaded in tension under service conditions. It is prescribed that under the frequent load combinations the tensile stresses should be limited to:

$\sigma_{t,max} = \min\{f_{ctm,el}; f_{ctfm}\}$

As mentioned in section 5.4.5, it is clarified in the guideline that this value is established in experiments where cyclic loads resulted in alternating compressive and tensile stresses. Because of this reason, this criterion is deemed to be appropriate for the verification of the given situation.

The beams are designed as such that the tensile stresses under the characteristic load combination in the SLS do not exceed the value of $\sigma_{t,max} = 6{,}7$ N/mm^2, see section 8.5.8. Therefore, this fatigue criterion was already implicitly satisfied. If the actual tensile stress of 1,1 N/mm^2 is divided by the maximum tensile stress of 6,7 N/mm^2, then this results in an indicative unity check value of 0,16. This is the most unfavourable result of the three approaches that have been discussed in this section. This result is therefore the governing result, which will be added to the overview of the verifications that have been performed.

End cross beams: Although these beams were not further considered for the optimization, the calculations indicated that the number of strands in the prestressing tendons could be reduced from 7 to 4 strands.

Buckling of the webs: A remark is made regarding the webs of the beams. The optimization has resulted in very slender webs, as a result the risk increases of the occurrence of instability phenomena that are generally not expected to be governing for more conventional structures: effects such as local buckling or plate buckling of the webs. Verifications for these phenomena have not been included because these are generally not expected to be governing for concrete elements, but given the slenderness of the webs these aspects are worth mentioning and should be included in the design procedure if the bridge is to be constructed.

If buckling of the webs turns out to be of relevance in such a design, extensive detailing will be involved. Such detailing aspects can be solved well in practice, for example by providing stiffeners. At the same time, it is expected that the application of such solutions will have a negligible effect on the results of the project; stiffeners result only in a limited increase of the self-weight of the structure, especially if this function is combined with that of the reinforcing diaphragm elements for ship collision.

Calculation results final design

Table 31 gives the results of the design verifications after implementing the aforementioned modifications.

Table 31 Results calculations optimization phase – Set II (final design)

Verification	Element	Unity check
Bending moment capacity	Main beams (global)	0,90
Shear force capacity	Main beams (global)	0,84
Torsional moment capacity	Main beams (global)	0,29
Combination shear and torsion	Main beams (global)	0,93
Combination shear and torsion – Compressive strut	Main beams (global)	0,65
Ship collision – Static equilibrium	Whole deck (global)	0,17
Bending moment capacity joint	Longitudinal joints (local)	0,38
Top flange transverse - Sagging moment	Top flange (local)	0,81
Top flange transverse - Hogging moment	Top flange (local)	0,76
Bending moment capacity longitudinal direction	Top flange (local)	0,83
Fatigue verification – Prestressing steel	Main beams (global)	0,18
Fatigue verification – Concrete at top fibre	Main beams (global)	≈0
Fatigue verification – Concrete at bottom fibre	Main beams (global)	0,16
Deflection	Main beams (global)	0,65
Bending moment capacity	End cross beams (global)	0,38
Shear force capacity	End cross beams (global)	0,72

A value not given in the table is the tensile stress in the bottom fibre at mid span for $t \to \infty$, this is a tensile stress of 6,2 N/mm^2.

9.4 Overview of the final design

The results of the calculations indicate that very limited room remains for further weight reduction if the current design approach remains to be used. If further substantial weight reductions are to be achieved, a different approach should be applied, such as the second and third option given in 9.1.2. Therefore, no further optimizations will be carried out and the design as defined in 9.3.5 will be taken as the final design, with which the design stage is concluded. Figure 95 gives the cross section of the optimized beam design: the final design.

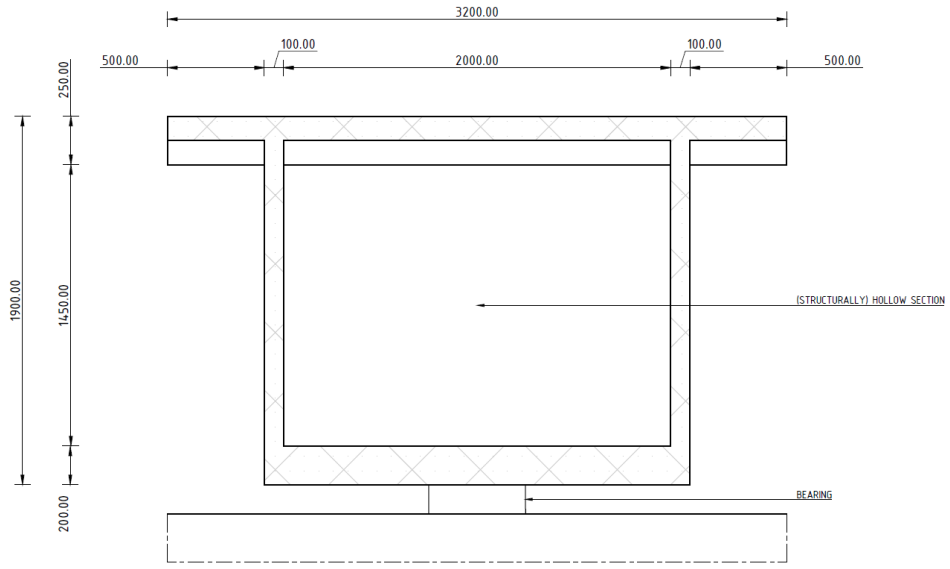

Figure 95 Optimized cross section main beams

The optimization has resulted in further weight reduction. Table 32 compares the weight of the final design to that of the detailed design, this equates to a reduction of the weight with an additional 18%.

Table 32 Weight comparison detailed design and final design

	Detailed design	**Final design**
Element	[kN]	[kN]
Prefab UHPC beams	14.703	11.864
In-situ UHPC joints	119	119
Cross beams	2887	2315
Asphalt layer	266	266
Kerbs	601	601
Capping beam	614	614
Total	19.190	15.779

To conclude the design stage, a number of key figures of the optimized prefab UHPC beams (the values correspond to a single beam) are summarized:

- Total number of pretensioned strands: 115 [pcs]
- Total volume of UHPC: 106,4 [m^3]
- Self-weight including solid beam end: 2660 [kN]

Reference is made to annex VII for the full elaboration of the optimization phase and final design, as well as for the corresponding drawing of the prefab beam deck.

10

GLOBAL ASSESSMENT FOUNDATION

10.1 Approach

10.1.1 Global assessment of the foundation

The design stage of the project has been concluded with the final design. The next phase is to determine whether the final design resulted in a weight reduction significant enough to allow for the reuse of the existing foundation of the Eefdesebrug. The most accurate way to determine whether the existing foundation can be reused is a full analysis. However, this falls outside the project scope. The analysis of the foundation is therefore limited to a comparison of the vertical loads acting upon it in the new and existing situation.

The formal requirement that has to be satisfied is given in equation (72), the design value of the permanent and variable vertical loads should be smaller than or equal to the design value of the permanent and variable vertical loads of the existing structure. This inequality is formulated under the assumption that in the design of the existing structure partial load factors were applied.

$$\gamma_{G,N} * G_N + \gamma_{Q,N} * Q_N \leq \gamma_{G,E} * G_E + \gamma_{Q,E} * Q_E \qquad \text{Equation (72)}$$

In this equation the symbols G_N and G_E represent the vertical actions due to permanent loads in the new design and existing situation, respectively. These values will be based on the final design from 9.4 and the design drawings of the existing bridge provided by Rijkswaterstaat. The symbols Q_N and Q_E represent the vertical variable actions in the new design and the existing situation, respectively. These values will be determined in accordance with the Eurocode and the codes used for the design of the existing structure, respectively.

In addition, four partial load factors are required. The factors $\gamma_{G,N}$ and $\gamma_{Q,N}$ are the partial load factors for permanent and variable actions for the new design, these are determined following the Eurocode. The factors $\gamma_{G,E}$ and $\gamma_{Q,E}$ are the partial load factors for permanent and variable loads for the design of the existing structure, these will have to be deduced from former codes that were in use in the period the Eefdesebrug was designed and built.

By using the formal approach given by equation (72), the design value of the vertical loads for the new design is compared to the design value of the vertical loads the foundation is originally designed for. This implies that if the vertical forces in the new situation are smaller than or equal to those in the existing situation, the capacity of the foundation should theoretically be sufficient for reuse.

Note that in reality the current horizontal variable loads are also higher than those that had to be applied in the past. However, these horizontal forces are excluded from the scope of the project. The reason is that a structure can be strengthened for increased horizontal variable loads in more practically applicable ways compared to strengthening for increased vertical variable loads.

10.1.2 Codes and guidelines existing structure

Identifying former design codes

To be able to follow the approach as given by equation (72), the codes that were used for the design of the existing structure have to be identified. This way the vertical variable loads and partial load factors can be established. Given the year of construction of the bridge, it is estimated that the design work for the Eefdesebrug must have taken place in the 1950 – 1955 period. Design codes from this period will therefore have to be sought for.

Technische Grondslagen voor Bouwvoorschriften (TGB) 1949

During the period in which the Eefdesebrug was designed, the starting point for the structural design of most structures was the N 1055, also referred to as the TGB 1949. This code covered the general aspects of the design such as actions on structures and maximum stress values for various materials (steel, timber and stone) and deflections. Provisions for the design of concrete structures were not given though, in the preface of the code the remark is made that the committee responsible for the TGB 1949 did not include the design of reinforced concrete structures, because this was part of the task of the reinforced-concrete committee.

Gewapend Beton Voorschriften (GBV) 1950

Because the TGB 1949 does not provide the required information the relevant code on reinforced concrete has to be identified. Table 33 is based on information from (Gijsbers, 2012) and gives an overview of all codes on reinforced or structural concrete since the first code on this topic was introduced in the Netherlands in 1912.

Table 33 Overview of codes on reinforced/structural concrete in The Netherlands

Year	Title of the code	Denoted as:
1912	Gewapend Beton Voorschriften	GBV 1912
1918	Gewapend Beton Voorschriften	GBV 1918
1930	Gewapend Beton Voorschriften	GBV 1930
1940	Gewapend Beton Voorschriften	GBV 1940
1950	Gewapend Beton Voorschriften	GBV 1950
1962	Gewapend Beton Voorschriften	GBV 1962
1974	Voorschriften Beton	VB 1974
1984	NEN 3880 – Voorschriften Beton	VB 1974/1984
1990	NEN 6720 – Voorschriften Beton	VBC 1990
1995	NEN 6720 – Voorschriften Beton	VBC 1995
2012	Eurocode 2: Ontwerp en berekening van betonconstructies	NEN-EN 1992

Based on the year of publication of these codes, it is most likely that the existing structure was designed using the GBV 1950. This code was a revision and extension of its predecessor, the GBV 1940, and comprised eight different sections: general provisions, materials, execution & construction, design calculations, allowable stresses, control of construction, deviations from the code and the then new topic of flat slabs.

The GBV 1950 cannot be used as a standalone document, it contains references to other codes as well. Although it gives a small number of additional provisions, it prescribes that loads should be determined following the provisions given in the TGB 1949, see article 28-d of section 4 for this reference. For variable loads due to traffic reference is made to the VOSB, the code to which a reference was found as well on the design drawings provided by Rijkswaterstaat.

Voorschriften voor het Ontwerpen van Stalen Bruggen (VOSB) 1938

The N 1008, also denoted as the VOSB, is a former code on the design of steel bridges and included load models for variable traffic loads. For concrete bridges the variable loads were also determined following this code, on one of the design drawings of the Eefdesebrug provided by Rijkswaterstaat it is mentioned that the variable loads used in the design were in accordance with ‘class A’ of the VOSB.

The code was revised multiple types and as a result three versions have been used: the version from 1933, 1938 and 1963. Given the years of publication the version of 1938 is most probably used. Because design calculations of the existing structure were not available, the variable loads will have to be determined in accordance with this code.

10.2 Determining vertical loads and factors

10.2.1 Self-weight existing structure

Although rough estimations of the self-weight of the existing structure have already been made to perform a weight comparison with the results of the preliminary and detailed design, a more accurate estimation will be made in this section. Figure 96 gives an overview of the structure in which ten different components are indicated that are distinguished and included in the calculation.

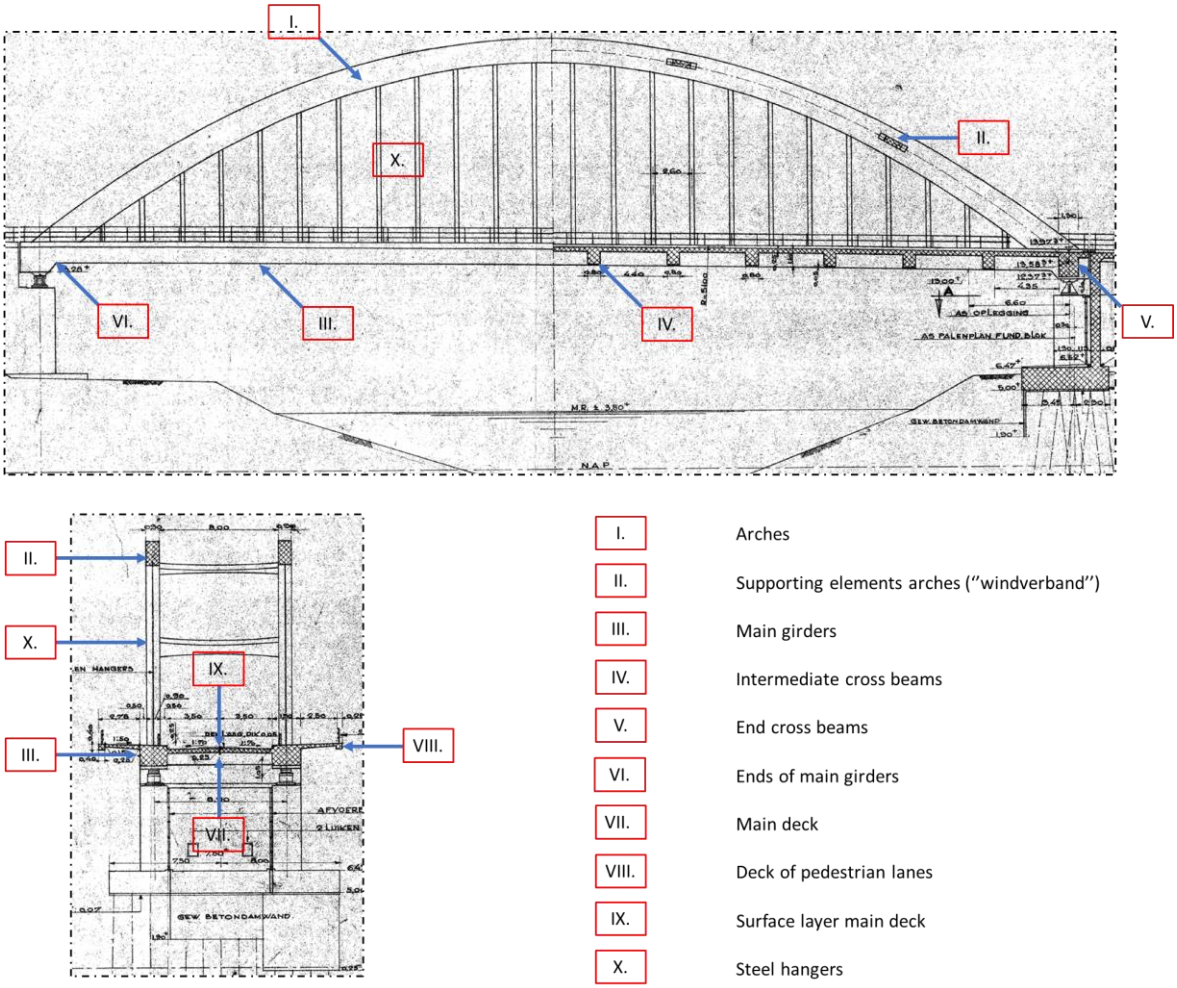

Figure 96 Components considered for weight calculation existing bridge – Part of drawing B.3806 (from Rijkswaterstaat archives)

To perform this calculation assumptions have to be made for the specific weight of the materials that are applied. For reinforced concrete γ_c is taken equal to 25 kN/m^3, for asphalt γ_a is taken equal to 23 kN/m^3 and for steel the value of γ_s is 78,5 kN/m^3.

Using these values for the specific weight and the design drawings of the existing structure, the weight contribution of each component is calculated. Subsequently the individual contributions to the self-weight of the structure are added up to obtain an estimation of the total self-weight G_E of the structure. Table 34 summarizes the results of the calculation, the complete calculation can be found in annex VII.

Table 34 Calculation weight of existing bridge deck

Component	Length	Height	Width	Cross-section	Number	Weight	Result
[-]	[m]	[m]	[m]	[m^2]	[-]	[kN/m^3]	[kN]
I	72,50	1,70	0,90		2	25	5546
II	8,00	0,36	1,60		4	25	461
III	70,70	1,30	1,90		2	25	8731
IV	7,00	0,80	0,80		12	25	1344
V	7,00	1,25	1,30		2	25	569
VI			1,90	1,13	4	25	215
VII	70,70	0,25	7,00		1	25	3093
VIII	70,70			0,636	2	25	2248
IX	70,70	0,05	7,00		1	23	569
X	133,62			$3,32*10^{-3}$	8	78,5	278
Total							23.055

10.2.2 Self-weight final design

The self-weight of the optimized final design is calculated by decomposing the deck into a total of seven components after which their individual contributions are added up to determine the total self-weight. The different components are the prefab UHPC beams (component 1), the solid end sections of the prefab beams (component 2), the in-situ cross beams (component 3), the in-situ UHPC joints (component 4), the surface layer (component 5), the kerbs (component 6) and the capping beams (component 7). The specific weight of the materials is in accordance with the assumptions from 8.2.3. Table 35 summarizes the results.

Table 35 Calculation weight of bridge deck final design

Component	Length	Height	Width	Cross-section	Number	Volume	Weight	Result
	[m]	[m]	[m]	[m^2]	[-]	[m^3]	[kN/m^3]	[kN]
1	70,70			1,3425	5		25	11.864
2	1,90	1,51	2,00		10		25	1437
3					2	17,57	25	878
4	70,70	0,1875	0,090		4		25	119
5	70,70	0,010	16,36		1		23	266
6	70,70	0,34	0,50		2		25	601
7	16,36	1,0	0,75		2		25	614
Total								15.779

10.2.3 Variable loads existing structure

Because no original design calculations of the existing structure have been found, the loads are determined by the VOSB 1938. Loads on bridges for road traffic are covered in articles 28 and 29.

Load classes: Based on article 28 the bridge has to be classified into one of the four given load classes, the Eefdesebrug is a bridge of ''class A'', which are bridges for main traffic roads for which diverting the traffic is not possible.

Load on carriageway: Article 29 defines the actual loads based on the classification of the previous article, for a bridge classified as ''class A'' and a carriageway with a width smaller than 5,0 m the code prescribes a uniformly distributed load of 400 kg/m^2 over the area of the deck combined with one set of concentrated loads comprising three axles of 20 tons. Figure 97 gives the load model.

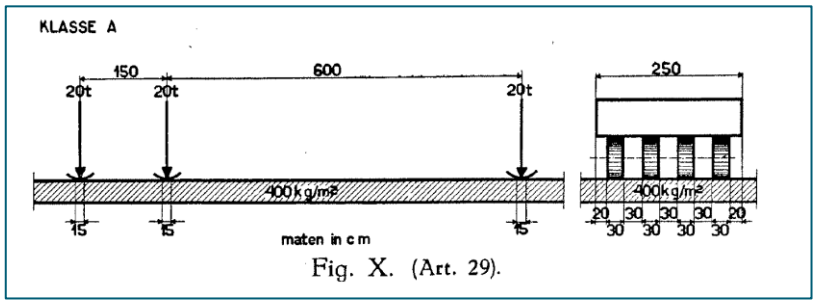

Figure 97 Variable load model ''Klasse A'' from the VOSB 1938 – VOSB 1938, p.55

Because the carriageway is wider than 5,0 m, multiple lanes (and thus heavy vehicles) can be placed adjacent to each other. Conforming the VOSB the maximum number of heavy vehicles is determined by dividing the width by 2,5 m and rounding off to the lower nearest integer, for the Eefdesebrug this results in two lanes.

Because two heavy vehicles can be positioned adjacent to each other the code prescribes that a 10% reduction may be applied to the concentrated and uniformly distributed loads. This results in a uniformly distributed load of 360 kg/m^2 applied over the full surface of the deck and two heavy vehicles comprising three axles of 18 tons each, resulting in a total of 108 tons.

Loads on pedestrian lanes: The vertical loads on bicycle and pedestrian lanes are covered in article 30, for bridges of ''class A'' a uniformly distributed load is prescribed of 400 kg/m^2. This load is to be applied over the full area of the pedestrian lanes provided that this gives the most unfavourable result.

Loads on railings: Article 38 covers loads acting on railings. Only horizontal loads are prescribed but because these are no part of the comparison of vertical loads, these actions are not taken into consideration.

Dynamic amplification factor: Contrarily to the Eurocode where the variable loads already include dynamic effects, this is not the case for the VOSB 1938 in which a separate factor is prescribed in article 34. The factor should be applied to the variable loads on the main carriageway and the loads on the pedestrian lanes and is calculated as follows:

$$S = 1 + \frac{40}{100 + L}$$

For the Eefdesebrug this results in a factor of 1,24. According to article 54 of the VOSB the factor has to be applied for the design of concrete decks, but (see article 34) not for the design of abutments made of concrete or stone. The factor will therefore not be included in further elaborations.

Total vertical variable loads: Figure 98 summarizes the results when applying the VOSB 1938 to determine the variable loads acting on the deck of the existing bridge. Note that the uniformly distributed loads are applied over the full length of the deck to obtain the most unfavourable situation and that each heavy vehicle comprises three axles.

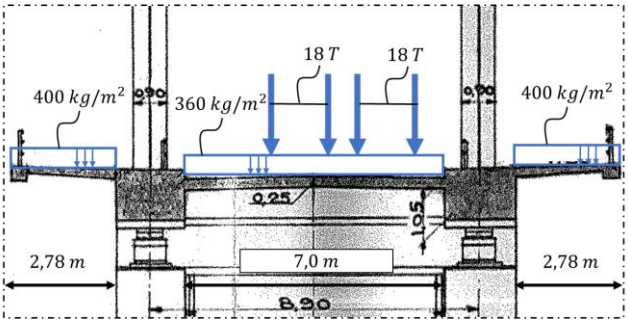

Figure 98 Traffic loads on the existing structure following the VOSB 1938 – Part of drawing B.5109 (from RWS archives)

10.2.4 Variable loads final design

The variable loads of the final design are determined in accordance with Eurocode 1-2, see sections 7.3.1 and 8.3.1. Both the first and second configuration of LM1 as given in Figure 46 or Figure 47 can be applied, this will give the most conservative results in the comparison of vertical loads. The first configuration is selected.

Figure 99 gives an overview of the different vertical variable loads that are applied, including the loads on the pedestrian lanes and the railing. By applying these load configurations and applying the uniformly distributed loads over the full length of the deck, the most unfavourable situation is obtained.

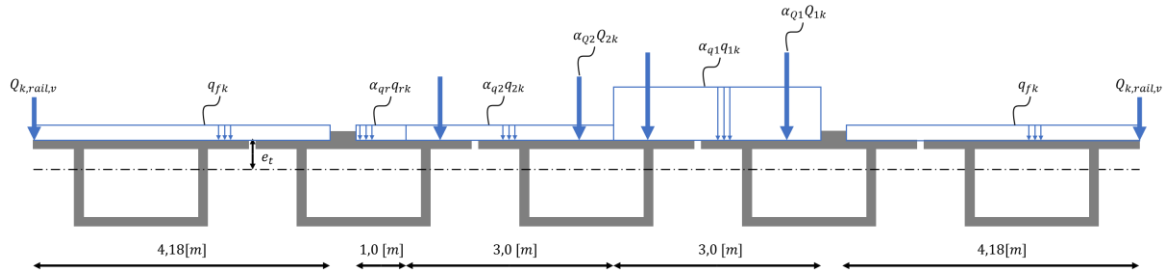

Figure 99 Total variable vertical load on the deck

For the sake of completeness, the values of the vertical variable loads are summarized in the following table.

Table 36 Values of variable vertical loads on the deck

Lane	Concentrated load	Line load	UDL
[-]	[kN/axle]	[kN/m]	[kN/m^2]
Theoretical lane 1	291	-	8,73
Theoretical lane 2	194	-	2,424
Remaining area	-	-	2,25
Pedestrian lanes	-	-	3,22
Railing	-	3,0	-

10.2.5 Comparison of design codes

Comparing safety philosophies

The global assessment is supposed to be carried out using equation (72) as the design criterion, this equation was formulated under the assumption that both the Eurocode and the codes used for the design of the existing structure make use of the same safety philosophy (method of partial factors). However, it has to be verified whether the proposed approach is valid or not.

Eurocode

Structural reliability in the Eurocode is demonstrated by verifying that the design value of effect of actions is smaller than or equal to the design value of the resistance, this can be written as follows:

$$\frac{E_d}{R_d} \leq 1{,}0 \qquad \text{Equation (73)}$$

The design value of the effect of the actions is obtained by multiplying the characteristic value of the effect of actions with the partial factor for actions. The design value of the resistance is obtained by dividing the characteristic value of the resistance by a partial factor associated to the resistance. The characteristic value is a value defined as such that the probability of the occurrence of an action larger or a resistance value smaller than the characteristic value is a certain percentage, typically this is 5%. The unity check of equation (73) can be written as follows:

$$E_k * \gamma_F \leq \frac{R_k}{\gamma_M} \qquad \text{Equation (74)}$$

GBV 1950 and VOSB 1938

In the GBV 1950 and VOSB 1938 a different method was used in the past to demonstrate the reliability of a structure. Variable traffic loads were determined in accordance with the VOSB 1938 while other loads were determined following the TGB 1949. Subsequently the force distribution was determined without applying partial load factors, the values of the actions therefore represent the actions under use conditions.

The verification subsequently took place using the GBV 1950, provisions were given in section 5. Verifications were based on maximum stress values, the stresses in the components were calculated and subsequently compared with the maximum allowable value. These maximum stress values included a global safety margin, the maximum value was dependent on the type of verification (e.g. centric compressive force or a beam in bending), the material (concrete or reinforcing steel) and whether supervision is present during construction.

An example is the maximum stress allowed in the reinforcement of structural elements loaded in bending or a combination of bending and axial force. The following table, from article 34b, gives the maximum stresses in the reinforcing steel if supervision during construction is present.

Staalsoort		Toelaatbare trekspanning in kg/cm²
a) Betonstaal QR 22		1300
b) „ QR 24		1400
c) „ QR 30	volgens V 1035	1600
„ QR 36 en QRn36		1800
„ QR 42 en QRn42		2000
„ QRn48		2200
„ QRn54		2400

Figure 100 Allowable stresses in reinforcement – GBV 1950, p.83

For steel of grade QR22 the minimum yield stress is 2200 kg/cm^2 (approximately 220 N/mm^2) while the maximum allowable tensile stress is 1300 kg/cm^2 (approximately 130 N/mm^2). That means that there is a theoretical safety margin incorporated in the allowable stress of:

$$\gamma = \frac{2200}{1300} \approx 1{,}7$$

Comparison

Before the comparison is further elaborated, it is mentioned that it was expected beforehand that differences would be found between the Eurocode and the GBV 1950 and VOSB 1938. Design practices change over time due to technological developments and codes always represent common practice at the moment of publication. New approaches may be added and older provisions may be replaced or removed because these have become obsolete. Differences were sought for in the way that reliability is incorporated in the design procedure, two main difficulties have been identified that complicate the method summarized by equation (72).

Uncertainties and effects: The first aspect is what the safety factors actually represent. The Eurocode applies the method of partial factors, this is relatively transparent because the partial load factor and partial material factor account for different uncertainties and effects. An example of what the partial load factors accounts for is the uncertainty in the magnitude of the load, which may vary from the value of the characteristic load.

This is contrary to the GBV 1950, which prescribes a global safety factor by reducing the maximum allowable stress in the concrete and reinforcing steel. This global factor accounts for all possible uncertainties in the design, both those on the side of the actions and the side of the resistance, and as a result the code is less transparent.

Safety margin in design of foundation: The second complicating factor is in the design of the foundations. The GBV 1950 prescribes different maximum allowable stresses for different materials and verifications, this implies that if the foundation is considered, it should be known what the safety margin is that was included in the design of the foundation if any sensible comparison with the Eurocode is to be made.

Because the dated GBV 1950 followed vastly different design approaches than those in the more modern Eurocode, this suggests that the approach to the design of the pile foundations will also have been different in the period the Eefdesebrug was designed and constructed. However, neither the GBV 1950 nor the VOSB 1938 give more information on the design of pile foundations.

A clarification for this lack of information can be found in (Van Tol, 1994), in which an overview is given of methods for the investigation of soil and the design of pile foundations in the Netherlands in the past. The design and construction of the Eefdesebrug falls in the period in which the cone penetration test was introduced only recently and in which the first attempts were made to derive empirical methods to determine the load bearing capacity of foundation piles directly from the results of such tests.

However, it would take decades until consensus on such approaches would be achieved and the first code on geotechnical design would be introduced (the NEN 6743 from 1992). The NEN 6743 was part of the TGB 1990 series. As a part of this series, statistics were first introduced in geotechnical design using the methods of partial factors. This is in correspondence with the codes for other materials that were also part of this series, such as concrete as covered in the VBC 1990, in which this method was also applied.

Implications for global assessment of the foundation

The Eurocode has been compared with the GBV 1950 regarding the incorporation and demonstrating the theoretical reliability of the structure. Two reasons have been identified that complicate the application of equation (72) as a means of performing a global assessment of the foundation.

The first factor is the fact that the GBV 1950 uses a global safety factor while the Eurocode uses the method of partial factors. The second complicating factor is that it remains unknown what safety margin was included in the design of the existing foundation, no specific information or specific safety factor for the design of pile foundations was found in the older codes that were considered. This is explained by the fact that at the time the Eefdesebrug was designed and constructed, methods for soil investigation and the design of pile foundations were still in their earlier stages of development, normalisation was only to follow decades later.

Given these two differences it is deemed not to be possible to perform a comparison using equation (72). In order to perform a global assessment of the foundation an alternative approach will have to be adopted.

10.3 Performing global assessment foundation

10.3.1 Verification criterion

In section 10.2 the vertical loads have been determined for the new design and existing structure. In addition, the design codes were compared from which it was concluded that the approach given by equation (72) is not valid. Therefore, a different approach will have to be applied.

As an alternative the global assessment of the foundation will be performed by comparing the total vertical forces for the new design and the existing structure without any additional load factors, and thus representing loads under use condition. Equation (72) is replaced by the following expression:

$$G_N + Q_N \leq G_E + Q_E \qquad \text{Equation (75)}$$

The principle behind this criterion is identical to the principle of the criterion from 10.1.1, expect for the fact that no load or combination factors are applied. This means that the representative values of the actions are

plugged into the equation. The requirement is that the representative value of the vertical forces in the new situation should be smaller than or equal to the value of these forces for the existing bridge.

10.3.2 Comparison of total vertical forces

Summation of all vertical forces

Table 37 summarizes the results from the weight calculation given in section 10.2.1 up to and including section 10.2.4. Figure 101 visualises the values given in the table.

Table 37 Vertical loads existing structure and optimized new design

Action	Existing structure	New design	Percentage change
[-]	[kN]	[kN]	[%]
Permanent loads	23.055	15.779	-32
Variable loads	4434	5822	31
Total vertical load	27.489	21.602	-21

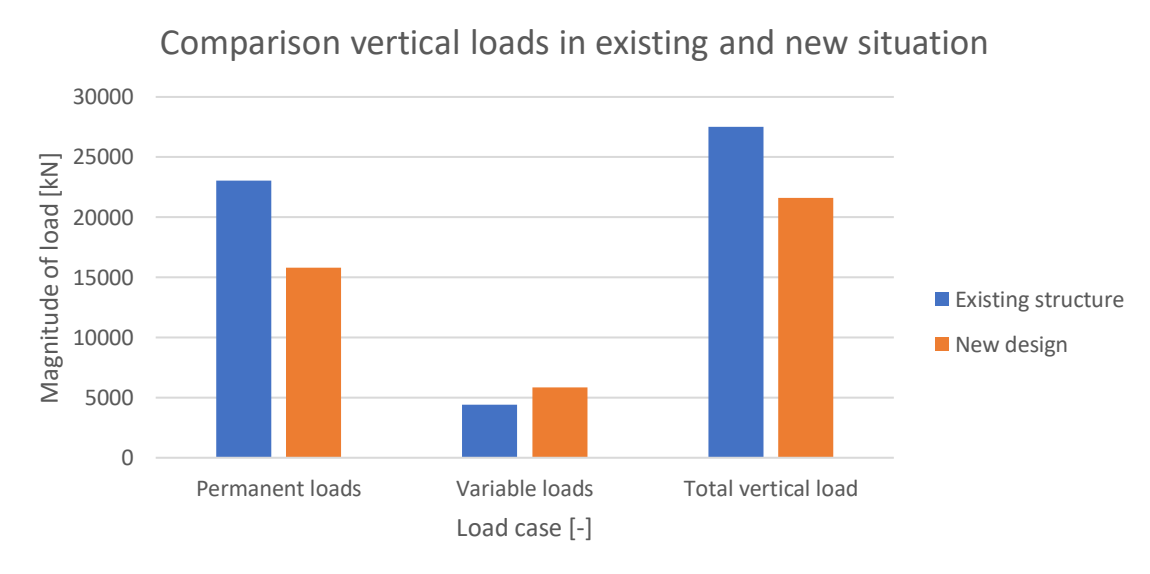

Figure 101 Comparison of vertical loads of existing structure and optimized new design

The results give an impression typical for concrete bridges with longer spans. For such bridges it is generally the self-weight that is the largest load. The following observations can be made with regard to the vertical loads:

- If only the permanent loads are considered, then the final design results in a reduction of 32% compared to the existing bridge;
- The variable loads determined following the Eurocode are in total 31% higher than those determined following the VOSB 1938;
- Although the increase of the variable load is significant in absolute terms, it is less significant in relative terms when compared to the self-weight. The weight reduction is more than sufficient to compensate for the increase of the variable loads, resulting in an overall decrease of the vertical forces of 21%.

The comparison of equation (75) can also be formulated in the form of a unity check. If the total vertical force in the new situation is denoted by $F_{V,N}$ and that in the existing situation by $F_{V,E}$, then:

$$UC = \frac{F_{V,N}}{F_{V,E}} \leq 1{,}0 \rightarrow \frac{21.602}{27.489} = 0{,}79$$

It is concluded that with a reduction of the total vertical forces of 21%, the criterion for the reuse of the existing foundation as formulated by equation (75) has been satisfied.

Summation of forces with axles near support

The results presented in Table 37 and Figure 101 do not include any load effects. It was assumed implicitly that the loads are centred around mid-span, as a result both abutments carry half the total load. In reality such situations usually do not occur and therefore a second situation will be analysed.

It is determined what the result would be if one abutment carries the total variable concentrated loads. Table 38 summarizes the results visualised by Figure 102. The permanent loads and uniformly distributed variable loads are distributed equally over both abutments while the concentrated variable loads are assumed to be positioned directly above the supports at one of the abutments.

Table 38 Vertical loads existing structure and optimized new design – Single abutment

Action	Existing structure	New design	Percentage change
[-]	[kN]	[kN]	[%]
Permanent loads	11.527	7890	-32
Variable loads	2757	3396	23
Total vertical load	14.284	11.286	-21

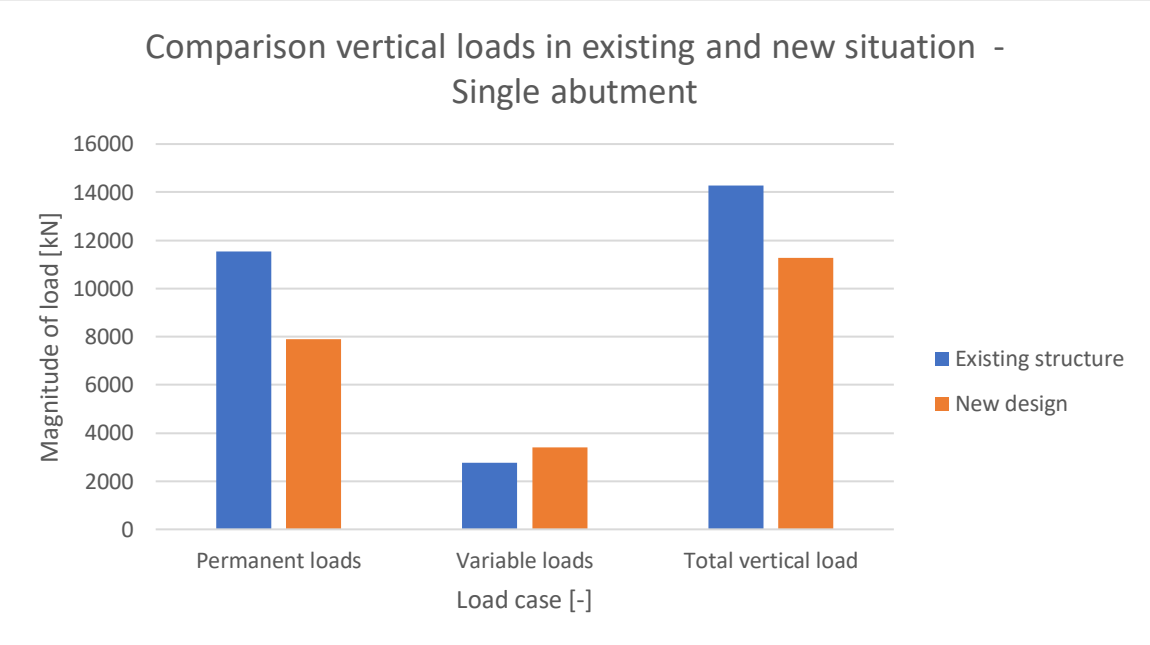

Figure 102 Comparison of vertical loads of existing structure and optimized new design – Single abutment

The percentual increase of the variable loads is lower compared to the previous case due to the fact that the Eurocode is more unfavourable than the VOSB 1938 if the uniformly distributed loads are considered, while for this calculation the contribution of the axle loads, where the difference is smaller, increased relatively to that of the uniformly distributed loads.

From the results it can be seen that on the whole there is no difference in percentual change. This indicates that although for a single abutment the situation is more unfavourable, the permanent loads are still the largest contributor to the vertical loads, the effect of positioning the concentrated variable loads directly above one of the supports is only marginal.

10.3.3 Additional analysis – Forces in foundation piles

Including additional analysis

A global assessment of the foundation of the Eefdesebrug has been carried out by comparing the vertical forces acting upon it in the new and existing situation. As an addition to the project aspects from the pile foundation will also be considered. Using a simplified model an approximating calculation of the forces in the foundation piles will be performed. This additional calculation is added because it is expected that it will provide useful additional insights that cannot be obtained by only comparing the vertical forces, insights such as:

- A rough estimate of the forces in the different pile groups;
- An indication to what extent the percentual change of total vertical forces relates to the percentual change of the forces in the foundation piles;
- The option of including the effects of the eccentricity of the bearings with respect to the centre of the pile group and that of horizontal forces acting on the bridge deck;
- Determine the heaviest loaded pile group of the foundation as well as the percentual change in the compressive forces in this pile group.

The calculation will be carried out using various simplifications and assumptions. The foundation block is reduced to a 2D model and all forces included are assumed to act in the direction of the longitudinal axis of the bridge deck. The calculation only includes actions due to permanent and variable loads due to and acting upon the superstructure, i.e. the self-weight of the deck, imposed permanent load on the deck, vertical variable loads acting on the deck and horizontal variable loads acting on the deck. Furthermore, the actions are considered without load factors. Figure 103 gives the approach to the calculation.

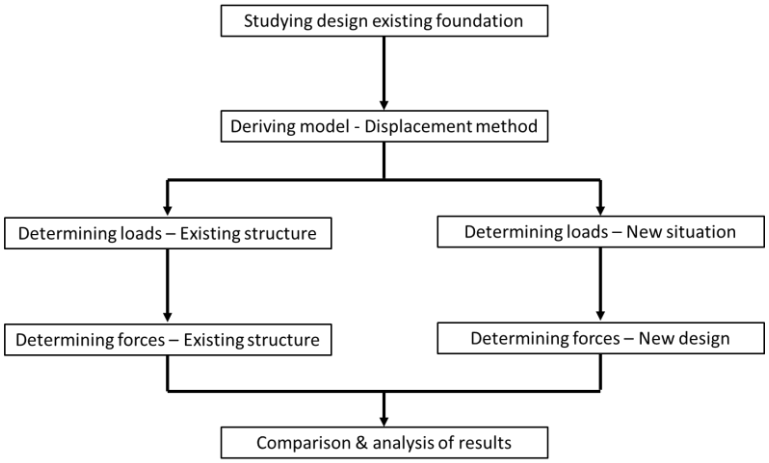

Figure 103 Approach to approximate forces in the foundation piles

Actions that are thus explicitly not included are actions in transverse direction (e.g. ship collision), rotational effects (e.g. due to eccentric horizontal traffic loads), elongation or shortening due to temperature effects, actions related to soil pressure acting upon the substructure and the self-weight of the substructure itself.

Analysis of foundation north side

The pile group of the northern foundation block will be analysed but given the large similarities in design these results hold for the southern block as well. Figure 104 gives a side view of the bridge and abutment (left) as well as the top view of the pile group of the foundation block (right). Along the horizontal axis five rows of piles can be distinguished and based on the inclination of the piles towards the left or right, a total of eight pile groups can be distinguished.

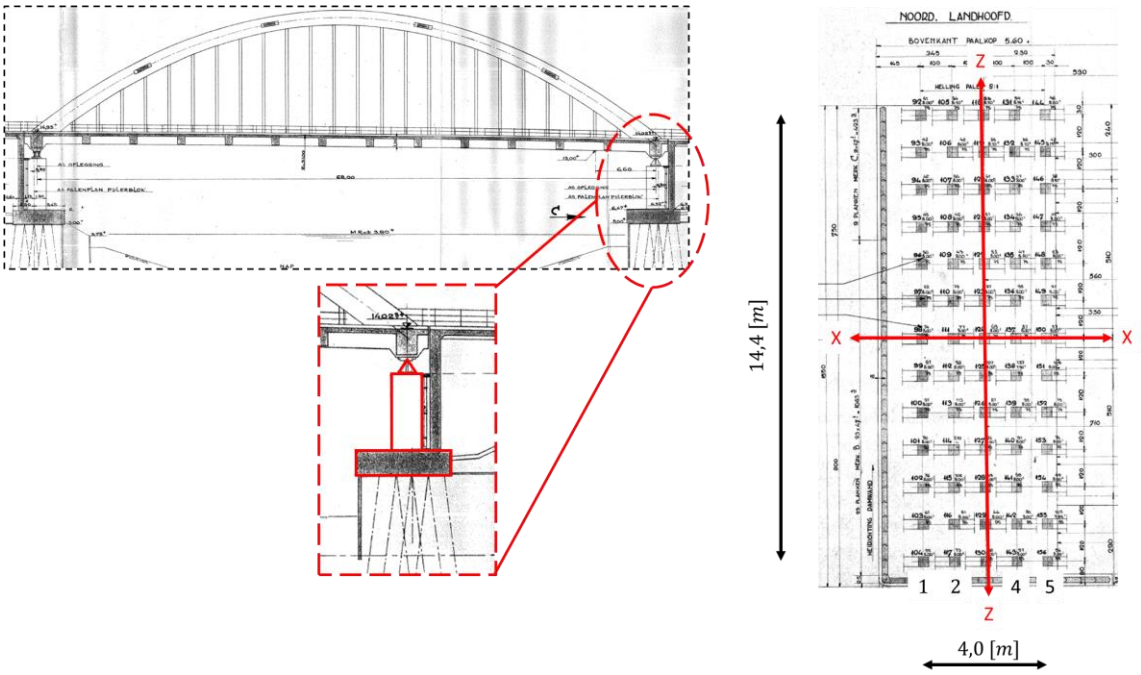

Figure 104 Abutment (left) and top view of the pile group (right) – Drawings B.5109 & B.3797 (from Rijkswaterstaat archives)

Figure 105 gives a side view of the foundation block as well as the main principles of the model. The foundation block is simplified into a 2D model with three degrees of freedom upon which three different loads are acting. If a force R_v acts upon the buttress due to the superstructure and the loads upon it (see part A of the figure), then via the buttress this load acts onto the foundation block (B). Due to an eccentricity 'e' with respect to the centre of the pile group, a moment M_v (C) is introduced. As a first approximation the foundation slab is assumed to be rigid and the foundation piles will be modelled as groups of parallel translational springs (D). These springs give reaction forces only to displacements in the direction of their longitudinal axis.

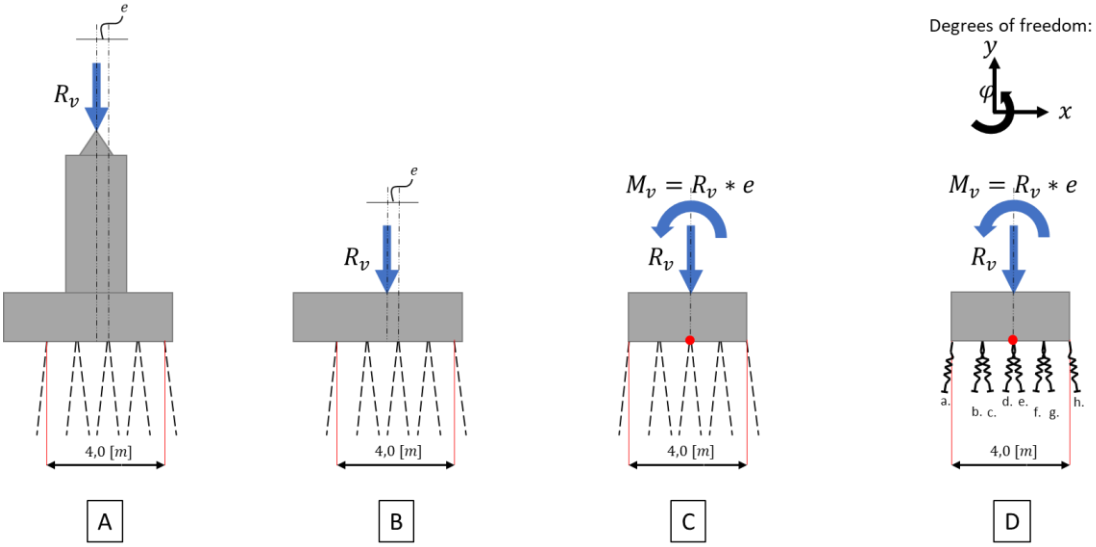

Figure 105 Model for the analysis

All individual piles are assumed to have the same stiffness k. Eight pile groups can be distinguished, the piles are grouped depending on their direction of the inclination, forming groups of parallel springs with the same deformation u_i. These pile groups are denoted with letters a – h. The reaction force N_i of a pile group consisting of n_i springs with the same stiffness k_i is the summation of individual capacities:

$$N_i = n_i * k_i * u_i$$

Further derivations of the model

Using the displacement method equations will be derived to determine the forces in the foundation piles for any combination of horizontal forces, vertical forces and moments. The degrees of freedom are a horizontal displacement, vertical displacement and rotation.

The system is moved in the positive directions of each of the individual degrees of freedom after which the pile forces due to the two displacements and the rotation are determined. This way a total of eight equations is formulated, one equation for each pile group which expresses the pile forces as a function of the displacements in the positive directions of the degrees of freedom. In matrix-vector form this is written as:

$$\underline{n} = \boldsymbol{K}\underline{u} \qquad \text{Equation (76)}$$

Subsequently the equilibrium equations are formulated. External forces are assumed in their positive directions as well as pile forces in their positive directions. The tensile forces in the piles are denoted as positive values. Formulating the horizontal equilibrium, vertical equilibrium and moment equilibrium of the foundation block results in three equations. In matrix-vector form these can be written as:

$$\boldsymbol{C}\underline{n} = \underline{f} \qquad \text{Equation (77)}$$

By substituting equation (76) into (77) the equilibrium of the system is expressed in the displacements of the springs, and the displacements of the springs required to obtain equilibrium with the given external forces are calculated. If the multiplication of matrices $\boldsymbol{C}$ and $\boldsymbol{K}$, which results in a 3 by 3 matrix, is denoted as $\boldsymbol{H}$, then the expression for the displacement vector is:

$$\underline{u} = \boldsymbol{H}^{-1}\underline{f} \qquad \text{Equation (78)}$$

By substituting the vector $\underline{u}$ back into equation (76) the forces of the individual piles are obtained that correspond to the displacements obtained by equation (78).

Determining loads

A model has been derived with which the forces in the foundation piles can be estimated. To use the model the forces acting on the foundation block have to be determined.

Vertical loads: Vertical loads are, both for the new design and existing situation, calculated by dividing the uniformly distributed loads and line loads equally over the abutments. In addition, it is assumed that the concentrated variable loads are positioned at the abutment under consideration and is therefore by approximation fully supported by this foundation block.

Horizontal loads: Because horizontal loads may result in significant forces in the foundation piles, these are included as well. For the existing structure the horizontal loads are determined following article 40 of the VOSB 1938, which prescribes that the braking forces are taken equal to 1/7 of the concentrated variable loads, which corresponds to 154 kN.

For the new design the horizontal loads are determined following section 4.4.1 of Eurocode 1-2, which prescribes that the horizontal loads are to be taken as a percentage of the vertical variable loads acting on the first theoretical lane according to LM1, with an upper limit of 800 kN. With a combination factor of 0,8 to account for load groups this results in a force of 428 kN.

To obtain the most unfavourable situation it is assumed that the full horizontal load is restrained by the foundation block under consideration, resembling the hinge in the mechanics scheme of a statically determinate beam.

Moments: A moment is imposed onto the foundation block and comprises two contributions: the eccentricity between the support and the centre of the foundation block and the eccentricity between the top of the deck where the horizontal forces act and the bottom of the foundation slab. The most

unfavourable situation is obtained if the direction of the horizontal forces is chosen as such that both contributions to the moment are of the same sign.

Total forces: Table 39 gives the components of the force vector $\underline{f}$, note that the signs of the forces follow from the sign conventions as given in Figure 103.

Table 39 Forces on foundation block including sign convention

Component force vector	Existing structure	New design
Horizontal force f_H [kN]	-154	-428
Vertical force f_V [kN]	-14.285	-11.286
Moment f_M [kNm]	+5815	+7893

Results and analysis

The results from the calculation indicate that pile group 'a' is the governing group, as was to be expected given the direction of the forces acting upon the foundation block. The actions corresponding to the existing structure result in a compressive force of 423,5 kN in a single pile while those corresponding to the new design result in a force of 387,6 kN, this means that the force in the governing pile is reduced by 8,5%.

When the results of the other piles are also considered and the limitations of this approach due to the incorporated simplifications are kept in mind, two conclusions can be drawn:

1. The reduction of the vertical force as calculated in 10.3.2 results in a reduction of the forces in the foundation piles, the reduction for the governing piles being 8,5%. This is with the exception of two pile groups but in those situations the pile forces remain low compared to the governing foundation pile;

2. The reduction of the total vertical load expressed as a percentual change does not result in a reduction of the forces in the foundation piles with a percentual change of equal magnitude.

These results illustrate that although the reduction of total vertical forces is an indicator that the forces in the piles will reduce as well, it does not fully capture the distribution of the loads over the foundation piles and does not give information specifically enough to determine the actual reduction of the forces on the level of a pile group or single pile. This discrepancy can be explained by the following factors:

- **Design of the foundation**: The design of the foundation with inclined piles and different numbers of piles per row causes an uneven distribution of the forces over the pile groups;

- **Introduction of moments**: The eccentricity of the support with respect to the centre of the pile group contributes to the difference;

- **Including horizontal forces**: The third factor is including horizontal forces and the moments caused by these forces, the effects of which were not accounted for in the comparison of vertical loads.

11

GENERALISATION AND APPLICATION OF THE SOLUTION

11.1 Generalisation of the solution for the Eefdesebrug

11.1.1 Overview results of representative bridge

In the introductory chapter of the report the Twentekanaal was introduced as the topic of the project. In chapter 4 an inventorying and characterisation was carried out of all bridges across the Twentekanaal. This resulted in the identification of a total of twelve bridges that are relevant to the project given their similar characteristics. Because it is not possible to perform in-depth analysis of all these bridges simultaneously, a representative bridge was selected for the redesign: the Eefdesebrug.

During chapters 6 to 9 of this report a design for a new deck for the Eefdesebrug constructed using prefabricated UHPC beams was elaborated in a series of steps, resulting in a value for the self-weight significantly lower than that of the existing concrete deck. Figure 106 gives the self-weight of the existing structure and the designs that have been elaborated during the different design phases.

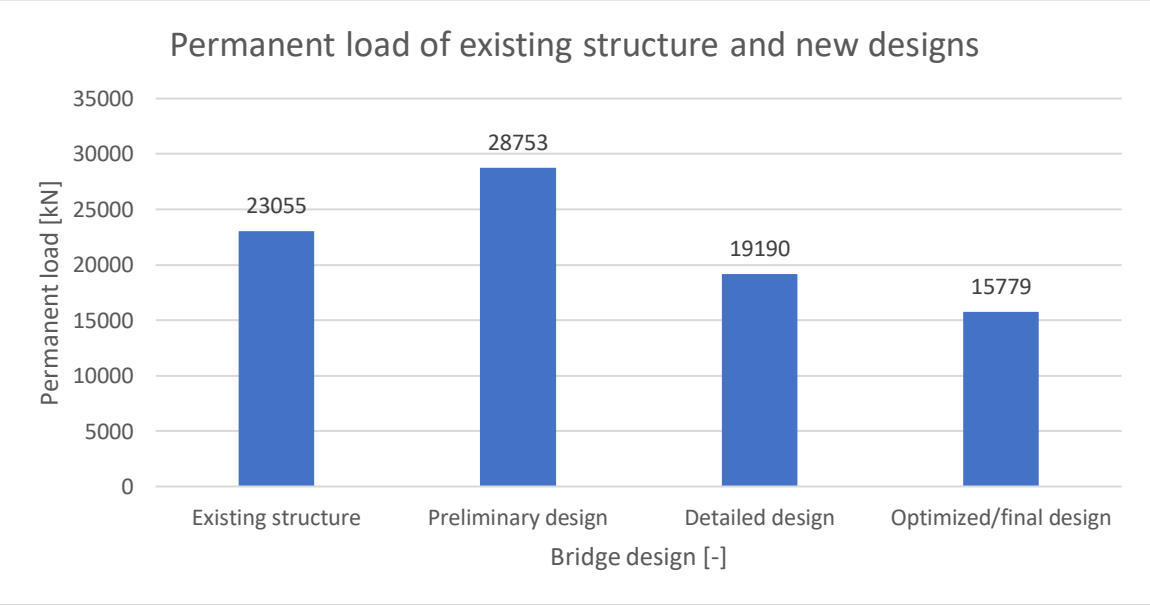

Figure 106 Permanent load of the existing structure and new design during the different design phases

After concluding the design stage for the Eefdesebrug, a comparison was made between the existing structure and the final design to determine whether the weight reduction was significant enough to satisfy the criterion for reuse of the foundation of the bridge. With the results of the design stage, this criterion for reuse was indeed satisfied.

11.1.2 Extending results to existing bridges Twentekanaal

In chapter 4 it was shown that the results for the Eefdesebrug can be of relevance to twelve bridges from a total of 37 bridges or bridges part of engineering structures across the Twentekanaal. The criterion for the

reuse of the existing foundation of the Eefdesebrug, as covered in chapter 10, has been satisfied. The subsequent step is to determine, based on the results for the Eefdesebrug, whether a similar solution is possible for all other bridges of the identified group. Two aspects have to be considered:

- **Dimensions of bridge decks**: Based on the results of the redesign of the Eefdesebrug an estimation can be made of the dimensions if a similar solution would be applied to the other bridges. The span, beam height and the width of the deck will be considered.

- **Substructure and actions on foundation**: To judge the reusability of the existing foundations, an indication has to be obtained of the actions acting upon these. In addition, it has to be determined whether the ratio of permanent and variable loads as found for the Eefdesebrug may also be expected to occur for the other relevant bridges.

Using the results of the redesign of the Eefdesebrug as the starting point, these two aspects will be considered in the subsequent sections.

11.1.3 Estimating dimensions of bridge decks

Relevant bridges and their key features

Table 40 gives the group of twelve bridges with similar characteristics as well as their features that are most important in the context of this report: the year of construction, span, and width of the deck. A visualisation of these features can be found in Figure 23, Figure 25 and Figure 26 of chapter 4.

Table 40 Relevant bridges and their key features

Bridge name	Year of construction	Span	Width	Estimated height
[-]	[-]	[m]	[m]	[m]
Eefdesebrug	1955	68,0	16,36	1,9
Almensebrug	1948	50,0	10,0	1,4
Exelsebrug	1955	67,09	16,0	1,9
Lochemsebrug	1947	41,2	11,0	1,2
Markelosebrug	1962	46,35	10,76	1,3
Weldammerbrug	1948	58,355	9,6	1,7
Hengelerbrug	1948	63,09	11,8	1,8
St. Annabrug	1965	55,0	15,0	1,6
Oelerbrug	1963	50,06	18,8	1,4
Lonnekerbrug	1958	48,2	16,0	1,4
Cottwicherbrug I	1947	42,035	12,0	1,2
Wierdensebrug	1952	44,0	19,0	1,3

The results for the Eefdesebrug are based on extensive design work and these results will be projected onto the other bridges to estimate their approximate dimensions. The dimensions considered are the span, height and width.

Span and beam height

The span and height of a beam are related through the slenderness. The slenderness of the beams designed for the Eefdesebrug (see chapter 9, the beam height is 1,9 m) is:

$$\lambda = \frac{68{,}0}{1{,}9} \approx 36 \qquad \text{Equation (79)}$$

Using the slenderness of the Eefdesebrug, which has the largest span of the group of bridges, and the dimensions of the spans of the other bridges, a substantiated estimation can be obtained of the required beam height for the decks of each of the bridges. This is under the assumption that beams of a similar type

and design are applied. Note that the results were rounded off to the nearest higher multiple of 0,1 m to obtain practically applicable dimensions. The results are given in the column 'estimated height' of Table 40.

Width of the deck

Table 40 indicates that there is a significant difference in the width of the different bridges, the smallest value being approximately half the width of the widest bridge. While a substantiated estimation of the required beam height could be made through the span and the slenderness value, the number of beams and width of each beam will depend on each individual bridge. A qualitative description will therefore be given on methods that can be applied to obtain the desired with of a new bridge deck.

Assuming that in the new situation the bridge decks have to have the same width as in the existing situation and that beams of the same type are used as in the redesign of the Eefdesebrug, three options can be distinguished to obtain a deck with the desired total width for each of the bridges. The different options are:

- **Increase or decrease the number of beams**: The most straightforward solution is to start with considering beams with the same width as those of the Eefdesebrug and increase or decrease the number of beams.

- **Width in-situ joints**: Box type beams have the advantage of allowing for adjustment of the width of the longitudinal joints up to some extent. If small deviations in deck width are to be compensated for, this can be achieved by a small increase or decrease of the joint width.

- **Adjusting the design**: If applying the two aforementioned options does not result in a deck of the desired width or if the ratio of width and height results in an unfavourable beam design, then the design of the beams can be adjusted, for example by reducing the width of the outstand flange or the inner width of the box.

Using these three options it will be possible to obtain a deck consisting of box beams and with the desired total width for each of the bridges. For the beams with larger spans, it is expected that the designs (i.e. proportionality between the cross section of the beams and width of the deck) will be similar to that of the Eefdesebrug because most of the differences in the width of the deck will be accounted for in varying the dimensions of the top flanges of the beams.

For the bridges with smaller spans, it is expected that adjustments to the design will be required, because unfavourable ratios of width and height will occur, as indicated in part A of Figure 107. In such situations a larger number of smaller beams with reduced width can be applied, as presented schematically in part B of the same figure.

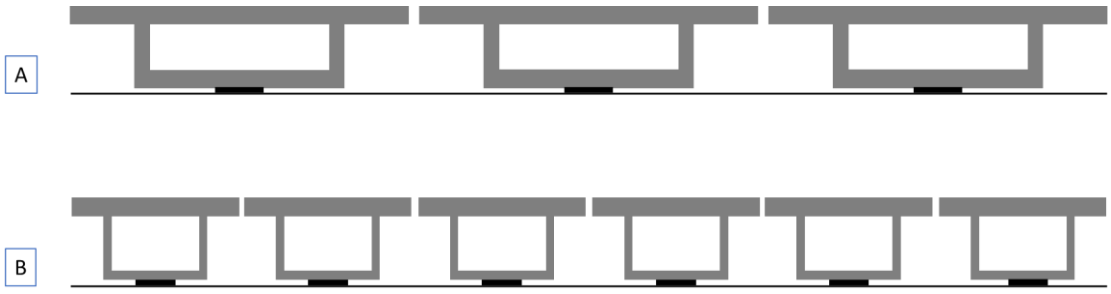

Figure 107 Schematic representation of different height to width ratios for prefab beam deck

Although the dimensions such as the web thickness and the thickness of the bottom flanges may be expected to be smaller than those of the box beams for bridges with larger spans, it is nonetheless expected that the total cross section over the total width of the deck will increase due to the additional webs and bottom flanges that are added compared to the situation of a smaller number of larger beams.

An additional aspect worth mentioning in relation to a change of the cross-sectional design, is the shear capacity of the beams. Especially at shorter spans shear might become governing over bending. Although

this is not expected to be the case for the bridges considered, if the beam height is reduced while the thickness of the webs remains constant, then the situation may arise where shear becomes the governing criterion.

11.1.4 Substructure and actions on foundation

Existing substructures

In addition to the dimensions of the different bridge decks, the second aspect to consider is the substructure and actions on foundations of all relevant bridges. One of the conclusions from chapter 4 was that the different bridges given in Table 40 vary regarding the design of their substructure and foundation. Some of the identified bridges might require more effort to modify their substructure in order to place a new deck comprising prefab beams than others and in addition it is known from the bridge inventory that not all bridges have a similar foundation.

Despite these differences, the verification criterion for the reuse of existing foundations as given by equation (75) in section 10.3.1 is still considered to be valid for all twelve bridges. If a structure has functioned under a certain vertical load acting upon the foundation that is larger than or equal to the vertical load in the new situation, it is not expected to be likely that such a new situation would result in failure.

Actions on existing foundations

With the criterion for the reuse of existing foundations as formulated for the Eefdesebrug determined to be valid for all bridges, the focus is placed upon the vertical actions on the foundations of the other bridges. As done for the Eefdesebrug, it has to be estimated what the total vertical loads will be that act upon the substructures of all bridges of the group. The results for the Eefdesebrug will again be projected onto the other bridges. This way it can be judged whether it is likely that the existing substructures and foundations of the other bridges can be reused.

By comparing the dimensions of the Eefdesebrug with those of the other bridges, an impression can be obtained of the order of magnitude of the loads that may be expected to act upon the substructures of the other bridges.

Differences are found in terms of the span and width of the deck and it is especially the span that is of importance. The redesign of the Eefdesebrug revolved around the goal of compensating the increased variable load by a decrease of the self-weight of the structure. This makes the ratio between the permanent loads and vertical variable loads into an important aspect to consider. This is dependent on the span of the deck while the width is of lesser importance for this consideration.

The results obtained for the Eefdesebrug were typical for concrete bridges of longer spans. The self-weight dominates the total variable load, see Figure 101, the contribution of the variable loads is significantly smaller. The Eefdesebrug has the largest span of the group of relevant bridges, and large differences occur in the values of the spans within the group. Therefore, it should be determined whether results similar to those found for the Eefdesebrug may be expected for the other bridges as well, especially for those with the smallest spans.

Figure 108 gives a first impression of what may be expected, the graph represents the contributions to the total vertical load on the governing beam of a bridge deck. The figure has been prepared by considering two types of loads, being the self-weight of the structure and the vertical variable loads.

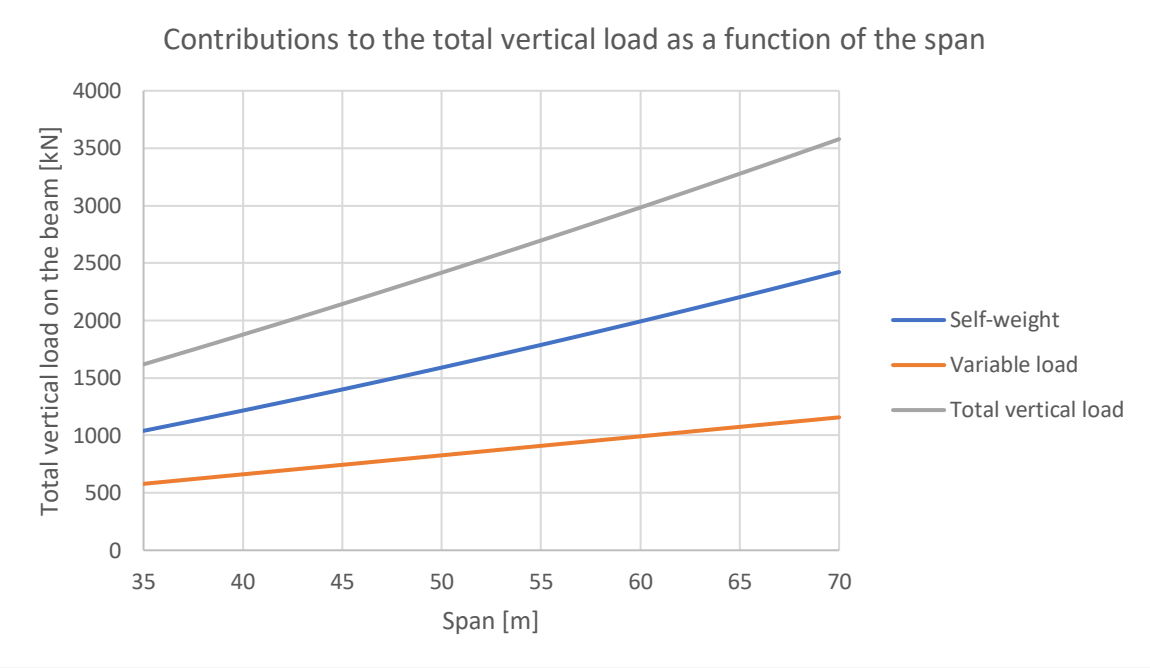

Figure 108 Contribution of self-weight and variable load to total vertical load on a beam – Concentrated loads at mid span

To obtain the graphs a single beam is considered on which a line load acts that represents the self-weight. The value of the line load is calculated by first estimating the total height of the beam by dividing the span by the slenderness. The cross section is estimated by taking a top flange with the mean thickness of 187,5 mm, the bottom flange with a thickness of 200 mm, the webs with a thickness of 100 mm each and determining the height of the web by subtracting the thickness of the top and bottom flange from the estimated total height. The other dimensions are identical to those given in chapter 9. The self-weight also includes the surface layer of 10 mm.

The variable loads are represented by taking the value of the bending moments due to the variable loads in the serviceability limit state at midspan for the governing beam as calculated for the optimized design, see Table 29. This bending moment (9553 kNm) is converted into an equivalent line load by applying equation (80), which results in a value of 16,5 kN/m. By applying this approach both the uniformly distributed and concentrated variable loads of LM1 at mid span are included as well as the effect of beam interaction.

$$M_{E,Q} = \frac{1}{8} * q_{eq} * l^2 \leftrightarrow q_{eq} = \frac{8 * M_{E,Q}}{l^2}$$ Equation (80)

The graphs for the self-weight, variable load and total vertical load are subsequently obtained by multiplying the values of the respective loads with the span of the beam. From the graph it can be observed that the contribution of the self-weight to the total vertical load increases. Its contribution is 64% for the smallest span while its contribution increases to 68% for the largest span considered. Although the calculations underlying the graph are only an approximation, they do give a first impression of the relative contributions of the self-weight and variable load to the total weight on the governing beam. The graph indicates that percentage wise there is no significant change in this contribution between beams with smaller and larger spans.

Effect of concentrated vertical loads to bridges with smaller spans

The aforementioned results should be interpreted with care for bridges with smaller spans because of two reasons. The first reason was already visualized in Figure 107. The situation may occur where the design has to be changed, resulting in a higher self-weight than would be predicted by projecting the results as found for the Eefdesebrug directly onto such bridges. The second reason is related to the positioning of the concentrated variable loads of LM1. The graph in Figure 108 was prepared under the assumption that these axle loads are positioned around mid-span, which is the situation as given in Figure 109 A. However, the situation may also occur where these forces are positioned directly above the support, see Figure 109 B.

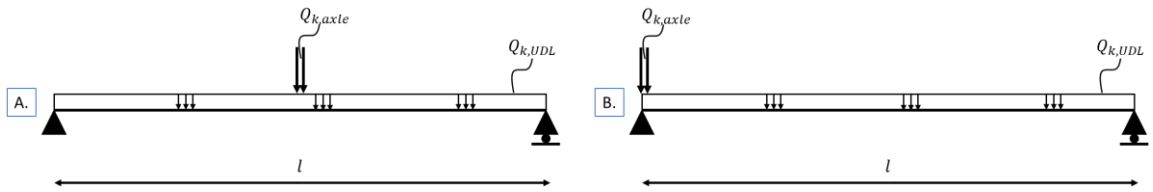

Figure 109 Positioning of concentrated loads of LM1 on governing beam

For shorter beams, this second situation may be governing over the first situation and give more unfavourable results than the graphs in Figure 108 suggest. To give an indication of this effect, the graphs in Figure 110 have been prepared. For this graph only half the span of the beam is considered and the self-weight is calculated in the same manner as in the previous case. For the variable actions, the equivalent line load is again calculated using equation (80), but this time only using the bending moments due to the uniformly distributed variable loads (5475 kNm). The axle loads are assumed to be positioned directly above the support of the beam under consideration. Their total value is 582 kN, which corresponds to the axle loads of LM1 on lane 1 and is assumed to be completely carried by the beam under consideration.

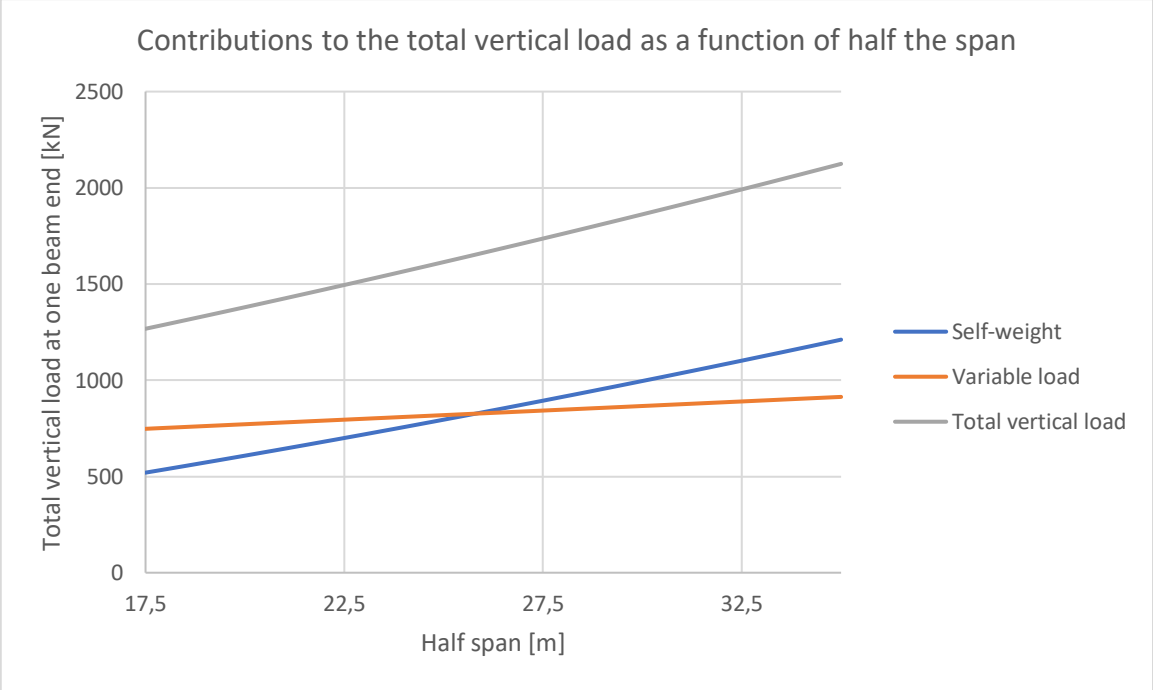

Figure 110 Contribution of self-weight and variable load to total vertical load on half a beam – Concentrated loads at support

There is a significant difference with the results of the first graph in Figure 108. It can be seen that the vertical action at the support is dominated by the concentrated axle loads. The contribution of the variable loads to the total loads exceeds the contribution of the self-weight up to a span of approximately 50 m. For the smallest span the contribution of the variable loads is 59%, which decreases to 43% for the largest spans considered.

However, it has to be noted that these two sets of graphs are based on the governing beam and represent two limit cases. If the same analysis would be performed on the level of the whole abutment, then the load effect related to the positioning of the axle loads would be less pronounced because the variable loads on the other beams are less significant. For the Eefdesebrug for example, Figure 102 demonstrated that this effect is virtually absent on the level of the whole abutment. It is therefore not expected that the effect of the positioning of the concentrated variable loads will affect the final conclusions of the project. Nevertheless, the effect of the positioning of these loads may be more pronounced for bridges with spans smaller than those of the Eefdesebrug.

11.1.5 Expected results for other bridges

In the previous sections a description was given of what may be expected if the solution as designed for the Eefdesebrug is applied onto the other bridges identified in chapter 4. Although in practice for each bridge an individual deck design and assessment of the foundation have to be carried out, this analysis sufficed for the elaboration of this project.

Based on the results from the redesign of the Eefdesebrug and the span of the existing structures a substantiated assumption was made of the required beam height. In addition, suggestions were given to obtain a new deck with the same total width as the existing structures. The substructure and existing foundation of the existing bridges were touched upon as well. Based on the bridge spans and the results for the Eefdesebrug it is expected that the ratio between the variable loads and self-weight will be approximately the same for all bridges in the group.

The remark was made that for bridges with the smaller spans the situation may occur where an unfavourable ratio between beam height and width is found, as presented in figure see Figure 107 (A). In such situations the design will have to be changed by applying a larger number of smaller beams and it is expected that the self-weight will increase compared to the results for the redesign of the Eefdesebrug scaled to the slenderness of the deck of the bridge under consideration.

In addition, it was mentioned that for shorter spans the situation may occur where positioning concentrated loads at the supports may be governing over the situation where these loads are positioned at mid span, thus giving more unfavourable results than is covered by the criterion for reuse of existing foundations and the results of the Eefdesebrug, which are based on the total structure. However, the results of the redesign of the Eefdesebrug also indicated that a margin remains between the total vertical loads in the existing and new situation. A limited increase of the vertical forces acting on the foundation due to an increase of the self-weight and an unfavourable effect due to the positioning of the concentrated variable loads can therefore be compensated for.

In judging whether or not a similar solution as the one designed for the Eefdesebrug is possible for all other bridges of the identified group, two key assumptions are made:

1. The criterion for reuse of the existing foundation as formulated for the Eefdesebrug also holds for the other bridges. This is a fair assumption because the capacity of a foundation is proportional to the dimensions of the superstructure of the bridge.

2. For bridges with smaller spans, it is assumed and expected that more unfavourable results due to an increase of the cross section compared to the scaled solution for the Eefdesebrug or related to a different positioning of the axle loads being governing over the positioning at mid span can be compensated for by the margin between the total vertical loads in the new and existing situation as found for the Eefdesebrug.

Based on the estimation of dimensions, the points considered regarding the substructure and foundation and the two key assumptions made, it is expected that the solution as designed for the Eefdesebrug can also be applied to all other bridges of the group and will result in satisfying the criterion for reuse of the existing foundations in all these cases.

11.2 Application of solution – Increase of beam height

11.2.1 Solutions for increase of beam height

Consequence of increase of beam height

One of the aspects of applying a new prefab beam deck to replace existing arch or truss bridges, is an increase of the height of the deck. All bridges considered span a canal with a clearly defined free height that is required to enable shipping, in practice this means that it is the height at the top of the deck that will

increase. In case of the Eefdesebrug the beam height increased from 1,3 m in the existing situation to 1,9 m in the new situation. It is expected that an increase of height will occur for the other bridges as well, albeit an increase smaller than the 0,6 m as found for the Eefdesebrug.

Although the focus of the project is on verifying whether existing foundations can be reused, the increase of the deck height is an important aspect of the application of the solution and is therefore briefly considered in this section.

Possible measures

It is expected that for all identified bridges the height of the deck will increase if a new prefab beam deck is applied. That means that for all bridges measures will have to be taken to obtain and guarantee an acceptable transition from the deck onto the adjacent abutment, approach bridge or embankment and road. The most appropriate solution will differ on a project-to-project basis, see Figure 27, which already shows differences between the bridges. Different solutions will be briefly described in the remainder of this chapter.

Modifications to the embankments: The first possible solution is to carry out soil works to the adjacent embankments. This is suitable for the situations where direct transitions are made from the deck to the adjacent embankments via the abutments and transition slabs. Note that modifications to the abutments are required as well. It is likely that all situations will involve earthwork to be carried out, because for all structures at some point a transition will have to be made from the structure (new deck or approach bridges) to the adjacent embankments.

To give an impression of the extent of the soil works, the length over which the vertical alignment of the embankment will have to be changed can be calculated using values from road design manuals. A height difference can be overcome by means of a transition curve, which comprises a crest curve and sag curve. The Eefdesebrug has a hight difference of 0,6 m and is taken as an example.

For a provincial road (N-road) with a speed limit of 80 km/h the crest curve has a prescribed minimum radius of 5012 m while in practice it is often sufficient to take the radius of the sag curve equal to twice that of the crest curve, i.e. 10.024 m. This results in a total transition length of 134 m, which is calculated as follows:

$$l_{tot} = \sqrt{(R_c + R_s)^2 - (R_c + R_s - \Delta h)^2}$$

Deck overlay: If only a limited difference in height between the new deck of the main span and the adjacent approach bridge or embankment has to be overcome, then the solution can be sought for in the form of application of an overlay.

By means of a new concrete layer (a structural layer) or an additional asphalt layer the height of the top surface of the adjacent approach bridge or embankment can be increased up to the required height. It has to be noted though that only a limited increase in height is possible because of the significant increase of the self-weight of the deck, if this solution is applied on an approach bridge or abutment.

Jacking superstructure of approach bridges: In case the deck height of the approach bridges has to be increased, an option can be the jacking of the decks of the approach bridges to the required height. By means of jacks the superstructure of the approach bridges is lifted until the decks are aligned with that of the new deck of the main span, after which the substructure of the approach bridges is modified as such that it can support the deck at the new height. This method is suitable if the deck of the approach bridges is expected to be able to fulfil the intended functions for a significant period of time.

Replacement of approach bridges: Another method is to combine the replacement of the superstructure of the main span with the replacement of the approach bridges. This way all the replacing work can be carried out at once and the new structure will be constructed using aligning decks.

Design of more slender beams: Another possibility is to investigate options to further optimize the design of the beams and reduce the height. In chapter 9 it was already shown that with the design approach as

applied in this report no new significant savings should be expected. However, alternative approaches were also given that still may result in more slender beams.

Regardless of the chosen approach for optimization it should not be expected that the beam height can be reduced to the height of the main girders of the existing deck, at a certain point the limits of what can be achieved with the beams will be reached. The first challenge that is expected to occur is that the type of cross sections of the beams of the deck will have to be changed, as visualized in Figure 107. At a certain point additional challenges will occur related to aspects such as dynamic effects, robustness in design and executional aspects of the work. These form the ultimate limit of what can be achieved within the framework of the project and the given type of beams.

11.2.2 Choosing a solution strategy

Different methods have been mentioned that can be applied to overcome differences in height between a new prefabricated UHPC beam deck and the adjacent existing abutment, approach bridge or embankment. Which solutions are selected depends on multiple factors and will vary on a project-to-project basis. Possible factors to consider are, among others, the difference in height that has to be overcome and the condition of the approach bridges. The measures can be applied individually or in combinations, where the modifications to the embankment and the road surface (asphalt layer) will have to be applied in most cases.

12

CONCLUSION AND RECOMMENDATIONS

12.1 Conclusion and recommendations

The project described in this report focussed on a concept where the use of Ultra-High Performance Concrete, an example of an advanced cementitious material, and an example of accelerated bridge construction in the form of reusing existing foundations, were combined. It was expected that this concept would prove to be promising as one of the potential solutions to the replacement task of existing bridges. This was expressed in the project goal of designing an ultra-high performance concrete (UHPC) bridge deck for the existing bridges across the Twentekanaal, in such a way that the existing foundations could be reused with only limited modifications.

This chapter starts with a reflection upon the challenges that were faced during the elaboration of the project, following by limitations to the results of the work, the conclusion and an overview of the recommendations.

12.1.1 Reflection on challenges

In this section a reflection is given to look back upon four distinct points that were encountered during the elaboration of the project and that have proven to be of prime importance for the direction of the work or that have provided specific challenges to the elaboration of the project.

Information existing structures

In order to describe or reassess an existing structure it is beneficial to have detailed information regarding the original design. For the Eefdesebrug original design drawings were provided that allowed for a detailed description of the structure, despite the fact that no original design calculations were available. In general terms, the availability of a larger number of original design documents allows for more accurate analysis of the structure to be carried out.

The availability of design drawings allows for accurately determining the overall design and the dimensions of the structure. For the Eefdesebrug this resulted in a detailed description and in-depth knowledge of the original design, as well as a more accurate weight calculation. For many of the existing bridges across the Twentekanaal sets of drawings were provided as well with varying degrees of completeness. As a result, dimensions such as the span and width could be established with accuracy. For bridges where this information was lacking, use had to be made of less reliable sources, such as Google Maps, to estimate the dimensions. This reduces the accuracy of the work.

The availability of calculations has the additional benefit of clarifying in what way the design codes relevant at the time of designing the structure were interpreted as well as the assumed parameters. For the Eefdesebrug no calculations were available, which means that the VOSB 1938 had to be interpreted and applied. This may result in a different approach compared to when the original design was worked out.

Acceptability and standardization of UHPC

Although the fundamentals on UHPC were already published in 1981 by H.H. Bache, its application remains limited to this day. Influencing factors are the technological advancements with respect to UHPC, standardization of designing in UHPC and the acceptability of UHPC as a solution, which are three

interrelated aspects. The use of UHPC is not as well established as the use of conventional concrete and it is not part of common practice in designing in structural concrete. Therefore, additional sources had to be identified and selected to complement the information missing in Eurocode 2.

Initially, the lack of guidance with regard to designing in UHPC was solved by publishing the first recommendations in the early 2000s. As time progressed, these guidelines became more comprehensive. This resulted in the AFGC-SETRA 2013, which was written as such that it can be used in accordance with Eurocode 2. Despite the progress, additional effort was required to incorporate designing in UHPC in the existing frameworks of design codes. The publication of NF P18-470, NF P18-710 and NF P18-451 in France or the SIA 2052 in Switzerland are another step up in this regard. By embedding the use of UHPC within the existing framework of design codes, it is expected that its use will be further promoted and the acceptability of UHPC as a solution will increase.

Transparency in material parameters and constitutive law

The Eurocode 2 for conventional concrete is very transparent in the sense that the properties related to strength and deformation are clearly defined for different concrete strength class. This means that for each strength class it is unambiguously defined what compressive and tensile strength, modulus of elasticity and strain values may be expected, this is contrarily to UHPC for which it is less straightforward to establish the material parameters and select the appropriate constitutive law. Two reasons are given:

- The first reason is the limitations captured in some of the codes or guidelines on UHPC themselves. For the project as described in this report the AFGC-SETRA 2013 guideline was applied, which is aimed at a limited number of commercially available types of UHPC instead of being focussed on the application of UHPC in general.

- The second reason is related to more intrinsic properties of the material. As is the case for conventional concrete, the properties of the material depend on the mix design. However, effects related to the execution of the work are more pronounced for UHPC due to the distribution and orientation of the steel fibres. This can especially be observed in the behaviour of the material in tension.

  While the behaviour of the material during the pre-cracking stage can be predicted with reasonable accuracy, the behaviour in the post-cracking stage is harder to predict and the scatter is larger. The behaviour at this stage is dictated by the fibres and it is the orientation and distribution of the fibres that is in turn influenced by the execution.

The selected guideline, the AFGC-SETRA 2013, gives certain guiding values for material parameters that can be used for preliminary design. However, as soon as a more detailed calculation is to be performed for a specific project the values have to be established. This has been solved by selecting values for the material parameters based on literature. To challenge the industry, optimistic values were chosen. In addition, the application of heat treatment was assumed. Furthermore, a practical constitutive law was assumed based on the guideline and literature.

However, given the aforementioned remarks it can be stated that the overview of the parameters and the constitutive law as given in the report may look relatively simple but do not cover the full extent of the challenges that are involved in defining and determining parameters as well as the uncertainty and scatter in values. It is for this reason that the guideline prescribes extensive testing to adjust and modify the design and execution procedure until both design and practice are in accordance with one another.

Knowledge on former codes and design methodologies

The final aspect is the required knowledge on former codes and design methodologies. To assess an existing structure, it is obvious that it is has to be established what the codes are that were followed during the design of the structure. This way a more 'fair' comparison can be made between the new design and existing structure. The availability of original design documents helps in establishing this information.

12.1.2 Limitations to the results

After the reflection upon four distinct points as well as the discussions in all previous chapters, a number of limitations to the results of the project can be identified. These limitations are either the result of one of two causes. Limitations can originate from the project scope, meaning that aspects that are relevant in practice were excluded from the project. Limitations can also originate from the various assumptions that have been made during the elaboration of the work to solve the challenges that were mentioned in the previous section. An overview will be given of the various limitations that have to be considered when interpreting the project results.

Material parameters

Because UHPC is not a single specific mixture but a group of materials, material parameters had to be assumed for the elaboration of the project. For the detailed design onwards, values were selected that were deliberately on the favourable side of the range of values given in literature on Ductal FM, a decision justified by ongoing technological advancement and in order to challenge the industry. However, defining such parameters introduces uncertainty into the design process.

The application of UHPC is not as common of that of conventional concrete and its properties and requirements are not as unambiguously defined. The AFGC-SETRA 2013 prescribes that the parameters that the UHPC is supposed to possess have to be verified via series of tests. To establish the parameters with full certainty, a mixture would have to be selected or designed and tests would have to be performed, which is also related to the following point of executional aspects.

Executional aspects

For UHPC there is a strong relationship between material parameters used in the design and the actual execution of the work, but this could only be included in the project by means of assumptions. Two examples of execution influencing material properties are:

- **Fibre distribution**: The fibre distribution and orientation heavily influence the mechanical properties of the material and these are influenced by the execution of the work. Because of this reason the AFGC-SETRA 2013 prescribes testing using representative mock-ups of the actual structure to determine to what extent the actual fibre distribution and orientation differs from a perfectly random distribution, and whether the parameters assumed for design are actually achieved.

- **Creep and shrinkage**: Another example are creep and shrinkage values of UHPC. Heat treatment was assumed to be applied to reduce the creep and control the shrinkage. However, this can be a demanding requirement for larger prestressed prefab elements and will challenge manufacturers.

Deflection and vibrations

Although deflections are included in the design calculations of the bridge, only a rough estimate was obtained using RFEM results and standard engineering equations. In practice determining the deflection of a beam is more complicated than that can be captured using this approach. Vibrations are mentioned in the report, but no calculations have been performed. This decision was made because vibrations are generally not the governing criterion for a concrete bridge with the dimensions as given in this report. However, because no calculation is performed, no numerical result can be presented to support this claim and it should therefore be included in practice.

Detailing

Various parts of the design of the deck have been discussed qualitatively, but corresponding calculations were not given. These were aspects that require extensive and detailed calculations while their results were not expected to change the results and conclusion of the project. Examples are the local verifications in case of ship collision and the detailing of the connections between the main beams and end cross beams (both referred to in the detailed design) and buckling of the webs of the main beams (referred to in the final design).

In practice such aspects should be part of the design procedure though. Other aspects were not included because these should be part of the next phase of the design if the project was to become reality, such as the surfacing and slope of the deck in transverse direction to guarantee dewatering.

Optimization
Although three different approaches were formulated that can be explored to optimize the design, only one of these approaches was put into practice because it was expected that this would suffice to achieve the goal of the project. Within this approach eventually only limited room remained for further optimization but the other two approaches can still be applied to optimize the design further, not all possible methods of optimization have been employed yet.

Horizontal actions
Solutions regarding increased horizontal actions due to variable loads and imposed deformations were excluded from the scope of the project under the assumption that measures to strengthen the substructure for increased horizontal forces is more practically applicable compared to strengthening measures for increased vertical forces. The project is elaborated under these assumptions, but in reality the horizontal forces cannot be neglected in the analysis.

Analysis of substructure and foundation
The scope of the project has been narrowed down to the analysis of the deck unless specifically stated otherwise, the substructure and foundation were not fully assessed. This was replaced by a global assessment of the foundation instead. Although this global assessment was sufficient to formulate conclusions for the project, it nonetheless introduced limitations. By performing additional calculations, it was demonstrated that it is not possible to capture the actual behaviour of the foundation and the distribution of forces over the foundation piles by only comparing vertical forces. The only method to assess the foundation with full certainty is to perform a complete reassessment of the structure as a whole, including the foundation.

Assessing other bridges
A total of twelve bridges has been identified that are relevant to the project because of their similar characteristics. By means of projecting the results of the Eefdesebrug onto these bridges, an indication was given of what to expect if the solution of the Eefdesebrug is applied to all bridges within this group. However, the remark is made that to obtain full certainty, each one of these bridges should be fully assessed because the conclusion was based only on the outer dimensions of the structure. For most of the structures these were established based on original design drawings, but these were not always complete and not always available for all structures.

The uncertainty increases to a limited extend for the bridges with the smaller spans, given possible additional unfavourable effects that are not captured by projecting the results of the Eefdesebrug directly onto these bridges. It is expected that for these bridges the relative weight reduction will be less significant than the weight reduction for the Eefdesebrug and other bridges from the group with larger spans.

Beam height
It has been demonstrated that the height of the deck increased for the Eefdesebrug compared to the existing situation. If the solution is applied to other bridges, then it is most likely that this situation will occur as well. Measures will have to be taken to cope with the increased height of the top surface of the deck in all cases. Different possible solutions can be sought for and these have been mentioned briefly, but no further elaboration was included in the project.

Construction of the prefab beam deck
During the design phase of a prefab project, the production, storage, transportation and placement of the beams are aspects that have to be considered. The most stringent aspects were taken into consideration during the different design phases. Load situations were defined as such that all different stages, from production to the bridge being in service, were covered. In addition, the number of strands in the final design is in correspondence with the maximum number that can be applied in practice. Furthermore, the transportation of the beams of the given size was proven to be feasible by means of a reference project: the Lienebrug in Wanssum. However, should a new prefab UHPC deck become reality for the Eefdesebrug or for one of the other relevant bridges, then such aspects of the project have to be elaborated in a more detailed and specific manner.

12.1.3 Conclusion

Conclusion to main research question

The hypothesis of the project was that if one would redesign the bridge deck of an existing bridge using UHPC, a higher slenderness and lower dead-weight would be achieved compared to the original situation, which would compensate for the increased traffic loads and therefore would increase the reusability of the existing foundation. A total of twelve bridges with similar characteristics across the Twentekanaal was identified, these bridges were subjected to the hypothesis. At the start of the project, the following main research question was formulated:

"What should the redesign of the existing bridges across the Twentekanaal in UHPC be like in order to obtain a design which complies to the current standards and enables the reuse of the existing foundation of the bridges without having to modify them due to the increase of vertical variable loads?"

The Eefdesebrug near Zutphen was selected as the test case for the redesign, and functioned as the representative structure for the aforementioned group of twelve bridges. Taking into account the scope of the project, the following answer is formulated based on the redesign of the Eefdesebrug and the subsequent analysis of the results as described in this report:

- *By means of a comparison of the total vertical loads between the optimized design and the existing structure, the possibility of reuse of the existing foundation of the Eefdesebrug without modifications for increased vertical loads has been demonstrated for a deck consisting of prefabricated UHPC box beams prestressed with pretensioned steel, with a span of 68 m, and a beam height of 1,90 m, resulting in a slenderness of 36.*

- *In addition, based on the results of the redesign of the deck of the Eefdesebrug it was shown that a similar solution can be applied to all twelve bridges across the Twentekanaal with characteristics similar to those of the Eefdesebrug.*

Clarification of the conclusion

After collecting the required basic information, a design for a new bridge deck was elaborated following the provisions from the Eurocode. Because the Eurocode lacks information on UHPC it was supplemented by the AFGC-SETRA 2013 as well as literature. The design was formulated in a stepwise approach, starting with a preliminary design and followed by a detailed design, optimization phase and concluded with a final design. After each step, the global goal of the project was reflected by means of a weight comparison.

The designs were improved and optimized with each step of the design process and the final design was compared with the existing structure, which dimensions and loads were established based on original design drawings and codes of the relevant period. The final design resulted in a 32% percent reduction of the self-weight. Despite an increase of the vertical variable loads of 31% between the VOSB 1938 and the Eurocode, this still resulted in a 21% decrease of the total vertical load, based on which it was concluded that reuse of the existing foundation of the Eefdesebrug is possible without having to modify it due to an increase of vertical variable loads, confirming the hypothesis of the project. This comparison was carried out without the use of load factors.

By comparing the characteristics of all bridges across the Twentekanaal with those of the Eefdesebrug it was determined that a total of 12 bridges would be relevant to the project. By means of projecting the results of the redesign of the Eefdesebrug onto this group it was concluded that the concept of the redesign of the Eefdesebrug can be applied to all bridges of the group. However, the remark has to be made that within this concept each individual bridge requires a deck design and assessment of the foundation that is structure specific.

These results demonstrate the potential of the concept of designing slender structures using UHPC in combination with reuse of the existing foundation as one of the possible solution strategies in dealing with the replacement task, in addition to more 'traditional solutions'. The application of the concept as described

in this report will result in saving time and material, which translates into a reduction of hindrance for traffic and the surrounding area, as well as a reduction of environmental impact. Although the initial costs related to the development of such new concepts may be higher, it is expected that further developments in the field of UHPC and its applications in the infrastructure will result in an increase of financial attractiveness and on the longer term will result in such concepts being competitive with conventional solutions.

12.1.4 Recommendations

Based on the reflection upon the project and the limitations to the results that have been formulated, a number of recommendations will be given. These recommendations are aimed at overcoming the difficulties and limitations that were encountered during the elaboration of the project.

The recommendations are subdivided into three categories. The first category comprises recommendations specifically aimed on further elaboration of the redesign of the Eefdesebrug. The second category comprises recommendations regarding the concepts as discussed in this report: the redesign of existing structures using UHPC in combination with the reuse of existing foundations. The final category is an additional category based on parts of the reflection from the start of this chapter, focussing on further introducing and promoting the use of UHPC in the infrastructure in the Netherlands.

Recommendations – Redesign of the Eefdesebrug

The following recommendations have been formulated with regard to further elaborating the redesign of the Eefdesebrug.

Include additional verifications: Various design verifications have only been discussed qualitatively, either because these aspects require extensive detailing while not changing the results and conclusions (e.g. local verifications of ship collision) or because these were not expected to be governing (vibrations). However, in practice such verifications cannot be omitted and it is therefore recommended to include these in the next design phase if the concept is to become reality.

Include further detailing: Detailed design aspects such as the slope of the deck to arrange dewatering have not been included because such points were deemed to be very detailed while not contributing to the goal of the project. However, in practice such points are part of the design and it is therefore recommended to include these in the next design phase if the concept is to become reality. Another aspect related to detailing is the use of conventional reinforcement. If the cross section is optimised further in a next phase or in one of the other bridges as mentioned in the report, the application of passive reinforcement can be considered.

Include analysis of substructure: To further concretize the design, it is recommended to include a full analysis of the substructure and foundation in the next design phase if a complete and accurate view of the forces acting on the foundation, as well as its capacity, is to be obtained. Horizontal forces have shown to have a significant effect on the forces of the foundation piles. Therefore, it is recommended to include these in the analysis.

Recommendations – Redesign of existing bridges in Ultra-High Performance Concrete

The following recommendations have been formulated with regard to the concept of redesigning existing concrete bridges in UHPC in combination with the reuse of the existing foundation.

Application of UHPC: If the development of the concept is to be continued, then it is recommended to invest in establishing more reliable values for the material parameters and constitutive laws, especially with regard to executional aspects. This can be done in one of the following two ways:

- If the development of the concept is continued with further theoretical studies, then information on reference projects can be collected with characteristics as close to the redesign of the bridges under consideration as possible. Examples of characteristics that are of importance are: mechanical properties, heat treated material and pretensioned beams.

- If the concept as described in this report is to become reality, then the design process of a suitable mixture and execution method have to be undertaken to obtain a material with the properties that meets the requirements in relation to the execution methods used.

This aspect is of relevance to the Eefdesebrug and other bridges considered in this report, but it is formulated more broadly to contribute to the further introduction of UHPC to the prefabrication industry for applications in the infrastructure.

Generalisation of the solution: It was concluded that it is likely that the solution as devised for the Eefdesebrug can be applied to a total of twelve bridges. However, this conclusion was based on a comparison of the main outer characteristics of all bridges and the results of the Eefdesebrug. If the solution as presented in this report is to be applied to other bridges, then it is recommended to extend the project and perform a more elaborate analysis for each individual structure.

Construction and application of the solution: The concept as presented in the report is promising, but practical aspects such as the construction and the application on the location have to be considered in more detail. Therefore, it is recommended to invest in further research on the production and construction of similar structures using prefab UHPC beams. The application of the solution on the actual location should be included in this step, to cope with aspects such as a difference in height between the new deck and the adjacent embankments or approach bridges.

Recommendations – Application of Ultra-High Performance Concrete in the infrastructure

This report demonstrated the potential of the application of UHPC in the infrastructure and especially in the replacement task. The material offers new opportunities that are not provided by conventional concrete. However, the application of UHPC is not part of common design practice and is accompanied by specific challenges, as was reflected upon in this chapter. To overcome these points, two recommendations will be given. These recommendations are related to standardization of the application of UHPC in the Netherlands and the expectation is that by following these recommendations the use of this material in the infrastructure will be promoted.

- **Include UHPC in Dutch code framework**: The first recommendation is to include UHPC in the Dutch framework of the design codes. This can be done in a similar way as done in France (NF P18-470, NF P18-710 and NF P18-451) and Switzerland (SIA 2052). For clients, this will increase the acceptability of designs in UHPC as a solution while for designers it will result in clear and comprehensive design procedures.

- **Transparency in determining material parameters**: The second recommendation is to include clear and transparent procedures to determine the material parameters and constitutive laws into such codes, which should be valid for all UHPC mixtures and products within a certain scope. This way, limitations of applicability of the code to certain types of mixtures are prevented from occurring.

It is expected that by applying these two recommendations UHPC will become gradually more established and will become part of the common construction practice. Standardization has an important role in this development and in the most ideal case the standardization effort progresses as such that in time the material will become as practically applicable in design as conventional concrete. This may result in, for example, having an overview of parameters of UHPC that may be expected for different strength classes in a similar fashion as presented in table 3.1 of Eurocode 2-1-1 for conventional concrete.

However, such a level of standardization has not been reached yet. It will require extensive study and gaining experience until such a degree of standardization will be achieved, if it can be achieved at all. After all, UHPC mixtures are often optimized for specific applications and properties are highly dependent on execution. Regardless of the question whether this aforementioned ideal case can be achieved, continuous standardization efforts will increase the reliability and acceptance of solutions in UHPC and will make the material more practically applicable for designers and manufactures in the Dutch infrastructural sector.

13

BIBLIOGRAPHY

Literature

Behloul, M., & Acker, P. (2004). Ductal Technology: A large spectrum of properties, a wide range of applications. In M. Schmidt, E. Fehling, & C. Geisenhanslüke (Red.), *Ultra High Performance Concrete* (pp. 11-23). Kassel: Kassel University Press.

Behloul, M., & Batoz, J.-F. (2008). Ductal applications over the last Olympiad. In E. Fehling, M. Schmidt, & S. Stürwald (Red.), *Ultra High Performance Concrete (UHPC)* (pp. 855-902). Kassel: Kassel University Press.

Behloul, M., Durukal, A., Batoz, J.-F., & Chanvillard, G. (2004). Ductal: Ultra High-Performance Concrete technology with ductility. In M. Di Prisco, & G. A. Plizzari (Red.), *6th International RILEM Symposium on Fibre-Reinforced Concretes (FRC)* (pp. 1281-1290). Varenna: RILEM.

Bertram, G., & Hegger, J. (2012). Bond Behavior of Strands in UHPC - Test and Design. In E. Schmidt, E. Fehling, C. Glotzbach, S. Fröhlich, & S. Piotrowski (Red.), *Ultra-High Performance Concrete and Nanotechnology in Construction* (pp. 525-532). Kassel: kassel university press.

Betoniek. (2017). Da's sterk! *Betoniek Standaard*, 1-12.

Braam, C., Kaptijn, N., & Buitelaar, P. (2003). Hogesterktebeton als brugdekoverlaging. *Cement*, 86-91.

DYWIDAG. (2017, juni 01). DYWIDAG Bonded Post-Tensioning Systems using Strands.

Fehling, E., Schmidt, M., Walraven, J., Leutbecher, T., & Fröhlich, S. (2014). *Ultra-High Performance Concrete UHPC*. Berlin: Wilhelm Ernst & Sohn.

fib. (2004). *Precast concrete bridges.* State-of-art report prepared by Task Group 6.4.

Gijsbers, J. (2012). 100 jaar betonvoorschriften. *Cement*, 68 - 77.

Hunger, M., & Spiesz, P. (2016). Praktijkproef bewijst potentie UHSB. *Betoniek Vakblad*, 12-16.

Kaptijn, N. (2002). Toekomstige ontwikkelingen van zeer-hogesterktebeton. *Cement*, 56-63.

Ketel, H., Willemse, R., Van Rijen, P., & Koolen, E. (2011). Dwarskracht- en kolomberekening VVUHSB. *Cement*, 86-91.

Ketel, H., Willemse, R., Van Rijen, P., & Koolen, E. (2011). Rekenmodel VVUHSB (1). *Cement*, 50-57.

Lafarge North America Inc. (sd). JS1000. *Field-cast UHPC closure pour solutions for prefabricated bridge element connections*. USA.

Lebet, J.-P., & Hirt, M. A. (2013). *Conceptual and Structural Design of Steel and Steel-Concrete Composite Bridges.* EPFL Press.

Markovic, I. (2006). High-Performance Hybrid-Fibre Concrete: Development and Utilisation. *Proefschrift*. TU Delft.

Ng, T. S., Voo, Y. L., & Foster, S. J. (2011). Sustainability with Ultra-High Performance and Geopolymer Concrete Construction. In M. N. Fardis, *Innovative Materials and Techniques in Concrete Construction* (pp. 81-98). Springer.

Reitsema, A., Lukovic, M., & Hordijk, D. (2016). Towards slender, innovative concrete structures for replacement of existing viaducts. *fib Symposium*.

Rijkswaterstaat. (2014, oktober). Twentekanaal . *Kijk op de ruimtelijke kwaliteit van kanalen*. (Rijkswaterstaat, Samensteller)

Rijkswaterstaat. (2020). *Vaarwegen in Nederland.* Rijkswaterstaat, CIV. Rijkswaterstaat Centrale Informatievoorziening.

Rijkswaterstaat. (sd). *Twentekanaal*. Opgeroepen op mei 18, 2020, van Rijkswaterstaat: https://www.rijkswaterstaat.nl/water/vaarwegenoverzicht/twentekanalen/index.aspx

Russell, H. G., & Graybeal, B. A. (2013). *Ultra-High Performance Concrete: A State-of-the-Art Report for the Bridge Community.* Federal Highway Administration (FHWA), Office of Inrastructure Research and Development.

Simon, A., Corvez, D., & Marchand, P. (2013). Feedback of a ten years assessment of fibre distribution using K factor concept. *Int. Symposium on Ultra-High Performance Fibre-Reinforced Concrete* (pp. 669-678). Marseille: RILEM-fib-AFGC.

Snijder, H., & Steenbergen, H. (2011). *Krachtswerking.* Zoetermeer: Bouwen met Staal.

Toutlemonde, F., Kretz, T., Généreux, G., Resplendino, J., Pillard, W., Guérinet, M., & Rougeau, P. (2017). French Standards for Ultra-High Performance Fiber-Reinforced Concrete (UHPFRC). *High Tech Concrete: Where Technology and Engineering Meet - Proceedings of the 2017 fib Symposium* (pp. 1601-1609). Maastricht: Springer.

Van Geffen, L., & Attahiri, M. (2016). UHSB als alternatief voor hout. *Cement*, 28-34.

Van Nalta, R. (2015). Let op bij ontwerpen met UHSB. *Cement*, 38-42.

Van Tol, F. (1994, juni 3). Hoe betrouwbaar is de paalfundering? *Intreerede*. Technische Universiteit Delft.

Verruijt, A. (2001). *Grondmechanica.* Delft: Technische Universiteit Delft.

Walraven, J. (2006). Ultra-hogesterktebeton: een materiaal in ontwikkeling. *Cement*, 57-61.

Walraven, J. (2012). UHSB op weg naar regelgeving. *Cement*, 50-55.

Walraven, J., & Braam, C. (2019, February). Prestressed Concrete.

Wikipedia. (2020, mei 8). *Lijst van bruggen over de Twentekanalen*. Opgeroepen op 05 19, 2020, van Wikipedia: https://nl.wikipedia.org/wiki/Lijst_van_bruggen_over_de_Twentekanalen

Wikipedia. (2020, mei 7). *Twentekanaal*. Opgeroepen op mei 18, 2020, van Wikipedia: https://nl.wikipedia.org/wiki/Twentekanaal

Yang, Y. (2020). Lecture Notes Concrete Bridges CIE5127.

Codes and guideline

Commissie F1 voor de normalisatie van technische grondslagen voor bouwvoorschriften. (1949). N 1055. *TGB 1949 - Technische Grondslagen voor Bouwvoorschriften*.

Gowripalan, N., & Gilbert, I. R. (2000, May). Design Guidelines for Ductal Prestressed Concrete Beams. School of Civil and Environmental Engineering, the University of New South Wales.

Groupe de travail BFUB. (2002, January). Ultra High Performance Fibre-Reinforced Concretes - Interim Recommendations. AFGC-SETRA.

Groupe de travail BFUP. (2013, June). Ultra High Performance Fibre-Reinforced Concretes. *Recommendations*. Association Francaise de Génie Civil.

International Federation for Structural Concrete (fib). (2012, March). Model Code 2010 - Volume 1.

International Federation for Structural Concrete (fib). (2012, April). Model Code 2010 - Volume 2.

Koninklijk Instituut van Ingenieurs (KIVI) - Afdeling voor Bouw- en Waterbouwkunde. (1938). N 1008. *VOSB 1938 - Voorschriften voor het Ontwerpen van Stalen Bruggen*.

Koninklijk Instituut van Ingenieurs (KIVI) - Afdeling voor Bouw- en Waterbouwkunde. (1950). N 1009. *GBV 1950 - Gewapend-Betonvoorschriften 1950*.

NEN. (2011, november). NEN-EN 1992-1-1+C2. *Eurocode 2: Ontwerp en berekening van betonconstructies - Deel 1-1: Algemene regels en regels voor gebouwen*.

NEN. (2011, december). NEN-EN 1992-2+C1. *Eurocode 2: Ontwerp en berekening van betonconstructies - Betonnen bruggen - Regels voor ontwerp, berekening en detaillering*.

NEN. (2015, oktober). NEN-EN 1991-1-7+C1+A1. *Eurocode 1: Belastingen op constructies - Deel 1-7: Algemene belastingen - Buitengewone belastingen: stootbelastingen en ontploffingen*.

NEN. (2015, oktober). NEN-EN 1991-2+C1. *Eurocode 1: Belastingen op constructies – Deel 2: Verkeersbelasting op bruggen*.

NEN. (2019, november). NEN-EN 1990+A1+A1/C2. *Eurocode: Grondslagen voor het constructief ontwerp*.

NEN. (2019, november). NEN-EN 1990+A1+A1/C2/NB. *Nationale bijlage bij NEN-EN 1990+A1:2006+A1:2006/C2:2019 Eurocode: Grondslagen van het constructief ontwerp*.

NEN. (2019, november). NEN-EN 1991-1-1+C1+C11. *Eurocode 1: Belastingen op constructies – Deel 1-1: Algemene belastingen – Volumieke gewichten, eigen gewicht en gebruiksbelastingen voor gebouwen*.

NEN. (2019, november). NEN-EN 1991-1-1+C1+C11/NB. *Nationale bijlage bij NEN-EN 1991-1-1+C1+C11: Eurocode 1: Belastingen op constructies - Deel 1-1: Algemene belastingen – Volumieke gewichten, eigen gewicht en gebruiksbelastingen voor gebouwen*.

NEN. (2019, november). NEN-EN 1991-1-7+C1+A1/NB. *Nationale bijlage bij NEN-EN 1991-1-7+C1+A1: Eurocode 1: Belastingen op constructies - Deel 1-7: Algemene belastingen - Buitengewone belastingen*.

NEN. (2019, november). NEN-EN 1991-2+C1/NB. *Nationale bijlage bij NEN-EN 1991-2+C1: Eurocode 1: Belastingen op constructies – Deel 2: Verkeersbelasting op bruggen*.

NEN. (2020, februari). NEN-EN 1992-1-1+C2/NB+A1. *Nationale bijlage bij NEN-EN 1992-1-1+C2 Eurocode 2: Ontwerp en berekening van betonconstructies - Deel 1-1: Algemene regels en regels voor gebouwen*.

Rijkswaterstaat. (2017, April). Richtlijnen Ontwerp Kunstwerken. *ROK 1.4*.

Societé suisse des ingénieurs. (2016). SIA 2052:2016. *Béton fibré ultra-performant (BFUP) - Matériaux, dimensionnement et exécution*. SIA.

Figures

Figure 15	From: *https://www.spanbeton.nl/content/files/Files/Kennisportaal/Volstortliggers/WEBSITE__SJP-FLEX_NIEUW.pdf*, on 12-06-2020
Figure 16	From: *https://www.spanbeton.nl/content/files/Files/Kennisportaal/Railbalk/WEBSITE__ZIPXL.pdf*, on 12-06-2020
Figure 17	From: *https://www.spanbeton.nl/content/files/Files/Kennisportaal/Kokerbalk/WEBSITE__SKK.pdf*, on 12-06-2020
Figure 19	From: *https://www.researchgate.net/profile/Vic_Perry/publication/340443134/figure/fig2/AS:876812158648320@1586059717555/Sherbrooke-Pedestrian-Bridge-Quebec-Canada-In-2001-the-US-Federal-Highway.jpg*, on 12-06-2020
Figure 27 Almensebrug	*Almensebrug*. (sd). Opgeroepen op 05 19, 2020, van Brueckenweb.de: https://www.brueckenweb.de/2content/datenbank/bruecken/3brueckenblatt.php?bas=6288
Figure 27 Exelsebrug	Bruntink, H. (2018, augustus 30). *Schilderbeurt Exelsebrug blijft voorlopig uit*. Opgeroepen op 05 19, 2020, van Lochems Nieuws: https://www.lochemsnieuws.nl/2018/08/30/schilderbeurt-exelsebrugblijft-voorlopig-uit/
Figure 27 Lochemsebrug	*Lochemsebrug (2)*. (2013, July 7). Opgeroepen op 05 19, 2020, van Wikipedia: https://upload.wikimedia.org/wikipedia/commons/thumb/7/72/Lochemsebrug_%282%29.jpg/727px-Lochemsebrug_%282%29.jpg
Figure 27 Markelosebrug	*Zware vrachtwagens weer over Markelosebrug*. (2018, mei 12). Opgeroepen op 05 19, 2020, van Maarkelsnieuws: https://www.maarkelsnieuws.nl/?p=70746
Figure 27 Weldammerbrug	Afdeling Multimedia Rijkswaterstaat. (1959, 8 27). *De Weldammerbrug over het Twenthe kanaal nabij Goor ID468742*. Opgeroepen op 05 19, 2020, van Beeldbank Rijkswaterstaat: https://beeldbank.rws.nl/MediaObject/Details/De_Weldammerbrug_over_het_Twenthe_kanaal_nabij_Goor_468742
Figure 27 Hengelerbrug	Eissink, J. (2019, July 3). *Hengelerbrug 2*. Opgeroepen op 05 19, 2020, van Wikimedia: https://upload.wikimedia.org/wikipedia/commons/8/82/2019-07 03_Hengelerbrug_2.jpg
Figure 27 Oelerbrug	Google Maps
Figure 27 Lonnekerbrug	Tubantia. (2019, 07 18). *Lonnekerbrug in Enschede volledig afgesloten voor verkeer*. Opgeroepen op 05 20, 2020, van Tubantia: https://www.tubantia.nl/enschede/lonnekerbrug-in-enschede-volledigafgesloten-voor-verkeer~af3405d6/
Figure 27 Cottwicherbrug I	Eissink, J. (2019, augustus 5). *Wikipedia*. Opgeroepen op 05 20, 2020, van https://nl.m.wikipedia.org/wiki/Bestand:2019-08-05_Cottwicherbrug_3.jpg
Figure 27 Wierdensebrug	*Wikipedia*. (2012, juni 2). Opgeroepen op 05 20, 2020, van https://nl.wikipedia.org/wiki/Bestand:Wierdense_brug_(2).jpg
Figure 86	From: *https://www.spanbeton.nl/nl/references/item/bleizo-vervoersknoop-lansinger-landzoetermeer/*, on 17-09-2020
Figure 87 (left)	From: *https://www.haitsma.nl/nieuws/brugliggers-wanssum/*, on 17-09-2020
Figure 87 (right)	From: *https://www.haitsma.nl/landingspagina/langste-prefab-voorgespannen-liggers-terwereld/*, on 17-09-2020

For the other figures either the sources have been mentioned in the text or the figures are own work.